Exploring the substrate specificity of the antimicrobial peptide transporter BceAB of Bacillus subtilis

Kobras, Carolin M

Award date:
2019

Awarding institution:
University of Bath

Exploring the substrate specificity of the antimicrobial peptide transporter BceAB of *Bacillus subtilis*

Carolin Martina Kobras

A thesis submitted for the degree of Doctor of Philosophy

University of Bath

Department of Biology & Biochemistry

January 2019

_____

Abstract

Cell wall biosynthesis is an important target of antimicrobial peptides (AMPs), which in light of the imminent shortage of antibiotics are considered promising candidates for future treatment of infections. Yet, numerous Gram-positive bacteria have developed specific resistance systems against many AMPs. These systems feature so-called BceAB-like ATP-binding cassette transporters consisting of ten transmembrane helices and a characteristic extracellular domain of around 200 amino acids.

So far, the mechanisms behind substrate recognition and binding as well as the nature of the physiological substrate of the transporters remained elusive. This is a major impediment to our understanding of the resistance mechanism, and multiple theories have been proposed regarding these important questions. The targets of AMPs are crucial membrane-anchored intermediates of the lipid II cycle. One hypothesis suggests that the transporters expel the AMP from the membrane, in which case the physiological substrate should be the AMP itself or the AMP bound to its cellular target. Alternatively, the transporters may flip the drug target to the cytoplasmic face of the membrane to remove it from access by the AMP.

Here, we investigate the substrate specificity of the transporter BceAB of *Bacillus subtilis*. We focus on characterising the binding capacity of its large extracellular domain *in vitro* and further aim to identify the physiological substrate of BceAB using *in vivo* approaches. Combining the findings of biochemical, biophysical and physiological assays conducted for this study, we propose the complex formed between the AMP and its cellular target to be the physiological substrate of BceAB, rather than the unbound AMP or the drug target alone. Considering this result in the context of previous findings and the literature enabled us to gain valuable insights into the potential resistance mechanism of BceAB-like transporters that play such a crucial role in antimicrobial resistance.

Acknowledgements

First of all, I would like to thank the University of Bath for financial support.

I would also like to thank my lead supervisor Susanne Gebhard. Thank you for giving me the opportunity to work with you on this exciting project and for being ever so enthusiastic and optimistic, especially when the science did not behave. Thanks for valuable advice and great support over the last six years, I have learnt an incredible lot from you. I am very lucky that I have found a PhD supervisor that genuinely wants the best for me.

Thanks to my second supervisor Chris Pudney for introducing me to plenty of super exciting biochemical and biophysical approaches to protein science.

A big thank you also goes to my lab group for support and troubleshooting ideas throughout my PhD, particularly to our postdoc Alan Koh, who is not only a very inspiring researcher, but also has become a very good friend of mine over the last three years. I will miss our Saturday chats in the lab!

Many thanks to the academic staff of the Department of Biology & Biochemistry for a supportive and friendly environment, encouraging words and many open doors whenever I needed advice.

Thanks to my peers in the lab and the office, the PGBio crew and other friends around the Department of Biology & Biochemistry. Thank you so much for the amazing time I had in beautiful Bath. For sharing my passion for science. For great food and great company. For cake and tea breaks. For board games, cycley bevs and pub quizzes. For dancing and exercising with me. For helping to pick up the pieces of broken hearts and broken beerfest bones. And, of course, for listening to Caro-stories over and over and over again.

Ich möchte mich auch gerne bei meiner Familie für all ihre Unterstützung während meiner Doktorarbeit bedanken, insbesondere bei meinen Eltern. Vielen Dank, dass ihr mir Sorgfalt und Gewissenhaftigkeit vorgelebt und mir von früh auf Entschlossenheit und Durchhaltevermögen mit auf den Weg gegeben habt. Danke, dass ihr mir nicht nur alle Freiheiten gelassen habt, meine eigenen Entscheidungen zu treffen, sondern mich auch immer in meinen Vorhaben unterstützt habt. Wer von uns hätte denn gedacht, dass es mich einmal zu einem ‚Doctor of Philosophy' führen würde, als ich als Vierjährige frech behauptet habe: „Aus mir wird nochmal was!"?

Danke, dass ihr den Weg dahin geebnet habt.

Table of contents

Abstract ... **III**

Acknowledgements ... **V**

Table of contents ... **VII**

List of figures ... **XIII**

List of tables ... **XV**

List of abbreviations ... **XVII**

Chapter I: Introduction ... **1**

1. Antimicrobial peptides as promising candidates to combat antimicrobial resistance. ... **3**

1.1 Emerging antimicrobial resistance is a global threat. ... 3

1.2 Strategies to tackle antimicrobial resistance ... 4

2. The cell envelope protects bacteria from the environment. ... **6**

2.1 Bacterial membranes comprise many phospholipids with anionic net charge. ... 6

2.2 The cell wall of Gram-positive bacteria and its biosynthesis ... 8

2.2.1 Peptidoglycan precursor synthesis in the cytoplasm ... 8

2.2.2 Precursor translocation via the lipid II cycle is the bottleneck of cell wall synthesis. ... 9

2.2.3 Peptidoglycan polymerisation and cross-linking in the extracellular space ... 15

3. The cell wall synthesis is a major target for antibiotics. ... **17**

3.1 Lipid II serves as a target for numerous classes of AMPs. ... 17

3.1.1 Non-ribosomally synthesized antimicrobial peptides that bind lipid II. ... 17

3.1.2 Ribosomally-synthesised AMPs that target lipid II. ... 18

3.2 The cyclic dodecapeptide bacitracin targets undecaprenyl pyrophosphate. ... 24

4. Resistance and self-protection against AMPs in Firmicutes ... **27**

4.1 Modifications of cellular targets to evade AMP action ... 27

4.2 Inactivation or degradation of AMPs in the extracytoplasmic space ... 28

4.3 Transport of AMPs as immunity and resistance strategy 29

4.3.1 LanFEG-type transporters mainly mediate self-protection in lantibiotic producers. 30

4.3.2 BcrAB-type transporters are ancestors of LanFEG-type transporters. 30

4.3.3 BceAB-like transporters confer resistance against a broader substrate range..... 31

4.4 Sequestration of AMPs by resistance and immunity proteins 32

4.4.1 The LanI proteins SpaI and NisI directly bind their substrates. 32

4.4.2 NukH and NukFEG use a cooperative immunity mechanism. 34

4.4.3 PepI seems to sequester the cellular target rather than the lantibiotic. 35

5. Substrate recognition of regulatory and resistance proteins 37

5.1 How do regulatory proteins sense AMPs in the extracytoplasmic space? 37

5.1.1 Prototypical periplasmic-sensing histidine kinases detect AMPs via an extracytoplasmic domain. 38

5.1.2 The formation of hydrophobic pockets allows substrate recognition in the membrane. 39

5.2 How do transporters recognise and bind AMPs in the extracytoplasmic space? 40

5.2.1 The periplasmic domains of RND-type multi-drug efflux pumps harbour the substrate binding sites. 41

5.2.2. Extracytoplasmic domains of ABC transporters are important for substrate interactions..... 42

6. The Bce system of *B. subtilis* is the paradigm for AMP resistance in Firmicutes. 44

6.1 The Bce-like systems of the Gram-positive model organism *B. subtilis* 44

6.2 The flux-sensing mechanism of BceAB-BceRS ensures need-based supply of resistance. 45

6.3 The resistance mechanism and substrate specificity of BceAB remain unclear. 48

7. Aims and objectives of this study 50

7.1 *In vitro* characterisation of the binding capacity of BceB-ECD 50

7.2 *In vivo* determination of the physiological substrate of BceAB 51

Chapter II: Material and Methods **53**

1. Chemicals **55**

2. Bacterial strains and growth conditions **55**

3. DNA manipulations and transformations **56**

3.1 Polymerase chain reaction 56

3.2 DNA digest and ligation 56

3.3 Plasmid extraction and verification of cloning 57

3.4 Bacterial transformations 57

3.4.1 Transformation of *E. coli* strains 57

3.4.2 Transformation of *B. subtilis* 57

4. Overproduction and purification of BceB-ECD **58**

4.1 Overproduction of BceB-ECD 58

4.2 Cell lysis 58

4.3 Refolding BceB-ECD from inclusion bodies 59

4.4 Protein purification techniques 59

4.4.1 Immobilized metal affinity chromatography 59

4.4.2 Anion exchange chromatography 60

5. Protein visualisation and quality determination **60**

5.1 Sodium dodecyl sulphate - polyacrylamide gel electrophoresis 60

5.2 Western blot 60

5.3 Mass spectrometry 61

5.4 Determination of protein concentration 61

5.5 Dynamic light scattering 61

6. *In vitro* characterisation of BceB-ECD using biophysical methods **62**

6.1 8-Anilino-naphthalene-1-sulphonic acid fluorescence spectroscopy 62

6.2 Circular dichroism spectroscopy 62

7. *In vivo* characterisation of the physiological substrate of BceAB. **64**

7.1 Growth assays for determination of the fasted doubling time. 64

7.2 Competition assays as measure of relative fitness 64

7.3 Determination of the minimal inhibitory concentration of bacitracin 65

7.4 Luminescence reporter assay for determination of BceAB transport activity 65

Chapter III: *In vitro* characterisation of the binding capacity of BceB-ECD **67**

1. Introduction 69

2. Results 72

2.1 *In silico* characterisation reveals high flexibility and partial intrinsic disorder of BceB-ECD. 72

2.2 *In vitro* characterisation of purified BceB-ECD does not imply bacitracin binding activity. 76

2.2.1 Initial attempts of overproduction and purification of BceB-ECD using plasmid pSG1601 76

2.2.2 Improvements on the purification of BceB-ECD and refolding the ECD from inclusion bodies 78

2.2.3 ANS fluorescence spectroscopy experiments suggest no conformational change of BceB-ECD in the presence of bacitracin. 82

2.2.4 CD spectroscopy experiments with refolded BceB-ECD do not show conformational changes upon addition of bacitracin. 86

2.3 A shortened version of BceB-ECD does not possess bacitracin binding capability *in vitro*. 89

2.3.1 Reduction of flexible ends increases yield and solubility of recombinant BceB-ECD. 89

2.3.2 Spectroscopy experiments on BceB-ECD with increased solubility do not unveil bacitracin-induced conformational changes. 92

2.4 The complex formation of [GPP-BAC] masks a potential binding reaction of BceB-ECD. 95

2.4.1 A potential increase of ANS fluorescence emission upon addition of [GPP‒BAC] is subject to high variation. 95

2.4.2 CD spectra of BceB-ECD remain inconclusive due to high variation of the [GPP-BAC] signal. 98

3. Discussion 100

3.1 BceB-ECD does not undergo a conformational change in the presence of bacitracin or GPP. 100

3.2 The membrane environment might be required for recognition of AMPs. 102

3.3 ECDs can combine substrate recognition in the membrane environment with a broad substrate range. 105

3.4 The isolated extracellular domain might not be functional *in vitro.* 109

Chapter IV: *In vivo* determination of the physiological substrate of BceAB **..... 113**

1. Introduction 115

2. Results 118

2.1 Investigating a potential interaction between BceAB and UPP using growth assays 118

2.1.1 Presence of BceAB does not alter the fastest doubling time. 118

2.1.2 Absence of BceAB seems beneficial to growth in competition assays when recycling of UPP is impaired. 121

2.2 Changing amounts of the [target-AMP] complex has impact on BceAB activity. 124

2.2.1 Accumulation of UPP increases BceAB activity at low concentrations of bacitracin. 126

2.2.2 UPP accumulation does not affect transport activity upon addition of lipid II binding AMPs. 130

2.2.3 Accumulation of C_{35}-PP in the cell does not alter BceAB activity. 134

3. Discussion 136

3.1 Our experimental data do not support a 'UPP import' model for BceAB. 136

3.2 The [target-AMP] complex is likely the physiological substrate of BceAB. 139

3.3 The 'hydrophobic vacuum cleaner' model as proposed mechanism for BceAB. 141

3.4 The challenges of manipulating the lipid II cycle intermediate levels of the cell wall biosynthesis 143

Chapter V: Conclusions and future perspectives **149**

1. Summary and main conclusions 151

2. BceAB removes bacitracin from its membrane-bound target and releases the AMP into the extracellular space. 152

3. BceAB is a mechanotransducer 156

3.1 Mechanotransmission rather than 'classic' transport 156

3.2 Could BceAB work according to an 'ATP-switch' model? 157

3.3 Mechanotransmission directly couples transport activity with flux sensing. 159

4. Target protection as resistance strategy 161

4.1 BceAB confers resistance by protecting its target 161

4.2 Target protection of cell wall synthesis might be more common than anticipated. . 163

5. Future Perspectives 165

5.1 Investigations on the physiological substrate of BceAB for lipid II-binding AMPs. 165

5.2 *In vivo* investigation of potential BceB-ECD binding site for target-bound bacitracin. 168

5.3 Analysis of the natural membrane environment and localisation of BceAB. 170

References 175

Supplement 197

Chapter II 197

Chapter III 202

Chapter IV 207

List of figures

Chapter I

Figure 1.1: The three stages of bacterial cell wall synthesis ……..12
Figure 1.2: Schematic structures of representative class I and class II lantibiotics that bind lipid II……..22
Figure 1.3: Bacitracin adopts an amphipathic configuration upon target binding……..26
Figure 1.4: Schematic domain architectures of ABC transporters subfamilies that mediate resistance or immunity against AMPs……36
Figure 1.5: The BceAB-BceRS resistance system operates according to a flux-sensing mechanism……..47

Chapter III

Figure 3.1: *In silico* characterisation reveals BceB-ECD to be highly flexible with an intrinsically disordered region……75
Figure 3.2: Initial purification attempts of BceB-ECD from pSG1601 result in a double band on SDS-PAGE……77
Figure 3.3: Improvements on overproduction and purification BceB-ECD from pSG1601 and refolding from inclusion bodies lead to increased yield and purity……81
Figure 3.4: ANS fluorescence spectroscopy experiments suggest no conformational change of BceB-ECD in the presence of bacitracin……84
Figure 3.5: CD spectroscopy experiments with refolded BceB-ECD do not show conformational changes upon addition of bacitracin……88
Figure 3.6: Reducing the length of flexible ends of BceB-ECD increases yield and solubility drastically……91
Figure 3.7: Spectroscopy experiments on BceB-ECD with increased solubility do not exhibit bacitracin-induced conformational changes……94
Figure 3.8: Potential increase of ANS fluorescence emission upon addition of [GPP-BAC] is subject to high variation……97
Figure 3.9: CD spectra of BceB-ECD remain inconclusive due to high variation of the [GPP-BAC]
signal……99
Figure 3.10: BceB (TMH7-10) has the characteristic features of type VII ABC transporters…108

Figure S3.1: The extracellular domains of bacitracin resistance-related BceB-like permeases have only poor amino acid conservation……..202
Figure S3.2: Circular dichroism spectra of polypeptides and proteins with representative secondary structures……204
Figure S3.3: Complex formation between bacitracin and GPP results in saturation at 50 µM BAC and 200 µM GPP……205
Figure S3.4. Schematic of BceB-ECD hybrid membrane proteins……206

Chapter IV

Figure 4.1: The doubling time of exponentially growing *B. subtilis* seems unaffected by presence of absence of BceAB……120
Figure 4.2: The absence of BceAB seems only beneficial upon accumulation of UPP……123
Figure 4.3: The flux-sensing mechanism as suitable strategy to monitor BceAB activity…….125
Figure 4.4: Varying the cellular UPP concentration affects BceAB transport activity in the presence of bacitracin……..129
Figure 4.5: Accumulation of UPP does not affect BceAB nor PsdAB transport activity in the presence of mersacidin, actagardine or nisin, respectively……132
Figure 4.6: Accumulation of C_{35}-PP in the cell does not affect BceAB activity in presence to bacitracin, but leads to decrease in resistance……135

Figure S4.1: AMP transport assay suggests bacitracin is neither imported nor inactivated by BceAB……207
Figure S4.2: Deletion of *ponA* does not lead to changes in BceAB activity……208
Figure S4.3: Combination of bacitracin or mersacidin with vancomycin does not alter BceAB activity……209
Figure S4.4: Deletion of *sigM* does not result in significant changes in the BceAB activity….210
Figure S4.5: Overproduction of UppS does not alter BceAB activity……211

Chapter V

Figure 5.1: BceAB is proposed to remove bacitracin from its target and to release the AMP into the extracellular space……138
Figure 5.2: Mechanotransmission of BceAB can couple ATP-driven bacitracin resistance with flux-sensing response through BceRS……144

List of tables

Table S1: *E. coli* strains used in this study……197

Table S2: *B. subtilis* strains used in this study……198

Table S3: Vectors used in this study……199

Table S4: Plasmids used in this study……200

Table S5: Oligonucleotides used in this study……201

List of abbreviations

ABC	ATP-binding cassette
Abu	aminobutyric acid
ACT	actagardine
AEX	anion exchange chromatography
Ala	alanine
AMP	antimicrobial peptide
amp^r	resistance to ampicillin
ANOVA	analysis of variance
ANS	8-anilino-1-naphthalenesulphonic acid
aPBP	class A PBP
Asn	asparagine
Asp	aspartate
ATP	Adenosine triphosphate
BAC	bacitracin
BceB-ECD	extracellular domain of BceB
$BceB\text{-}ECD^{ref}$	refolded BceB-ECD
$BceB\text{-}ECD^{sol}$	soluble BceB-ECD
C_{15}-PP/FPP	farnesyl pyrophosphate
C_{35}-PP/HPP	heptaprenyl pyrophosphate
C_5-PP/IPP	isoprenyl pyrophosphate
CD	circular dichroism
CFU	colony forming units
CI	competition index
cm^r	resistance to chloramphenicol
D-Ala	D-alanine
DDM	n-dodecyl-β-D-maltoside
dH_2O	deionised water
Dha	didehydroalanine
Dhb	didehydrobutyrine
DHNA	1,4-dihydroxy-2-naphthoic acid
DLS	dynamic light scattering
DNA	deoxyribonucleic acid
dNTP	deoxyribonucleotide triphosphate
DTT	dithiothreitol

EC_{50}	half maximal effective concentration
ECD	extracellular domain
ECF	extracytoplasmic function
EDTA	ethylene-diamine-tetra-acetic acid
EF-G	elongation factor G
GlcNAc	N-acetylglucosamine
Gln	glutamine
Glu	glutamate
Gly	glycine
GPP	geranyl pyrophosphate
His	histidine
IDP	intrinsically disordered protein
Ile	isoleucine
IMAC	immobilised metal affinity chromatography
IPTG	isopropyl-β-D-thiogalactopyranoside
kan^r	resistance to kanamycin
LB	lysogeny broth
Leu	leucine
Lys	lysine
*m*DPA	*meso*-diaminopimelic acid
MERS	mersacidin
Met	methionine
MH	Müller-Hinton broth
MIC	minimal inhibitory concentration
mls^r	resistance to macrolide-lincosamide-streptogramin B
MoRF	molecular recognition feature or element
mRNA	messenger RNA
MurNAc	N-acetylmuramic acid
NBD	nucleotide binding domain
NIS	nisin
OD_{600}	optical density at 600 nm wavelength
Orn	ornithine
P_{bceA}-*lux*	P_{bceA}-*luxABCDE*
PBP	penicillin binding protein
PCR	polymerase chain reaction
Phe	phenylalanine
Pro	proline

PVDF	polyvinylidene fluoride
RLU	relative luminescence units
RNA	ribonucleic acid
RND	resistance, nodulation, division
rRNA	ribosomal RNA
Sabre	small alpha/beta rich extracytoplasmic
SDS	sodium dodecyl sulphate
SDS-PAGE	sodium dodecyl sulphate - polyacrylamide gel electrophoresis
SEDS	shape, elongation, division and sporulation
Ser	serine
sgRNA	single guide RNA
SMA	styrene-maleic acid
SMALP	SMA lipid particles
$spec^r$	resistance to spectinomycin
TCS	two component system
tet^r	resistance to tetracycline
Thr	threonine
TMH	transmembrane helix
tRNA	transfer RNA
Trp	tryptophan
Tyr	tyrosine
UDP-GlcNAc	uridine diphosphate-N-acetylglucosamine
UDP-MurNAc	uridine diphosphate-N-acetylmuramic acid
UP	undecaprenyl phosphate
UPP	undecaprenyl pyrophosphate
UV	ultraviolet
Val	valine
WT	wild-type

Chapter I

Introduction

1. Antimicrobial peptides as promising candidates to combat antimicrobial resistance.

1.1 Emerging antimicrobial resistance is a global threat.

Infectious diseases like tuberculosis, pneumonia and diphtheria were the leading causes of death in humans for a long time (Zaffiri *et al.*, 2012). Over the course of the last century, advances in sanitation and hygiene, but mainly the development and clinical use of antibiotics and vaccinations, helped to tackle the impact of infectious diseases and majorly contributed to the extraordinary reduction of morbidity and mortality associated with those illnesses (Alanis, 2005, Zaffiri *et al.*, 2012). Antibiotics kill bacteria by impeding vital metabolic processes including the cell wall biogenesis or nucleic acid or protein biosynthesis, thereby inhibiting their growth and replication (Anderson, 2012). Originating from naturally-occurring microbial products, more antibiotics were discovered in the 1950s and 1960s and soon chemically synthesised (Davies, 2006). This has paved the way for impactful application of antimicrobial agents against acute bacterial infections, and has increased the health and longevity of humans.

Yet, humankind is at risk of being thrown back into the dark age of the pre-antibiotic era. Naturally, bacteria continuously evolve to resist antibiotics, making treatments less powerful or often totally ineffective (Alanis, 2005). As a result, common bacterial infections like food-borne illness, let alone sepsis, meningitis and the diseases mentioned above, can become life-threatening again (World Health Organization, 2019).

Antibiotic resistance is on the rise, with new resistance mechanisms emerging and spreading globally. Every year, several hundred thousand people worldwide die because of infections caused by antimicrobial resistant bacteria (O'Neill, 2014). Future scenarios predict antimicrobial resistance to even claim around 10 million lives every year by 2050 (O'Neill, 2014). But antimicrobial resistance has the potential to undermine public health even further. To prevent bacterial infections in immuno-suppressed patients or other risk groups, antibiotics are often administered prophylactically. Secondary implications of antimicrobial resistance would thus make routine surgery like caesarean sections or joint replacements precarious procedures, and cancer treatments even more worrisome (O'Neill, 2014).

Although the development of antimicrobial resistance is evolutionarily inevitable, combatting antimicrobial resistance promptly is crucial to avoid a 'post-antibiotic' global health crisis (O'Neill, 2014).

1.2 Strategies to tackle antimicrobial resistance

To tackle the emerging threat of antimicrobial resistance, several strategy papers have been compiled (World Health Organization, 2015, O'Neill, 2016, European Commission, 2017).
Some of the proposed policies aim at reducing the occurrence of antimicrobial resistance and preventing spreading of infections. Examples include improved sanitation and hygiene and better surveillance of drug resistance. To avoid unnecessary administration of antibiotics in humans and agriculture, regulations on their medical use and as food additives should be implemented and novel rapid diagnostic tools developed. Taken together, these measures are meant to maximise the life span of current antibiotics. At the same time, the action plans demand the discovery and clinical development of new antimicrobial agents as well as the further advancement of existing antibiotics and the investigations of underlying resistance mechanisms (O'Neill, 2016).
In the quest for new antibiotics, antimicrobial peptides (AMPs) have raised attention. AMPs are short, often cationic peptides that are produced by virtually all life forms, and are also known as host-defence peptides (Hancock & Sahl, 2006). In higher organisms, AMPs can modulate the innate immune response of the host to infections, while prokaryotes produce AMPs to gain an advantage over other microbes, competing for the same environmental niche and resources (Mahlapuu *et al.*, 2016). Aiming at the development of a novel therapeutic strategy, these host-defence peptides without direct antimicrobial activity are a promising research focus. They are able to adjust the innate immunity response and thereby can potentially indirectly promote pathogen clearance (Hancock & Sahl, 2006, Mahlapuu *et al.*, 2016).
Yet, with several in clinical trials, AMPs are first in line to potentially become future therapeutics for infection treatment (Hancock & Sahl, 2006, Mahlapuu *et al.*, 2016). The reasons as to why AMPs are regarded as propitious are plenty. Many AMPs possess a direct and fast-acting antimicrobial potency (Hancock & Sahl, 2006). Generally, they have a broader-than-average target spectrum, preferring several low-affinity targets over a single high-affinity one. It is thus difficult for bacteria to accomplish resistance by developing only a single defence strategy (Lai & Gallo, 2009, Mahlapuu *et al.*, 2016).

AMPs act by disrupting the physical integrity of the microbial cell envelope or by translocating across the membrane into the cytoplasm to act on intracellular targets (Hancock & Sahl, 2006, Mahlapuu *et al.*, 2016). This membrane interference is often effectuated by the cationic and amphipathic characteristics of AMPs. Bacteria have a significant amount of anionic phospholipids displayed on the cell surface. AMPs thus mainly interfere with the negatively charged bacterial membrane via electrostatic forces (Andersson *et al.*, 2016). Differences in lipid composition and distribution are thought to be responsible for the selectivity of AMPs for bacterial membranes. Plasma membranes of many mammalian cells have an asymmetrically-distributed lipid composition (Quinn, 2002). For example, phospholipids with negatively-charged head groups like phosphatidylserine are primarily featured in the inner leaflet of the plasma membrane of human erythrocytes. The outer face of the plasma membrane mainly consists of phospholipids with zwitterionic properties and a neutral net charge, such as phosphatidylethanolamine, phosphatidylcholine, and sphingomyelin (Quinn, 2002, Andersson *et al.*, 2016).

Many structures of membrane and cell wall synthesis are non-proteinaceous and procedures often well-conserved, posing a challenge to bacteria to develop resistance against AMP stress while still having to secure functionality and structural integrity of the cell wall (Lai & Gallo, 2009). As the interaction with the bacterial membrane seems to be a key factor for the antimicrobial activity of AMPs, features and characteristics of the bacterial cell envelope are described in the following section.

Despite their considerable potential, there are several obstacles to overcome in the development of AMPs for clinical use (Marr *et al.*, 2006). These drawbacks include for example the high cytotoxicity and haemolytic activity displayed by certain AMPs against human cells (Maher & McClean, 2006, Mader & Hoskin, 2006). In addition, AMPs or host-defence molecules can be immunogenic and even lead to allergic reactions (Mader & Hoskin, 2006). Further, some AMPs only display poor serum stability and show degradation by proteases or inactivation by high salt concentrations (Marr *et al.*, 2006). Although the broad substrate activity of AMPs can be listed as an asset of AMPs, at the same time the broad-range activity can lead to complications in clinical use by disrupting the indigenous host microbiome (Aoki & Ueda, 2013).

For these reasons, most AMPs that have been applied in health care so far have found use as topical medication. Further research and development are required to target the stability, safety, and efficacy of AMPs. One example of a promising candidate from the family of lanthionine-containing antibiotics is nisin. The lantibiotic is already used as food preservative

and treatment in animal care due to its broad potency against Gram-positive bacteria, including drug-resistant microbes and the causative agents of food spoilage (Dischinger *et al.*, 2014, Shin *et al.*, 2016). Recent bioengineering approaches have aimed at increasing the antimicrobial activity of nisin against *Escherichia coli* and other Gram-negative bacteria (Zhou *et al.*, 2016, Li *et al.*, 2018) and improving nisin's resistance against protease degradation (Field *et al.*, 2018). Based on these and other advances, nisin is hoped to be applied in future infection treatment, oral health and possibly even cancer treatment of humans (Shin *et al.*, 2016).

2. The cell envelope protects bacteria from the environment.

The cell envelope is a bacterium's multi-layered, protective barrier to the environment. Based on the differences and characteristics of their complex cell envelopes, bacteria can generally be divided into two major groups, Gram-positive and Gram-negative bacteria (Silhavy *et al.*, 2010). In Gram-positives, the cytoplasmic membrane is surrounded by numerous layers of peptidoglycan, forming a thick cell wall. Gram-negative bacteria in contrast only possess a few peptidoglycan layers. They are additionally surrounded and protected by another membrane containing lipopolysaccharides (Silhavy *et al.*, 2010, Lin & Weibel, 2016). The two membranes of Gram-negative bacteria are referred to as 'inner' and 'outer' membrane, the space between them is named the periplasm.

2.1 Bacterial membranes comprise many phospholipids with anionic net charge.

The composition of bacterial membranes is not only highly variable between different species, bacteria are also able to modify their membrane composition in response to environmental changes, such as temperature, salinity and pH (Lin & Weibel, 2016). Cytoplasmic membranes of both, Gram-positive and Gram-negative bacteria, can be described as fluid bilayers containing oriented globular proteins and phospholipids (Singer & Nicolson, 1972). The proteins occurring in cytoplasmic membranes are either 'peripheric' and only weakly-attached, or 'integral' proteins that intercalate into the membrane and often contain a high content of α-helices (Singer & Nicolson, 1972).

The (glycero-)phospholipids of bacterial membranes generally contain two fatty acid chains and a variable polar phosphate headgroup. The phospholipid acyl chains determine the

membrane viscosity and permeability, and by this, influence many membrane-associated functions, including transport and protein–protein interactions (Zhang & Rock, 2008). Most abundant in many bacterial species are phosphatidylethanolamine, phosphatidylglycerol and cardiolipin, but also phosphatidylinositol and phosphatidylserine, or even lipids that lack a phosphate group can be found, but usually to a lesser degree (Sohlenkamp & Geiger, 2016). While phosphatidyl-ethanolamine is zwitterionic, phosphatidylglycerol and cardiolipin are both negatively charged, causing the overall anionic net charge of the bacterial membrane.

Phospholipids are heterogeneously distributed along the cytoplasmic membrane and form specific lipid domains with particular functions (Strahl & Errington, 2017). For example, it has been hypothesised that the formation of anionic phospholipid lipid domains is involved in the initiation of DNA replication and cell division (Mileykovskaya & Dowhan, 2005). Yet, this hypothesis is still subject to debate and not generally accepted. Antimicrobial compounds, like the cationic AMPs described above, can also affect the membrane environment, and *vice versa*, the phospholipid composition can affect the efficacy of AMPs (Epand & Epand, 2009, Epand *et al.*, 2016).

Highly conserved in most bacteria, but prevalent to a lesser degree in the cytoplasmic membrane, are poly-isoprenoid carriers (C_{55}). Their role is the translocation of activated sugar intermediates that are required for envelope biogenesis (Raetz & Dowhan, 1990). Their structure and function will be further described in I.2.2.2.

Gram-negative specifications: the outer membrane

The outer membrane of Gram-negative bacteria functions as selective permeability barrier and protects the cell against harsh environmental conditions. The phospholipids of the outer membrane are restricted to the inner leaflet. The outer leaflet consists of lipopolysaccharides that extend into the extracellular space and can serve as virulence factor in pathogens (Silhavy *et al.*, 2010, May & Silhavy, 2017). The outer membrane further contains mainly two types of proteins. These are either bilayer-anchored lipoproteins or β-barrel transmembrane proteins responsible for nutrient uptake or efflux of waste products (May & Silhavy, 2017).

Gram-positive specifications: teichoic acids

In contrast, Gram-positive bacteria lack an outer membrane and a distinct periplasm. The cell envelope of Gram-positive bacteria is heavily modified by the incorporation of carbohydrate-based anionic polymers, so-called teichoic acids (Weidenmaier & Peschel, 2008, Silhavy *et al.*, 2010). Lipoteichoic acids are linked to the outer face of the membrane via a lipid anchor

(Percy & Grundling, 2014). Wall teichoic acids are covalently attached to peptidoglycan (Brown *et al.*, 2013). Both polymer types are highly complex polysaccharides, based on either polyribitol- or polyglycerol phosphate and vary for each bacterial strain (Silhavy *et al.*, 2010). Together, both structures extend from the bacterial cell surface beyond the outermost layers of the cell wall. Accounting for as much as 60 % of the molecular composition of the cell wall, teichoic acids can influence membrane permeability and cell envelope stability majorly, and serve as scaffolds for extracytoplasmic enzymes required for cell wall growth and degradation (Weidenmaier & Peschel, 2008, Silhavy *et al.*, 2010).

2.2 The cell wall of Gram-positive bacteria and its biosynthesis

In Gram-positive bacteria, the cell wall is the principal barrier to environmental stresses, and its integrity is of critical importance to cell viability. The cell wall ensures osmotic stability and, because of its rigidity, determines the cell shape. With between 30 and 100 nm in width, the multi-layered cell wall of Gram-positives is drastically thicker than the sometimes only single-layered cell wall of Gram-negatives (Silhavy *et al.*, 2010).

The cell wall is made up by a mesh-like polymer called peptidoglycan (Vollmer *et al.*, 2008). The basic structure of peptidoglycan is similar in most bacteria except *Mycoplasma* and few other species that lack a cell wall. Peptidoglycan consists of long, about parallel glycan strands that in rod-shaped cells are thought to run perpendicularly to the long axis of the bacterium (Vollmer *et al.*, 2008). Glycan strands are assembled and polymerised from alternating 1,4-linked N-acetylglucosamine (GlcNAc) - N-acetylmuramic acid (MurNAc) disaccharide units (Scheffers & Pinho, 2005). Glycan strands are cross-linked with adjacent strands via the pentapeptide side chains of the MurNAc units, which connects the peptidoglycan sacculus to one very large polymer. The composition of the so-called stem peptide can vary between bacterial species, but the most common pentapeptide is L-alanine-D-glutamate-*meso*-diaminopimelic acid (*m*DPA)-D-alanine-D-alanine (Scheffers & Pinho, 2005, van Heijenoort, 2007). The cell wall synthesis is a highly complex process that can be divided into three stages. Their details will be described in the following sections.

2.2.1 Peptidoglycan precursor synthesis in the cytoplasm

The first stage of bacterial cell wall synthesis takes place in the cytoplasm where the nucleotide sugar-linked precursors are synthesised (Fig. 1.1). The leading enzymes of this stage are a series of Mur enzymes (El Zoeiby *et al.*, 2003).

Uridine diphosphate-N-acetylglucosamine (UDP-GlcNAc) is synthesised from fructose-6-phosphate in several steps (van Heijenoort, 1998). UDP-GlcNAc is not only required for assembly of lipid II in the second stage of cell wall synthesis, it also serves as precursor for synthesis of uridine diphosphate-N-acetylmuramic acid (UDP-MurNAc). This two-step reaction is catalysed by the enolpyruvyl transferase MurA and the flavin-dependent reductase MurB (El Zoeiby *et al.*, 2003, Bugg *et al.*, 2011). UDP-MurNAc is then further modified by the stepwise addition of the first three amino acid residues of the stem peptide, commonly L-alanine, D-glutamic acid and *meso*-diaminopimelic acid (Fig. 1.1). The residues are successively added to the reduced lactyl group of UDP-MurNAc by the ATP-dependent synthetases MurC, MurD and MurE, respectively. Finally, a D-alanine-D-alanine dipeptide is linked to the UDP-MurNAc-tripeptide in a MurF-catalysed step, bringing the last soluble peptidoglycan precursor UDP-MurNAc pentapeptide to completion (Fig. 1.1, van Heijenoort, 1998, El Zoeiby *et al.*, 2003, Bugg *et al.*, 2011).

2.2.2 Precursor translocation via the lipid II cycle is the bottleneck of cell wall synthesis.

The next steps of the cell wall synthesis involve membrane-anchored lipid intermediates and begins at the inner leaflet of the cytoplasmic membrane, before the peptidoglycan precursors are translocated across the membrane to its outer face (Fig. 1.1). As the membrane-anchored lipid carrier is recycled to take up another peptidoglycan precursor, this stage of the cell wall synthesis is known as the lipid II cycle.

The membrane-anchored lipid carrier: undecaprenyl phosphate

The membrane carrier that accepts the UDP-MurNAc pentapeptide and later translocates it across the membrane is called undecaprenyl phosphate (UP, Fig. 1.1), also known as bactoprenol. UP belongs to the ubiquitous, functionally highly diverse family of isoprenoids (Ogura *et al.*, 1997). The shortest isoprenoid unit is isopentenyl pyrophosphate (IPP), which consists of five carbon atoms and an allylic pyrophosphate group (C_5-PP, IPP). This fundamental building block results from acetyl-CoA via the mevalonate pathway (Thorne & Kodicek, 1966), or the non-mevalonate MEP pathway (Desai *et al.*, 2016). Isoprenoids with longer carbon chains are assembled from IPP via head-to-tail condensation reactions catalysed by prenyl transferases (Ogura *et al.*, 1997). The synthesis of the lipid carrier takes place on the cytoplasmic face of the membrane and is catalysed by the enzyme undecaprenyl pyrophosphate synthase (UppS, Fig. 1.1, Takahashi & Ogura, 1982, Apfel *et al.*, 1999). UppS

catalyses consecutive reactions of a farnesyl pyrophosphate (C_{15}-PP, FPP) with eight IPP units. The resulting undecaprenyl pyrophosphate (C_{55}-PP, UPP) is then dephosphorylated by undecaprenyl phosphatases to produce UP (Manat *et al.*, 2014, Liu & Breukink, 2016).

Lipid I formation

In the first step of the lipid II cycle, the membrane-associated translocase MraY catalyses the ligation of the phosphoryl-MurNAc pentapeptide moiety onto the lipid carrier UP (Fig. 1.1, Bouhss *et al.*, 2004). This results in the formation of undecaprenyl-pyrophosphoryl-MurNAc-pentapeptide, typically referred to as lipid I (van Heijenoort, 1998, Liu & Breukink, 2016).

Lipid II formation

The second step at the inner leaflet of the membrane is the synthesis of undecaprenyl-pyrophosphoryl-1,4-MurNAc-pentapeptide-GlcNAc, better known as lipid II (Fig. 1.1, Liu & Breukink, 2016). The reaction between lipid I and UDP-GlcNAc, the first precursor formed in the cytoplasm, is catalysed by the glycosyltransferase MurG. Lipid II carries the final substrate for the polymerisation of peptidoglycan strands (van Heijenoort, 1998, Manat *et al.*, 2014).

Lipid II translocation

Lipid II is subsequently translocated from the inner side of the membrane to the outer face (Fig. 1.1). The identity of the flippase that is responsible for lipid II translocation has been much-debated (Young, 2014, Ruiz, 2015, Scheffers & Tol, 2015, Zhao *et al.*, 2017). For a while, the SEDS (shape, elongation, division and sporulation) family protein FtsW was believed to be a lipid II flippase (Mohammadi *et al.*, 2011). However, more recent evidence discounted this idea (Sham *et al.*, 2014, Meeske *et al.*, 2015) and supported the original hypothesis proposed by Ruiz (2008). According to these studies, MurJ in *E. coli* and MurJ and its homolog Amj in *Bacillus subtilis* serve as lipid II flippases (Sham *et al.*, 2014, Meeske *et al.*, 2015). Recently, insights into the underlying flipping mechanism emerged. MurJ directly binds lipid II *in vitro*, likely by recognising the GlcNAc-MurNAc-pentapeptide moiety (Bolla *et al.*, 2018). The crystal structure of MurJ in the absence of its substrate revealed 14 transmembrane helices that form a closed-gate, inward-open conformation with a distinct central cavity (Zheng *et al.*, 2018). MurJ was thus proposed to translocate lipid II across the membrane according to an alternating-access mechanism, in which MurJ alternates between an inward-open, then outward-open conformation. Structure-guided cysteine crosslinking indicated that MurJ is able to adopt both conformations, supporting the rocker-switch model for lipid

II transport (Kumar *et al.*, 2018, Zheng *et al.*, 2018). Once on the outer face, the GlcNAc-MurNAc-pentapeptide moiety of lipid II is incorporated into already existing glycan strands as described in 2.2.3.

Lipid carrier recycling

When the GlcNAc-MurNAc-pentapeptide moiety of lipid II is incorporated, the lipid carrier is released as undecaprenyl pyrophosphate (UPP). This is the same pyrophosphate form of the lipid carrier that results from *de novo* synthesis (Manat *et al.*, 2014). To be recycled for membrane translocation of peptidoglycan precursors, UPP is dephosphorylated to UP. This reaction is catalysed by UPP phosphatases (El Ghachi *et al.*, 2005, Manat *et al.*, 2014). In *B. subtilis*, two phosphatases can catalyse this reaction, UppP and BcrC (Bernard *et al.*, 2005, Zhao *et al.*, 2016). Both enzymes are located in the cytoplasmic membrane, but it is currently unknown whether their catalytic activity takes place at the inner or outer face of the membrane. UppP and BcrC form a synthetic lethal pair, which means that one phosphatase becomes essential in the absence of the other, suggesting that their function is interchangeable to some degree (Zhao *et al.*, 2016, Radeck *et al.*, 2017a). Yet, BcrC seems to play a more important role during growth and particularly when facing antimicrobial stress, whereas UppP was found to be crucial for sporulation (Radeck *et al.*, 2017a).

Further, UPP is localised in the outer membrane leaflet, and thus needs to translocate back into its cytoplasmic face (Manat *et al.*, 2014). Not much is known about this reverse flippase reaction. Due to the chemical properties of UP, the translocation of the lipid carrier is thought to be actively facilitated (Zhao *et al.*, 2017). A spontaneous flipping reaction of UP across the membrane is considered too slow for the high turnover rates of the lipid II cycle (de Kruijff *et al.*, 2008). It is further unknown if such a flippase would translocate UP, UPP, or potentially would be able to translocate both forms of the lipid carrier (Manat *et al.*, 2014).

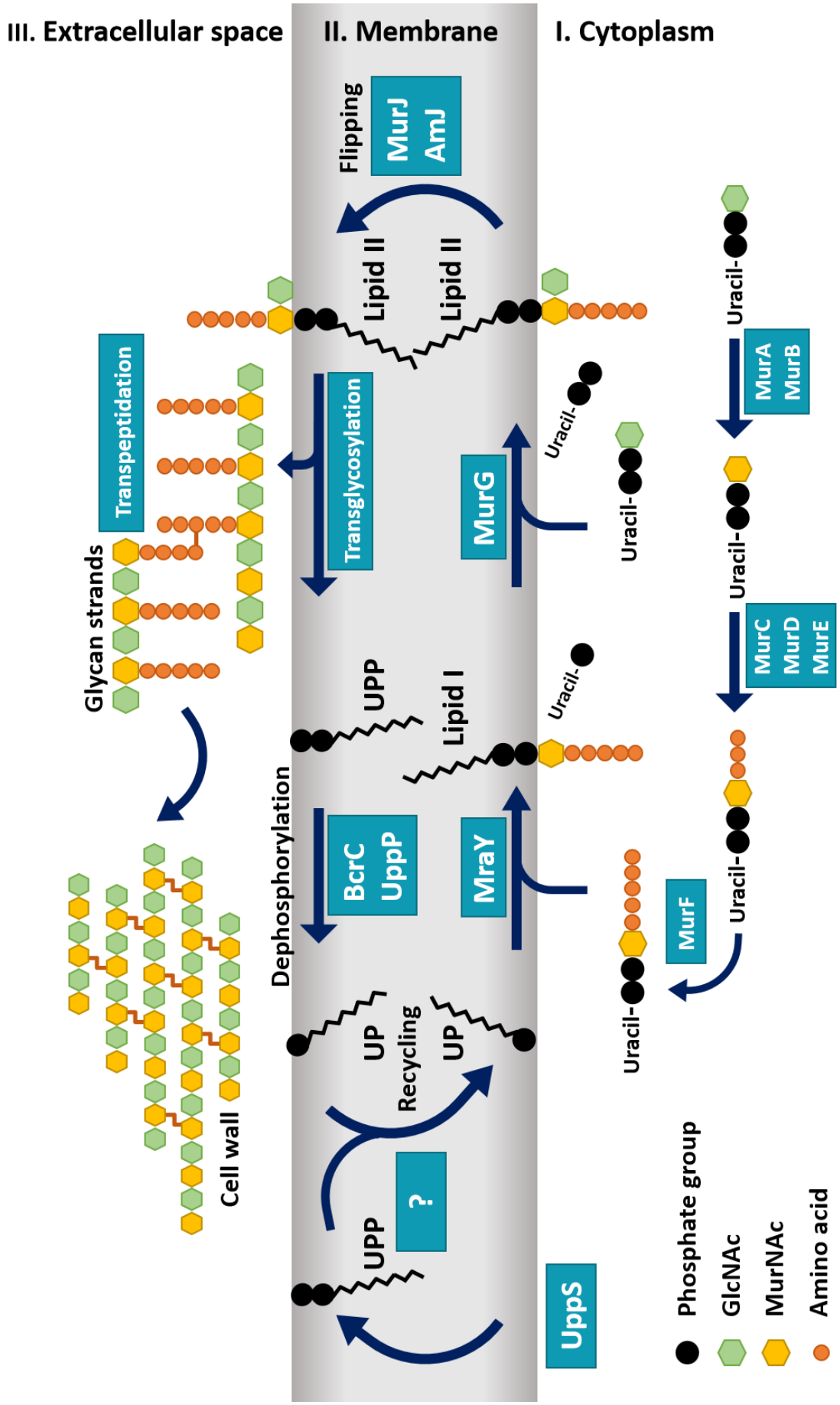
III. Extracellular space
II. Membrane
I. Cytoplasm
Flipping
MurJ
AmJ
Lipid II
Lipid II
Transpeptidation
Transglycosylation
MurG
Uracil-
Uracil-
Uracil-
MurA
MurB
Uracil-
MurC
MurD
MurE
Glycan strands
UPP
Lipid I
Uracil-
Dephosphorylation
BcrC
UppP
MraY
MurF
Uracil-
UP
Recycling
UP
UPP
?
UppS
Cell wall
Phosphate group
GlcNAc
MurNAc
Amino acid

Figure 1.1: The three stages of bacterial cell wall synthesis. I: Cell wall synthesis begins in the cytoplasm with the assembly of peptidoglycan precursors. These precursors are transferred onto membrane-anchored lipid carriers and translocated across the cytoplasmic membrane in the so-called lipid II cycle (II). III: The incorporation of peptidoglycan precursors into the existing glycan strands and the cross-linking between stem peptides takes place in the extracellular space. Glycan strands can be further modified, e.g. by incorporation of wall teichoic acids. These modifications are not depicted in this schematic. The lipid carrier UPP is recycled by dephosphorylation to UP and imported back into the cell. UPP can also be formed by *de novo* synthesis, which is catalysed by UppS. Enzymatic reactions are indicated by enzyme names in turquois boxes, where known. Enzymes involved in transglycosylation and transpeptidation are not listed individually for clarity. Green hexagon: N-acetylglucosamine (GlcNAc), yellow hexagon: N-acetylmuramic acid (MurNAc), black circle: phosphate group, two black circles: pyrophosphate group, orange circle: amino acids that form the stem pentapeptide. UP: undecaprenyl phosphate, UPP: undecaprenyl pyrophosphate, Lipid I: undecaprenyl-pyrophosphoryl-MurNAc-pentapeptide, Lipid II: undecaprenyl-pyrophosphoryl-1,4-MurNAc-pentapeptide-GlcNAc.

The lipid II cycle as bottle neck of cell wall synthesis

Efficient lipid carrier recycling and quick re-introduction into the cell wall synthesis are crucial to ensure growth and cell wall integrity. UP and its derived lipid II cycle intermediates exist only in very limited amounts in bacterial membranes (van Heijenoort, 1998). The lipid II cycle is thus thought to have an extremely high turnover rate, with one to three transits per second per molecule (van Heijenoort, 1998, Breukink & de Kruijff, 2006). The lipid carrier is further involved in other cell wall pathways, like wall teichoic acid synthesis and capsular polysaccharide synthesis (Manat *et al.*, 2014, Liu & Breukink, 2016). The synthesis of the different intermediates is thus tightly regulated and temporally coordinated (Breukink & de Kruijff, 2006, Liu & Breukink, 2016). Nevertheless, the rate-limiting factor seems to remain UP availability.

Direct measurement of these pool levels remains challenging. Hence, indirect measurements like the analysis of *in vivo* peptidoglycan synthesis using radiolabelled UDP-GlcNAc were used to approximate the number of lipid intermediates (Kramer *et al.*, 2004). In *E. coli*, pool levels of UPP are estimated to lie around 1.2×10^5 molecules per cell (Barreteau *et al.*, 2009), the peptidoglycan precursor-carrying lipid I and lipid II are thought to be very small with maximal 700 and 2000 molecules per cell, respectively (van Heijenoort *et al.*, 1992). Further, the ratio between the soluble precursor UDP-MurNAc pentapeptide and lipid I is greater than 100:1 (van Heijenoort, 1998), stressing that the availability of the lipid carrier is the limiting factor of cell wall synthesis.

Pool levels of lipid carrier intermediates seem to vary between bacterial species. The cell wall of Gram-positive bacteria contains higher amount of peptidoglycan. In agreement, the pool levels of lipid carrier intermediates are increased in Gram-positives (van Heijenoort, 2007). *Listeria monocytogenes* and *Micrococcus sp.* were found to contain around 2×10^5 molecules per cell of the lipid carrier forms UP or UPP (Storm & Strominger, 1974, Kramer *et al.*, 2004). *Staphylococcus aureus* was shown to contain maximal 5×10^4 lipid II molecules per cell (van Heijenoort, 2007). In comparison, the rod-shaped *Bacillus subtilis* has even lower lipid II levels (Qiao *et al.*, 2017) and the lipid II levels of *Bacillus megaterium* were estimated to lie around 3.4×10^4 molecules per cell (van Heijenoort, 2007).

The lipid II cycle is therefore considered to be the bottleneck of the cell wall synthesis. Due to low lipid carrier pool levels and high turnover rates, even small discontinuities can lead to major disruptions of cell wall synthesis. The lipid II cycle is thus particularly susceptible to antimicrobial action (Schneider & Sahl, 2010, Bugg *et al.*, 2011). Amongst all enzymes and lipid intermediates involved, lipid II is regarded as the Achilles' heel of the cycle, due to the

particularly small pool size and the (at least at times) localisation at the extracellular face of the membrane. Numerous antibiotics and AMPs have been described to directly recognise and bind lipid II, thereby inhibiting its action (Breukink & de Kruijff, 2006, de Kruijff *et al.*, 2008, Scheffers & Tol, 2015, Ng & Chan, 2016). The group of lanthionine-containing antibiotics (lantibiotics) seem to comprise particularly many lipid II-binding agents and will be discussed in the next main section of the introduction (I 3.1).

2.2.3 Peptidoglycan polymerisation and cross-linking in the extracellular space

The third stage of the cell wall biosynthesis takes place at the outer side of the cytoplasmic membrane and involves the incorporation of the peptidoglycan precursors from lipid II into the growing cell wall mesh via two reactions called transglycosylation and transpeptidation (Fig. 1.1).

The principal enzymes of this stage are penicillin-binding proteins (PBPs) that belong to the family of acyl serine transferases (Scheffers & Pinho, 2005). PBPs can be subdivided into high molecular weight PBPs and low molecular PBPs (Sauvage *et al.*, 2008, Sauvage & Terrak, 2016). The latter are mono-functional peptidases required for transpeptidation. High molecular weight PBPs are composed of two modules. The C-terminal module harbours the penicillin-binding domain, which catalyses the transpeptidase reaction. The N-terminal domain of this type of PBPs links it to the outer face of the cytoplasmic membrane. The catalytic properties of this domain allow the subdivision high molecular weight PBPs further into two major groups, simply termed class A and class B PBPs. While class B PBPs only possess peptidase activity, class A PBPs (aPBPs) are bi-functional enzymes (Scheffers & Pinho, 2005, Sauvage *et al.*, 2008). Their N-terminal module comprises a transglycosylase site, which enables aPBPs to perform both, transglycosylation and transpeptidation (Scheffers & Pinho, 2005, Sauvage *et al.*, 2008).

Transglycosylation: glycan strand formation

In the first extracellular step of cell wall synthesis, the reducing end of MurNAc of a nascent glycan strand is connected with the lipid II-linked GlcNAc-MurNAc-pentapeptide moiety. Hereby, the peptidoglycan precursor gets polymerised into the glycan strand and the lipid carrier is released (Scheffers & Pinho, 2005). Until recently, this step called transglycosylation was known to be performed by two classes of enzymes, mono-functional transglycosylases and aPBPs, with aPBPs considered as the principle transglycosylases (Zhao *et al.*, 2017).

The amount of different aPBPs varies between bacterial species, depending on the availability of proteins with redundant function and cell shape (Scheffers & Pinho, 2005, Sauvage *et al.*, 2008). The Gram-positive model organism *B. subtilis* was shown to possess four aPBPs (PBP1a, PBP4, PBP2c, PBP2d, McPherson & Popham, 2003, Scheffers & Pinho, 2005). Despite some differences in their membrane localisation, these aPBPs seem to be functionally redundant to a certain degree (Pedersen *et al.*, 1999, Scheffers & Pinho, 2005). Recently, the SEDS protein RodA of *B. subtilis* was shown to possess transglycosylase activity (Meeske *et al.*, 2016, Emami *et al.*, 2017). This also answered the long-standing question as to why *B. subtilis* was viable when all aPBPs had been removed, despite the lack of traditional mono-functional transglycosylases (McPherson & Popham, 2003).

Transpeptidation: cross-linking of glycan strands via their stem peptides

During the second step, transpeptidation, the newly built glycan strands are cross-linked via their stem peptides. Peptidases recognise and form a complex with the D-Ala-D-Ala amino acids of the stem peptide. A serine residue in the enzyme's active site interacts with a carbon atom of the terminal D-Ala, which leads to an acyl-enzyme intermediate and the concomitant release of the C-terminal D-Ala residue (Sauvage *et al.*, 2008). This is followed by the deacylation of the enzyme, by which a peptide bond between the penultimate D-Ala residue and the amino acid at position 3 of a different stem peptide (often *meso*-diaminopimelic acid or L-lysine) is formed. The transpeptidation reaction can be mediated by both, bi-functional aPBPs or mono-functional transpeptidases of class B PBP (Scheffers & Pinho, 2005, Sauvage et al., 2008). The peptide bonds cross-link the glycan strands with their neighbouring ones in all directions, resulting in a mesh-like network that is responsible for the shape and rigidity of the bacterial cell (Scheffers & Pinho, 2005, Silhavy et al., 2010).

3. The cell wall synthesis is a major target for antibiotics.

The cytoplasmic membrane and the membrane-embedded cell wall biosynthesis are major targets for numerous classes of antibiotics (Schneider & Sahl, 2010, Mahlapuu *et al.*, 2016). Localised on the extracellular side of the membrane, and thus first in line as antibiotic targets are penicillin-binding proteins (PBPs). PBPs serve as targets for most commercially available β-lactam antibiotics, including cephalosporins, carbapenems, monobactams, and the famous group of penicillins (Sauvage & Terrak, 2016). As the name 'penicillin-binding protein' implies, PBPs can bind to β-lactam antibiotics, because the antibiotics have a high structural similarity to the C-terminal D-Ala-D-Ala moiety of the peptidoglycan stem peptide (Tipper & Strominger, 1965). In doing so, the antibiotics seem to irreversibly bind to the serine residue of the active site of the transpeptidase domain, resulting in inhibition of peptidoglycan cross-linking (Sauvage *et al.*, 2008).

Further, the moenomycin family of antibiotics was shown to inhibit PBP function (Ostash & Walker, 2010). In contrast to penicillins, moenomycin A binds to the enzymatic cavity of the transglycosylase module of bi-functional aPBPs (Lovering *et al.*, 2007). This leads to the blocking of conserved consensus motifs that are important for substrate recognition and thus, prevents cell wall biosynthesis at the step of transglycosylation (Sauvage & Terrak, 2016).

3.1 Lipid II serves as a target for numerous classes of AMPs.

3.1.1 Non-ribosomally synthesized antimicrobial peptides that bind lipid II.

Highly conserved membrane-embedded lipid II cycle intermediates, like lipid II, are also among popular targets of antibiotics, including numerous antimicrobial peptides (AMPs).

AMPs fall into two different classes, based on whether they are synthesised by standard transcription and translation on the ribosome or whether the AMPs are produced non-ribosomally on multi-enzyme complexes (Hancock & Chapple, 1999). The vast class of non-ribosomally synthesized AMPs contains many examples that interfere with lipid II (Breukink & de Kruijff, 2006, Oppedijk *et al.*, 2016). Members of the mannopeptimycins and katanosins AMP subfamilies have been shown to directly interact with lipid II (Ruzin *et al.*, 2004, Lee *et al.*, 2016). Another example is the glycopeptide vancomycin that was shown to bind lipid II at its C-terminal D-Ala-D-Ala moiety (Breukink & de Kruijff, 2006, Wang *et al.*, 2018). Furthermore, the recently discovered teixobactin directly binds to lipid II (Ling *et al.*, 2015).

The lipoglycopeptide ramoplanin was shown to target any variant of lipid II cycle intermediates, as long as they contained a pyrophosphate (Walker *et al.*, 2005).

3.1.2 Ribosomally-synthesised AMPs that target lipid II.

The other major class of antimicrobial peptides are ribosomally-synthesised and often undergo extensive post-translational modifications (Hancock & Chapple, 1999). These modifications lead to the introduction of characteristic features that are often essential for the antimicrobial activity of the AMPs and are used for their further classification (Cotter *et al.*, 2013).

Amongst those heavily-modified AMPs that often interfere with lipid II cycle intermediates is the subgroup of lanthionine-containing antibiotics. These so-called lantibiotics (Schnell *et al.*, 1988) are heat-stable molecules with a molecular weight below 4 kDa that were shown to be active in a nanomolar range (Cotter *et al.*, 2005). Yet, their main distinction from other ribosomally-synthesised AMPs is due to their high content of unusual amino acids, synthesized by extensive post-translational side-chain modifications. The most prominent and name-giving examples are the thioether amino acids lanthionine and β–methyllanthionine (Bierbaum & Sahl, 2009, Cotter *et al.*, 2013). These unusual residues form covalent thioether bridges between amino acids, which result in internal ‘rings’ and give lantibiotics their characteristic structural features (Cotter *et al.*, 2005). Additionally, many lantibiotics contain other rare amino acids, like didehydroalanine or didehydrobutyrine.

Lantibiotics are mainly produced by Gram-positive bacteria of the Firmicutes or Actinomycetes phyla and target other microbes, while the producer is protected by specific immunity mechanisms (Colin *et al.*, 2008, Alkhatib *et al.*, 2012). The activity spectra of lantibiotics are mainly directed against other low-GC content Gram-positive species, including multi-resistant bacterial strains (Dischinger *et al.*, 2014). Numerous lantibiotics are known to directly interact with lipid II (Breukink & de Kruijff, 2006). Yet, the mode of target binding and the mechanism by which certain groups of lantibiotics inhibit the cell wall synthesis differ.

Class I lantibiotics: lipid II binding and subsequent pore formation.

Class I lantibiotics often have a dual mode of action, based on target binding and subsequent pore formation (Wiedemann *et al.*, 2001, Parisot *et al.*, 2008). They can form pores and increase membrane permeability by interacting non-specifically with negatively charged phospholipids or via a highly specific, lipid II-targeted mechanism (Kordel *et al.*, 1989, Brötz *et al.*, 1998b, Breukink & de Kruijff, 2006).

The class I lantibiotic nisin was first described over 90 years ago (Rogers, 1928). Since then it has been studied extensively and is a well-known lantibiotic representative due to its application as a food preservative (Dischinger *et al.*, 2014). Nisin is a 34-residue-long, elongated lantibiotic that is produced by *Lactococcus lactis*. It contains five lanthionine or β-methyllanthionine rings and exhibits an overall positive charge (+5, Fig. 1.2 A, Draper *et al.*, 2015). The lantibiotic is the holotype for other nisin-like lantibiotics, including nisin derivatives and the *B. subtilis* ATCC6633-produced AMP subtilin (Fig. 1.2 B). All nisin-like lantibiotics are very similar in size and charge, and contain several highly conserved and structurally important residues (Dischinger *et al.*, 2014).

At high concentrations, nisin was shown to interact non-specifically with phospholipids of the cytoplasmic membrane, likely due to its highly cationic nature (Wiedemann *et al.*, 2001). In doing so, nisin leads to the deformation the membrane, destabilising membrane curvature, symmetry and lipid packing density and pore formation (Wiedemann *et al.*, 2001, Prince *et al.*, 2016). In addition to these unspecific effects, nisin was shown to specifically interact with lipid II. *In vitro* binding experiments with phospholipids and model membrane vesicles showed that the affinity of nisin for lipid II was much higher (2×10^7 M^{-1}, Breukink *et al.*, 1999) than for membranes containing anionic phospholipids (1.8 × 103 M–1,Breukink *et al.*, 2000). In addition, membrane permeability assays using vesicles with and without lipid II revealed a 1000-fold higher nisin activity in the presence of lipid II (Breukink *et al.*, 1999, Breukink & de Kruijff, 2006).

By binding lipid II, nisin inhibits the sequestration of lipid II to the cell division site and block the cell wall biosynthesis (Wiedemann *et al.*, 2001, Hasper *et al.*, 2006). Nisin recognises and binds to the pyrophosphate group, the MurNAc moiety and the first isoprene unit of lipid II (Hsu *et al.*, 2004). The interaction is mediated via the structurally well-conserved N-terminus. The lanthionine rings A and B of nisin are thought to interact with the pyrophosphate via hydrogen bonds, and in doing so form a pyrophosphate cage which explains why nisin also interacts with lipid I (Fig. 1.2 A). Except for some well-conserved amino acids, the backbone scaffold of the cyclic structures seems to play a more important role than the side chain

composition of nisin (Hsu *et al.*, 2004). The pyrophosphate cage-binding mechanism thus also applies to other lipid II binding class I lantibiotics (Fig. 1.2 A).

Lipid II binding is also the first step towards the second mode of action of this type of lantibiotics: specific lipid II-mediated pore formation (Brötz *et al.*, 1998b, Wiedemann *et al.*, 2001). Once bound, four lipid II-nisin complexes assemble together and recruit four additional nisin molecules (Breukink *et al.*, 2003, Hasper *et al.*, 2004). This very stable 'pore complex' enables nisin to insert perpendicularly into the membrane and span the phospholipid bilayer via its C-terminus (Willey & van der Donk, 2007, Oppedijk *et al.*, 2016). During this process, nisin undergoes drastic conformational changes. Recent studies demonstrated the configuration of the C-terminal and the hinge region between lanthionine ring C and D seem to be particularly flexible and responsive to environmental changes (Fig. 1.2 A), indicating their importance to adapt to the target membrane of a given bacterium (Medeiros-Silva *et al.*, 2018). Pore formation leads to an immediate efflux of cytoplasm followed by rapid cell death (Wiedemann *et al.*, 2001, Hasper *et al.*, 2004).

Class II lantibiotics: inhibition of cell wall biosynthesis by lipid II-binding

Class II lantibiotics usually also target lipid II to inhibit the cell wall synthesis, but they often lack a nisin-like targeted pore formation mechanism. The paradigm of this group is mersacidin. The peptide is a 19 amino acid long lantibiotic, which contains four lanthionine ring structures and is produced by *B. subtilis* HIL Y-85,54728 (Fig. 1.2 C, Bierbaum *et al.*, 1995). Unlike class I lantibiotics, mersacidin is a globular peptide and does not possess a positive net charge. In contrast, a conserved, functionally crucial glutamate residue at position 17 within lanthionine ring C gives mersacidin an anionic net charge (Breukink & de Kruijff, 2006). Structurally similar to mersacidin, also actagardine and its derivatives that are produced by *Actinoplanes liguriae* contain the conserved negatively-charged residue (Fig. 1.2 D, Dischinger *et al.*, 2014). Thus, they were classified as mersacidin-like lantibiotics.

Mersacidin was shown to inhibit the cell wall synthesis at the stage of transglycosylation by binding to lipid II, albeit with a lower affinity than nisin (Brötz *et al.*, 1997, Brötz *et al.*, 1998a). However, this interaction does not lead to pore-formation. As mersacidin binding includes the GlcNAc moiety of lipid II, it specifically recognises lipid II but not lipid I (Oppedijk *et al.*, 2016).

A lipid II-binding motif is conserved in all mersacidin-like lantibiotics, comprising the lanthionine-ring structure around the glutamate residue (Fig. 1.2 C, D, Brötz *et al.*, 1998a). As lipid II is mostly negatively charged, direct charge interactions between mersacidin and lipid

II seem unlikely. Mersacidin-like lantibiotics were found to be more active in a calcium-rich environment (Böttiger *et al.*, 2009). These divalent cations are thought to form a bridge between the glutamate of the peptide and lipid II.

Despite the lack of perpendicular membrane insertion, the conformation of mersacidin was found to be highly flexible and crucial for its antimicrobial activity (Hsu *et al.*, 2003). A small hinge region (Ala-12-Abu-13) allows the lantibiotic to modulate the accessibility of the charged residues upon lipid II binding (Fig. 1.2 C, Hsu *et al.*, 2003). This reinforces the indications that electrostatic interactions play an important role in the lantibiotic-target interaction (Breukink & de Kruijff, 2006, Oppedijk *et al.*, 2016).

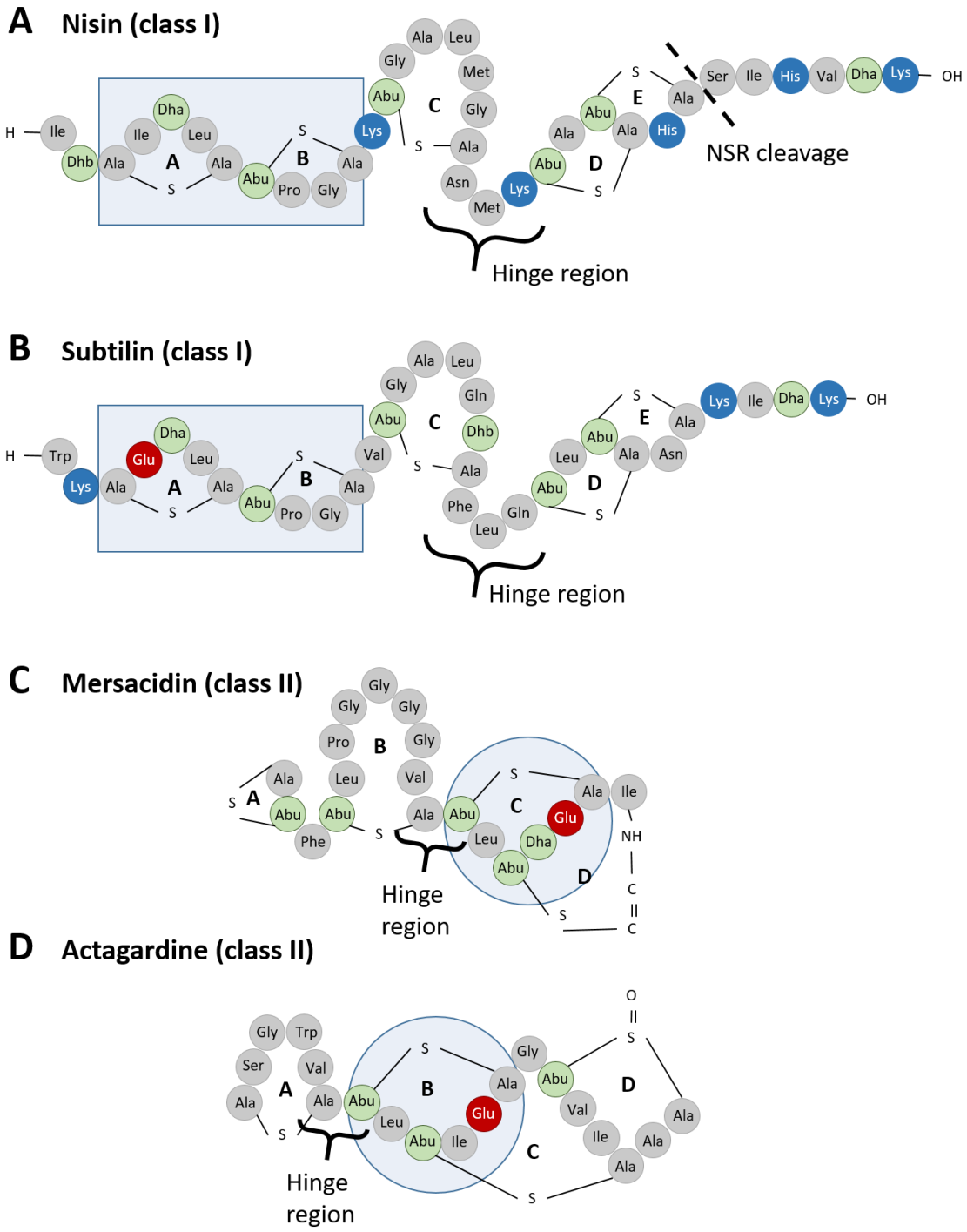
A Nisin (class I)
NSR cleavage
Hinge region
B Subtilin (class I)
Hinge region
C Mersacidin (class II)
Hinge region
D Actagardine (class II)
Hinge region

Figure 1.2: Schematic structures of representative class I and class II lantibiotics that bind lipid II. A: Nisin. **B:** Subtilin. **C:** Mersacidin. **D:** Actagardine. Lanthionine and methyllanthione rings are indicated by letters A-E. Nisin and subtilin share a conserved lipid II binding motif (blue box). Mersacidin and actagardine contain a different conserved lipid II binding motif (blue circle). Hinge regions are indicated for all lantibiotics. The cleavage site of the NSR peptidase is indicated in the nisin molecule (A). Grey: no charge, red: negatively charged, blue: positively charged, green: post-translationally modified amino acids: Dhb: didehydrobutyrine, Dha: didehydroalanine, Abu: aminobutyric acid. Ala: alanine, Gly: glycine, Val: valine, Ser: serine, Leu: leucine, Ile: isoleucine, Pro: proline, Phe: phenylalanine, Tyr: tyrosine, Trp: tryptophan, Met: methionine, Gln: glutamine, Glu: glutamate, His: histidine, Lys: lysine, Asn: asparagine. Figures are based on Willey and van der Donk (2007), Staron *et al.* (2011), Knerr and van der Donk (2012).

3.2 The cyclic dodecapeptide bacitracin targets undecaprenyl pyrophosphate.

The peptide antibiotic bacitracin was shown to disturb the cell wall synthesis by interfering with the lipid carrier intermediates. Yet, bacitracin does not target lipid II, but the lipid carrier in its undecaprenyl pyrophosphate form (Stone & Strominger, 1971).

Bacitracin is a cyclic peptide antibiotic, produced by *B. subtilis* or *B. licheniformis* strains (Johnson *et al.*, 1945). It is active against many Gram-positive bacteria, including pathogens of the *Staphylococcus*, *Streptococcus* and *Clostridium* genera (Ming & Epperson, 2002). It is thus not surprising that bacitracin has been applied in human and veterinary medicine as topical ointment to prevent infection or administered orally against gastrointestinal infections (Ming & Epperson, 2002).

Bacitracin is synthesised by non-ribosomal peptide synthases as mixture of closely related derivatives (bacitracin A, B, D, F and variations thereof), with bacitracin A being the most antimicrobially potent, and the oxidised form, bacitracin F, being the least active (Storm & Strominger, 1973). Bacitracin A consists of twelve amino acid residues (L-Ile$_1$-L-Cys$_2$-L-Leu$_3$-D-Glu$_4$-L-Ile$_5$-L-Lys$_6$-D-Orn$_7$-L-Ile$_8$-D-Phe$_9$-L-His$_{10}$-D-Asp$_{11}$-L-Asn$_{12}$), of which residue 1 and 2 form a thiazoline ring at the N-terminus (Fig. 1.3 A). The condensation of the C-terminal asparagine and the lysine at position 6 results in a lariat-shaped structure, typical for cyclic peptides (Ming & Epperson, 2002).

The antimicrobial activity of bacitracin is based on specifically binding the undecaprenyl pyrophosphate lipid carrier (UPP), and in turn preventing its dephosphorylation (Stone & Strominger, 1971, Storm, 1974). This inhibits the recycling of the lipid carrier and arrests the lipid II cycle. While bacitracin binds UPP and other pyrophosphate-containing isoprenoids with a K_d of around 1 µM, it has much lower affinity to the dephosphorylated form, UP (Storm & Strominger, 1973).

Bacitracin requires divalent metal cations for its antimicrobial activity. Its activity has been shown to increase in the presence of Mg^{2+}, Ca^{2+} and Cu^{2+} ions, amongst others. In complex with Zn^{2+} ions, bacitracin was shown to be in its most active state (Stone & Strominger, 1971). The crystal structure of bacitracin in complex with both, zinc ions and the shorter geranyl pyrophosphate as surrogate for UPP, was solved recently giving an excellent insight into the target recognition and binding (Economou *et al.*, 2013). Bacitracin binds tightly to the pyrophosphate moiety by forming a closed, dome-like structure around it (Fig. 1.3 C). Direct interactions between bacitracin and the phosphate groups of the lipid, as well as indirect interactions mediated via Zn^{2+} and Na^{+} ions were observed. Upon UPP binding, bacitracin

undergoes an extensive conformational change (Economou *et al.*, 2013). Remarkably, target-bound bacitracin has a truly amphipathic configuration, with almost all polar residues interacting with the pyrophosphate group and facing the membrane surface (Fig. 1.3 B). All non-polar residues are buried towards the membrane environment and some of them are thought to interact with the adjacent isoprenoid unit (Economou *et al.*, 2013). The structural insights also give an explanation as to why, in contrast to other antimicrobial peptides, bacitracin does not target lipid II. The sugar and peptide moieties attached to the pyrophosphate are simply too large to fit into the tight amphipathic shell formed by bacitracin (Fig. 1.3 C, Economou *et al.*, 2013).

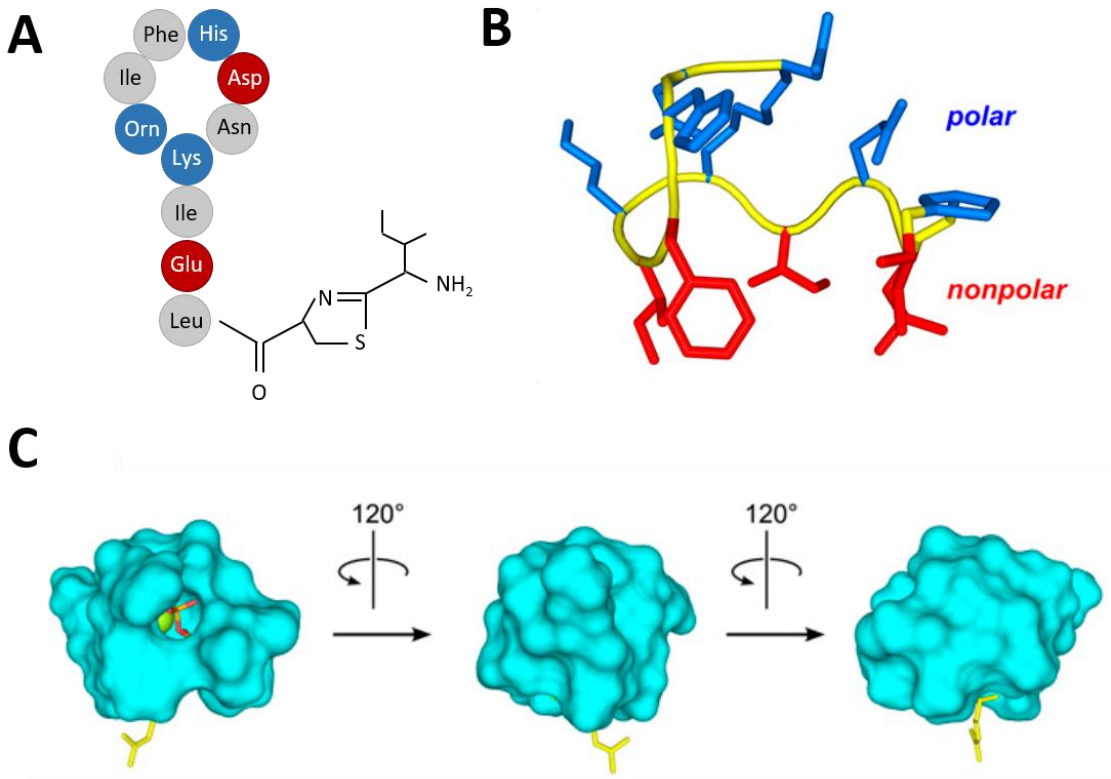

Figure 1.3: Bacitracin adopts an amphipathic configuration upon target binding. A: Schematic structure of bacitracin A, indicating the amino acid residues. Grey: no charge, red: negatively charged, blue: positively charged. Leu: leucine, Glu: glutamate, Ile: isoleucine, Lys: lysine, Orn: ornithine, Phe: phenylalanine, His: histidine, Asp: aspartate, Asn: asparagine. **B:** Amphipathic configuration of bacitracin. The peptide backbone is coloured yellow, hydrophilic side chains are coloured blue, and hydrophobic side chains are coloured red (Economou *et al.*, 2013). **C:** Opaque surface representation of bacitracin bound to geranyl pyrophosphate from different angles. This depiction highlights the almost complete burial of the pyrophosphate group (Economou *et al.*, 2013).

4. Resistance and self-protection against AMPs in Firmicutes

Similar to resistance against other classes of antibiotics, bacteria have evolved different defence strategies to circumvent growth inhibition or even death caused by antimicrobial peptides. Further, the producer strains of AMPs of course need to protect themselves from the antimicrobial action of their products. Among these adaptations are modifications of the cell wall and the cell membrane or the destruction of AMPs. Furthermore, different variants of transporters or specific resistance proteins have been described (Draper *et al.*, 2015, Revilla-Guarinos *et al.*, 2014, Joo *et al.*, 2016). Numerous mechanisms of immunity and resistance against AMPs could be discussed, but the following paragraphs focusses on examples of resistance mechanisms of low GC content Gram-positive bacteria, also known as Firmicutes.

4.1 Modifications of cellular targets to evade AMP action

Modifications of the cellular targets of AMPs can include alterations of membrane charge or fluidity or structural modifications of the targets to avoid interaction with AMPs.

One example of phospholipid modifications is the lysinilation of membrane phospholipids (Peschel *et al.*, 2001). In *S. aureus* and other Gram-positives, the phosphatidylglycerol lysyl-transferase MprF modifies the membrane lipid phosphatidylglycerol with L-lysine, thereby neutralising the anionic net charge of the membrane (Draper *et al.*, 2015). MprF-mediated AMP resistance is thus most likely based on repulsion of cationic AMPs.

Another well-described example is the D-alanylation of lipo- and wall teichoic acids (Neuhaus & Baddiley, 2003, Revilla-Guarinos *et al.*, 2014). Facilitated by the *dltABCD* operon, a D-alanine residue is added onto a free hydroxyl group of the repeating sugars of lipo- and wall teichoic acids (Perego *et al.*, 1995). The D-Ala esterification leads to the incorporation of positive residues into the cell envelope and higher resistance against many cationic AMPs (Draper *et al.*, 2015). Moreover, also vancomycin resistance in several Gram-positive strains is caused by target alteration. These strains contain operons encoding enzymes that are able to modify the stem peptide of lipid II (Courvalin, 2006). In the presence of vancomycin stress, these enzymes are produced and alter the C-terminal D-Ala residue to D-lactate or D-serine. As vancomycin only targets the D-Ala-D-Ala moiety of the lipid II stem peptide (Wang *et al.*, 2018), it has much lower affinity to the modified stem peptide, and thus cannot block the cell wall synthesis anymore (Courvalin, 2006).

Target alteration further plays a role in bacitracin resistance. Bacitracin targets the pyrophosphate moiety of undecaprenyl pyrophosphate (UPP), but has significantly lower affinity to UP (Storm & Strominger, 1973). In *B. subtilis*, the dephosphorylation reaction of UPP to UP is catalysed by the UPP phosphatases BcrC and UppP (Bernard *et al.*, 2005, Zhao *et al.*, 2016, Radeck *et al.*, 2017a). By removing a phosphate group the phosphatases contribute to resistance against bacitracin. To adjust the levels of UPP dephosphorylation, BcrC production is regulated by the extracytoplasmic function (ECF) σ factors, σ^M and σ^X (Cao & Helmann, 2002). In the presence of antimicrobial stress, including bacitracin, the production of BcrC is upregulated, providing additional protection against bacitracin.

4.2 Inactivation or degradation of AMPs in the extracytoplasmic space

While the just described resistance mechanisms focus on modifications of the cellular target, most more specific defence strategies involve a direct interaction with the AMP. In many cases, resistance determinants neutralise the AMP by degradation or inactivation in other ways.

An example for inactivation of an AMP in the extracellular space is the phospholipid-shedding mechanism, observed in Agr-defective *Staphylococcus aureus* mutants, resulting in resistance against the last-resort lipopeptide antibiotic daptomycin (Pader *et al.*, 2016). Daptomycin targets the bacterial cell membrane and leads to inhibition of the cell wall synthesis and decrease of the membrane potential by rearrangement of lipid domains (Muller *et al.*, 2016). In response to daptomycin, *S. aureus* cells are thought to release phospholipids from the membrane that bind daptomycin, and thereby inactivate the antibiotic (Pader *et al.*, 2016).

As an alternative to inactivation via binding the AMPs in the extracellular space, many Gram-positive bacteria produce extracellular proteases that degrade the AMPs by proteolysis. In general, AMP degrading proteases possess a broad substrate range and can either be secreted into the extracellular space or attached to the outer face of the cytoplasmic membrane (Nawrocki *et al.*, 2014).

The nisin resistance protein NSR is an example for peptidases that specifically provide resistance against nisin and potentially also closely-related lantibiotics (Sun *et al.*, 2009). Conserved *nsr* operons are present in various Gram-positive species, including human pathogens (Khosa *et al.*, 2013, Khosa *et al.*, 2016b). NSR is a 35 kDa lipoprotein and anchored

to the cytoplasmic membrane via an N-terminal hydrophobic transmembrane helix (Khosa *et al.*, 2013).

Nisin and other lantibiotics are generally well-protected against proteolysis by their stable lanthionine and methyllanthionine rings. Nevertheless, NSR peptidases that belong to the family of C-terminal processing serine peptidases inactivate the AMPs by degradation. The mechanism of nisin degradation has been revealed for NSR of *Lactococcus lactis* TS1640 (Sun *et al.*, 2009). NSR cleaves the peptide bond between the methyllanthionine residue at position 28 that builds the methyl-lanthionine ring E and the serine at position 29. In doing so, nisin loses its six amino acids-long C-terminal tail, and in turn its antimicrobial potency decreases 100-fold (Sun *et al.*, 2009).

The structure of NSR of *Streptococcus agalactiae* has recently been revealed and showed that NSR forms a central, hydrophobic tunnel, which likely harbours both, the substrate binding domain and the active site required for peptidase activity (Khosa *et al.*, 2016a). The core domain of NSR exhibits a 'TASSAEM' motif, which is highly conserved within the NSR superfamily and contains the catalytically active serine at position 236, facing the inside of the tunnel. The serine residue lies in close vicinity of a conserved histidine residue, and jointly they form the active site responsible for nisin cleavage (Khosa *et al.*, 2016a). A structural model suggests the C-terminal lanthionine rings D and E of nisin to play a major role in substrate recognition as well as for the orientation and accurate positioning of the peptide in the active site of NSR. Accordingly, residues asparagine, methionine and isoleucine at positions 172 to 174 seem to form a hydrophobic pocket to accommodate rings D and E of nisin (Khosa *et al.*, 2016a).

4.3 Transport of AMPs as immunity and resistance strategy

A well-known strategy to mediate resistance against antibiotics as well as AMPs is by transport. In the superfamily of ATP-binding cassette (ABC) transporters, several subgroups contain members involved in either resistance or immunity against AMPs in Firmicutes (Gebhard, 2012). Here, 'resistance' is defined as the protection against exogenously-produced compounds, while 'immunity' describes the self-protection of producer strains against their own product.

4.3.1 LanFEG-type transporters mainly mediate self-protection in lantibiotic producers.

LanFEG transporters consist of two permeases of 200 to 250 amino acids. Each permease comprises six transmembrane helices and is linked to one ATPase (Fig. 1.4 A, Gebhard, 2012). Most of the transporters described in this family are involved in self-protection of producer strains against lantibiotics, and co-produced in the biosynthesis gene cluster of the corresponding lantibiotic (Colin *et al.*, 2008, Alkhatib *et al.*, 2012). Well-studied examples include the immunity to nisin in *L. lactis*, conferred by NisFEG (Stein *et al.*, 2003) and self-protection against subtilin in *B. subtilis* ATCC6633 provided by SpaFEG (Stein *et al.*, 2005). Generally, the substrate specificity of LanFEG transporters was found to be very narrow and specifically directed against the endogenously produced lantibiotic or structurally very closely related derivatives (Gebhard, 2012). The transporter EpiFEG can recognise the highly similar class I lantibiotics epidermin and gallidermin, but does not confer protection against nisin (Otto *et al.*, 1998). Consistently, no cross-immunity has been observed for nisin and subtilin by SpaFEG and NisFEG, respectively (Stein *et al.*, 2003, 2005).

In contrast to immunity-conferring transporters, the transporter CprABC of *Clostridium difficile* is not associated with a biosynthesis cluster typical for lantibiotics, and thus it provides resistance to exogenously-produced antimicrobial peptides rather than self-protection (McBride & Sonenshein, 2011, Gebhard, 2012). Interestingly, the substrate range of CprABC seems to be broader than observed for lantibiotic immunity transporters. CprABC confers resistance to nisin and gallidermin (McBride & Sonenshein, 2011).

The direction of substrate transport has been determined for several LanFEG-type transporters. Studies using peptide release assays or transport studies with fluorescently-labelled lantibiotics concluded unambiguously that the substrate is exported away from the membrane, where the targets of lantibiotics, lipid II cycle intermediates, are located (Otto *et al.*, 1998, Stein *et al.*, 2003, Stein *et al.*, 2005, Okuda *et al.*, 2008).

4.3.2 BcrAB-type transporters are ancestors of LanFEG-type transporters.

BcrAB-like transporters consist of one permease of around 230 amino acids with six predicted transmembrane helices and one ATPase (Fig. 1.4 B, Gebhard, 2012). To be functional, this type of transporters forms an A_2B_2 dimeric transporter. A well-characterised member is BcrAB of *B. licheniformis* ATCC10716, a bacitracin producer strain. The genes encoding BcrAB are clustered within the bacitracin biosynthesis locus (Neumüller *et al.*, 2001). Thus, it is not surprising that BcrAB confers immunity against the antimicrobial peptide bacitracin

(Podlesek *et al.*, 1995, Podlesek *et al.*, 2000). A second characterized transporter is BcrAB of *Enterococcus faecalis* (Manson *et al*., 2004). In this case, BcrAB is not associated with bacitracin production, but confers high levels of resistance against the cyclic peptide in numerous *Enterococcus* species including clinical isolates (Manson *et al.*, 2004, Matos *et al.*, 2009).

The transport mechanism of this group remains elusive. BcrAB of *B. licheniformis* was proposed to act akin to the mammalian multidrug transporter P-glycoprotein, which binds its substrate directly in the hydrophobic membrane environment and expels it from the membrane into the extracellular space (Higgins & Gottesman, 1992, Gottesman & Pastan, 1993, Podlesek *et al.*, 1995). This hypothesis, however, has never been proven experimentally for BcrAB. Experimental evidence for AMP expulsion from the membrane is only available for LanFEG-type transporters that have been shown to descend from BcrAB transporters (Gebhard, 2012). Thus, a similar transport mechanism is likely.

4.3.3 BceAB-like transporters confer resistance against a broader substrate range.

BceAB-like transporters comprise two proteins, one ATPase and one large permease of approximately 650 amino acids (Fig. 1.4 C, Gebhard, 2012). The permease consists of ten predicted transmembrane helices with a large extracellular domain of around 200 amino acids, located between helices 7 and 8 (Fig. 1.4 C). In contrast to other ABC transporters, the permeases of BceAB-like transporters do not further dimerise. Yet, BceB-like permeases possibly form 'pseudo heterodimers' with themselves, as they were found to contain conserved domains (TMH1-4, TMH7-10, Khwaja *et al.*, 2005, Dintner *et al.*, 2014).

BceAB-like transporters are, with some exceptions, not associated with the biosynthesis gene clusters of AMPs (Gebhard, 2012). In contrast to the described LanFEG- and BcrAB-type transporters, BceAB-like transporters were shown to generally possess a broader substrate range by conferring resistance against several AMPs (Gebhard, 2012). The substrates of BceAB-like transporters are often structurally very different from each other and not restricted to the group of lantibiotics, but can also include cyclic peptides, glycopeptides or β-lactam antibiotics. Furthermore, BceAB-like transporters provide protection against defensins and cathelicidins of mammalian origin (Dintner *et al.*, 2011, Gebhard & Mascher, 2011, Staron *et al.*, 2011, Gebhard, 2012).

For this type of transporter, the transport mechanism remains puzzling. Several opposing hypotheses have been proposed, but only a few are supported by direct experimental data

(Ohki *et al.*, 2003, Rietkötter *et al.*, 2008, Kingston *et al.*, 2014, Reiners *et al.*, 2017). Furthermore, the molecular mechanism of substrate recognition and specificity are currently unknown.

The characteristic large extracellular domain of BceAB-like transporters poses a major difference to the domain architectures of the other here described transporters that confer resistance or immunity against AMPs in Firmicutes (Fig. 1.4 C). As BceAB-like transporters showed a much broader substrate range, this extracellular domain could be responsible for substrate recognition and specificity. The extracellular domain was shown to be essential for transporter function (Rietkötter *et al.*, 2008, Coumes-Florens *et al.*, 2011). Further, domain swap experiments between two *S. aureus* transporters led to an exchange of substrate specificity and indicated that the domain was likely responsible for the determination of the substrate specificity (Hiron *et al.*, 2011).

4.4 Sequestration of AMPs by resistance and immunity proteins

In an alternative mechanism to transport, many Gram-positives produce proteins that sequester AMPs in the extracellular space to counteract their antimicrobial effect on the cell surface.

One example of a protein that is secreted into the extracellular environment and confers resistance against AMPs by sequestration is SIC (Streptococcal inhibitor of complement) of *Streptococcus pyogenes* (Neuhaus & Baddiley, 2003). This hydrophilic protein acts by binding AMPs, including α-defensin and LL-37. In doing so, SIC keeps the AMPs away from the membrane, and in turn inhibits their antimicrobial activity against the bacterium (Frick *et al.*, 2003).

Other proteins that bind specific AMPs in the extracytoplasmic space, but are anchored or at least tethered to the membrane, are LanI or LanH immunity proteins. As described before, self-protection against lantibiotics is generally conferred by LanFEG-type ABC transporters. In addition, lantibiotic biosynthesis loci regularly contain genes encoding LanI or LanH lipoproteins (Fig. 1.4 A, Colin *et al.*, 2008, Alkhatib *et al.*, 2012).

4.4.1 The LanI proteins SpaI and NisI directly bind their substrates.

Among the best-described LanI immunity proteins are NisI and SpaI, which protect their corresponding lantibiotic producer strains against nisin or subtilin, respectively. Both proteins mediate some level of immunity when produced in the absence of the LanFEG

transporters, but full protection was only achieved when NisI or SpaI and the cognate immunity transporter were both present (Stein *et al.*, 2003, Stein *et al.*, 2005). As the effect of both immunity determinants was additive, the immunity is thought to be provided by two independent protection mechanisms, rather than by a cooperative mode of action (Stein *et al.*, 2003, 2005).

NisI and SpaI both interact directly with their substrate (Stein *et al.*, 2003, Takala *et al.*, 2004, Stein *et al.*, 2005). They were not shown to modify or degrade the lantibiotic and are thus thought to confer immunity by sequestration of the lantibiotic (Khosa *et al.*, 2016b). Although subtilin and nisin are similar peptides, no cross-immunity against the other lantibiotic is provided by either of the proteins, pointing towards a highly specific mode of substrate recognition. Additionally, the two LanI proteins seem to differ significantly in size and were found to only have little sequence homology (Christ *et al.*, 2012a, Hacker *et al.*, 2015b).

SpaI is a 16.8 kDa lipoprotein that is attached to the surface of the cytoplasmic membrane via a covalent diacylglycerol anchor (Fig. 1.4 A). The positively-charged N-terminus forms a flexible linker between the lipid anchor and the SpaI core domain. When in the membrane environment, the N-terminus is thought to form an amphipathic helix. The structured part of SpaI mainly consists of β-strands and α-helices that assemble to a novel three-dimensional fold. They form a twisted antiparallel β-sheet, which is flanked by an unusually long β-hairpin (Christ *et al.*, 2012a, 2012b).

The exact subtilin binding site of SpaI remains puzzling. Two possibilities have been proposed: a hydrophobic patch surrounded by negatively charged residues facing the periplasm, or the surprisingly negatively charged surface in vicinity to the likewise negatively charged membrane. This anionic surface is thought to bind the overall positively charged subtilin, either by competing with the pyrophosphate moiety of lipid II as alternative target for subtilin or by binding the two positively charged residues within the C-terminus of lipid II-bound subtilin (Christ *et al.*, 2012a, 2012b). In agreement, also the structures of the LanI homologs EntI and EriI revealed this negatively charged surface, indicating it is important for binding the positively charged lantibiotics, entianin and ericin, respectively (Christ *et al.*, 2012a).

NisI consists of two independent domains (12.7 and 14 kDa), connected by a flexible linker (Fig. 1.4 A, Hacker *et al.*, 2015a, Hacker *et al.*, 2015b). Interestingly, the three-dimensional fold of both domains is highly similar to each other, and to the core domain of SpaI. Despite their structural similarity, the two NisI domains possess quite different surface properties. Similar to SpaI, the surface of the N-terminal domain is positively charged and was shown to interact with the membrane. The C-terminal domain of NisI is highly negatively charged, as

is the core region of SpaI. The anionic C-terminal domain was shown to harbour the nisin binding site (Hacker *et al.*, 2015b). The amino acids thought to be responsible for nisin binding are located in proximity to the N-terminal domain and are involved in interaction between the domains in the absence of nisin. NisI binds nisin with a K_d in the micromolar range (Takala *et al.*, 2004). The low-affinity interaction is surprising, considering that nisin has antimicrobial activity in the low nanomolar range. This finding led to the idea that the immunity mechanism of NisI might not be the simple sequestration of nisin from the extracellular environment, but might involve the membrane-anchored target, lipid II (Hacker *et al.*, 2015b). Supporting this argument, a possible lipid II binding site of NisI was determined recently (Jeong & Ha, 2018).

4.4.2 NukH and NukFEG use a cooperative immunity mechanism.

A direct binding interaction between substrate and the extracytoplasmic immunity determinant was also observed for the LanH immunity protein, NukH (Colin *et al.*, 2008). With three predicted transmembrane helices, NukH is located at the cytoplasmic membrane (Fig. 1.4 A), and structurally different from the LanI proteins described above (Okuda *et al.*, 2005). NukH provides protection against the class II lantibiotics nukacin ISK-1 and lacticin 481 and was shown to directly recognise and capture nukacin ISK-1 via its C-terminus (Okuda *et al.*, 2008). Interestingly, NukH in combination with the LanFEG-type transporter NukFEG provided a much higher degree of immunity than the sum of both together, suggesting a cooperative immunity mechanism (Aso *et al.*, 2005). It was thus proposed that NukH acts as substrate binding protein for NukFEG, and that nukacin ISK-1 is being transported away from the membrane by NukFEG after being sequestered by NukH (Okuda *et al.*, 2008).

4.4.3 PepI seems to sequester the cellular target rather than the lantibiotic.

Yet, not all Lan immunity proteins seem to work by sequestration of the lantibiotic (Colin *et al.*, 2008). Immunity of Pep5-producer *Staphylococcus epidermidis* against this class I lantibiotic is solely mediated by PepI, as it has not been found to be associated with a LanFEG-type transporter. PepI is located and functions at the outer face of the cell membrane (Fig. 1.4 A, Reis *et al.*, 1994, Hoffmann *et al.*, 2004). It consists of a hydrophobic, likely membrane-associated N-terminus, and a hydrophilic C-terminus that is essential for mediation of immunity (Fig. 1.4 A, Hoffmann *et al.*, 2004). The C-terminal region contains multiple positively charged residues, which makes it unlikely to directly interact with the likewise cationic Pep5 (Kaletta *et al.*, 1989). Instead, PepI was proposed to bind the cellular target of the lantibiotic, shielding the target from the inhibitory effect of Pep5. The exact target of Pep5 has not yet been determined (Oppedijk, 2017), but it is likely to be an anionic compound of the cell envelope, which could then directly be bound by the positively charged stretches of PepI (Hoffmann *et al.*, 2004, Colin *et al.*, 2008).

While the described LanI and LanH immunity proteins all seem to either sequester the lantibiotic or bind the cellular target to shield it from inhibition by the AMP, their structural and other characteristic features are highly variable and also the immunity mechanisms seem to differ between Lan immunity proteins. These examples demonstrate the enormous variety of resistance and immunity strategies bacteria are able to develop to confer resistance, even against AMPs, the promising candidates for new therapeutics.

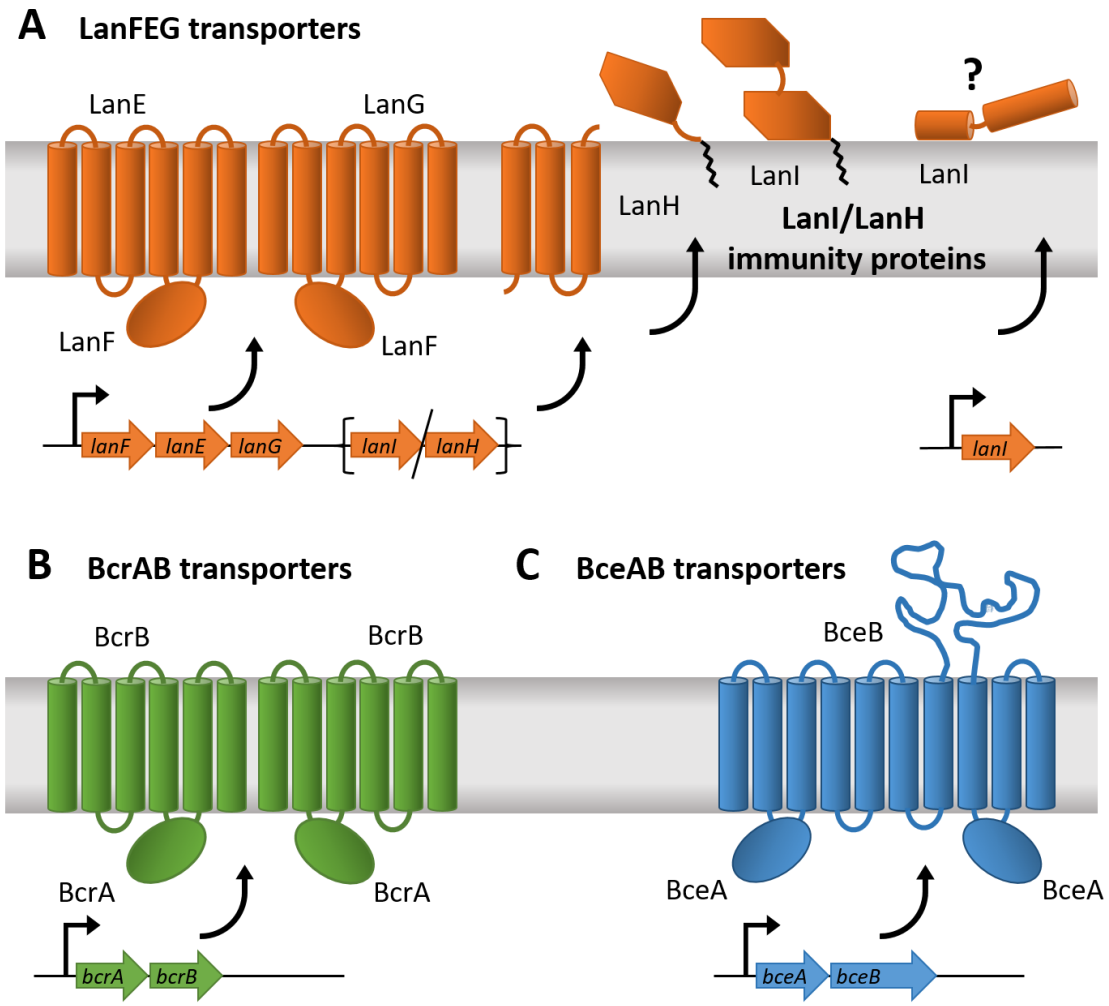

Figure 1.4: Schematic domain architectures of ABC transporters subfamilies that mediate resistance or immunity against AMPs. A: LanFEG-like transporters are encoded in a *lanFEG* operon and are composed of two ATPase units (LanF) and two permeases (LanE and LanG), containing six TMHs each. LanFEG-like transporters are often co-produced with LanI or LanH immunity proteins. These proteins have variable domain architectures with some examples depicted. These immunity proteins are not in all cases associated with LanFEG transporters. **B:** BcrAB-like transporters are encoded in a *bcrAB* operon and are composed of two ATPase units (BcrA) and two permeases (BcrB), containing six TMHs each. **C:** BceAB-like transporters are encoded in a *bceAB* operon and are composed of two ATPase units (BceA) and one permease (BceB), containing ten TMHs. A characteristic large extracellular domain (around 200 amino acids) is located between TMH7 and TMH8.

5. Substrate recognition of regulatory and resistance proteins

It is of great importance to investigate and understand the immunity and resistance mechanisms bacteria already have developed, including the molecular details behind substrate recognition. AMPs can then be modified to escape the resistance determinants, while still maintaining their antimicrobial potency. A recent example is the development of a nisin variant in which the serine residue at position 29 was replaced with a proline. The nisin variant S29P upheld the level of antimicrobial activity against a variety of target strains, and revealed increased activity against strains producing the NSR resistance protein (Field *et al.*, 2018). The reason for the decrease in resistance of the NSR producing strain is that the serine peptidase NSR could not cleave off the six C-terminal amino acids as it requires the serine for this action (Sun *et al.*, 2009). Thus, NSR could not confer its usual level of resistance against nisin S29P.

5.1 How do regulatory proteins sense AMPs in the extracytoplasmic space?

Substrate recognition is the initial step of any resistance mechanism that involves direct interaction with AMPs. Additionally, many resistance determinants are regulated by sensory proteins, which can perceive their stimulus by direct binding of the AMPs, and subsequently facilitate the production of the resistance determinant. This task is often performed by two-component regulatory systems, comprising a sensor kinase and a response regulator, or regulators that combine both functions in a single protein. When stimulus perception and signal transfer of these regulatory proteins are impaired, the response of bacteria against antimicrobial stress cannot be upregulated, leaving the cell vulnerable. Understanding the mechanistic details of substrate recognition of regulatory proteins is thus as important as understanding the resistance mechanism itself. As most AMPs target the cell envelope of bacteria, the following focusses on stimulus perception in the extracytoplasmic space or membrane interface.

5.1.1 Prototypical periplasmic-sensing histidine kinases detect AMPs via an extracytoplasmic domain.

Many LanFEG-type transporters like NisFEG or SpaFEG are associated with and their production regulated by LanRK systems (NisRK and SpaRK, respectively, Alkhatib *et al.*, 2012). The sensor kinases LanK have been shown to act by auto-inducing lantibiotic biosynthesis and immunity in response to the extracellular lantibiotic itself (Kleerebezem, 2004, Gebhard, 2012). The induction of LanK is highly-specific to the corresponding lantibiotic, and with detection of the lantibiotic in the picomolar range, also highly sensitive (Kuipers *et al.*, 1995). LanK kinases are classified as prototypical periplasmic-sensing histidine kinases (Mascher *et al.*, 2006, Gebhard, 2012). The N-terminal stimulus-perceiving input domain of these kinases consists of two transmembrane helices, connected via a 50 to 300 amino acid-long extracytoplasmic domain. Their C-terminal cytoplasmic transmitter domain contains a conserved histidine residue for autophosphorylation, followed by the highly conserved catalytic domain (Mascher *et al.*, 2006). The extracellular domain has been shown to be important for substrate recognition and specificity by domain swap experiments between SpaFEG and NisFEG (Kleerebezem, 2004). The domains are thought to directly bind the lantibiotic, but the details behind the binding mechanism remain enigmatic (Kleerebezem, 2004).

The related prototypical periplasmic-sensing histidine kinase PhoQ is involved in regulation of antimicrobial peptide resistance in many Gram-negative bacteria (Bader *et al.*, 2005, Mascher *et al.*, 2006). The substrate binding mechanism of PhoQ, mediated by its periplasmic sensory domain, is well-understood and serves as example of substrate recognition of AMP-sensing kinases. PhoQ is activated by low concentrations of cations and upon increasing concentrations of various AMPs, yet is repressed when divalent cations are abundant in high amounts (Bader *et al.*, 2005). The periplasmic sensory domain of PhoQ does not contain a cavity or discrete binding pocket for substrate binding, but a rather flat and negatively charged surface on one side of the protein. This anionic surface is located in close proximity to the likewise negatively charged cytoplasmic membrane. In its repressed state, the sensory domain of PhoQ is tethered to the membrane by ionic interactions mediated by divalent cations (Bader *et al.*, 2005). Recognition of cationic AMPs that often target the cell membrane disrupt the bond between the membrane and the kinase domain, as does the decrease of cations to low levels. As a result, the periplasmic domain is lifted off the negatively charged membrane. The concomitant structural rearrangement is transmitted via the

transmembrane helices and ultimately results in auto-phosphorylation of PhoQ and subsequent signal transfer (Bader *et al.*, 2005, Mascher *et al.*, 2006).

5.1.2 The formation of hydrophobic pockets allows substrate recognition in the membrane.

Two-component regulatory systems containing kinases that lack such periplasmic sensory domains often perceive the stimulus at or within the membrane interface (Mascher et al., 2006). In the phylum of Firmicutes, several types of such 'intramembrane'-sensing kinases were found to be involved in AMP sensing (Gebhard, 2012). These kinases can be responsible for regulation of resistance determinants (I 6.2). However, some examples instead regulate AMP production, often by a quorum sensing regulatory mechanism.

Quorum sensing-based systems enable communication within a bacterial species, which is used to coordinate their collective behaviour (Miller & Bassler, 2001). The involved histidine kinases are thus classified as peptide quorum sensor kinases and contain six transmembrane helices, but lack a prominent extracellular domain (Mascher et al., 2006). When a certain threshold concentration of AMPs in the extracellular environment is reached, the corresponding kinase can detect them. Stimulus detection by these quorum sensor kinases involve substrate binding and recognition in the membrane environment. The transmembrane helices of such kinases form a hydrophobic pocket between them, in which a first non-sequence specific interaction with the substrate takes place. Subsequently, a sequence-specific interaction with one of the kinase's extracellular loops triggers the signalling cascade (Mascher *et al.*, 2006, Gebhard, 2012). Via the cognate response regulator, AMP production is upregulated, which ultimately results in a positive feedback loop (Mascher *et al.*, 2006).

In multiple cases, the production of antibiotic resistance is regulated by members of the xenobiotic response elements (XRE) regulator family, which include DNA-binding transcriptional regulators containing a helix–turn–helix motif (Gebhard, 2012). Bacitracin resistance of *E. faecalis* conferred by BcrAB, for example, is regulated by such a one-component regulatory system. The transcriptional repressor BcrR is responsible for both, direct stimulus perception and signal transfer to the DNA-binding domain, which then facilitates the appropriate response to counteract the antimicrobial stress (Manson *et al.*, 2004, Gebhard *et al.*, 2009). The N-terminus of BcrR contains the DNA binding domain. This region of BcrR was shown to be constitutively bound to two inverted repeat regions of the

bcrA promotor DNA *in vitro*, irrespectively of the presence or absence of the stressor (Gauntlett *et al.*, 2008). The C-terminus is located in the cytoplasmic membrane and predicted to comprise four transmembrane helices, but lacks longer extracellular domains (Gauntlett *et al.*, 2008). BcrR thus seems to be associated with its target DNA while localised in the membrane. This would require the respective DNA locus to be pulled towards the cell membrane. Yet this hypothesis has not been addressed further.

BcrR was shown to directly bind the AMP bacitracin when it is in complex with Zn^{2+} ions (Gebhard *et al.*, 2009). As bacitracin is unlikely to be imported into the cell due to its amphipathic nature, and because of BcrR's lack of obvious input domains, bacitracin binding was suggested to potentially take place at the membrane interface (Gebhard *et al.*, 2009). In agreement, a recent study suggested the putative bacitracin binding site in the second extracellular loop of the C-terminal transmembrane domain (Darnell *et al.*, 2019). Further investigations are required to shed light on the details of the binding interaction between BcrR and bacitracin. Yet, also here substrate recognition in a hydrophobic pocket, formed between membrane-spanning helices, seems plausible.

5.2 How do transporters recognise and bind AMPs in the extracytoplasmic space?

On the grounds of recent structural studies, we have gained valuable insights into the substrate recognition of LanI-type immunity proteins (I 4.4.1) and other resistance proteins (I 5.1, Christ *et al.*, 2012a, Hacker *et al.*, 2015b, Khosa *et al.*, 2016a, Jeong & Ha, 2018). However, little is known about how the resistance transporters described above recognise and bind their substrates in the extracytoplasmic environment, nor about which factors influence substrate specificity or binding affinity. Similar to prototypical periplasmic-sensing kinases, extracytoplasmic domains also seem to play an important role in substrate recognition and specificity of other resistance transporters.

5.2.1 The periplasmic domains of RND-type multi-drug efflux pumps harbour the substrate binding sites.

A well-described example is the resistance-nodulation-division (RND)-type multidrug efflux pump AcrB of *E. coli* (Pos, 2009, Du *et al.*, 2018). *acrB* encodes a membrane-embedded transporter that forms a tripartite efflux pump by interacting with the periplasmic adapter protein AcrA (Murakami *et al.*, 2002). The adapter molecule in turn stabilises the interaction with the outer membrane channel TolC, granting efflux across the outer membrane. Characteristically for multidrug pumps, AcrAB confers resistance against a vast number of lipophilic and amphipathic molecules including drugs, dyes and detergents (Elkins & Nikaido, 2002). Conversely, the RND-family multidrug efflux pump AcrD has a fairly narrow substrate range and transports mainly hydrophilic substrates like aminoglycosides (Aires & Nikaido, 2005).

Both efflux pumps possess two characteristic large extracellular domains per protomer (Elkins & Nikaido, 2002). In domain swap experiments, in which the periplasmic loops of AcrB and AcrD were exchanged, Elkins and colleagues (2002) demonstrated that $AcrD^{loop(AcrB)}$ acquired the broader AcrB-like substrate specificity, while the substrate range of $AcrB^{loop(AcrD)}$ narrowed down to substrates characteristic for AcrD, confirming that the periplasmic loops were responsible for substrate specificity in RND-type multidrug efflux pumps.

The periplasmic loops of AcrB form a so-called ‘pore’ domain on top of the central cavity that is located between the transmembrane domains (Murakami *et al.*, 2002). The four subdomains of the pore harbour the main substrate binding sites. Access to these binding pockets is possible through several channel pathways, allowing the transporter to bind substrates directly from the periplasm, the periplasm-membrane interface or through the central cavity (Aires & Nikaido, 2005, Zwama *et al.*, 2018). Proximal and distal binding pockets of this highly flexible domain are equipped with various polar, aromatic and hydrophobic residues, which makes them eminently suitable for binding a wide range of substrates (Nakashima *et al.*, 2011). Conformational changes driven by the proton-motive force lead to substrate extrusion to the extracellular space via a funnel-like structure and the outer membrane channel TolC (Pos, 2009, Du *et al.*, 2018), and thus to resistance against the transported molecule. The pore domain of the AcrB transporter is an excellent example for extracytoplasmic substrate binding domains that recognise substrates located in the membrane and feature a broad substrate range due their conformational flexibility.

5.2.2. Extracytoplasmic domains of ABC transporters are important for substrate interactions.

Stressing their importance in substrate recognition and binding even further, extracytoplasmic binding domains are also important in ATP-binding cassette (ABC) transporters, which are closer related to the AMP resistance and immunity transporters described above (I 4.3).

The ABC transporter MacB is known to form a tripartite efflux pumps with its adapter molecule MacA and the outer membrane channel TolC in various Gram-negative bacteria (Rouquette-Loughlin *et al.*, 2005, Fitzpatrick *et al.*, 2017, Crow *et al.*, 2017, Okada *et al.*, 2017). With only four transmembrane helices and dimerisation instead of trimer formation, MacB has a very different membrane architecture to AcrB-type tripartite efflux pumps described above. Further, MacB contains only one large periplasmic domain between TMH1 and TMH2. MacB confers resistance against macrolide antibiotics like erythromycin (Kobayashi *et al.*, 2001) and is involved in secretion of enterotoxins (Yamanaka *et al.*, 2008). Recently, MacB was also shown to mediate resistance against the AMPs bacitracin and colistin (Crow *et al.*, 2017). Extensive site-directed mutagenesis revealed a cluster of mutations in the periplasmic domain that reduced antibiotic resistance to erythromycin as well as bacitracin and colistin *in vivo*. The mutation of eight polar and aromatic residues that lie in close proximity to each other and are located at the interior interface of the dimeric periplasmic domains had the most prominent effect on antibiotic resistance (Crow *et al.*, 2017). This region was therefore concluded to play a role in substrate recognition and binding. ATP-dependent dimerisation of the nucleotide binding domains (NBD) of MacB induces the opening and closing of the periplasmic domains via conformational changes of the transmembrane segments (Crow *et al.*, 2017). By this, the substrate is thought to be extruded from its binding domains into the extracellular space, via the MacA-TolC efflux duct.

Yet, extracytoplasmic domains are not only involved in AMP recognition and binding. LolCDE is an ABC transporter comprising a homodimer of the ATPase subunit LolD and one of each membrane-located proteins LolC and LolE forming a heterodimer (Yakushi *et al.*, 2000). LolC and LolE both possess four transmembrane helices with a large extracellular domain between TMH1 and TMH2. In contrast to MacB, LolCDE does not form a tripartite drug efflux pump. Instead, LolCDE is crucial for the extraction of lipoproteins that are specific for the outer membrane of Gram-negative bacteria from the cytoplasmic membrane (Yakushi *et al.*, 2000, Narita & Tokuda, 2017). Substrate binding of particular lipoproteins by LolCE was shown to

take place in the outer leaflet of the inner membrane. While the exact mechanism is controversial (Okuda & Tokuda, 2009, Mizutani *et al.*, 2013, Crow *et al.*, 2017), it is known that the hydrophobic lipoprotein is passed on to the periplasmic chaperone LolA (Taniguchi & Tokuda, 2008). The lipoprotein is then transferred to LolB, which facilitates its incorporation into the outer membrane. The recently determined structure of the periplasmic domain of LolC revealed a similar fold to the MacB substrate binding domain (Crow *et al.*, 2017). Further, ATP binding by LolD, but not its hydrolysis, was shown to release the substrate from the LolCDE-substrate complex (Ito *et al.*, 2006, Narita & Tokuda, 2006). These analogies to MacB suggest a similar role of the periplasmic domains in substrate binding and similarities in the transport mechanism.

Moreover, FtsEX is a widely conserved protein among bacteria. Although it possesses an ABC transporter-like structure (Schmidt *et al.*, 2004), FtsEX does not seem to play a role in drug efflux or substrate transfer. Its responsibility revolves around the coordination of peptidoglycan hydrolysis with cell division in numerous Gram-positive and Gram-negative bacteria (Yang *et al.*, 2011, Sham *et al.*, 2013, Meisner *et al.*, 2013, Mavrici *et al.*, 2014) or sporulation initiation in *B. subtilis* (Garti-Levi *et al.*, 2008). FtsX contains a large extracytoplasmic loop, located between TMH1 and TMH2 of its four transmembrane helices. Several *in vitro* and *in vivo* studies of FtsX of various bacteria have shown that this domain directly interacts with its respective binding partner, proteins involved in peptidoglycan hydrolysis (Yang *et al.*, 2011, Sham *et al.*, 2013, Mavrici *et al.*, 2014). Structures of FtsX of *Mycobacterium tuberculosis* revealed that the extracellular domain forms two flexible lobes with a hydrophobic cleft between them (Mavrici *et al.*, 2014). Exposing four phenylalanine residues, the cleft was proposed to be the interaction site with the binding partner. Due to flexible hinge regions, the domain can acquire different conformations, thereby opening and closing the cleft (Mavrici *et al.*, 2014). The signal inducing the structural readjustment to an activated state of FtsX is thought to be passed on from the ATPase FtsE (Mavrici *et al.*, 2014).

6. The Bce system of *B. subtilis* is the paradigm for AMP resistance in Firmicutes.

6.1 The Bce-like systems of the Gram-positive model organism *B. subtilis*

To gain further insights into the substrate specificity of ABC transporters in Firmicutes and to ultimately elucidate their resistance mechanism against AMPs, we here focus on investigations on a resistance system of *Bacillus subtilis* 168 (from here onwards referred to as *B. subtilis*, if not further specified).

B. subtilis serves as model organism of the phylum of low-GC content Gram-positive bacteria. The rod-shaped, soil-dwelling organism is amongst the best-characterised prokaryotes with regards to molecular and cell biology (Graumann, 2007). *B. subtilis* is non-pathogenic, and thus safe to work with, while closely related *Bacillus* species like *B. cereus* or *B. anthracis* are the cause of food-borne illness or anthrax, respectively. Full genome sequences (Kunst *et al.*, 1997, Barbe *et al.*, 2009), and lists of essential genes and correlating gene deletion libraries of non-essential genes are available (Kobayashi *et al.*, 2003, Peters *et al.*, 2016, Koo *et al.*, 2017), as well as databases from other systems approaches (Moszer *et al.*, 2002, Michna *et al.*, 2014, Zhu & Stulke, 2018). Several ever-developing vector systems and toolboxes have been established for *B. subtilis*, facilitating molecular work (Radeck *et al.*, 2013, Popp *et al.*, 2017, Radeck *et al.*, 2017b, Liu *et al.*, 2018). *B. subtilis* has thus also drawn attention as a chassis for synthetic biology approaches and as workhorse in biotechnology. Over decades, endless studies have shed light on the physiology, metabolic processes and the numerous differentiation strategies of *B. subtilis*, which include sporulation, cannibalism and competence (Lopez & Kolter, 2010). It is thus not surprising that also the resistance against AMPs via BceAB-like resistance transporters is best understood in *B. subtilis*.

Three AMP sensing and resistance transporters of this type were found in *B. subtilis.* The YxdLM transporter is induced by the cathelicidin LL-37, while PsdAB mainly responds to lantibiotics, including nisin, subtilin, gallidermin and actagardine, but also the non-lantibiotic enduracidin (Staron *et al.*, 2011). The name-giving paradigm of these transporters is BceAB, which senses and confers resistance against mersacidin, actagardine and the fungal AMP plectasin (Staron *et al.*, 2011). Yet, the transporter is mainly known to act as the primary resistance determinant in the bacitracin resistance network of *B. subtilis* (Radeck *et al.*, 2016b).

6.2 The flux-sensing mechanism of BceAB-BceRS ensures need-based supply of resistance.

Production of BceAB-like transporters is regulated via two-component regulatory systems. More than 200 BceAB-like transporters were found to be associated with such systems, consisting of a BceS-like histidine kinase and a BceR-like response regulator (Dintner *et al.*, 2011). A phylogenetic analysis classified BceB-like permeases and BceS-like kinases and revealed that they have co-evolved to form unique, self-sufficient resistance systems against AMPs in Firmicutes bacteria (Dintner *et al.*, 2011). Yet, the distribution of resistance systems into phylogenetic groups did not allow further predictions of the function or substrate range of uncharacterised transporters, neither did the sequence analysis of their extracellular domains (Dintner *et al.*, 2011).

Signalling within the BceAB-BceRS system of *B. subtilis* operates according to a flux sensing mechanism (Fritz *et al.*, 2015). The transmembrane segment of BceS-like kinases consists of two transmembrane helices, but lacks an obvious extracellular input domain (Mascher *et al.*, 2006). Classified as 'intramembrane' sensing histidine kinase, BceS cannot perceive the stimulus directly (Mascher *et al.*, 2006, Mascher, 2014). Its N-terminus instead acts as a signal transfer domain. Even in the absence of antimicrobial stress, the kinase BceS interacts directly with the transport permease BceB, forming a sensory complex for the detection of AMPs (Dintner *et al.*, 2014). As BceB was shown to directly bind bacitracin *in vitro,* the transporter is thought to have dual function and acts as both, the true sensor of AMPs as well as the resistance-mediating determinant against them (Dintner *et al.*, 2014).

In this novel way of sensing, the monitored parameter is the transport activity of BceAB resistance transporters. BceAB acts as a 'flux sensor', which passes information on its current transport rate on to the kinase BceS, rather than sensing the antibiotic concentration or downstream effects on the bacterial physiology (Fritz *et al.*, 2015). BceAB transmits the signal onto BceS, which leads to intramolecular signal conversion and enables the ATP-dependent auto-phosphorylation of the highly conserved histidine residue of the kinase (Mascher, 2014).

Subsequently, the phosphate group is transferred onto an aspartate residue of the cognate response regulator BceR, which in turn binds to its target promotor P_{bceA}. By this, expression of the *bceAB* operon is initiated and the ABC transporter BceAB is produced and incorporated into the cell membrane. This flux sensing mechanism allows the cell to constantly assess its current detoxification capacity and cost-efficiently adjust its level of transporter *de novo*

synthesis to the required level of protection (Fritz *et al.*, 2015). The BceAB-BceRS system is the paradigm for more than 200 systems (Dintner *et al.*, 2011) and recently other BceS-like kinases have been found to directly interact with their associated transporters (Randall *et al.*, 2018). It is thus likely that this type of signalling is wide spread in the regulation of antimicrobial resistance among the phylum of Firmicutes.

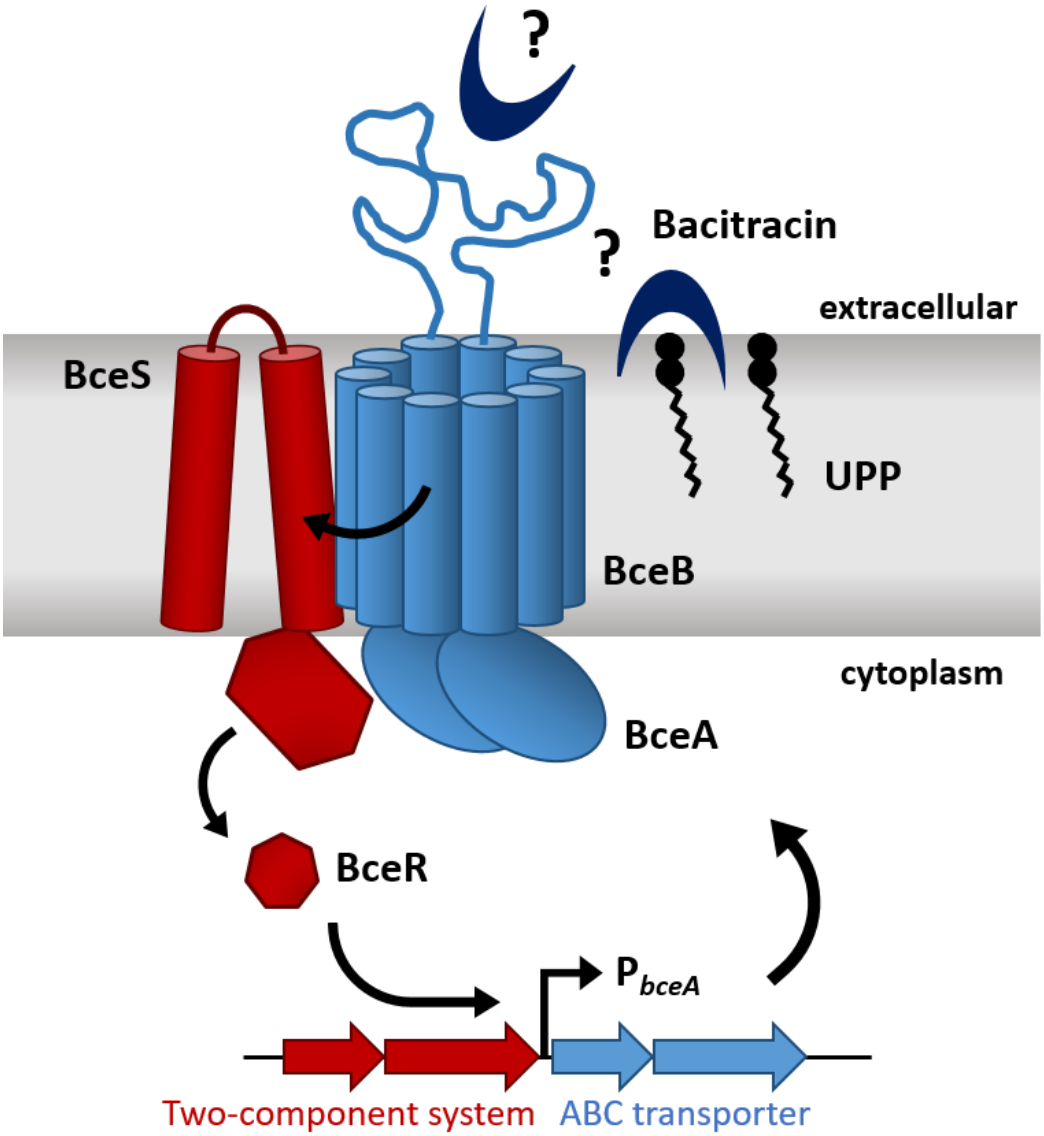

Figure 1.5: The BceAB-BceRS resistance system operates according to a flux-sensing mechanism. The schematic depicts the auto-regulation of the BceAB-BceRS system. The transporter BceAB (blue) and the histidine kinase BceS (red) form a sensory complex in the membrane (grey). BceAB acts as flux sensor and perceives the stimulus by a not yet understood mechanism (question mark). BceAB passes the signal on to BceS, which in turn triggers a signal cascade and activates its cognate response regulator BceR (red). BceR binds to the P_{bceA} promotor region and activates transcription of *bceAB* (operon indicated by black and blue arrows), resulting in adjusted resistance levels. Dark blue crescent: bacitracin, UPP: undecaprenyl pyrophosphate. Arrows indicate the signal transfer and *de novo* production of BceAB.

6.3 The resistance mechanism and substrate specificity of BceAB remain unclear.

While the insights into the communication between BceB and BceS taught us a lot about the regulation of BceAB-like transporters, the mechanism of resistance is not yet understood. Several different hypotheses have been proposed, which range from BceAB acting as an importer that internalises the AMP for degradation to BceAB exporting the AMP (Ohki *et al.*, 2003, Rietkötter *et al.*, 2008). Recently, first indications were obtained that another BceAB-like system might confer resistance by expulsion of the AMP away from the membrane into the extracellular space (Reiners *et al.*, 2017). If and how such a mechanism could effectively provide protection from antimicrobial action has been subject to debate.

It is further not known how the resistance transporters recognises or binds its substrate, and which features allow them to distinguish between them. While many BceAB-like systems are known to confer resistance against several AMPs, the basis of their substrate specificity remains elusive, with no pattern detected or prediction possible so far.

The PsdAB-PsdRS system of *B. subtilis* is, for example, able to recognise structurally different AMPs like the lantibiotic nisin and the lipoglycopeptide enduracidin, but not ramoplanin, which is closely related to enduracidin (Gebhard & Mascher, 2011, Staron *et al.*, 2011). PsdAB further confers resistance against actagardine, but not mersacidin, which is structurally very similar to actagardine. Within the same bacterial strain, however, BceAB recognises both, actagardine and mersacidin, but is not induced by nisin. Then again, BceAB also provides protection against bacitracin, which even targets a different molecule in the cell (Gebhard & Mascher, 2011, Staron *et al.*, 2011). In contrast, a BceAB-like transporter of *S. aureus* has been found to mediate resistance against both, bacitracin and nisin (Hiron *et al.*, 2011).

To add to the confusion, it has been proposed that the transporter might not actually use the AMP as its physiological substrate. Instead, the transporter may import the cellular target of AMPs (Kingston *et al.*, 2014), or was suggested to recognise the AMP in complex with its cellular target only (Mascher *et al.*, 2003, Bernard *et al.*, 2007).

Extracytoplasmic domains often seem to play a key role in substrate recognition by kinases and resistance transporters that sense membrane-targeting AMPs. Due to its exposed location at the extracellular face of the membrane and its requirement for bacitracin sensing and resistance, the large extracellular domain of BceAB was proposed as potential binding domain (Rietkötter *et al.*, 2008, Coumes-Florens *et al.*, 2011). In *S. aureus*, this domain was shown to be responsible for the substrate specificity (Hiron *et al.*, 2011). Yet, sequence analysis of all known extracellular domains did not reveal any correlations to a certain

substrate specificity (Dintner *et al.*, 2011). Hence, the molecular bases and mechanisms behind substrate specificity and AMP binding remain unclear.

The goal of this study was to understand the substrate specificity of BceAB and to test the role of its extracellular domain as the substrate binding domain. We also aimed to identify the true physiological substrate of BceAB. In doing so, we hope to shed light onto the controversies around the mechanism of the AMP resistance transporter BceAB.

7. Aims and objectives of this study

The overall aim of my PhD project was to explore the substrate specificity of the antimicrobial resistance transporter BceAB of *B. subtilis*. Deciphering the underlying substrate specificity and recognition is enormously valuable to ultimately understand the resistance mechanism by which BceAB-like transporters confer resistance against AMPs. This knowledge can be used as a stepping stone to develop AMPs that are able to escape this type of resistance determinant as future therapeutics. The development of potent antimicrobial agents combined with tighter regulations of their use is crucial to counteract the emerging antimicrobial crisis, and to implement and secure global health.

As we here investigate the substrate specificity of BceAB using both *in vitro* and *in vivo* approaches, the study was divided into two main sections, based on the nature of the experiments involved.

7.1 *In vitro* characterisation of the binding capacity of BceB-ECD

In the first part of this study, we focussed on the characterisation of the binding capacity of the putative binding domain of BceAB, its large extracellular domain (ECD). To this end, we used *in vitro* biochemical and biophysical techniques. The main objectives were:

- To gain further insights into the predicted structural features and potential substrate binding sites by conducting an *in silico* analysis of BceB-ECD.
- To facilitate the *in vitro* characterisation of BceB-ECD by establishing an optimised protocol for the overproduction and purification of this domain.
- To examine the substrate binding ability of isolated and purified BceB-ECD *in vitro* by using biophysical approaches.
- To investigate the substrate specificity and binding affinities of BceB-ECD for several antimicrobial peptides, as well as their cellular targets or surrogates thereof.

7.2 *In vivo* determination of the physiological substrate of BceAB

In the second part of this study, we aimed to identify the physiological substrate of BceAB using *in vivo* approaches. To this end, we had the following objectives:

- To examine the effect of BceAB on growth of *B. subtilis* and whether the transporter has an affinity to undecaprenyl pyrophosphate by performing growth and competition assays in the presence of different levels of BceAB.
- To determine the variables that lead to changes in BceAB transport activity by using a P_{bceA} luminescence reporter assay as proxy for transport activity and monitoring its response to varying concentrations of antimicrobial peptides, alterations of the amounts of cellular targets of AMPs available in the cell, or both.

Chapter II

Material and Methods

1. Chemicals

Media and buffer components and other materials used in this project were purchased from Merck, Sigma-Aldrich®, VWR® or Thermo Fisher Scientific Inc., if not stated otherwise. The antibiotics used in this study were purchased from Sigma-Aldrich®. Reagents used for molecular microbiological techniques (e.g. enzymes) were purchased from New England BioLabs Inc., unless stated otherwise.

2. Bacterial strains and growth conditions

E. coli and *B. subtilis* strains were routinely grown at 37 °C with agitation (180 – 200 rpm) in lysogeny broth medium (LB; 1 % (w/v) tryptone, 0.5 % (w/v) yeast extract, 1 % (w/v) sodium chloride, Bertani (1951)) or Müller-Hinton medium (MH, 0.2 % (w/v) beef extract, 1.75 % (w/v) acid hydrolysate of casein, 0.15 % (w/v) starch). Solid media contained 1.5 % (w/v) agar. Where required, *B. subtilis* strains were supplemented with 0.2 % (w/v) xylose.

Selective media for *E. coli* strains contained ampicillin (100 µg/ml), chloramphenicol (30 µg/ml) or spectinomycin (20 µg/ml). For *B. subtilis* strains chloramphenicol (5 µg/ml), kanamycin (10 µg/ml), spectinomycin (100 µg/ml), tetracycline (10 µg/ml) or erythromycin (1 µg/ml) and lincomycin (25 µg/ml, macrolide-lincosamide-streptogramin B, MLS) were used for selection.

Bacitracin was purchased as zinc-salt from Sigma-Aldrich®. Mersacidin and deoxy-actagardine B (for convenience hereafter actagardine) were kindly provided by Cantab Anti-infectives Ltd. Stock solutions of antimicrobial peptides used for this study were prepared in dH_2O+HCl (bacitracin), dH_2O (nisin) or 100 % methanol (mersacidin, actagardine) at concentrations of 10 mM for *in vitro* and 10 mg/ml for *in vivo* experiments.

Determination of the optical density at 600 nm wavelength (OD_{600}) of liquid cultures was performed using a spectral photometer (Jenway 6320D, Bibby Scientific Limited) in cuvettes with a 1 cm light path length. All bacterial strains used in this study are listed in tables S1 and S2 (supplement).

3. DNA manipulations and transformations

Vectors, plasmids and oligonucleotides involved in this study are depicted in tables S3, S4 and S5 (supplement).

3.1 Polymerase chain reaction

Polymerase chain reactions (PCRs) for general cloning were performed using Q5® High-Fidelity DNA polymerase (0.02 U/µl) according to the manufacturer's instructions. The PCR reaction contained final concentrations of 1 × reaction buffer, 200 µM dNTPs, 0.5 µM forward primer, 0.5 µM reverse primer and up to 1 ng of plasmid DNA, when filled to final volume of 50 µl with deionised H_2O. PCR reactions were carried out in a PCR cycler (Biometra TPersonal, LABGENE Scientific SA) with a typical reaction cycle of: 30 s at 98 °C for initial denaturation, 35 cycles of 10 s at 98 °C, 30 s at 58-60 °C and 30 s/kb at 72 °C. A final extension step was performed for 2 minutes at 72 °C. The resulting DNA fragments were separated by agarose gel electrophoresis (1 % w/v) in 0.5 × TAE buffer (20 mM Tris, 10 mM acetic acid, 0.5 mM EDTA, pH 8.0) containing 0.1 µl SYBR® Safe DNA gel stain (Thermo Fisher Scientific Inc.) per ml agarose solution for detection of bands using the ChemiDocTM XRS imaging system (Bio-Rad Laboratories, Inc.). PCR products were purified using the E.Z.N.A® Cycle-Pure Kit (Omega Bio-tek) or extracted from an agarose gel using Monarch® DNA Gel Extraction Kit (New England BioLabs Inc.). Where genes were commercially synthesised, the procedure was performed by GenScript®. The downstream cloning was carried out as usual.

3.2 DNA digest and ligation

PCR products and vectors were digested with the respective enzymes as instructed by the manufacturer. Incubation was carried out at 37 °C for at least one hour. To avoid re-ligation, digested vector fragments were dephosphorylated by addition of alkaline phosphatase and incubated at 37 °C for another hour. Digested DNA fragments were purified using E.Z.N.A® Cycle-Pure Kit (Omega Bio-tek). Concentrations of purified DNA fragments and vectors were quantified by agarose gel electrophoresis. Generally, ligations were performed for one to two hours at room temperature or overnight at 4 °C in an at least 3:1 ratio of insert to vector and by using T4 DNA Ligase (final amount 400 units/reaction) following to the manufacturer's instructions.

3.3 Plasmid extraction and verification of cloning

Plasmids were extracted using a GeneJET Plasmid MiniPrep Kit (Thermo Fisher Scientific Inc.) or via alkaline lysis. For this, cells were harvested from an overnight culture and resuspended in 300 µl buffer P1 (50 mM Tris/HCl, 10 mM EDTA, 100 µg/ml DNase-free RNase, pH 8.0). 300 µl lysis buffer were added (P2, 0.2 M NaOH, 1 % (w/v) SDS) as well as after inversion of the tubes, 300 µl buffer P3 for precipitation of chromosomal DNA (3 M potassium acetate, 5 % formic acid). The mixture was centrifuged and the supernatant transferred into a fresh tube. For precipitation of plasmid DNA, 0.7 volumes of 100 % isopropanol were added and after another centrifugation step, the pelleted DNA was washed with 70 % ethanol, air-dried and dissolved in dH_2O.

The correct insertion of the fragment was either verified by colony PCRs using OneTaq® 2 × Master Mix, following the manufacturer's instructions or by restriction digest. Sequencing of plasmid DNA was performed by Eurofins Genomics GmbH, according to the instructions. The resulting sequences were analysed *in silico* using the freewares BioEdit (version 7.0.0, Hall, 1999, Hall *et al.*, 2011) and SerialCloner (version 2.5).

3.4 Bacterial transformations

3.4.1 Transformation of *E. coli* strains

For transformations regarding general cloning, chemically competent cells of *E. coli* DH5α from the laboratory stock were used. Transformations for protein overproduction was carried out using *E. coli* BL21(DE3), purchased commercially from New England BioLabs Inc. Cells were gently defrosted and incubated with ~150 ng plasmid DNA on ice for at least 20 minutes. A heat shock was performed at 42 °C for 90 s, followed by 2 minutes recovery on ice. Cells were further incubated in 1 ml LB for roughly 1 hour at 37 °C with agitation. Cells were gently harvested, the cells resuspended and plated on selective medium. Plates were incubated overnight at 37 °C.

3.4.2 Transformation of *B. subtilis*

B. subtilis transformations were performed using a modified version of the Paris protocol (Kunst & Rapoport, 1995). Overnight cultures of recipient strains were grown in 500 µl Paris medium (60 mM K_2HPO_4, 44 mM KH_2PO_4, 1 mg/ml trisodium citrate, 1 % (w/v) glucose, 0.4 % (w/v) potassium L-glutamate, 0.1 % (w/v) casamino acids, 2.2 µg/ml ferric ammonium

citrate, 3 mM $MgSO_4$, 25 µg/ml tryptophan) at 37 °C with aeration (180 rpm). Day cultures were inoculated 1:50 in fresh, pre-warmed Paris medium and grown for 3 hours (37 °C, 180 rpm). 50 µl of isolated genomic DNA were added to each transformation reaction. Genomic DNA was isolated by mixing an overnight culture 1:1 with SC buffer (150 mM NaCl, 10 mM sodium citrate, pH 7.0) and harvesting the cells by centrifugation (5 min, 13000 × *g*). The pellet was resuspended in SC buffer and incubated with lysozyme at 37 °C for 15 minutes. The solution was mixed 1:1 with 5 M NaCl and filter sterilised. Transformation cultures were grown for another 5 hours and plated on selective media. For MLS or chloramphenicol resistance, cultures were pre-induced to a 1:40 final concentration of the respective antibiotic one hour before plating.

4. Overproduction and purification of BceB-ECD

4.1 Overproduction of BceB-ECD

Overnight cultures were inoculated in LB with fresh transformants and grown at 37 °C shaking incubation. Cultures for overproduction of BceB-ECD were inoculated 1:100 from an overnight culture of *E. coli* BL21(DE3) carrying the respective plasmid. Cells were incubated at 37 °C with agitation (180 – 200 rpm). Gene expression was induced with 1 mM isopropyl β-D-1-thiogalactopyranoside (IPTG, Thermo Fisher Scientific Inc.) during the exponential growth phase (OD_{600} of 0.5 – 0.6). The cultures were further incubated at 16 °C, 180 – 200 rpm for 18 – 24 h. Depending on the culture size, cells were either harvested at by centrifugation in an Avanti® J-25 centrifuge (Beckman Coulter, Inc., JLA-10.500) at 18,600 × *g* for 10 min or in a Centrifuge 5804R (Eppendorf AG, A-4-44) at 4500 × *g* for 20 min. Both centrifugation steps were performed at 4 °C. Pellets were stored at - 80 °C until further use.

4.2 Cell lysis

Cell pellets were defrosted in lysis buffer (1 ml/g pellet; 50 mM Tris/HCl [pH8], 0.5 M NaCl, 5 mM dithiothreitol (DTT), 0.1 mM n-dodecyl-β-D-maltoside (DDM, GLYCON Biochemicals GmbH), 0.2 U/ml Benzonase® nuclease (Sigma-Aldrich®), lysozyme and protease inhibitor cocktail (cOmplete™ ULTRA Tablets, EDTA-free, Roche). Cells were lysed by sonication (30 s for every 5 ml of cell suspension). The supernatant was separated from debris by centrifugation using an Avanti® J-25 centrifuge (Beckman Coulter, Inc., JA-25.50, 75600 × *g*,

30 min, 4 °C). The pellet was stored at - 80 °C and used for SDS PAGE and attempts of refolding protein from inclusion bodies. The supernatant was filtered (0.45 µm) and immediately used for downstream purification steps.

4.3 Refolding BceB-ECD from inclusion bodies

Pellets of lysed cells were defrosted and resuspended in wash buffer (4 ml/g pellet, 50 mM Tris/HCl [pH8], 0.5 M NaCl, 1 % (v/v) Triton X-100). Inclusion bodies were harvested using a pre-cooled centrifuge at 4500 × *g* for 20 min. The wash and centrifugation steps were repeated until the pellet appeared white. The pellet was split and transferred into microcentrifuge tubes labelled with the weight of the sample. Inclusion bodies were stored at -40 °C until further use. For refolding attempts, the pellets were resuspended in solubilisation buffer (50 mM Tris/HCl [pH8], 50 mM NaCl, 0.1 mM DDM, 8 M urea) to a concentration of 100 mg/ml and incubated at room temperature for 30 - 60 minutes. The suspension was centrifuged (17000 × *g*, 30 min, 4 °C) to remove any insoluble parts. The supernatant was diluted 1:10 – 1:100 in solubilisation buffer and dialysed overnight at 4 °C into refolding buffer (20 mM Tris/HCl [pH8], 20 mM NaCl, 0.1 mM DDM) using SnakeSkin™ (7 kDa molecular weight cut off). Purity and presence of BceB-ECD were confirmed by SDS-PAGE and mass spectrometry.

4.4 Protein purification techniques

4.4.1 Immobilized metal affinity chromatography

The first purification step was an immobilized metal affinity chromatography (IMAC) using a 1 ml HisTrap FF column (GE Healthcare Life Sciences) connected to an ÄKTAstart purification system (GE Healthcare Life Sciences). All buffers were freshly prepared and filtered (0.45 µm). Buffers and protein samples were kept at 4 °C or on ice at all times. Buffers A and B contained 50 mM Tris/HCl [pH8], 0.5 M NaCl, 0.1 mM DDM and 10 mM imidazole or 1 M imidazole, respectively. All purification and wash steps were performed at a flow rate of 1 ml/min and attention was paid to pressure limits. The sample was loaded using a 50 ml superloop (GE Healthcare Life Sciences). The protein was washed and eluted with 0, 10, 20, 30 and 100 % buffer B over 10 column volumes per concentration at a flow rate of 1 ml/min. The collected fractions were analysed by SDS-PAGE. Fractions containing the protein of interest were

dialysed (SnakeSkin™, 7 kDa molecular weight cut off) into 20 mM Tris/HCl [pH8], 20 mM NaCl, 0.1 mM DDM overnight at 4 °C.

4.4.2 Anion exchange chromatography

Where necessary, further purification by anion exchange (AEX) chromatography was performed using a HiTrap Q HP column (1 ml, GE Healthcare Life Sciences). Buffers QA and QB contained 20 mM Tris/HCl [pH8], 20 mM NaCl or 1 M NaCl, respectively, 0.1 mM DDM. Proteins were eluted in a 20 column volumes gradient from 0 % to a final concentration of 100 % buffer QB at a flow rate of 1 ml/min and analysed by SDS-PAGE. The samples containing pure protein were dialysed (SnakeSkin™, 7 kDa molecular weight cut off) overnight at 4 °C into 20 mM Tris/HCl [pH8], 20 mM NaCl, 0.1 mM DDM.

5. Protein visualisation and quality determination

5.1 Sodium dodecyl sulphate - polyacrylamide gel electrophoresis

Sodium dodecyl sulphate - polyacrylamide gel electrophoresis (SDS-PAGE) was performed using precast polyacrylamide gels (10 %; RunBlue, Expedeon) and 1 × RunBlue SDS Running Buffer (Expedeon). Gels were run at 120 V for roughly 60 minutes. For visualisation of protein bands, gels were stained with Coomassie staining solution (45 % (v/v) methanol, 10 % (v/v) acetic acid, 0.25 % (w/v) Coomassie Brilliant Blue G-250) and destained by using destaining solution (45 % (v/v) methanol, 10 % (v/v) acetic acid). Alternatively, InstantBlue™ Protein Stain (Expedeon) was used.

5.2 Western blot

Western blot analysis was performed using polyvinylidene fluoride (PVDF) membranes (Merck Millipore, activated in 100 % MetOH). Membranes, SDS-PAGE gels and Whatman filter paper were soaked in transfer buffer (1 × RunBlue SDS Running Buffer, Expedeon, 20 % (v/v) methanol) prior to blotting. The transfer was performed at 75 mA for 70 minutes using a PerfectBlue™ Sedec™ Semi-Dry Electroblotter (Peqlab). For Western Blot analysis of His•tag®-constructs, the membrane was blocked with 7.5 % (w/v) skimmed milk powder in PBST (137 mM NaCl, 2.7 mM KCl, 10 mM Na_2HPO_4, 1.8 mM KH_2PO_4 [pH7.4], 0.1 % (v/v) Tween 20) overnight at 4 °C, gently shaking. Membranes were washed three times with PBST (15

ml), each step taking 5 to 10 minutes with gentle shaking. Subsequently, the PDVF membrane was incubated for two hours at room temperature in 10 ml 1 % (w/v) bovine serum albumin containing the primary antibody (Penta·His Antibody, QIAGEN®, 1:4000 dilution). After another three wash steps with PBST, the membrane was incubated in milk containing the secondary antibody (Peroxidase-AffiniPure Goat Anti-Rabbit IgG, Jackson ImmunoResearch Europe Ltd, 1:4000) for at least an hour at room temperature and washed three times with PBST (see above). Pierce™ ECL Western Blotting Substrate (Thermo Fisher Scientific Inc.) was used as enhanced chemiluminescence substrate to enable detection of peroxidase activity. The Western blots were exposed for 3 s using a Qiagen CCD camera with Fusion software.

5.3 Mass spectrometry

Sample preparation and mass spectrometry analysis of protein bands cut out of SDS-PAGE gels were performed by the proteomics unit of the Chemical Characterisation and Analysis Facility of the University of Bath. The protein ID was determined by nanoLC-MS/MS and results were compared to both *E. coli* and *B. subtilis* database entries.

5.4 Determination of protein concentration

Protein concentrations were determined by absorbance spectroscopy using a 1 cm optical pathway quartz cuvette. According to the Beer-Lambert law ($A = \varepsilon * c * l$), the absorbance A at 280 nm wavelength and the molar extinction coefficient for BceB-ECD ($\varepsilon = 7450\ M^{-1}\ cm^{-1}$) were used to determine the protein concentration.

5.5 Dynamic light scattering

Protein solutions were filtered (0.45 µM) or centrifuged to remove contaminants like dust and insoluble aggregates prior to experiments. Protein solutions (100 µl) transferred into a black quartz cuvette. Dynamic light scattering (DLS) experiments were performed using a Zetasizer Nano S controlled by the Malvern Panalytical Software (Malvern Panalytical Ltd). Measurements were taken at 20 °C. Measurements with a count rate (kcps) below 200 were disregarded due to poor quality of the result. Z-average and polydispersity index were provided by the Malvern Panalytical Software. The reported average diameter in nm was the result of at least three independent measurements based on the size distribution by volume rather than by intensity.

6. *In vitro* characterisation of BceB-ECD using biophysical methods

6.1 8-Anilino-naphthalene-1-sulphonic acid fluorescence spectroscopy

8-Anilino-naphthalene-1-sulphonic acid (ANS) and protein solution were diluted from stock solutions into buffer (20 mM Tris/HCl [pH8], 20 mM NaCl, 0.1 mM DDM) to a final concentration of 100 µM ANS and 4 µM protein (1 ml volume). Substrates were added gradually from 10 mM stock solutions to final concentrations between 0 and 50 µM. Where substrate was administered in a single step, final concentrations of 50 µM bacitracin, 500 µM GPP or a premixture of 50 µM bacitracin and 500 µM GPP were used. To ensure steady-state measurements, samples were left to equilibrate in a quartz cuvette (optical pathway: 10 mm) for at least three minutes before initial measurements and after every addition of substrate. Fluorescence measurements were performed at 20 °C using the fluorescence spectrometer LS 55 (PerkinElmer®). The following settings of the FL WinLab software were used: Excitation wavelength: 380 nm, slit width: 3 nm, mean of three repeats. Where substrate concentrations were added in a single step, the mean of ten measurements was used for further analysis. Spectra were determined from 400 – 640 nm and exported into the freeware Spekwin32 (Menges, 2016) and Microsoft Excel for further analysis. Fluorescence emission was determined by addition of the intensity values of the spectra. To measure specific rather than total binding, the spectra were buffer corrected (Motulsky & Christopoulos, 2004). Results were set relative to 1 = 0 µM substrate and averaged across independent measurements as indicated in figure legends. Non-linear single site binding curves were plotted to the equation:

$$1 + \frac{B_{max} * x}{K_d + x},$$

where possible, using Graphpad Prism® (Motulsky & Christopoulos, 2004). K_d values were determined using the same software. Where applicable, data were approximated with a linear regression fit (Motulsky & Christopoulos, 2004).

6.2 Circular dichroism spectroscopy

Circular dichroism (CD) spectroscopy experiments were performed at 10 °C using a Chirascan qCD spectrometer (Applied Photophysics Ltd.). Purified protein at a final concentration of 4.5

µM in 20 mM Tris/H_2SO_4 [pH8], 20 mM NaCl, 0.1 mM DDM was either measured alone or in the presence of a potential substrate. Bacitracin and nisin were added to a final concentration of 50 or 90 µM, respectively. GPP and premixed [GPP-BAC] were added to final concentrations of 500 µM GPP, or 50 bacitracin and 500 µM GPP, respectively. To ensure steady-state measurements, samples were left to equilibrate in a quartz cuvette (optical pathway: 1 mm) for at least three minutes before initial measurements. Spectra of the ellipticity (mdeg) were obtained from 195 or 200 to 260 nm wavelength with a spacing of 1 nm and five repeats per cuvette. Experiments were carefully performed without exceeding an HT (voltage) value of 700 V. Spectra were buffer corrected and moving averages (n=5) were applied manually. Spectra obtained from independent measurements were averaged. For the secondary structure estimation, the online circular dichroism analysis tool Dichroweb was used. (Whitmore & Wallace, 2004, Whitmore & Wallace, 2008). CD spectra of BceB-ECD were approximated using the CONTIN-LL algorithm (Provencher & Glockner, 1981) and the reference set 4 (Sreerama & Woody, 2000).

For determination of the 222/208 nm ratios the values at 222 were divided by the respective value at 208 nm. The ratios were averaged across independent measurements and the standard deviation determined. Values were set relative to 222/208 nm ratio of BceB-ECD. Statistical analyses were performed using Graphpad Prism®.

7. *In vivo* characterisation of the physiological substrate of BceAB.

7.1 Growth assays for determination of the fasted doubling time.

For the determination of the fastest doubling time, overnight cultures of the strains of interest were diluted 1:1000 into fresh LB. 100 µl of each diluted culture were dispensed into 96-well microtiter plates. All wells around the edge of the plates were filled with water to reduce evaporation. Cultures were grown at 37 °C with shaking incubation (180 rpm) using a Tecan® Spark® microplate reader controlled by the SparkControl™ software (Tecan Trading AG, Switzerland). The optical density (OD_{600}) was measured every 5 min at 600 nm over 8 hours. Growth curve measurements were corrected against blank wells that only contained media. log(OD_{600}) values were plotted against time using Microsoft Excel. From this, the fastest doubling time (t_d) during exponential growth phase was calculated for each strain using the equation:

$$t_d = \frac{ln_{(2)}}{k},$$

where *ln* is the natural logarithm and *k* is the growth rate (Powell, 1956). Doubling times of independent measurements were averaged from at least six biological replicates. Mean and standard deviation are depicted in results figures and specific values given in accompanying tables.

7.2 Competition assays as measure of relative fitness

To compare the relative fitness of strains in competition assays, overnight cultures of each strain to be competed were grown and their optical density was determined. Based on the OD_{600} measurements, two strains were mixed in a 50:50 ratio. 1:1000 dilutions of the mixed cultures were prepared in 2 ml of LB broth, and cultures were incubated at 37 °C with agitation (180 rpm). To determine the initial amount of colony forming units (CFUs) in the cultures, serial dilutions of the mixed culture were plated onto selective and non-selective LB agar plates in two technical replicates. After 24 h of incubation of the plates at 37 °C, colonies were counted and CFUs/ml determined. Experiments in which the initial 50:50 ratio deviated more than 40:60 were excluded. Every 24 hours, the mixed cultures of the competing strains were diluted 1:1000 into fresh LB and further incubated. The CFUs were determined after 24

and 72 hours of growth as described. The CFU concentrations were used to calculate the competition index (CI) of the competing pairs after 24 hours and 72 hours incubation.

$$CI = \frac{\frac{cfu\ ml^{-1}\ of\ mutant\ (t_f)}{cfu\ ml^{-1}\ of\ reference\ (t_f)}}{\frac{cfu\ ml^{-1}\ of\ mutant\ (t_i)}{cfu\ ml^{-1}\ of\ reference\ (t_i)}}$$

The mutant strain refers to the deletion mutant which contains an extra gene for antibiotic selection over the reference strain in the competing pair. t_i refers to the initial CFU concentration, t_f refers to the CFU concentration after 24 hours of incubation (Auerbuch *et al.*, 2001, Wiser & Lenski, 2015).

7.3 Determination of the minimal inhibitory concentration of bacitracin

The sensitivity of *B. subtilis* strains to bacitracin was determined using the minimal inhibitory concentration (MIC). For this, dilutions of Zn^{+}-bacitracin were prepared in 2 ml of Müller-Hinton medium and inoculated 1:500 from overnight cultures. Cultures were incubated overnight (37 °C, 180 rpm) and examined for growth after 24 h. The MIC was determined as the lowest concentration at which no visible growth was detected. All experiments were performed in biological triplicates.

7.4 Luminescence reporter assay for determination of BceAB transport activity

LB or MH (10 ml) were inoculated 1:1000 from overnight cultures of each strain to be tested. Day cultures were grown at 37 °C with agitation (180 rpm) to an optical density at OD_{600} of around 0.5, to ensure exponential growth. Cultures were then diluted to an OD_{600} of 0.01 and dispensed into 96 well microplates (Corning®, black, clear flat bottom), with 100 µl culture volume per well. All wells around the edge of the plates were filled with water to reduce evaporation. Luciferase activity of strains was determined in a Tecan® Spark® microplate reader controlled by the SparkControl™ software (Tecan Trading AG, Switzerland). Cells were grown in the microplate reader for 5 hours with continuous shaking incubation (37 °C, 180 rpm, circular motion, intensity: 3). After 1 hour of incubation, cells were challenged with 5 µl of freshly diluted antibiotic stock solutions per well to make up the desired concentration. The OD_{600} and the corresponding luminescence (relative luminescence units, RLU) were

measured every 5 minutes. Luminescence output was normalized to cell density by dividing each data point by its corresponding blank-corrected OD_{600} value (RLU/OD). For dose response curves, RLU/OD values were determined from the average of three measurements (25, 30 and 35 min). Data are shown as mean ± standard deviation of at least three biological replicates.

Chapter III

In vitro characterisation of the binding capacity of BceB-ECD

1. Introduction

The mechanism by which the BceAB-BceRS detoxification system confers resistance against AMPs is still not entirely understood. It is however known that the regulatory two-component system (TCS) BceRS requires the active transporter BceAB for the detection of the AMP (Bernard *et al.*, 2007). In the absence of BceAB, or when transport activity was impaired, the resistance system did not only lose its ability to provide protection against AMPs, but also could not induce the signalling cascade through the TCS (Bernard *et al.*, 2007, Rietkötter *et al.*, 2008). The histidine kinase BceS lacks an extracellular input domain, which is a characteristic feature for sensor kinases to perceive their stimulus (Mascher, 2014). Instead, the kinase was shown to form a sensory complex with the transporter even in the absence of bacitracin (Dintner *et al.*, 2014). The transporter BceAB was therefore proposed to be entirely responsible for substrate recognition and interaction. In recent work, Dintner and colleagues (2014) showed that purified BceB was able to bind bacitracin with a steady-state K_d of 60 nM, using surface plasmon resonance spectroscopy. However, the exact site of interaction between the transporter and its substrate remains unknown.

One conserved feature of all BceB-like permeases is a large extracellular domain located between transmembrane helices (TMH) 7 and 8 (Dintner *et al.*, 2011). Generally, these domains were found to consist of approximately 180 to 230 amino acids (Dintner *et al.*, 2011). The extracellular domain of BceB (BceB-ECD) was shown to be essential for resistance against and sensing of bacitracin, as replacing the ECD with a truncated version resulted in a non-functional protein (Rietkötter *et al.*, 2008, Coumes-Florens *et al.*, 2011) and thus, was suggested as the substrate binding domain of BceB. In support of this, Hiron and colleagues (2011) found these large extracellular domains of resistance transporters to be responsible for substrate specificity in *S. aureus*. A domain-swap experiment between the ECDs of the closely related permeases VraG and VraE was performed, resulting in a chimeric VraFG transporter that had its native ECD replaced by the VraE-ECD ($VraFG^{loop(VraE)}$). Interestingly, the hybrid transporter conferred resistance against bacitracin, which is usually the substrate of VraDE, but not any longer against colistin, the original substrate of VraFG. In other words, the resistance conferred by the transporter changed accordingly to its ECD, suggesting the ECD to be responsible for substrate recognition.

In a phylogenetic analysis of all known Bce-like detoxification systems, the transporters could be distributed into eight different groups. However, the ECD sequences had been removed

for this analysis. Less than 10 % pairwise sequence identity and low sequence similarity had led to very poor alignments across that region (Dintner *et al.*, 2011). Similar results were found in an independent study by Coumes-Florens and colleagues (2011). The extracellular domains of the most closely related transporters were their least conserved regions. Further, no correlation between the phylogenetic group of the transporter and their substrate specificity could be drawn (Dintner *et al.*, 2011). Even when ECDs of transporters that provide resistance against the same AMP, for example bacitracin, were aligned, hardly any sequence conservation was found (Fig S3.1, blue box). When comparing the secondary structure predictions of the ECDs however, Dintner and colleagues (2011) discovered a conserved arrangement of α-helices and β-sheets across all phylogenetic groups, according to α-β-α-β_{2-3}-α-β_{3-4}-α-β-α_{1-2} pattern. Despite the poor sequence alignments, some conserved residues could be identified. These were mainly hydrophobic residues and found in close proximity of the central α-helix or the penultimate β-sheet (Dintner *et al.*, 2011).

Our analysis of this domain's secondary structure revealed that parts of the ECD lack a fixed or ordered three-dimensional structure, which suggested that regions of the protein are intrinsically disordered (Fig. 3.1). An analysis of BceB using several different disorder prediction tools showed the extracellular domain to be comparatively flexible in contrast to the transmembrane domains of BceB and also its other loops (III 2.1). Unanimously, the region between amino acid residues 370 to 385 was found to be particularly disordered (see below for details).

Only over the last few decades, our understanding of binding interactions deviated from the traditional linear sequence-to-structure-to-function paradigm and intrinsically disordered proteins (IDPs) moved into focus (Wright & Dyson, 1999). Many IDPs were characterised, and their importance in signalling and regulatory pathways through specific protein-protein, protein-nucleic acid and protein-ligand interactions became clear (Dunker *et al.*, 2008b). Numerous IDPs were shown to fold in a disorder-to-order transition manner upon binding their substrate (Wright & Dyson, 2009). The substrate-induced coupled folding and binding mechanism of IDPs has several advantages over binding mechanisms of structurally-ordered proteins. Benefits include the binding diversity that is mediated by high conformational flexibility. Their unstructured regions allow flexible domains to interact with a variety of targets, whereas ordered enzymes are thought to select their substrates based on the classic key-lock theory (Fischer, 1894, Koshland Jr., 1995). Yet, disorder-to-order transitions that IDPs can undergo upon substrate binding still assure a high substrate specificity (Kriwacki *et al.*, 1996). As BceB-ECD contains intrinsically disordered regions, a substrate-induced coupled

folding and binding mechanism is also conceivable for BceAB. Such a mechanism could also explain the broad but highly specific substrate range of BceAB. Aside from bacitracin, BceAB also confers resistance against other AMPs, including plectasin, mersacidin and actagardine, but not to the lipid II-binding AMP nisin (Staron *et al.*, 2011).

For IDPs, high substrate specificity is complemented by low affinity binding (Kriwacki *et al.*, 1996, Huang & Liu, 2009). Specific protein-ligand interactions can thus easily come apart, which is not only important in regulatory interactions (Dunker & Obradovic, 2001), but might also be advantageous in transport reactions.

While some IDPs have been described to be entirely unstructured prior to and during the binding event, most IDPs were suggested to comprise so-called molecular recognition features or elements (MoRFs, Mohan *et al.*, 2006, Dunker *et al.*, 2008a). With around 10 – 70 amino acid residues, these relatively short amphipathic motifs are found within longer regions of disorder. Upon interaction with their substrate, these motives can obtain helical, β-strand or different non-regular structures. Often IDPs even acquire a different structure on binding different substrates (Wright & Dyson, 2009). Short MoRFs were identified in the unstructured regions of BceB-ECD (III 2.1), which highlighted this region again as potential binding domain of the transporter.

The so-called 'fly casting' model suggests the flexible region of some IDPs to comprise a greater capture radius than orderly-structured proteins do (Shoemaker *et al.*, 2000, Huang & Liu, 2009). That way, the IDP can partially and weakly bind to targets from a larger distance. The IDP then fully ropes its substrate in while simultaneously undergoing a disorder-to-order structural transition. This model is based on the observations that IDPs generally have faster binding rates than structured proteins and encounter a substrate less often before they can bind it (Huang & Liu, 2009). In addition, IDPs possess lower binding energy barriers, which makes it easier for them to reach transition state (Shoemaker *et al.*, 2000, Huang & Liu, 2009). A fly-casting mechanism, in which the highly flexible BceB-ECD reels in bacitracin thereby removing it from its target, is also imaginable for substrate binding by BceAB.

Thus, we hypothesise that the highly-flexible extracellular domain of BceB acts as the substrate binding domain and hypothesise that the binding mechanism functions according to a 'fly-casting' mechanism, in which BceB-ECD undergoes conformational changes upon substrate binding. To test this, we overproduced and purified BceB-ECD using different protein purification strategies, including immobilised metal affinity and anion exchange chromatography and refolding BceB-ECD from inclusion bodies. We then characterised the binding reaction between BceB-ECD and its substrate using biochemical and biophysical *in*

vitro methods, including fluorescence spectroscopy and circular dichroism spectroscopy. As no interaction was measured between the BceB-ECD and the AMPs alone, our approaches re-focussed on BceB-ECD potentially binding the AMPs in complex with their cellular target as suggested previously (Bernard *et al.*, 2007, Kingston *et al.*, 2014).

2. Results

2.1 *In silico* characterisation reveals high flexibility and partial intrinsic disorder of BceB-ECD.

To begin investigations on BceB-ECD, we performed *in silico* analyses to find out the characteristics of the protein. The domain architecture of BceB was analysed using SMART database (Letunic *et al.*, 2015, Letunic & Bork, 2018). As described before (Rietkötter *et al.*, 2008), the large extracellular domain of BceB is located between the transmembrane helices 7 and 8 and predicted to consist of 213 amino acids from S313 to G525. The molecular weight (24043.27 Da) and further parameters, including the theoretical isoelectrical point and the extinction coefficient were determined using the ExPASy ProtParam tool (Fig. 3.1 A, Gasteiger E., 2005). These parameters were used to select suitable purification methods and determine the protein concentration via absorbance spectroscopy.

Alignments of the ECD revealed low sequence conservation in a phylogenetic analysis (Dintner *et al.*, 2011, Coumes-Florens *et al.*, 2011). Even within their phylogenetic groups, the ECDs showed very low sequence identity. Here, we aligned the BceB from *B. subtilis* with sequences of several BceB-like permeases that were known to either sense bacitracin or confer resistance against it (Fig. S3.1). Permeases from *Staphylococcus aureus* (Hiron *et al.*, 2011, Yoshida *et al.*, 2011), *Listeria monocytogenes* (Collins *et al.*, 2010), *Streptococcus mutans* (Tsuda *et al.*, 2002, Ouyang *et al.*, 2010), *Streptococcus pneumoniae* (Becker *et al.*, 2009) and *Enterococcus faecalis* (Gebhard *et al.*, 2014) were included in the analysis. The alignment was performed using the integrated ClustalW application (Thompson *et al.*, 2003) of the sequence alignment editor BioEdit (Hall, 1999, Hall *et al.*, 2011). A threshold of 75 % was set for shading of identical residues and or amino acids with similar characteristics. Although the permeases were not part of the same phylogenetic groups, the transmembrane domains were comparatively well-conserved (8 % sequence identity, 27 % sequence similarity, Fig. S3.1). In contrast to this, hardly any identical or even similar residues were

found within the ECD. A proline (P) residue at position 340 seems best-conserved but is missing in BceB. Most other shaded amino acids have hydrophobic side chains like tyrosine (Y), valine (V), and isoleucine (I, Fig S3.1), which agreed with previous findings (Dintner *et al.*, 2011).

The secondary structure of BceB-ECD was predicted using JPred4 (Drozdetskiy *et al.*, 2015) and I-TASSER (Roy *et al.*, 2010). Our results confirmed the conserved α-β-α-β_{2-3}-α-β_{3-4}-α-β-α_{1-2} secondary structure pattern described previously (Dintner *et al.*, 2011). The secondary structure of BceB-ECD was predicted to comprise a combination of α-helices (22.8 %) and β-strands (25 %), with a considerable amount of unstructured regions (52.2 %).

I-TASSER and UCSF Chimera were used to predict a 3D model of the BceB-ECD secondary structure (Fig. 3.1 B, Roy *et al.*, 2010, Yang & Zhang, 2015, Zhang *et al.*, 2017, Pettersen *et al.*, 2004). In this model, the blue and red residues depict the beginning and the ending of the ECD, where the extracellular region would usually be linked to transmembrane helices (Fig. 3.1 B). This model also clearly illustrated non-structured elements within the extracellular domain (Fig. 3.1 B, particularly disordered regions are highlighted in green and yellow). The flexibility of BceB was analysed using several disorder prediction tools (IUPred (Dosztanyi *et al.*, 2005a, Dosztanyi *et al.*, 2005b), DisEMBL (Linding *et al.*, 2003), PONDR® (Molecular Kinetics, Inc.), prDOS (Ishida & Kinoshita, 2007)). The disorder probability of the ten transmembrane regions was consistently under 5 %, thus these domains were concluded to be fairly rigid. The flexibility of the shorter cytoplasmic and extracellular domains was also not increased, with the exception of the cytoplasmic linker between TMH 8 and 9 that had disorder probabilities of up to 30 % (amino acid residues 544 – 580).

The large ECD between TMH 7 and 8 was found to be the most flexible region of BceB, with one major peak at residue 381 (Fig. 3.1 C). The region between amino acid 370 and 385 was predicted to be intrinsically disordered (threshold: > 0.5). Two minor peaks of high flexibility were found to lie at amino acid residues 432 and 471. In further agreement with this, the domain architecture prediction tool SMART describes the region between residues 386 and 401 as region of low complexity (Letunic *et al.*, 2015, Letunic & Bork, 2018).

Proteins with intrinsically disordered regions often contain so-called molecular recognition features (MoRFs). These short elements are involved in the molecular recognition of binding partners and undergo disorder-to-order transitions upon binding (Mohan *et al.*, 2006). Further supporting the idea of BceB-ECD comprising the substrate binding domain of the resistance transporter, BceB-ECD was also predicted to contain such MoRFs. The MoRF

prediction tool found potential binding sites from amino acid residues 377 to 384 and between residues 432 and 435 (Fig. 3.1 B, green, yellow, Disfani *et al.*, 2012).

Taken together, the findings of the *in silico* characterisation suggested BceB-ECD to contain some unstructured regions that might be involved in the substrate binding mechanism and potentially undergo a conformational change upon binding. Therefore, the protein domain was further investigated *in vitro* using techniques that are typical for the characterisation of intrinsically disordered proteins, including circular dichroism and fluorescence spectroscopy (Dunker *et al.*, 2001, Wright & Dyson, 2009).

A

Parameter	Value
Residues	213 amino acids
Molecular weight	23695.86
Theoretical pI	5.70
Extinction coefficient	7450 M^{-1} cm^{-1}

B

C

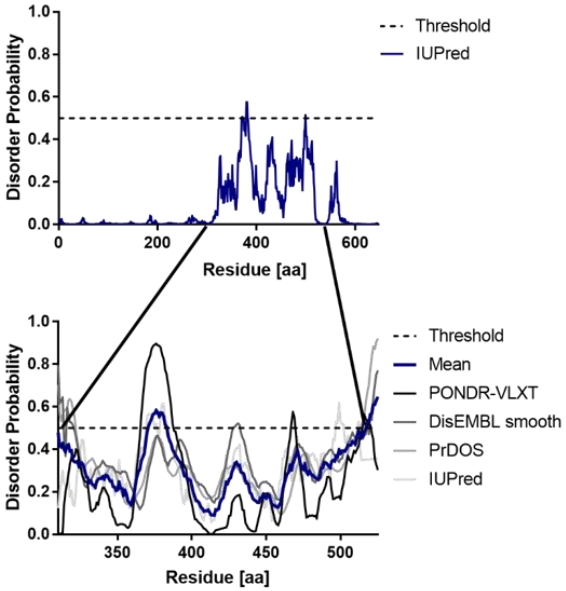

Figure 3.1: *In silico* characterisation reveals BceB-ECD to be highly flexible with an intrinsically disordered region. A: Characteristics of the extracellular domain of BceB determined by the ProtParam prediction tool. **B:** I-TASSER secondary structure model predicted BceB-ECD to consist of mainly α-helices, some β-strands and unstructured regions. The N- and C-terminal domains that were membrane-bound in native BceB are coloured in blue and red, respectively. The disordered regions that contain a molecular recognition feature (MoRF) are shown in green and yellow. **C:** Analysis of flexibility and intrinsic disorder of full-length BceB (top) and BceB-ECD (bottom) using several disorder prediction tools. The consensus of the prediction is depicted in blue. The extracellular domain was found to be highly flexible compared to any other domains of BceB. The peak around amino acid residue 380 suggested this part of BceB-ECD to be intrinsically disordered.

2.2 *In vitro* characterisation of purified BceB-ECD does not imply bacitracin binding activity.

2.2.1 Initial attempts of overproduction and purification of BceB-ECD using plasmid pSG1601

To characterise the isolated ECD, we first needed a strategy to overproduce and purify the BceB-ECD. Previous work had pointed out plasmid pSG1601 (pET-16b-*bceB*-ECD) as a suitable starting point for overproduction of BceB-ECD (Fig. 3.2 A). This plasmid contained the nucleotide sequence for BceB-ECD, encoding amino acids A310 to G525 of BceB. Expression from the vector pET-16b led to a fusion protein with an N-terminal histidine decapeptide (His_{10}-tag, Franke & Hruby, 1993). First overproduction attempts were made using the expression strain *E. coli* BL21(DE3) (Wood, 1966). Exponentially growing cells were induced with 1 mM IPTG. After overnight growth at 16 °C, cells were lysed and protein purified from the soluble fraction using immobilised metal affinity chromatography (IMAC) purification with a linear elution gradient. Fractions were then analysed by SDS-PAGE. Most of the overproduced BceB-ECD was found in the insoluble pellet fraction, displayed as a single band at 26 kDa (Fig. 3.2 B). This was consistent with the predicted molecular weight of this construct of 26.7 kDa (ExPASy ProtParam, Gasteiger E., 2005). Some BceB-ECD was eluted at around 200 mM imidazole, alongside other proteins (not shown). As the BceB-ECD produced from pSG1601 had a theoretical isoelectric point of 6.52 (ExPASy ProtParam, Gasteiger E., 2005) and hence, probably possessed a negative surface charge at pH 8.0, the second purification method used was an anion exchange (AEX) chromatography. SDS-PAGE analysis of the eluted fractions showed BceB-ECD as a double band at around 26 kDa (Fig. 3.2 B). Although mass spectrometry analysis of the two bands confirmed the presence of BceB-ECD in both bands (not shown), comparison with the insoluble fraction led to the conclusion that the lower band resulted from a degraded version of BceB-ECD or a contaminant. With around 1 mg of purified protein per 10 L of culture also the yield of the overproduction and purification was poor and restricted the *in vitro* characterisation of BceB-ECD.

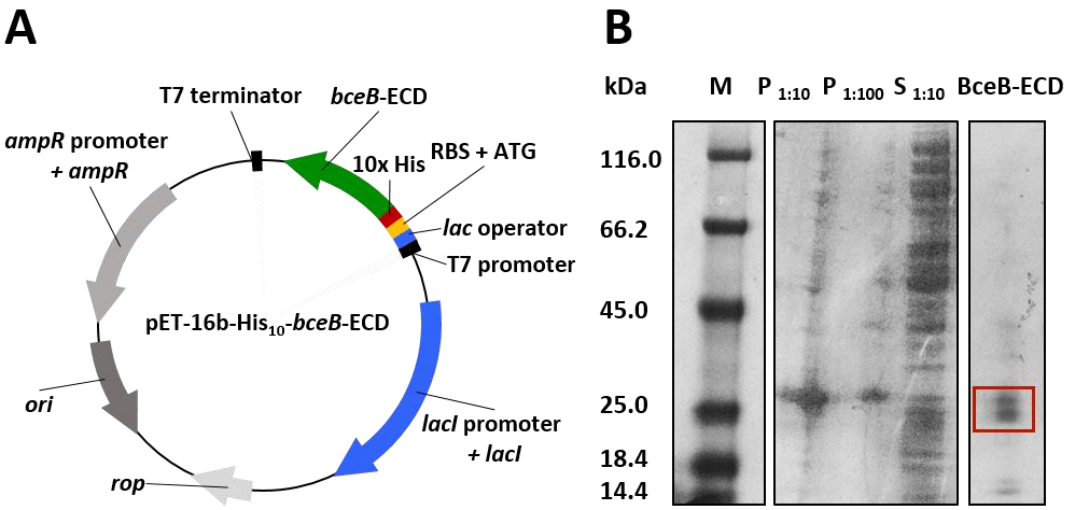

Figure 3.2: Initial purification attempts of BceB-ECD from pSG1601 result in a double band on SDS-PAGE. A: Schematic of the plasmid pSG1601. *bceB*-ECD was expressed with an N-terminal His_{10}-tag from the IPTG-inducible vector pET-16b. **B:** SDS-PAGE analysis of pellet fraction and supernatant after cell lysis. kDa: kilodalton, M: marker, P: pellet (diluted, 1:10 or 1:100), S: supernatant (diluted, 1:10). BceB-ECD purification from soluble fraction by IMAC (not shown) and AEX chromatography resulted in double band (red box) at around 25 kDa on a Coomassie-stained SDS-PAGE gel.

2.2.2 Improvements on the purification of BceB-ECD and refolding the ECD from inclusion bodies

To obtain higher quantities of BceB-ECD and an improved degree of purity, improvements on the purification protocol or even alternative strategies were required.

As shown in Fig. 3.2 B, most of the overproduced BceB-ECD was found in the insoluble pellet fraction after cell lysis. The large amounts of non-native protein that result from overproduction of recombinant plasmid-encoded proteins in heterologous systems like *E. coli* often induce a stress response in the host (Villaverde & Carrio, 2003). This consequently leads to production of heat-shock proteins or other chaperones and often also results in the aggregation of the encoded protein in inclusion bodies. These are particles of insoluble and densely-packed denatured or partially folded protein molecules. Generally, the recombinant protein aggregated in inclusion bodies was shown to be highly enriched and homogenous with only few other contaminants like chaperones (Singh & Panda, 2005, Singh *et al.*, 2015). Refolding of inclusion bodies to recover the bio-active forms of protein *in vitro* has therefore been regarded as alternative strategy for protein overproduction and purification (Rudolph & Lilie, 1996, Villaverde & Carrio, 2003).

To obtain higher amounts of BceB-ECD, refolding of BceB-ECD from inclusion bodies was attempted using a protocol based on the considerations of Tsumoto *et al.* (2003), and Singh *et al.* (2015). The recovery included the isolation of inclusion bodies by centrifugation with several wash steps, followed by the denaturation and solubilisation of the protein by chaotropic reagents, in this case 8 M urea. The solution was then diluted and BceB-ECD refolded by slowly removing the denaturants by dialysis.

SDS-PAGE analysis of the refolded samples revealed large quantities of BceB-ECD (Fig. 3.3 A). The main band at 29 kDa was confirmed to contain BceB-ECD by mass spectrometry (data not shown). BceB-ECD was found to be almost pure even before further purification steps had been performed, with only one other band at 26 kDa. This double band was observed before (2.2.1). The slight up-shift in protein mass is likely an artefact due to the use of a different protein standard. While refolding of proteins from inclusion bodies brings several advantages over soluble expression of proteins, this method can result in poor recovery of the bio-active form of the protein, as the protein might not take on its native fold after harsh treatment. To resolve this concern, we aimed to compare and validate the secondary structure of the refolded protein with the soluble version.

For this, we sought to improve overproduction and purification of soluble BceB-ECD in a parallel approach. To this end, we first focussed on improvements of cell lysis. Longer sonication pulses and the use of different types and higher amounts of DNAse or Benzonase® seemed particularly efficient. This led to enhanced overall protein yield and also simplified the sample handling during centrifugation and purification steps. These changes, however, affected the purity of protein after IMAC and AEX chromatography. To counteract, the culture volume was reduced from 10 L to 2 L, while maintaining the same volumes for cell lysis buffers and purification buffers, and higher salt concentrations were used in all purification buffers. Further, several changes to the purification protocol were undertaken to retain pure protein, e.g. the use of increased amount of protease inhibitor cocktail (cOmplete™ ULTRA Tablets). It also seemed beneficial to use freshly transformed cells and to not store the cell pellet longer than overnight at – 80 °C.

These modifications to the purification protocol resulted in a split of the elution of the protein that made up the typically observed BceB-ECD double band on SDS-PAGEs (Fig. 3.2 B). The protein of the former top band was eluted as faint band in a pure fraction at a concentration of 200 mM imidazole or higher (29 kDa, red box). The protein that made up the lower band (26 kDa, blue box) was eluted earlier from the column, together with other proteins. Downstream purification using AEX chromatography led to a fairly pure and concentrated protein sample. Mass spectrometry was used to confirm the identity of the proteins. Only the former top band (red box) seemed to contain the desired BceB-ECD, whereas the second analysed band (blue box) was found to result from the *E. coli* protein SlyD.

SlyD is a well-described enzyme that is ubiquitous in bacteria and has dual function (Löw, 2012). Aside from acting as peptidyl-prolyl cis-trans isomerase, SlyD also possesses chaperone activity (Scholz *et al.*, 2006). Chaperones assist in the folding mechanism of other proteins. In SlyD, this chaperone activity is performed by a so-called 'inserted-in-flap' domain that was shown to have high affinity to unfolded polypeptide chains (Weininger *et al.*, 2009). During overproduction of recombinant proteins, the host cells often upregulate chaperone production to deal with the large amount of unfolded protein (Villaverde & Carrio, 2003). Production of BceB-ECD might have acutely induced this stress response. In agreement with this, SlyD seemed far less abundant in expression trials using an empty pET-16b vector that did not contain the *bceB*-ECD coding region (data not shown). SlyD consists of 196 amino acids, which results in a molecular weight of around 22 kDa (P0A9K9, UniProtKB, Boutet *et al.*, 2007). Its size and molecular weight were similar to BceB-ECD, which led to the narrow double band on SDS-PAGE gels (Fig. 3.2 B).

Intriguingly, SlyD was categorised as metallochaperone and shown to be highly enriched in histidine (Löw, 2012). The C-terminal tail that harbours the metal binding domain (amino acids 150 to 196 in *E. coli*) contains a total of 15 histidine residues and can bind divalent cations via a conserved HGHXH motif. The chaperone was shown to bind Ni^{2+} ions with a K_d of 1.8 µM (Hottenrott *et al.*, 1997, Kaluarachchi *et al.*, 2009). This characteristic explained why SlyD is so often co-purified as contaminant during IMAC purification of recombinant proteins (Bolanos-Garcia & Davies, 2006). Just like the His_{10}-tagged BceB-ECD, SlyD could bind the nickel-charged IMAC column and co-purify. Due to a comparable theoretical isoelectrical point to BceB-ECD (4.81, ExPASy ProtParam, Gasteiger E., 2005), SlyD was eluted at a similar salt concentration to BceB-ECD during AEX chromatography (Fig. 3.2 C).

Refolding BceB-ECD from inclusion bodies and the described improvements to the purification protocol were two successful approaches to obtain higher quantities of BceB-ECD with a higher degree of purity. Hence, the *in vitro* characterisation of a potential binding reaction between bacitracin and $BceB\text{-}ECD^{ref}$ or $BceB\text{-}ECD^{sol}$, respectively, could proceed. The AMP bacitracin was shown to require zinc ions in a 1:1 ratio for biological activity (Stone & Strominger, 1971), and thus was applied as bacitracin zinc-salt throughout this study. In metal selectivity studies, SlyD was shown to also bind Zn^{2+} ions with high affinity in the sub-micromolar range (Kaluarachchi *et al.*, 2011). This makes SlyD likely to also bind the Zn^{2+} ion of bacitracin and the metallochaperone was therefore included in our *in vitro* assays as a positive control.

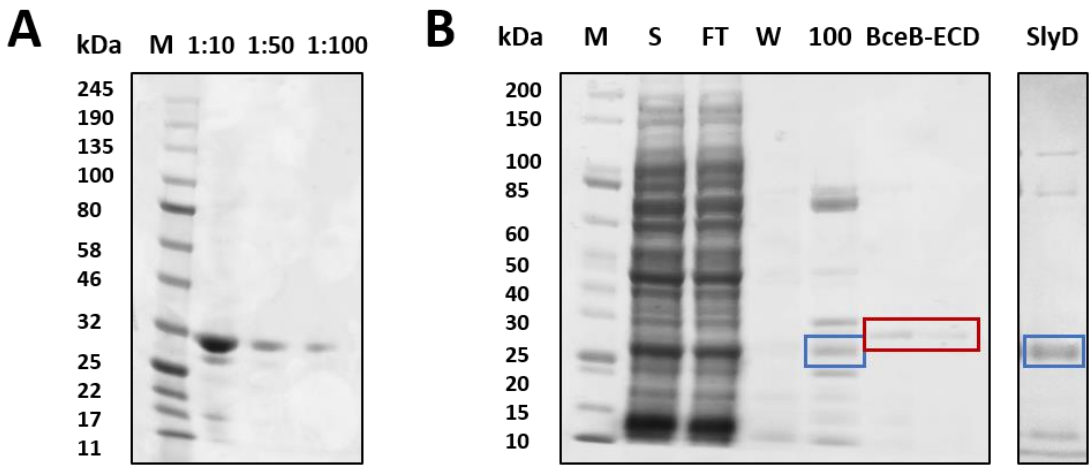

Figure 3.3: Improvements on overproduction and purification BceB-ECD from pSG1601 and refolding from inclusion bodies lead to increased yield and purity. A: SDS-PAGE analysis of diluted BceB-ECD samples, refolded from inclusion bodies using urea and slow removal thereof by dialysis. A clear band at 29 kDa was detected and confirmed as BceB-ECD by mass spectrometry. A minor band was revealed just below. M: marker, dilutions of refolded protein: 1:10, 1:50, 1:100. **B:** Improved cell lysis and changes to the purification protocol resulted in the separation of the usually observed double band by SDS-PAGE. IMAC purification using a 1 ml HisTrap led to elution of pure BceB-ECD at concentrations higher than 100 mM imidazole (former top band, red box). Follow-up AEX chromatography of the 100 mM fraction led to almost pure elution of SlyD, a metallochaperone with metal ion binding capacity (former bottom band, blue boxes). kDa: kilodalton, M: marker, S: supernatant, FT: flow through, W: wash, 100: 100 mM imidazole elution step. Proteins were visualised on SDS-PAGE gels using Coomassie staining solution or InstantBlue™ Protein Stain as indicated in II 5.1.

2.2.3 ANS fluorescence spectroscopy experiments suggest no conformational change of BceB-ECD in the presence of bacitracin.

A common approach to investigate binding reactions of highly dynamic proteins *in vitro* is the use of fluorescence spectroscopy (Wright & Dyson, 2009). To examine whether BceB-ECD comprised the substrate binding domain of the resistance transporter that interacts with the AMPs, ANS-based fluorescence assays were performed. 8-anilino-1-naphthalenesulphonic acid (ANS) is an organic compound with fluorescing properties that binds to hydrophobic regions on the surface of proteins (Gasymov & Glasgow, 2007). The dye has been extensively used to monitor conformational changes upon substrate binding. One example is the induced-fit binding mechanism between MurA, a crucial enzyme of the cell wall biosynthesis, and its substrate UDP-GlcNAc (Schonbrunn *et al.*, 1998). Upon conformational changes during substrate binding, the hydrophobic residues on the surface of the protein of interest alter their position. These hydrophobic residues are likely to be either more or less exposed to ANS, which results in an increase or quenching of the fluorescence signal during steady-state spectroscopy. Hence, experiments with BceB-ECD in the presence and absence of the substrate should allow conclusions on changes in the protein conformation, and thus on a binding interaction. This indirect assay was chosen as BceB-ECD does not contain any tryptophan residues and thus lacks sufficient auto-fluorescent properties to do direct measurements (Chen & Barkley, 1998). Yet, the indirect ANS measurement has potential drawbacks. The substrates to be tested in this assay are peptides and if they expose hydrophobic patches, they might also interact with ANS. This can lead to unspecific signal, and in case the substrate undergoes conformational changes upon binding, further experiments are required to investigate whether it is the AMP or BceB-ECD that rearranged its conformation.

Purified refolded or soluble BceB-ECD (BceB-ECD^{ref}, BceB-ECD^{sol}) or SlyD, respectively, were pre-mixed with ANS, before different AMPs were added in a stepwise fashion up to a concentration of 50 µM. The emission spectra were determined from 400 – 640 nm after excitation at 380 nm, and buffer corrected. Representative spectra of BceB-ECD^{ref}, BceB-ECD^{sol} and SlyD without substrate (0 µM) and at 50 µM for each substrate are depicted in Fig. 3.4 A, B, C. As expected from its previously described Zn^{2+}-binding ability, addition of Zn^{2+}-bacitracin resulted in an increased fluorescence emission for SlyD. The increased signal served as an indicator for the conformational changes that SlyD underwent upon binding Zn^{2+}-bacitracin, from which we concluded that our ANS fluorescence assay was functional

and suitable to detect binding reactions. The relative change in fluorescence emission was plotted against the substrate concentration and the data were modelled according to a saturating single-site binding curve (Fig. 3.4 D). From this, the dissociation constant K_d for Zn^{2+}-bacitracin was determined to be 9.89±2.45 µM. As nisin is not a substrate of BceAB and neither has divalent cations bound for biological activity, the lantibiotic served as negative control in these assays to identify potential unspecific binding. In agreement with our expectations, nisin did not cause any change in fluorescence emission, and therefore no binding reaction was detected when added to SlyD. Also the binding properties to mersacidin and actagardine were tested as they are substrates of BceAB. Their addition did not lead to changes in fluorescence emission which suggested no binding interaction between the AMPs and SlyD. Both AMPs require Ca^{2+} ions for biological activity, but SlyD was not shown to have affinity to calcium ions during metal selectivity studies (Kaluarachchi *et al.*, 2011).

Addition of bacitracin to BceB-ECD^{ref} and BceB-ECD^{sol} did not result in changes of the fluorescence emitted by ANS that could be fitted with a saturating single-site binding curve (Fig. 3.4 E, F). Although the fluorescence signal of the sample containing BceB-ECD^{sol} decreased upon addition of bacitracin the data was best approximated with a linear regression fit (Fig. 3.4 E). A non-saturating, linear proportionality equates a non-specific binding reaction (Motulsky & Christopoulos, 2004). The data for BceB-ECD^{ref} could also be approximated with a linear regression fit.

The graphs of panels E and F indicate that BceB-ECD^{ref} and BceB-ECD^{sol} potentially show different behaviour. This can however be redeemed, as BceB-ECD^{ref} and a shorter version BceB-ECD^{sol} showed highly similar CD spectra in III 2.2.3. The decline of ANS signal in panel E is likely an artefact caused by subtracting the buffer control containing only ANS and bacitracin. This distortion can be caused by inaccurate ANS or bacitracin concentrations in the cuvette, or a slightly different positioning of the cuvette in the spectrometer. Further, the graphs result from only two independent experiments each. Additionally, no decline or unspecific binding was observed in experiments with the shorter version of BceB-ECD^{sol} (III 2.2.3), supporting the linear decline in panel E to be an artefact.

These results suggested that BceB-ECD did not undergo a conformational change upon addition of bacitracin or that the ANS based assay was not able to reveal this interaction.

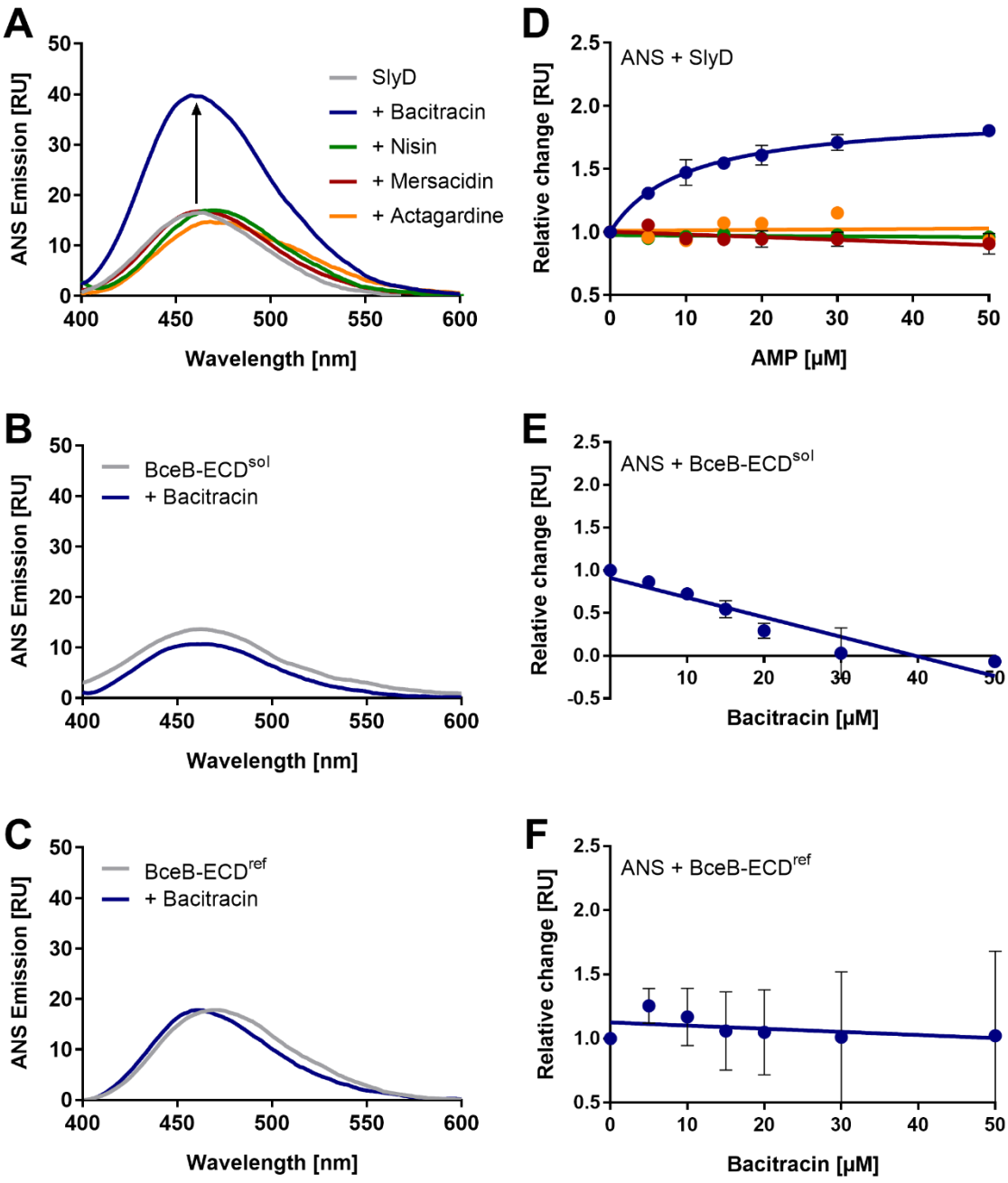
A
ANS Emission [RU]
Wavelength [nm]
SlyD
+ Bacitracin
+ Nisin
+ Mersacidin
+ Actagardine
B
BceB-ECD^sol
+ Bacitracin
C
BceB-ECD^ref
+ Bacitracin
D
ANS + SlyD
Relative change [RU]
AMP [µM]
E
ANS + BceB-ECD^sol
Bacitracin [µM]
F
ANS + BceB-ECD^ref
Bacitracin [µM]

Figure 3.4: ANS fluorescence spectroscopy experiments suggest no conformational change of BceB-ECD in the presence of bacitracin. Soluble or refolded BceB-ECD, SlyD or buffer, respectively, were pre-mixed with 100 µM ANS in a 1 cm quartz cuvette (4 µM protein concentration). Potential substrates were added to final concentrations of 5, 10, 15, 20, 30 and 50 µM. To ensure steady-state measurements, cuvettes were incubated in the spectrometer at 20 °C for 3 minutes after mixing and prior to each measurement. ANS fluorescence emission was measured every 0.5 nm wavelength over a spectrum from 400 to 640 nm, after excitation at 380 nm. Measurements were taken in triplicates with an automated average calculated. For each spectrum, the ANS emission at each determined wavelength was added up. Buffer measurements containing the respective concentration of substrate were subtracted from protein-containing samples. **A+B+C:** Representative buffer-corrected ANS fluorescence spectra of A: SlyD, B: BceB-ECD^{sol} and C: BceB-ECD^{ref} (grey) before stepwise addition of AMPs to a final concentration of 50 µM (bacitracin: blue, nisin: green, mersacidin: red, actagardine: orange). Spectra generally comprised a single emission peak at wavelength of 470 nm. Specific protein-substrate interaction that result in a conformational change should alter the ANS emission, as observed for the positive control SlyD in the presence of bacitracin. Spectra were smoothed with LOWESS smoothing for illustration. **D:** Dose response curve showing the relative change of ANS fluorescence in the presence of SlyD upon addition of AMPs. Bacitracin data were fit with a non-linear single-site binding curve, while all other data were approximated with a linear regression fit. **E+F:** Dose response curve of E: BceB-ECD^{sol} and F: BceB-ECD^{ref} showing the relative change of ANS fluorescence upon addition of bacitracin. Best fits of data were approximated with linear regression. Bacitracin data result from at least two independent measurements.

2.2.4 CD spectroscopy experiments with refolded BceB-ECD do not show conformational changes upon addition of bacitracin.

As a non-ANS based alternative approach to investigate the potential binding reaction between BceB-ECD and its substrate, circular dichroism (CD) spectroscopy experiments were performed.

CD spectroscopy is a frequently used method to examine intrinsically disordered proteins. Aside from conformational changes upon substrate binding, far-UV CD spectroscopy also gives insights into structural properties of proteins in solution (Dunker *et al.*, 2001). CD spectroscopy provides information on the secondary structure of a compound based on its ability to absorb left- and right-handed circularly polarized light (Kelly *et al.*, 2005, Greenfield, 2006). The difference in absorption of UV-light by the compounds is recorded in CD spectra. From the characteristic CD spectra of proteins with representative secondary structures, approximations of the secondary structure of a protein can be made. Far-UV CD spectra of prominent structural elements have been reported and representative spectra are depicted in Fig S3.2, modified from Greenfield (2006). An all-α-helical protein was reported to have two minima of similar magnitude at 222 and 208 nm, while it possesses very positive ellipticity at around 190 nm (black). A protein consisting of only antiparallel β-sheet has its minimum between 210 and 220 nm (red), and a maximum at around 195 nm. Random coils and intrinsically disordered proteins were described to have a very negative minimum at around 200 nm (green, Greenfield, 2006). According to secondary structure predictions in III 2.1, BceB-ECD was expected to contain a combination of all structural elements mentioned. A potential binding reaction between BceB-ECD and bacitracin should lead to a change of this secondary structure disclosed by a change in the CD spectra.

The experiments were performed on refolded BceB-ECD in absence and presence of AMPs, again using the *E. coli* protein SlyD as a positive control. The far-UV CD spectra were recorded from 195 or 200 to 260 nm wavelength and the respective spectra of buffer controls with or without AMPs were subtracted.

The spectra of purified SlyD without AMPs revealed the maximum of the spectrum at 195 nm with an extended minimum between 210 and 220 nm (Fig. 3.5 A, grey). Comparison with the exemplary spectra (Fig. S3.2) suggested a high content of antiparallel β-sheet, which is in agreement with the reported solution structure of SlyD obtained by nuclear magnetic resonance and CD spectroscopy (Weininger *et al.*, 2009, Martino *et al.*, 2009). As expected, the addition of nisin did not result in changes to the CD spectra. Also addition of mersacidin

and actagardine did not lead to changes of the CD spectra (data not shown). Upon addition of bacitracin, the ellipticity of SlyD increased at around 208 nm to a less negative value (Fig 3.5 A, blue). The minimum at 220 nm remained unaltered. The ellipticity at 222 and 208 nm is known to serve as an indicator for helicity (Hirst & Brooks, 1994, Wang *et al.*, 2006). A change of ellipticity towards a more positive value implies a loss, a more negative value suggests an increase of helicity. The comparison of the 222/208 nm ratio of a protein in the absence and presence of the substrate could thus be used to identify conformational changes upon substrate binding. For SlyD, the 222/208 nm ratio changed to a value significantly higher than 1 in the presence of bacitracin (Fig. 3.5 B), which suggested a loss in helicity. This finding is consistent with CD data for SlyD, which were interpreted as an increase of β-turn upon binding Ni^{2+} ions (Hottenrott *et al.*, 1997, Martino *et al.*, 2009). As the performed assay showed the structural rearrangements of SlyD upon binding the Zn^{2+} ions of bacitracin and did not suggest unspecific binding activity, we concluded the assay to be suitable for investigations on binding reactions that involve conformational changes.

The CD spectra recorded for refolded BceB-ECD displayed two minima at 208 and 222 nm (Fig. 3.5 grey). While the minima indicated some α-helical content, the minimum at 208 nm was more negative than the shoulder at 222 nm, which likely resulted from the predicted disordered content (III 2.1). CD measurements of BceB-ECD^{ref} in the presence of bacitracin resulted in a slight overall shift of the spectra to more positive values. However, the comparison of the 222/208 nm ratio of BceB-ECD without and with bacitracin did not result in a significant change of helicity. The shift might be the result of inaccuracies in protein or substrate concentrations in the cuvettes. This suggested that the secondary structure of refolded BceB-ECD was not altered in the presence of bacitracin.

These results were consistent with the findings of the ANS fluorescence assays (III 2.2.3), and indicated that refolded BceB-ECD did not undergo a conformational change upon addition of bacitracin. A possible explanation for the observed results was that refolding BceB-ECD from inclusion bodies did not recover biological activity during the failure-prone refolding process. CD spectra for BceB-ECD^{sol} were not obtained, as ANS fluorescence assays (III 2.2.3) suggested that there was no bacitracin binding activity. In contrast to refolded BceB-ECD, the amounts of pure BceB-ECD^{sol} were very low and restricted further experiments.

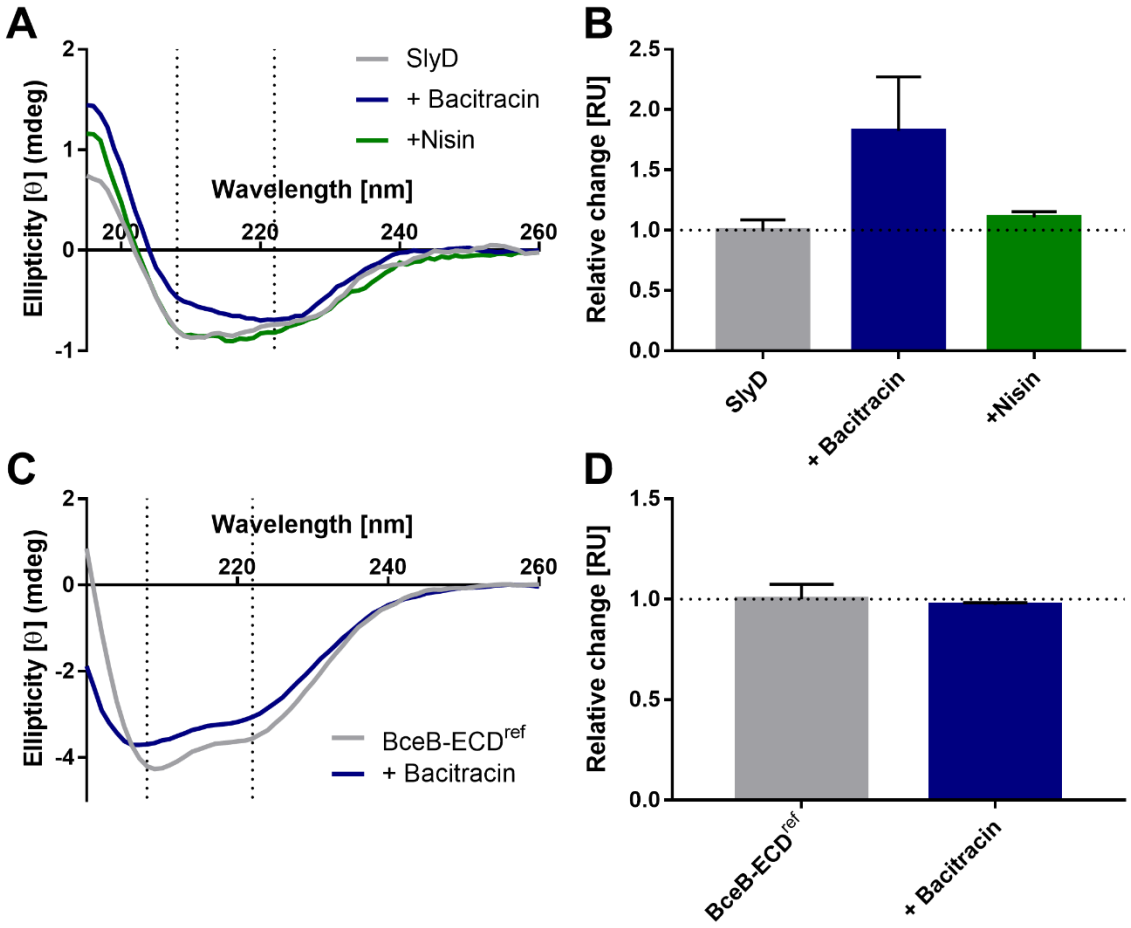

Figure 3.5: CD spectroscopy experiments with refolded BceB-ECD do not show conformational changes upon addition of bacitracin. Protein solutions (4 µM) or buffer were freshly mixed with potential substrates (90 µM) or buffer in a 1 mm quartz cuvette. Far-UV CD spectra were measured between wavelengths 195 or 200 and 260 nm. Five technical repeats were taken for each cuvette and averaged. The respective buffer controls were subtracted to unveil changes in the spectra of the protein sample. Vertical dotted lines mark the wavelengths 222 nm and 208 nm that are important indicators for helicity of a protein. **A+C:** Representative spectra of SlyD and refolded BceB-ECD in the absence (grey) or presence of bacitracin (blue) or nisin (green). **B+D:** The 222/208 nm ratio was determined from CD spectra and depicted relative to the 222/208 nm ratio of the protein sample without any potential substrates. Depicted are mean and standard deviation of three (SlyD) or two (refolded BceB-ECD) independently measured repeats.

2.3 A shortened version of BceB-ECD does not possess bacitracin binding capability *in vitro*.

2.3.1 Reduction of flexible ends increases yield and solubility of recombinant BceB-ECD.

The ECD of BceB as encoded on the so far used plasmid pSG1601 started at residue A310, which according to the *in silico* characterisation of BceB-ECD conducted for this chapter, was still predicted to be located in the membrane (III 2.1). In the full-length protein, the ends of the ECD are attached to transmembrane helices anchored in the membrane. The newly-acquired flexibility (Fig. 3.1 C) might lead to unspecific interactions and result in aggregation of the protein. This was possibly not only a cause for poor soluble production of BceB-ECD, but also could have resulted in preventing the binding activity of this domain.

To exclude that the highly-mobile ends interfered with biological activity, we produced shorter versions of BceB-ECD. We shortened the BceB-ECD encoding sequence of pSG1601 on both sides by taking away the nucleotides that encoded for either five or ten amino acids. This resulted in four different His_{10}-tagged constructs (pCKET1601, pCKET1602, pCKET1603, pCKET1604**,** schematic depicted in Fig. 3.6 A).

Overproduction in *E. coli* and cell lysis were performed according to the improved protocol described in III 2.2.2. Analysis of the cell lysate using SDS-PAGE revealed an additional band above the 25 kDa marker in the fractions of all shortened constructs (Fig. 3.6 B (3, 4, 5, 6)). The analysed lysate of the empty vector control and the original construct did not show any obvious additional bands (Fig. 3.6 B (E, B)).

For further work on BceB-ECD, the construct encoding BceB-ECD-3 was chosen (pCKET1601), which lacked the first and last five amino acids. Culture volumes for overproduction of BceB-ECD-3 were reduced to 50 – 200 ml and only a single IMAC purification step was performed. The eluted fractions resulted in a clear single band at 28 kDa, when analysed by SDS-PAGE (Fig. 3.6 C). Mass spectrometry (data not shown) and Western blot analysis (Fig. 3.6 D) confirmed that this band resulted from BceB-ECD. Taken together, shortening the flexible ends of BceB-ECD led to around 40-times higher yields of the protein, while maintaining high purity in a simple one-step purification. Reducing the length of the ECD also decreased the aggregation of BceB-ECD into inclusion bodies and greatly increased solubility.

To further investigate the quality of the protein, dynamic light scattering (DLS) experiments were performed. DLS is an established technique for the determination of particle size and homogeneity of a sample and therefore suitable to investigate protein aggregation (Li *et al.*, 2011, Stetefeld *et al.*, 2016). DLS on BceB-ECD led to a single peak that suggested the average

diameter of BceB-ECD to lie at around 20 nm (volume distribution, data not shown). If the BceB-ECD was a perfectly globular protein, with its predicted size of 26 kDa (including His_{10}-tag), it should theoretically have a minimal diameter of around 4 nm (Erickson, 2009). While the high flexibility of BceB-ECD indicated that BceB-ECD could have a larger diameter, it was still likely that BceB-ECD aggregated to a low degree in solution. Yet, the polydispersity index (PdI) was determined to be 0.270, which suggested a monodisperse size distribution of BceB-ECD with few bigger aggregates, and thus can be considered as homogenous sample.

While protein aggregates might have reduced or no biological function, aggregation is often reversible (Cromwell *et al.*, 2006). Soluble aggregates in particular have generally only weak interactions with each other that can be reversed when encountering a binding partner with higher binding affinity. As the aggregates were formed in a purified sample, the aggregation of BceB-ECD is likely the result of self-association, which describes the non-specific interaction with the same type of protein (Wang *et al.*, 2010). Self-associating proteins are likely to directly aggregate or oligomerise in their folded state, without any unfolded intermediates. We concluded from these considerations that despite low degree aggregation, purified BceB-ECD could be tested for its binding activity.

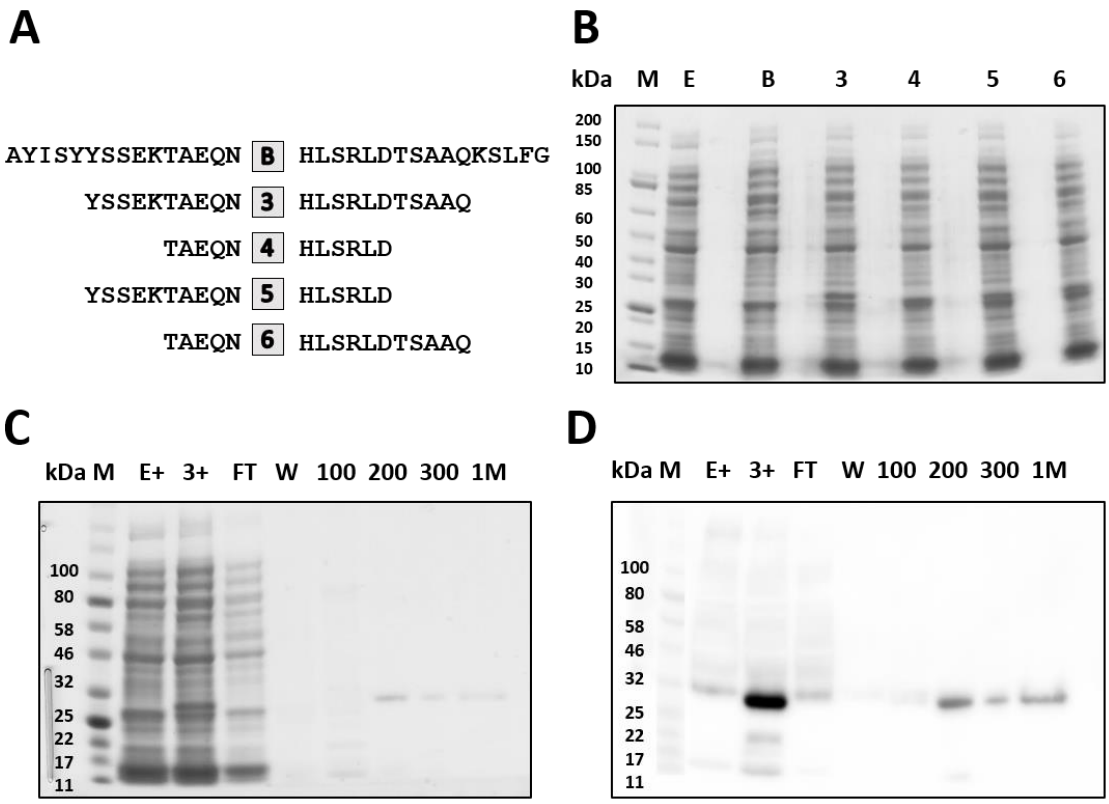

Figure 3.6: Reducing the length of flexible ends of BceB-ECD increases yield and solubility drastically. A: Schematic of the N- and C-terminal amino acid sequence of original and shortened BceB-ECD constructs. B: original BceB-ECD sequence as produced from pSG1601. 3-6: Nucleotide sequence of *bceB*-ECD was shortened to encode five or ten fewer amino acids on either side of the ECD (3: pCKET1601, 4: pCKET1602, 5: pCKET1603, 6: pCKET1604). **B:** Overproduction of shortened BceB-ECD proteins. Unpurified cell lysate supernatants of E: empty vector control, B: original construct, 3-6: shorter versions of BceB-ECD as depicted in A. Additional bands can be identified in fractions 3-6, but are absent in E and B. **C:** SDS-PAGE of samples after IMAC purification of BceB-ECD-3 resulted in a pure band in fractions containing 200 mM imidazole or more. Proteins were visualised on SDS-PAGE gels using InstantBlue™ Protein Stain as described in II 5.1. **D:** Western blot analysis of samples described in C using an α-His antibody. kDa: kilodalton, M: marker, E+: empty vector control, IPTG-induced, 3+, lysate of cells with construct BceB-ECD-3, FT: flow through, W: wash, 100, 200, 300: imidazole concentration in mM, 1M: 1 M imidazole.

2.3.2 Spectroscopy experiments on BceB-ECD with increased solubility do not unveil bacitracin-induced conformational changes.

To investigate the bacitracin-binding properties of the shortened construct, the steady-state ANS fluorescence spectroscopy assay was repeated. As described before, purified BceB-ECD was pre-mixed with ANS, and bacitracin was added in steps until a final concentration of 50 µM was reached. Addition of bacitracin to the BceB-ECD-ANS solution did not result in a change of fluorescence emission (Fig. 3.7 A + B).

This particular experiment was only performed once. Further measurements on purified BceB-ECD were conducted at a final concentration of 50 µM only (III 2.4.1). As these experiments did also not indicate conformational changes of BceB-ECD in the presence of bacitracin, the step-wise titration performed here was not repeated.

Further, the potential interaction between BceB-ECD and bacitracin was examined by far-UV CD spectroscopy in the presence and absence of bacitracin. The spectra of soluble BceB-ECD revealed a shoulder at 222 nm and an absolute minimum at 208 nm (Fig. 3.7 C). With an ellipticity value of 0.68 mdeg, the spectra hardly reached into positive ellipticity at 195 nm. To calculate the secondary structure content from experimental data, the spectra were analysed using DichroWeb (Whitmore & Wallace, 2004, Whitmore & Wallace, 2008). The experimental data were approximated using the CONTIN-LL algorithm (Provencher & Gloeckner, 1981, Sreerama & Woody, 2000). BceB-ECD was found to consist of 10.5 % helical content, 34 % β-strand and of 55.5 % non-regular, unordered structures. The high percentage of disordered content (> 50 %) is consistent with the *in silico* predictions of the secondary structure of BceB (III 2.1). The values found for regular structures differed from predictions (α-helix: 10.5 % versus 22.8 %, β-strand: 34 % versus 25 %). Explanations for the difference could be deviations in the approximations of the data (NRMSD (normalised root mean square deviation): 0.106), and only few known similar structures that online tools can base their secondary structure predictions on.

The addition of nisin, which was used as negative control, did not result in changes of the CD spectra of Bce-ECD (Fig. 3.7. C, green). In the presence of bacitracin, the BceB-ECD spectra (Fig. 3.7 C, blue) were found to be almost identical to the 'BceB-ECD only' spectra (Fig. 3.7 C, grey). Also the 222/208 nm ratio did not show significant changes (Fig 3.7 D). These findings indicate that BceB-ECD did not undergo a conformational change. This led to the conclusion that also the shorter version of BceB-ECD was unlikely to bind bacitracin, unless the binding mechanism did not involve structural changes.

It is also possible that the quality of purified BceB-ECD was too poor and the protein could not adopt its native, biologically-active fold. Increased solubility and monodispersity argue against this explanation. Further, the recorded far-UV CD spectra of the refolded and the soluble BceB-ECD were not significantly different and reproducible throughout different protein samples.

Another explanation for the lack of apparent binding could be that free bacitracin was not the physiological substrate of BceAB. It has been shown previously that the full-length BceAB transporter bound bacitracin (Dintner *et al.*, 2014). Nevertheless, it could not be excluded that bacitracin was recognised as it was bound to its target in the outer face of the membrane, co-solubilised undecaprenyl pyrophosphate (UPP). A direct interaction of BceAB with the UPP-bacitracin ([UPP-BAC]) complex has been discussed by several studies (Mascher *et al.*, 2003, Bernard *et al.*, 2007) and even UPP alone was proposed to be the physiological substrate of BceAB (Kingston *et al.*, 2014).

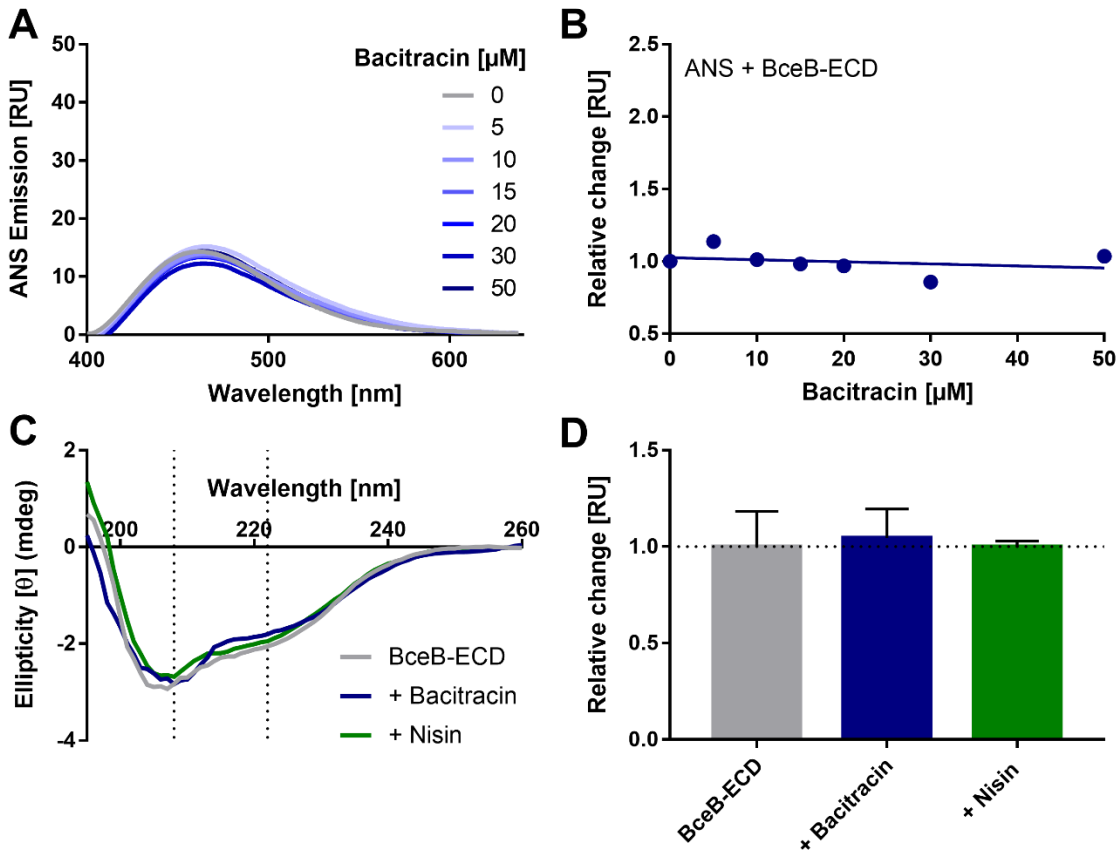

Figure 3.7: Spectroscopy experiments on BceB-ECD with increased solubility do not exhibit bacitracin-induced conformational changes. ANS fluorescence and CD spectroscopy experiments were performed as described before (Fig. 3.4 + Fig. 3.5), but with the shortened version of BceB-ECD. **A:** ANS fluorescence spectra of BceB-ECD in the presence or absence of different concentrations of bacitracin, as indicated. Spectra were smoothed with LOWESS smoothing or illustration. B: Dose response curve of ANS emission upon addition of bacitracin to BceB-ECD. Data points were approximated using a linear regression fit. **C:** Representative spectra of BceB-ECD in the absence (grey) or presence of bacitracin (blue) or nisin (green). **B+D:** The 222/208 nm ratio was determined from CD spectra and depicted relative to the 222/208 nm ratio of the protein sample without any potential substrates. Depicted are mean and standard deviation of three independently measured repeats.

2.4 The complex formation of [GPP-BAC] masks a potential binding reaction of BceB-ECD.

2.4.1 A potential increase of ANS fluorescence emission upon addition of [GPP-BAC] is subject to high variation.

We thus investigated the proposal that the bacitracin-target complex in the membrane was the physiological substrate of BceAB (Bernard *et al.*, 2007, Fritz *et al.*, 2015), rather than free bacitracin. Further, we sought to examine whether the cellular target alone could act as substrate (Kingston *et al.*, 2014) and characterise a potential BceB-ECD binding activity *in vitro*.

In a previous study, bacitracin was shown to bind tightly around the pyrophosphate group and to interact with only the first prenyl group (Economou *et al.*, 2013). The crystal structure of bacitracin was obtained in complex with geranyl pyrophosphate (GPP). With only two isoprenoid units (C_{10}), GPP has a shorter lipid chain compared to UPP (C_{55}), and thus better solubility in the aqueous buffers used in our experiments. We therefore chose GPP as artificial bacitracin target to examine a potential binding reaction between BceB-ECD and either the GPP-bacitracin ([GPP-BAC]) complex or GPP alone.

Bacitracin undergoes a conformational change when binding its membrane-located target (Economou *et al.*, 2013). Hence, to avoid an overlay of signal, we had to make sure that most bacitracin in the assay was already in complex with its target. To test at which concentration the complex formation between bacitracin and its target GPP was saturated, ANS fluorescence-based titration assays were performed.

Titration of GPP or bacitracin alone to an ANS-containing buffer resulted in a linear increase of the ANS fluorescence signal (Fig. S3.3 A, B), which corresponds to a non-specific binding reaction (Motulsky & Christopoulos, 2004). When GPP was gradually added to 50 µM bacitracin that had been pre-incubated with ANS, the fluorescence signal plateaued from around 150 µM GPP onwards. The data could be approximated with a non-linear regression fit, indicating the specific binding interaction between bacitracin and GPP and the saturation of the [GPP-BAC] complex formation (K_d = 90 µM, Fig. S3.3 C). Thus, for the reverse experiment, a GPP concentration of 200 µM was chosen. Bacitracin was gradually added to the GPP and showed saturation of the fluorescence signal at around 50 µM bacitracin (Fig S3.3 D). Again, the data could be approximated with a non-linear single site binding curve. These findings suggested that at concentrations of 50 µM bacitracin and 200 µM GPP, most bacitracin is in complex with GPP. Addition of bacitracin to concentrations higher than 50 µM

led to a linear increase in fluorescence (Fig S3.3 D grey, linear regression fit), which resulted from the unspecific binding between excess free bacitracin and ANS. As we aimed to avoid free bacitracin in our assays, we ensured an excess of GPP by using 500 µM GPP for further experiments.

Rather than a gradual increase of the substrate concentration as described in III 2.2.3, the steady-state ANS fluorescence assay was performed in the absence and presence of final concentrations of bacitracin (50 µM), GPP (500 µM) or the premixed [GPP-BAC] complex (50 µM + 500 µM GPP).

As shown before (III 2.3.2), ANS fluorescence experiments between BceB-ECD and free bacitracin did not result in a significant change of the fluorescence intensity (Fig. 3.8). Further, the addition of GPP did not affect the signal, suggesting that BceB-ECD did not undergo a GPP binding-induced conformational change. In the presence of the premixed [GPP-BAC] complex, the ANS fluorescence signal was seemingly increased (Fig. 3.8 A). However, statistical analysis of the relative ANS fluorescence did not show a significant difference between the fluorescence emission of the BceB-ECD sample without and with [GPP-BAC] added (Fig. 3.8 B). The measurements in the presence of [GPP-BAC] were subject to high variation in both, samples containing BceB-ECD and respective buffer controls. Despite efforts to account for the variations, they were likely caused by structural changes resulting from the complex formation between GPP and bacitracin. It is therefore unclear whether this non-significant trend was caused by a conformational change of BceB-ECD upon binding [GPP-BAC] or whether it was an artefact from [GPP-BAC] complex formation.

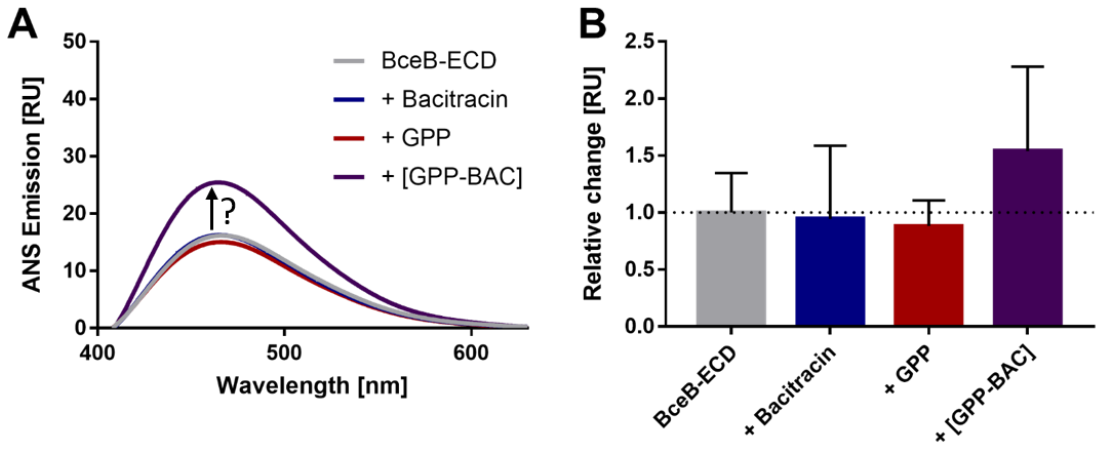

Figure 3.8: Potential increase of ANS fluorescence emission upon addition of [GPP-BAC] is subject to high variation. Steady-state ANS fluorescence experiments of BceB-ECD and potential substrates were performed as described in Fig. 3.4. In this assay, ten technical repeats were measured and averaged for each cuvette. Rather than gradual addition, substrates were administered in a single step to a final concentration of 50 µM bacitracin, 500 µM GPP or 50 µM + 500 µM pre-mixed [GPP-BAC]. **A:** Representative ANS fluorescence spectra of BceB-ECD (grey) before addition of potential substrates (bacitracin: blue, GPP: red, [GPP-BAC]: purple). Spectra were smoothed with LOWESS smoothing for illustration. **B:** Change in ANS emission relative to the signal for BceB-ECD without any potential substrates added. Bar graphs show the mean ± standard deviation of at least two independent measurements, BceB-ECD alone and in the presence of [GPP-BAC] were measured at least in four independent repeats.

2.4.2 CD spectra of BceB-ECD remain inconclusive due to high variation of the [GPP-BAC] signal.

To further examine the potential binding reaction between the shortened BceB-ECD and the [GPP-BAC] in a non-ANS based assay, far-UV CD spectroscopy was used. CD spectra of BceB-ECD in the absence of any potential substrate were found to be consistent with the spectra described in 2.3.2 (Fig. 3.9 A, grey). Addition of free GPP or free bacitracin, respectively, resulted in similar curves to the spectra without any potential substrates added (Fig. 3.9 A, blue, red). In line with the findings of ANS fluorescence spectroscopy, these observations did not indicate any conformational changes induced by GPP or bacitracin. Slight changes in the spectra as displayed in the representative curves for bacitracin lie within experimental error and were not reproducible. In agreement with this, the analysis of the 222/208 ratio did not show significant changes (Fig. 3.9 B).

The addition of [GPP-BAC] to BceB-ECD resulted in highly variable CD spectra (spectra of eight independent measurements are depicted in Fig. 3.9 C). The shapes of the spectra differed considerably from spectra that had been determined for BceB-ECD before. Instead of the absolute minimum at 208 nm and a shoulder 222 nm, the spectra measured in the presence of [GPP-BAC] comprised a minimum at 222 nm and a peak at 200 nm, or an absolute minimum at 200 nm (Fig. 3.9 C, purple). At wavelength 200 nm, CD spectra for BceB-ECD-[GPP-BAC] even fluctuated between minimal and maximal ellipticity values of -5 and 5 mdeg. This variation could be explained by the structural change bacitracin undergoes upon complex formation with GPP (Economou *et al.*, 2013). CD spectra of free GPP and unbound bacitracin by themselves only showed little or moderate CD signal intensity, respectively (Fig. 3.9 D, red, blue). CD spectra of the [GPP-BAC] complex revealed a stark increase in amplitude, with positive ellipticity of almost 5 mdeg at 222 nm and a negative absolute minimum of nearly -20 mdeg at 200 nm wavelength (Fig. 3.9 D, purple). The combination of GPP and bacitracin ([GPP-BAC]) clearly resulted in a larger ellipticity signal than simple addition of the spectra determined for free bacitracin and free GPP. This super-additive effect confirmed the changes of the secondary structure upon [GPP-BAC] complex formation.

Due to the increased magnitude of the around 5-times stronger ellipticity signal, variations of the protein and substrate concentrations in the cuvette were more pronounced. Even slightest differences in [GPP-BAC] concentration between buffer controls and cuvettes containing the BceB-ECD-[GPP-BAC] mix or between repeats led to substantial variation of the spectra and inaccurate buffer subtractions. As this variation masked any potential

conformational change of BceB-ECD, we could not conclude on whether this domain interacted with the [GPP-BAC] complex.

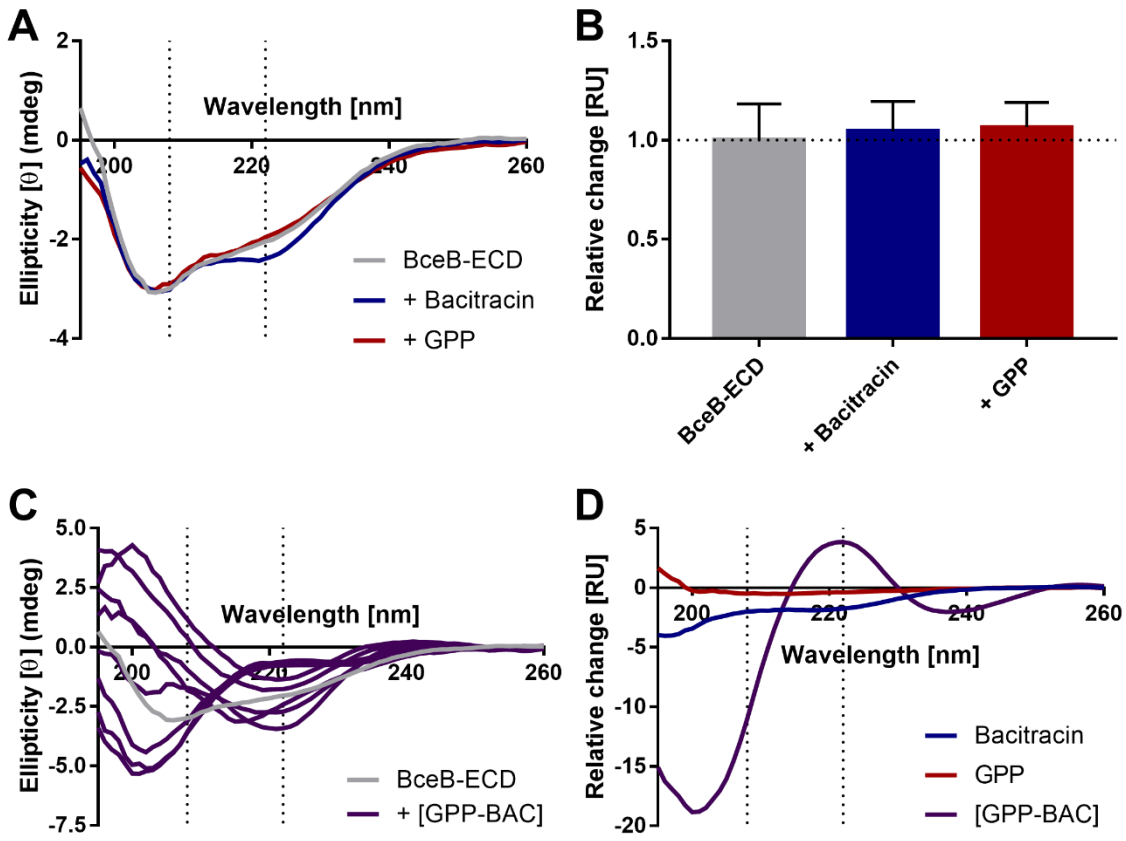

Figure 3.9: CD spectra of BceB-ECD remain inconclusive due to high variation of the [GPP-BAC] signal. Far-UV CD spectroscopy experiments were performed as described before (Fig. 3.5) at a final concentration of 50 µM bacitracin, 500 µM GPP or 50 µM + 500 µM pre-mixed [GPP-BAC]. **A:** Representative CD spectra of BceB-ECD alone (grey) and after addition of potential substrates (bacitracin: blue, GPP: red). **B:** The 222/208 nm ratio was determined from CD spectra and depicted relative to the 222/208 nm ratio of the protein sample without any potential substrates. Depicted are mean and standard deviation of six independently measured repeats. **C:** CD spectra of eight independent measurements of BceB-ECD in the presence of [GPP-BAC] after buffer subtraction. **D:** Representative CD spectra of the potential substrates (blue: bacitracin, red: GPP, purple: [GPP-BAC]), normalised against buffer.

3. Discussion

In this chapter, we focussed on investigating whether the large extracellular domain of BceB (BceB-ECD) is the binding domain of the resistance transporter. Due to low sequence conservation of BceB-ECD (Dintner *et al.*, 2011, Coumes-Florens *et al.*, 2011), the function of BceB-ECD, which is thought to be responsible for substrate specificity (Hiron *et al.*, 2011), is likely to be conserved on a structural level rather than by sequence. This idea was reinforced by the *in silico* analysis of BceB-ECD performed in this chapter (III 2.1). BceB-ECD was found to contain an intrinsically disordered region with a so-called molecular recognition feature (MoRF). MoRFs have been shown to play an important role in binding interactions, which often involve a conformational change with a disorder-to-order transition (Mohan *et al.*, 2006). We therefore proposed BceB-ECD to undergo substrate-induced coupled binding and folding, similar to a 'fly-casting' mechanism (Shoemaker *et al.*, 2000). To test this hypothesis using biochemical and biophysical methods, we first successfully established an optimised protocol for the overproduction and purification of BceB-ECD. The isolated domain was then tested for *in vitro* binding activity using ANS fluorescence and far-UV circular dichroism (CD) spectroscopy techniques.

3.1 BceB-ECD does not undergo a conformational change in the presence of bacitracin or GPP.

ANS fluorescence and CD spectroscopy-based experiments were performed on refolded and soluble recombinant BceB-ECD. Despite the use of several techniques and different BceB-ECD constructs, the domain did not seem to undergo a significant conformational change in the presence of bacitracin. These results suggested that purified BceB-ECD did not bind bacitracin *in vitro*, unless the highly-flexible domain did not undertake a detectable structural transition upon binding bacitracin. As an alternative to assays that were mainly based on the detection of conformational changes, preliminary isothermal titration calorimetry (ITC) experiments were performed. This powerful method is based on the direct measurement of the heat absorbed or released by a binding event and can not only give information on the binding constant (K_d) but also on enthalpy, entropy and reaction stoichiometry (Pierce *et al.*, 1999, Leavitt & Freire, 2001). However, the results were inconclusive (data not shown), due to technical challenges including problems to equalise the buffer concentrations and pH

between the cell containing the protein solution and the concentrated bacitracin in the injection syringe, which required a more acidic pH to stay soluble.

Although the quality and solubility of the recombinant BceB-ECD seemed suitable for an *in vitro* binding characterisation, no binding activity between BceB-ECD and bacitracin was discovered with the methods used. It was, however, possible that free bacitracin alone was not the physiological substrate of BceAB. It is well-known that BceAB confers resistance against bacitracin (Ohki *et al.*, 2003), and it has also been demonstrated that the full-length BceB transport permease interacted with bacitracin (Dintner *et al.*, 2014). However, the experiments could not exclude that the physiological substrate was bacitracin in complex with its target undecaprenyl pyrophosphate (UPP) in the outer face of the membrane. The identity of the true substrate of BceAB has been a much-debated question, with various proposed hypotheses. While recognition and transport of the free AMP seemed most intuitive, the UPP-bacitracin ([UPP-BAC]) complex as physiological substrate has been discussed by several studies (Mascher *et al.*, 2003, Bernard *et al.*, 2007). Furthermore, a computational analysis of the signalling dynamics in the Bce system by Fritz and colleagues (2015) was based on the hypothesis that BceAB only recognised target-bound bacitracin or the complex between bacitracin and UPP as a whole. Kingston and colleagues (2014) took this line of reasoning a step further and proposed transport of UPP rather than AMPs.

ANS fluorescence and CD spectroscopy experiments did not reveal any conformational changes of BceB-ECD in the presence of geranyl-pyrophosphate (GPP), which was used as surrogate for the cellular target of bacitracin, undecaprenyl pyrophosphate (UPP). These findings suggested that also the cellular target alone was not recognised as substrate and bound by BceB-ECD *in vitro*.

Similar experiments were performed in the presence of the [GPP-BAC] complex. Attention was paid to pre-mix both compounds at a ratio that should saturate complex formation. Yet, the conformational change that bacitracin undergoes when binding its target led to enormous variation in the measurements, even in the absence of BceB-ECD. While ANS fluorescence measurements might have indicated a slight conformational change of BceB-ECD (III 2.4.1), the results derived from CD spectroscopy were too variable to analyse (III 2.4.2). This made firm conclusions on a potential binding interaction between BceB-ECD and the [GPP-BAC] complex impossible. Based on the results of this chapter, also bacitracin in complex with UPP could be neither confirmed nor excluded as physiological substrate of BceAB.

As we sought to investigate if BceB-ECD was the binding domain and worked according to a 'fly-casting mechanism' (Shoemaker *et al.*, 2000, Huang & Liu, 2009), the techniques chosen for this chapter were based on detecting conformational changes. Although the methods were functional and generally suitable to investigate substrate binding, they were seemingly not optimal for BceB-ECD binding assays that included the [GPP-BAC] complex, due to the variable background signal during GPP binding by bacitracin.

We thus attempted to measure binding between BceB-ECD and bacitracin, when it is in its amphipathic, 'bound' configuration, but in the absence of its target. For this, high pressure ANS fluorescence experiments with BceB-ECD and free bacitracin were envisaged. The high pressure was thought to potentially constrain bacitracin to the conformation that it adopts in complex with GPP (Lullien & Balny, 2002, Maeno & Akasaka, 2015). However, preliminary experiments were unsuccessful as the high pressure resulted in irreversible precipitation of bacitracin and BceB-ECD (data not shown).

3.2 The membrane environment might be required for recognition of AMPs.

The idea that proteins require the membrane-association of antimicrobial peptides to be able to recognise them as substrate is not unprecedented. Other than potential bacitracin recognition by BceAB when in complex with its membrane-bound target (Bernard *et al.*, 2007, Kingston *et al.*, 2014), several other examples of substrate recognition in the membrane environment have been discussed that stand in direct context with this study.

SdpC (sporulation delaying protein) is an antimicrobial peptide intrinsically-produced by *B. subtilis* (González-Pastor *et al.*, 2003). Described as a cannibalism toxin, SdpC production is activated upon nutrient limitation during stationary growth phase in order to kill neighbouring *B. subtilis* cells. As toxin-producing cells are protected by the immunity protein SpdI (Ellermeier *et al.*, 2006), survivors can take up the nutrients released by their lysed siblings (González-Pastor *et al.*, 2003). The production of SdpI is regulated by the presence of the SdpC toxin. SdpC was shown to form a complex with the membrane protein SdpI. In turn, the autorepressor SdpR is recruited to the membrane, and expression of the *sdpRI* operon is de-repressed (Ellermeier *et al.*, 2006). It has recently been discovered that SdpC production intrinsically activates the Bce system of *B. subtilis* (Hofler *et al.*, 2016). Despite strong induction of the BceR target promotor P_{bceA} by such cannibalism toxins, no contribution of BceAB to resistance or immunity against SdpC could be detected (Hofler *et al.*, 2016). Although expression of *spdC* and production of the toxin seemed unimpaired, removal of the

immunity protein SdpI resulted in the total loss of the signalling response through BceAB-BceRS. This indicated that complex formation between SdpI and the toxin in the membrane environment is potentially required for SdpC perception by the Bce system (Hofler *et al.*, 2016), similar to our hypothesis that bacitracin may only be recognised in complex with UPP. Moreover, the transcription regulator BcrR of *E. faecalis* is known to activate transcription of the bacitracin resistance operon *bcrABDE* (I 5.1.2, Manson *et al.*, 2004, Gauntlett *et al.*, 2008). In contrast to BceRS-BceAB-like resistance systems, where the stimulus is perceived indirectly via the BceAB transporter, here the regulator BcrR directly binds Zn^{+}-bacitracin (Gebhard *et al.*, 2009). Though, the distinct AMP binding site has not yet been identified. BcrR is localised in the membrane and its four predicted transmembrane helices are connected by short extracellular and cytoplasmic linkers, lacking an obvious binding site (Manson *et al.*, 2004, Gebhard *et al.*, 2009). Also binding via the cytoplasmic N-terminal DNA binding domain was unlikely, as the targets of bacitracin are generally located in the outer face of the membrane. Bacitracin was shown to affect the cell membrane not only by interactions with cell wall synthesis precursors (Hancock & Fitz-James, 1964, Ming & Epperson, 2002). It was therefore proposed that BcrR might recognise and bind bacitracin when the AMP is associated with or inserted into the membrane (Gebhard *et al.*, 2009), even in the absence of UPP.

Further, the LanI-type immunity proteins SpaI and NisI of *B. subtilis* and *L. lactis,* respectively were discussed to recognise their corresponding substrates in the membrane environment (I 4.4.1). The exact resistance mechanism by LanI proteins remains puzzling, yet direct binding interactions with their substrates subtilin (SpaI) and nisin (NisI) have been demonstrated (Stein *et al.*, 2003, 2005, Takala *et al.*, 2004). Both proteins are brought in close contact with the negatively charged membrane via their highly positively charged N-terminal domains. The substrate binding sites of NisI and SpaI seem to be located on the extracellular regions of the lipoproteins, which exhibit negatively charged patches proximal to the membrane (Christ *et al.*, 2012a, Hacker *et al.*, 2015b). The immunity proteins might thus sequester their substrates when they are associated with the membrane. It is therefore conceivable that also substrate binding of BceAB operates according to a similar principle and recognises the membrane-bound substrate via its extracellular domain.

With a binding affinity in the micromolar range, the interaction between NisI and nisin was shown to be rather weak (Takala *et al.*, 2004). Considering that nisin is biologically active in a nanomolar range, the low affinity raised doubts about how NisI could effectively provide resistance. It has therefore been proposed that lipid II might be required in addition (Hacker *et al.*, 2015b). The affinity of NisI to its membrane-bound substrate has not yet been

determined. In agreement with the potential requirement of lipid II, the crystal structure of NisI revealed a deep cleft formed between the N- and C-terminal domains and the flexible linker region (Jeong & Ha, 2018). This cleft was proposed to bind the pyrophosphate moiety of lipid II, indicating that NisI can specifically recognise both components of the [lipid II-nisin] complex.

The core domain of the immunity protein SpaI was shown to possess a very negatively charged surface, which directly faces the likewise negatively charged cytoplasmic membrane (Christ *et al.*, 2012a). Homology models of the LanI-type proteins EriI and EtnI that confer immunity to ericin S and entianin, respectively, revealed the same membrane-orientated negative patches. As their respective substrates have an overall positive charge, it was conceivable that the negatively charged surface was responsible for possible interactions with membrane-associated lantibiotics (Christ *et al.*, 2012a). It was therefore speculated that upon target binding via the N-terminal lanthionine rings, the C-terminal positive residues of subtilin are exposed and might serve as binding sites for SpaI (Christ *et al.*, 2012a).

These examples demonstrate that it is indeed likely that AMPs can be recognised when associated with their membrane bound targets rather than in their free form. A common feature of bacitracin and class I lantibiotics like nisin and subtilin is that the peptides undergo major structural rearrangements when binding their targets (Economou *et al.*, 2013, Hsu *et al.*, 2004, Medeiros-Silva *et al.*, 2018). These adjusted 'bound' conformations might expose structural cues that allow resistance and regulatory proteins to recognise them as substrate. Many other AMPs undergo a conformational change when binding their target, membrane-based lipid II cycle intermediates (Breukink & de Kruijff, 2006, Oppedijk *et al.*, 2016). Depending on the surrounding environment, the class II lantibiotic mersacidin can acquire various conformations (Hsu *et al.*, 2003). When bound to its target lipid II, the structure of mersacidin is distinctly different from its free form. Similar to nisin (Medeiros-Silva *et al.*, 2018), mersacidin was shown to contain a hinge region with which it can adjust the exposure of charges upon binding and in that way adapt to its environment. Containing the same hinge-region, similar conformational flexibility was also suggested for actagardine and its derivatives (Hsu *et al.*, 2003, Breukink & de Kruijff, 2006). Further, NMR solution structures suggest two distinct conformations for the class II lantibiotic nukacin ISK-1 (Fujinami *et al.*, 2018). In only one of the states nukacin ISK-1 is capable of binding lipid II.

It is therefore possible that certain resistance proteins are able to distinguish between the free and target-bound form of the AMPs. This would bring the advantage that the resistance determinant removes the AMP directly from its inhibited target, rather than binding free

AMPs in the periphery. When UPP and lipid II are released from the inhibitory grip of the AMP, they can be transmitted to the next stage in the lipid II cycle. The AMP is often unable to recognise the resulting lipid II cycle intermediate or only binds it with much lower affinity, and hence the cell wall synthesis can be kept intact.

Analogously to these resistance proteins, it is quite possible that also BceAB can differentiate between the two configurations of its substrates. This would explain, why the data in this chapter suggested no interaction between BceB-ECD and bacitracin in its free form, but indicated a possible affinity to the [UPP-BAC] complex. Bacitracin might not have adopted the correct amphipathic configuration required for binding by BceB-ECD, when it was not associated with its target.

3.3 ECDs can combine substrate recognition in the membrane environment with a broad substrate range.

Most of the BceAB-like resistance transporters described so far were shown to confer resistance against several substrates (Staron *et al.*, 2011, Gebhard, 2012). LanFEG-type transporters were shown to mediate resistance against the same type of substrates as BceB-like transporters, mostly antimicrobial peptides (AMPs). Yet, LanFEG transporter were generally found to only confer resistance against a single specific substrate (Gebhard, 2012). Only few exceptions are described where the transporter also binds almost identical derivatives of a certain AMP, e.g. EpiFEG that recognises both, gallidermin and epidermin (Otto *et al.*, 1998). One explanation for this substrate exclusivity is that LanFEG transporters usually protect their host against a specific endogenously produced AMP, and thus confer immunity rather than resistance against exogenously stimuli (Stein *et al.*, 2003, 2005, Okuda *et al.*, 2008). Notably, LanFEG transporters lack an obvious binding site, while the large extracellular domain between TMH7 and TMH8 is one of the main characteristics of the BceAB family (Gebhard, 2012, Dintner *et al.*, 2011). It is thus plausible that the large, flexible ECD of BceB enables recognition of a broader substrate range, as it is shown for multidrug efflux pumps like AcrAB (Chapter I). In this type of transporters, the periplasmic domains are responsible for substrate recognition and binding. The conformational flexibility of these binding domains facilitates the characteristic broad substrate range of AcrB-like efflux pumps (Yu *et al.*, 2003).

Extracytoplasmic domains also play an important role in the substrate binding of MacB-like transporters (for details, refer to Chapter I). MacB is an efflux pump in several Gram-negative

bacteria that provides resistance against macrolide antibiotics and AMPs like bacitracin and colistin. The ECDs of MacB were suggested to be the substrate binding domains (Crow *et al.*, 2017). A similar role has been proposed for the ECDs of the lipoprotein extractor LolCDE (Crow *et al.*, 2017). Furthermore, the ECDs of FtsEX, prevalent in many Gram-positive and Gram-negative bacteria, were shown to be responsible for the direct interaction with the respective binding partner of FtsX, after the ECDs have acquired their active conformation (Mavrici *et al.*, 2014, Sham *et al.*, 2013).

These insights suggest that it is also very likely that BceB-ECD acts as the substrate binding domain of the resistance transporter, in a similar way to the here described examples. In this study, we probably could not show this interaction, as the ECD might have not bound free bacitracin, or because the ECD was not functional in isolation without the TMHs.

The MacB-like proteins described here are all classified as part of the type VII ABC transporter family, of which MacB is the holotype. With four transmembrane helices and one large extracytoplasmic the described transporters feature a homologous topology (Fig. 3.10). Further homologues are found amongst Gram-positive as well as Gram-negative bacteria, as recently reviewed by Greene and colleagues (2018).

Also BceAB of *B. subtilis* has been proposed to be a member of this family (Greene *et al.*, 2018). BceAB was shown to consist of two conserved ATPase units (BceA), but only a single transmembrane subunit (BceB) with ten predicted transmembrane helices (Dintner *et al.*, 2014). Some homologues of MacB harbour more than the 'basal unit' of four transmembrane helices with one large ECD between TMH1 and TMH2 in one monomer (Greene *et al.*, 2018). Transmembrane domains with eight or ten transmembrane helices per monomer have been described to be the result of gene duplication (Khwaja *et al.*, 2005). Each large monomer contains two repeat 'basal units' (TMH1-4, TMH5-8). The two additional helices of the transmembrane domain with ten predicted TMH seem to have inserted centrally between the functional units (TMH5 and TMH6). Further dimerisation of the transmembrane domain is not expected, and in the case of BceAB not observed (Dintner *et al.*, 2014), as the two basal units were suggested to form a pseudo-heterodimer (Khwaja *et al.*, 2005). In the case of BceB-like transporters, a rare intragenic deletion is thought to have led to the loss of the first large ECD between TMH1 and TMH2 (Khwaja *et al.*, 2005). Generally, the C-terminal repeat unit was found to be better conserved than its N-terminal equivalent. In agreement with this, the hydropathy profile of BceB TMH7-10 suggests BceB to have the same topology to MacB-like transporters (Fig. 3.10).

Crystal structures and secondary structure predictions of the extracytoplasmic domain revealed a conserved pattern for most MacB-like transporters. The ECDs seem to comprise two so-called 'Porter' subdomains (β-α-β) at their N- and C-termini, across all tested type VII ABC transporters (Crow *et al.*, 2017). All but FtsX-like domains showed a conserved Sabre (Small alpha/beta rich extracytoplasmic) subdomain between the Porter domains (Crow *et al.*, 2017). Comparison with the predictions for BceB-ECD (Fig. 3.10) and the previously discovered secondary structure pattern for most BceB-like extracellular domains (Dintner *et al.*, 2011), revealed a very similar secondary structure to MacB. We thus propose that also BceB-like ECDs can be differentiated into Porter and Sabre subdomains. The N- and C-terminal helices predicted in this study and the phylogenetic analysis by Dintner and colleagues (2011), are likely the continuation of TMH7 and TMH8 (or TMH1 and TMH2 in MacB, respectively) that form the so-called stalk of MacB-like transporters (Crow *et al.*, 2017). Indeed, secondary structure predictions of full-length BceAB revealed a continuation of the membrane-spanning helices 7 and 8 into the extracellular regions (data not shown).
The homology of the transmembrane regions and the potential structural similarity of BceAB and MacB-like transporters indicate a potential mechanistic similarity. This means that BceAB possibly recognises its substrate at the interface between the membrane and the extracellular space via its large extracellular domain akin to MacB-like proteins.

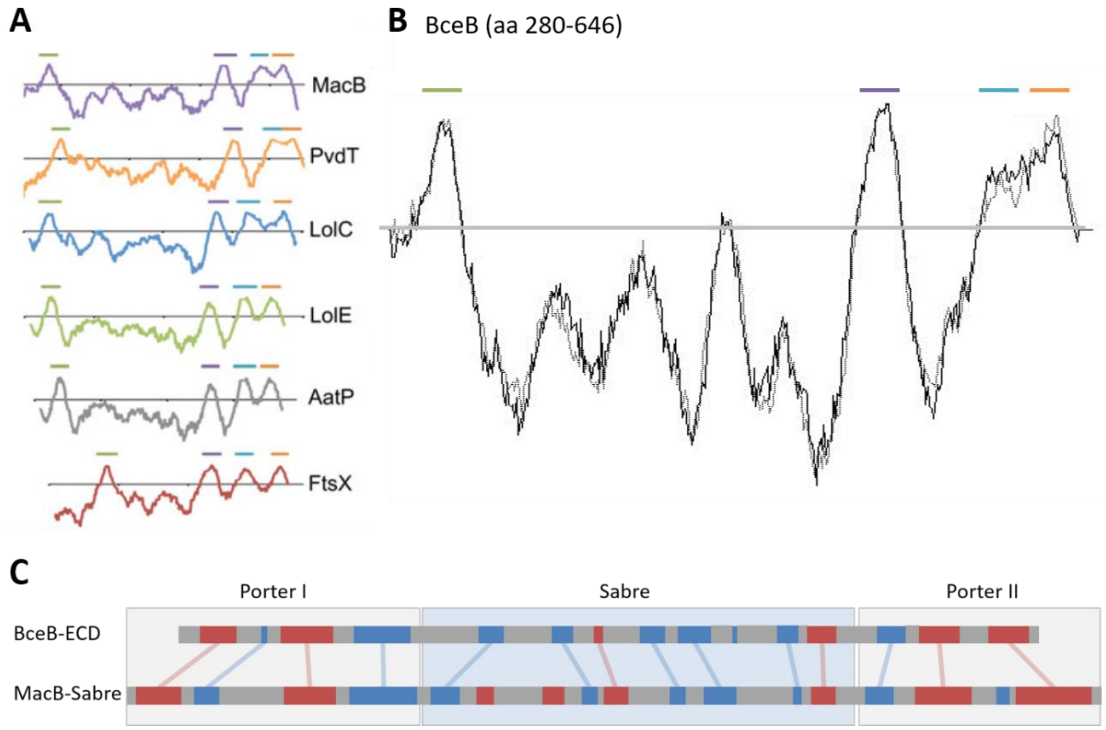

Figure 3.10: BceB (TMH7-10) has the characteristic features of type VII ABC transporters. **A:** Hydropathy profile of members of the type VII ABC transporter family, modified from Crow *et al.* (2017). **B:** Hydropathy profile of TMH 7-10 of BceB using the online tool TMpred (Hofmann, 1993). **C:** Comparison of the secondary structure of BceB-ECD and the periplasmic domain of MacB. Secondary structures were predicted using the JPred online prediction tool (Drozdetskiy *et al.*, 2015). Visualisation: red: α-helix, blue: β-sheet, grey: unstructured/coil. Porter and Sabre domains are indicated by grey and blue boxes.

3.4 The isolated extracellular domain might not be functional *in vitro.*

Although seemingly predestined for substrate binding, BceB-ECD could not be confirmed as the binding domain *in vitro.* Despite successful characterisations of *in vitro* binding by similar isolated domains (Mavrici *et al.*, 2014), it was possible that BceB-ECD, overproduced and purified as described above, was not functional.

The requirement of the extracellular domain to sense and confer resistance against bacitracin, as it is described in the literature (Rietkötter *et al.*, 2008, Coumes-Florens *et al.*, 2011), does not necessarily mean that the ECD alone is responsible for substrate binding. It is thus possible that BceB-ECD requires another extracellular loop of BceB to recognise and bind the substrate together. This is for example the case for protein-protein interactions by FtsEX in *S. pneumoniae*. Extracellular activation of the peptidoglycan hydrolase PcsB does not only require the large extracellular domain, which is located between transmembrane helices (TMH) 1 and 2. Also the shorter extracellular loop between TMH3 and TMH4 is needed to bind the coiled-coil region of PcsB (Sham *et al.*, 2013).

Random mutagenesis of BceAB has identified several mutations that abolish resistance and or signalling activity of BceAB. Two of these mutations are located at the membrane interface of two shorter extracellular loops of BceB (Kallenberg *et al.*, 2013). These mutations lie between TMH6 and TMH7, and TMH9 and TMH10, respectively. As bacitracin resistance was found to be moderately reduced, these extracellular loops might be additionally required for substrate binding.

Alternatively, it is plausible that BceAB interacts with its substrate in the membrane, or requires a combination of both, intramembrane interactions and recognition by BceB-ECD. The physiological substrate of BceAB has been proposed to consist of the AMP bound to its membrane-located target or even to be the target alone (Bernard *et al.*, 2007, Kingston *et al.*, 2014). Interactions between BceAB and isoprenoids are likely to take place in the membrane, potentially mediated by one or several transmembrane helices. To investigate this hypothesis, truncated versions of BceB could be produced as membrane proteins and tested for binding activity. Truncation studies are often used to identify the minimal functional unit of proteins (Lee *et al.*, 2002, Mavrici *et al.*, 2014, Hacker *et al.*, 2015b).

Furthermore, the membrane environment was shown to affect *in vitro* activity of membrane proteins (Lee, 2004, Shen *et al.*, 2013). BceB-ECD is natively the soluble domain of a membrane-protein, and thus in close proximity to the cytoplasmic membrane. Production of BceB-ECD as an isolated soluble protein might have affected its biological activity. To address

this issue, BceB-ECD could be reattached to the membrane. So far, we have designed and synthesised BceB-ECD hybrid proteins that anchor BceB-ECD onto the membrane by unrelated transmembrane helices (TMH) as described in Fig. S3.5 (GenScript, NJ, USA). In doing so, we hoped to re-create the natural environment of the ECD, but could still exclude other parts of BceB interacting with the substrate. Such a fusion protein has successfully been used for the characterisation of a periplasmic loop of similar length to BceB-ECD before (Saaf *et al.*, 1995). Initial attempts at overproduction, solubilisation of the membrane proteins in detergent and Strep-Tactin®-based purification of one of the BceB-ECD hybrid proteins according to a protocol modified from Dintner and colleagues (2014) were successful. However, no further binding experiments were performed due to time restrictions.

Recently, solubilisation of integral membrane proteins using styrene-maleic acid (SMA) copolymers has become a widely used method in membrane protein research (Dorr *et al.*, 2016).

In contrast to solubilisation of membrane proteins with detergent, SMA copolymers have the advantage that they can preserve the native membrane environment around the protein (Dorr *et al.*, 2016, Pollock *et al.*, 2018). SMA copolymers form so-called nanodiscs, which are SMA lipid particles that encompass the membrane protein and the lipid bilayer. This often secures biological activity and stabilises the protein for *in vitro* characterisation (Stroud *et al.*, 2018). Attempts to solubilise BceAB or the hybrid proteins in SMA copolymers have not yet been successful. Once established, this approach could also be used to investigate whether BceAB has affinity to and interacts with certain lipid II cycle intermediates.

In the ABC transporter superfamily, successful substrate transport is driven by ATP-hydrolysis (Locher, 2016). In agreement, various members of the Type VII ABC transporter family were found to be non-functional when key motifs of their nucleotide binding domains (NBD) were mutated (Frelet & Klein, 2006, Tikhonova *et al.*, 2007, Yang *et al.*, 2011, Crow *et al.*, 2017).

Conformational changes of FtsX in *M*. *tuberculosis* seem to be driven by ATP hydrolysis performed by the nucleotide binding domains (NBD) of FtsE. This allows the large extracellular domain of FtsX to adopt its active conformation FtsX, which enables it to interact with its binding partner (Mavrici *et al.*, 2014).

BceAB activity was also found to depend on functional NBDs. *B subtilis* cells carrying mutations in the conserved Walker A motif of BceA, which disturbs ATP-binding as well as the hydrolysis thereof, were not able to sense bacitracin or confer resistance against it (Rietkötter *et al.*, 2008). A BceAB-Walker B mutant, which can bind ATP but not further process it, showed minimal *in vivo* activity in our study (data not shown). Although purified

BceB alone was seemingly able to bind bacitracin *in vitro* (Dintner *et al.,* 2014), ATP binding or hydrolysis might be required for the substrate recognition of BceB-ECD (Rietkötter *et al.*, 2008).

Taken together, the work in this chapter was based on the *in vitro* characterisation of the extracellular domain of BceAB. Because no interaction between BceB-ECD and free bacitracin could be detected, BceB-ECD could not be confirmed as the binding domain of BceAB and no further investigations into a potential fly-casting binding mechanism could be performed (Shoemaker *et al.*, 2000). The target of bacitracin, UPP, had been discussed to potentially be at least part of the substrate (Bernard *et al.*, 2007, Kingston *et al.*, 2014). However, due to high background signal, *in vitro* analyses on the [GPP-BAC] complex remained ambiguous. The lipid carrier UPP is membrane-bound, and thus also the [UPP-BAC] complex would natively located in the membrane. If the [UPP-BAC] complex was the physiological substrate of BceAB, it is possible that substrate recognition happens directly in the hydrophobic membrane environment (Mascher *et al.*, 2003, Bernard *et al.*, 2007), according to a 'hydrophobic vacuum cleaner' mechanism (Podlesek *et al.*, 1995). Recently, extensive evidence has been published demonstrating that extracytoplasmic domains function as substrate binding domains in transporters homologous to BceAB (Crow *et al.*, 2017, Greene *et al.*, 2018). Despite their extracytoplasmic location, these domains are able to recognise and bind substrates from the membrane. A 'hydrophobic vacuum cleaner' hypothesis would thus be compatible with the indications that BceB-ECD may play a role in substrate recognition, but not of free bacitracin itself, which explains the lack of binding activity observed in this chapter (Rietkötter *et al.*, 2008, Hiron *et al.*, 2011). Hydrophobic vacuum cleaners basically confer resistance by shifting the equilibrium of the AMP binding reaction from the membrane more towards the extracellular environment. If BceAB acted according to such a mechanism, the ability to differentiate between free bacitracin and the [UPP-BAC] complex would be crucial. To gain further insights into the potential mechanism, the *in vivo* identification of the physiological substrate will be addressed in the following chapter.

Chapter IV

In vivo determination of the physiological substrate of BceAB

1. Introduction

While it has been shown that BceAB successfully confers resistance against certain AMPs, including bacitracin, mersacidin and actagardine (Staron *et al.*, 2011, Ohki *et al.*, 2003), the question of the resistance mechanism remains puzzling, and even the physiological substrate is still subject to debate. When first described, the transporter was named Bce for bacitracin efflux (Ohki *et al.*, 2003), although no evidence for the direction of transport was given. This assumption was based on the suggested self-protection mechanism of the Bcr transporter of *B. licheniformis* ATCC10716 (Podlesek *et al.*, 1995, 2000). The transporter of the bacitracin producer was thought to work according to a 'hydrophobic vacuum cleaner' model akin to the human multidrug resistance transporter P-glycoprotein (Higgins & Gottesman, 1992, Gottesman & Pastan, 1993). As it was difficult to envision how a membrane-located ABC-transporter could effectively confer resistance against AMPs that target molecules at the outer face of the membrane, BceAB was speculated to import bacitracin into the cytoplasm, where it is subsequently degraded (Rietkötter *et al.*, 2008). This idea was based on the differences in protein architecture of the permeases BceB and BcrB. BceB comprises ten predicted transmembrane helices and a large extracellular domain, whereas the permease BcrB consists of six transmembrane helices, but lacks the extracellular domain (I 4.3.2, Podlesek *et al.*, 1995, Rietkötter *et al.*, 2008, Gebhard, 2012). In general, ATP-binding cassette (ABC) transporters that are involved in substrate uptake were shown to require extracytoplasmic binding proteins (Davidson & Chen, 2004, Dawson *et al.*, 2007). Particularly in low GC-content Gram-positive bacteria, these substrate-binding proteins can be fused to the transmembrane segments of the transporter (van der Heide & Poolman, 2002). In contrast, efflux pumps seem to lack external substrate-binding proteins and acquire their substrate directly from the cytoplasm or the inner leaflet of the membrane (Dawson *et al.*, 2007, Du *et al.*, 2018).

More recently, several suggestions for the physiological substrate, and subsequently the resistance mechanism, have been made. Kingston and colleagues (2014) proposed that the transporter acted as a undecaprenyl pyrophosphate (UPP) translocase. BceAB was thought to confer resistance by transporting UPP and/or UP (undecaprenyl phosphate) across the membrane to the cytoplasmic face, thereby removing the cellular target for bacitracin rather than transporting bacitracin itself. In the presence of bacitracin, BceAB was hypothesised to bind the [UPP-BAC] complex, which was proposed to act as a transport inhibitor and lead to

activation of signalling through the BceRS regulatory two-component system (Kingston *et al.*, 2014).

In contrast, Dintner and colleagues (2014) showed that purified BceB was able to bind bacitracin with a steady-state K_d of 60 nM using surface plasmon resonance (SPR) spectroscopy, which was similar to the bacitracin threshold concentration required to induce the target promotor P_{bceA} *in vivo*. Without excluding the possibility of BceAB recognising the [UPP-BAC] complex, this finding stressed the likelihood of the transporter directly interacting with and possibly transporting the AMP rather than the lipid carrier. When revealing that signalling through BceRS worked according to a novel flux-sensing mechanism, the original hypothesis of BceAB acting as a 'hydrophobic vacuum cleaner' was proposed again (Ohki *et al.*, 2003, Fritz *et al.*, 2015). This model suggests that BceAB recognises the [target-AMP] complex in the membrane (Mascher *et al.*, 2003, Bernard *et al.*, 2007), and in turn removes the AMP and releases it in the extracellular space. By this, the cellular targets, which are usually lipid II cycle intermediates, are freed from the inhibitory grip of the AMP. This unblocks the lipid II cycle, enables recycling of the lipid carrier and secures an intact cell wall. For a mechanism like this to work, the transporter would need to be able to specifically recognise the [target-AMP] complex and distinguish it from the unbound versions of both, the AMP and the cellular target.

This would be possible if BceAB specifically bound both components of the [target-AMP] complex as it has been proposed for [lipid II-nisin] binding by the immunity protein NisI of *L. lactis* (Jeong & Ha, 2018). As discussed in Chapter III, many AMPs including the AMPs BceAB confers resistance against (bacitracin, actagardine and mersacidin) were shown to undergo extensive conformational changes upon target binding (Hsu *et al.*, 2003, Breukink & de Kruijff, 2006, Economou *et al.*, 2013). This rearrangement might expose structural cues that can serve as binding site by BceAB.

It is becoming more apparent that bacterial cells respond differently to antimicrobial stress depending on the physiological context and the metabolic state of the cells. Recently, aspartate deficiency was shown to reduce peptidoglycan synthesis and to increase the susceptibility to cell wall-active antibiotics (Zhao *et al.*, 2018). Further, genetic manipulations that disturb the levels of lipid II cycle intermediates were shown to affect antibiotic sensitivity. Lee and Helmann (2013) described a mutation in the ribosome-binding site of the promoter P_{uppS}, which was proposed to result in lower levels of UppS in the cell, the enzyme that catalyses assembly of UPP. Lower levels of UPP led to an increased resistance to

antibiotics that target early stages in the cell wall synthesis, whereas the cells responded more sensitively to antimicrobial compounds that target later stages, including bacitracin (Lee & Helmann, 2013). It is also well-known that the removal of the UPP phosphatases BcrC and UppP leads to increased bacitracin susceptibility in *B. subtilis* (Cao & Helmann, 2002, Bernard *et al.*, 2005, Zhao *et al.*, 2016, Radeck *et al.*, 2017a). As both are redundant in function to some degree and catalyse the dephosphorylation of UPP to UP, this change can likely be explained by an accumulation of the pyrophosphate form of the lipid carrier. In addition, Kingston and colleagues (2014) found that accumulation of heptaprenyl pyrophosphate (C_{35}-PP) sensitises *B. subtilis* to bacitracin. This effect was observed following deletion of *ytpB*, when MenA activity was limited at the same time. Both enzymes use C_{35}-PP as their substrate. C_{35}-PP was suggested to compete with UPP for translocation by BceAB and to potentially inhibit signalling through the two-component system BceRS (Kingston *et al.*, 2014). In a previous study, bacitracin was shown to bind tightly around the pyrophosphate group and to interact with only the first prenyl group (Economou *et al.*, 2013). The association constant between UPP and bacitracin was determined to be 1.05 μM^{-1}, but also the shorter farnesyl pyrophosphate (C_{15}-PP) was shown to bind bacitracin at a comparable association constant (K_a= 0.83 μM^{-1}, Storm & Strominger, 1973). Therefore, it is very likely that bacitracin also targets C_{35}-PP.

If the cellular target of the AMPs was at least part of the physiological substrate of BceAB, the described changes in lipid II-cycle intermediate levels should change the effective substrate concentration, and thus alter BceAB activity. In this chapter, we aimed to reveal the identity of the physiological substrate and the potential role of both, the cellular target and the AMPs, by monitoring growth behaviour and BceAB transport activity in cells with such variation.

In contrast to most assays used in Chapter III, in which we focussed on the *in vitro* characterisation of the substrate binding domain, this chapter describes *in vivo* approaches to identify the physiological substrate of BceAB. We used physiological assays, including growth and competition assays, to investigate the effect of BceAB on growth to identify a potential affinity to UPP. Further, we used a P_{bceA}-*lux* reporter assay to investigate the BceAB transport activity in response to genetic manipulations of genes important to the lipid II cycle. Previous data on bacitracin transport assays were used to gain further insights into the potential resistance mechanism. Our data suggest that the complex formed between the antimicrobial peptide and its corresponding cellular target acts as physiological substrate of

BceAB and are in support of a hydrophobic vacuum cleaner-like substrate recognition at the membrane interface.

2. Results

2.1 Investigating a potential interaction between BceAB and UPP using growth assays

2.1.1 Presence of BceAB does not alter the fastest doubling time.

The lipid II cycle is known to be the bottle neck of cell wall synthesis, with the availability of the lipid carrier being the rate-limiting step (van Heijenoort, 1998). It is further thought that lipid carrier recycling instead of *de novo* synthesis is the pacemaker of the lipid II cycle (Piepenbreier, Fritz, unpublished). Impairment of UPP recycling thus potentially affects the doubling time of during the exponential growth phase of bacteria. In agreement with this, Radeck *et al.* (2016b) found a *B. subtilis* Δ*bcrC* mutant to have an a higher doubling time than the WT and also detected a growth difference between *bceAB*$^{+}$ and *bceAB*$^{-}$ strains, supporting the hypothesis that cell wall synthesis is growth-limiting.

In several of the proposed resistance mechanisms of BceAB against antimicrobial stress, the transporter was suggested to interact with UPP. For example, BceAB was proposed to act as UPP importer (Kingston *et al.*, 2014). According to this hypothesis, the lipid carrier would serve as the true physiological substrate and even in the absence of bacitracin, the transporter should increase the turnover of the lipid II cycle.

Furthermore, also the 'hydrophobic vacuum cleaner' model indicates that BceAB can recognise the complex of the cellular target and the AMP (Mascher *et al.*, 2003, Bernard *et al.*, 2007). This could mean that BceAB has a certain affinity to UPP alone (Radeck *et al.*, 2016b). This potential binding interaction might help the transporter to monitor the UPP levels in the absence of AMP stress. By interacting with the lipid carrier, BceAB might withhold some UPP from cell wall biogenesis. When bound to BceAB, the lipid carrier is unlikely to be dephosphorylated and recycled. The interaction between BceAB and the lipid II cycle intermediate might therefore lead to a delay in UPP turnover in the absence of bacitracin. Thus, the absence of BceAB might be beneficial to growth when resistance to bacitracin is not required, as all available UPP can be directly recycled. Supporting this hypothesis, a Δ*bceAB* mutant was shown to have faster doubling times in the absence of

bacitracin (Radeck *et al.*, 2016b). While *in vitro* binding assays between the extracellular domain of BceAB and GPP did not indicate such an interaction (Chapter III), it seemed reasonable to investigate this interaction *in vivo* with the whole transporter and the lipid carrier in its natural environment. To test if the potential interaction between BceAB and UPP leads to benefits or disadvantages for the cell, growth and competition assays were performed by a project student (Laura Richardson) under my supervision.

Growth curves of the wild-type *B. subtilis* W168 (WT) and a Δ*bceAB* (SGB575) and a Δ*bcrC* mutant (TMB297), as well as a Δ*bceAB* Δ*bcrC* double mutant (SGB01) were obtained by recording the OD_{600}. The fastest doubling time (t_d) during exponential phase was determined for each of the strains (Fig. 4.1 A, B). For the WT, a doubling time of 23.50±1.77 minutes was calculated. In contrast to observations by Radeck and colleagues (2016b), deletion of Δ*bceAB* did not lead to a significantly different doubling time (23.23±2.28 minutes, p = 0.9913). The effect of BceAB on the growth rate was also tested in a Δ*bcrC* background. Deletion of *bcrC* is expected to lead to UPP accumulation and might highlight a potential interaction between BceAB and UPP. In the Δ*bcrC* mutation strain the doubling time was found to be 25.23±1.51 minutes, and the doubling time of the Δ*bceAB* Δ*bcrC* mutant was recorded as 25.95±1.93 minutes, which again did not show a significant difference (p = 0.8576). This suggests that removal of BceAB had no detectable impact on the fastest doubling times. A possible explanation for this was that in the absence of activity-inducing antimicrobial stress, the basal level of BceAB might simply be too low to cause a difference. To investigate this further, *bceAB* was expressed ectopically under xylose-inducible control. We hypothesised that if BceAB withheld some of the UPP from cell wall synthesis, increasing the amounts of BceAB upon xylose induction should lead to slower growth. If BceAB was able to import the lipid carrier, it should lead to faster growth.

Growth behaviour of the WT, a BceAB overproduction strain (SGB576, WT P_{xylA}-*bceAB)*, and a BceAB complementation strain (SGB577, Δ*bceAB* P_{xylA}-*bceAB*) were re-tested as described above. MIC assays showed increased bacitracin resistance when ectopically producing BceAB in the presence of 0.2 % xylose (MIC: Δ*bceAB* P_{xylA}-*bceAB* -xylose: 16 µg/ml, Δ*bceAB* P_{xylA}-*bceAB* +xylose: 64 µg/ml, WT P_{xylA}-*bceAB*: 128 µg/ml) confirming the successful production of BceAB. Doubling times of all tested strains revolved around 23 minutes (Fig. 4.1 C, detailed t_d in Fig. 4.1 D). None of the tested strains showed any significant difference in their doubling time when compared to their corresponding controls that did not overproduce BceAB. These findings show that even in the presence of ectopically produced BceAB the growth rate of *B.*

subtilis does not change in the tested conditions. This indicates that BceAB might not interact with free UPP.

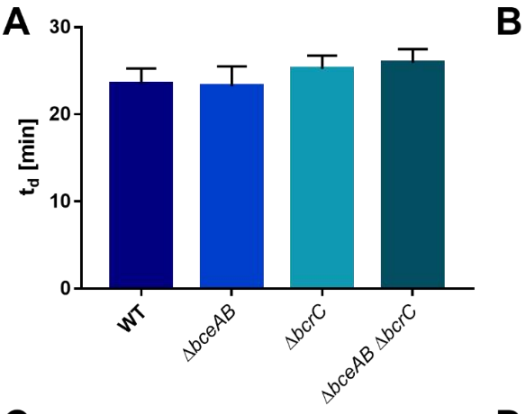

B

Strains	Doubling time t_d [min]
WT	23.50±1.77
Δ*bceAB*	23.23±2.28
Δ*bcrC*	25.23±1.51
Δ*bceAB* Δ*bcrC*	25.95±1.53

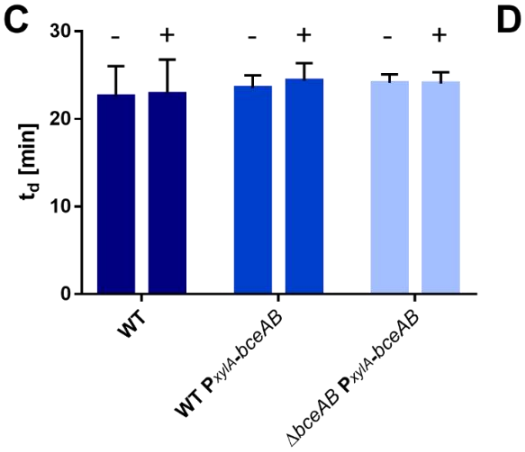

D

Strains	Doubling time t_d [min]	
	0 % xylose	0.2 % xylose
WT	22.57±3.45	22.87±3.90
WT P_{xylA}-*bceAB*	23.52±1.43	23.24±2.10
Δ*bceAB* P_{xylA}-*bceAB*	24.03±1.30	24.08±1.01

Figure 4.1: The doubling time of exponentially growing *B. subtilis* seems unaffected by presence of absence of BceAB. *B. subtilis* strains were grown in LB medium at 37 °C shaking incubation over 8 hours in a 96-well microplate reader. OD_{600} measurements were taken every 5 minutes. The fastest doubling time for each strain was determined. Bar graphs show means ± standard deviation from at least 6 biological replicates. **A:** Comparison of doubling times (t_d) of WT (W168), a Δ*bceAB* (SGB575) and a Δ*bcrC* mutant (TMB297), as well as a Δ*bceAB* Δ*bcrC* double mutant (SGB01), values are listed in panel **B**. **C:** Doubling times of BceAB overproduction (SGB576, centre) and BceAB complementation strains (SGB577, right) in the presence (+) or absence (-) of 0.2 % xylose compared to WT doubling times (left), values are listed in panel **D**. Statistical analysis using a Tukey's multi comparisons test did not show a significant difference upon removal of BceAB. Displayed data were obtained in collaboration with Laura Richardson.

2.1.2 Absence of BceAB seems beneficial to growth in competition assays when recycling of UPP is impaired.

An interaction between BceAB and UPP in the absence of bacitracin might only cause minor differences in the doubling times, and it is possible that growth in the 96-well plate might be insufficient to resolve these. As a more sensitive approach to investigate if the presence of BceAB is beneficial or even a burden on growth, competition assays were performed (Laura Richardson).

In contrast to comparison of the maximal growth rate (V_{max}) or the fastest doubling time (t_d), which measure the absolute fitness of a bacterial strain, competition assays are based on competing two bacterial strains directly against each other (Wiser & Lenski, 2015). By this, the relative fitness of a mutant to its wild type strain is determined and smaller differences have a better chance to be established. We hypothesised that if BceAB had an affinity to free UPP and withheld some of the lipid carrier from cell wall synthesis, a Δ*bceAB* strain would outcompete strains containing BceAB, like the WT. If BceAB acted as UPP importer and accelerated UPP turnover, the WT should outcompete the Δ*bceAB* strain. To test this, *B. subtilis* strains (WT versus Δ*bceAB* (SGB575), and Δ*bcrC* (TMB297) versus Δ*bceAB* Δ*bcrC* (SGB01)) were inoculated in a 50:50 ratio. A WT versus Δ*bcrC* pair was used as control, as the WT was expected to outcompete the UPP phosphatase deletion mutant (Radeck *et al.*, 2016b). Mixed cultures were grown in LB medium at 37 °C shaking incubation, and diluted 1:1000 into fresh broth every 24 hours. Viable cells were counted and the competition index (CI) determined for each of the pairs (Auerbuch *et al.*, 2001, Wiser & Lenski, 2015). The CI gives indication on whether one strain outcompetes the other, with CI = 1 implying equal growth rates, CI < 1 meaning the mutant strain was outcompeted and a CI value > 1 to be interpreted as the mutant outcompeting the wild type strain. The WT versus Δ*bcrC* pair revealed a mean CI of 0.76±0.06 after 24 hours, and 0.08±0.52 after 72 hours (Fig. 4.2). These results confirm that the WT strain had a growth benefit over the Δ*bcrC* mutant. It further validated the assay to be more sensitive, as this difference in fitness was not observed when comparing doubling times (IV 2.1.1). For the Δ*bcrC* versus Δ*bceAB* Δ*bcrC* pair, the CI lies at 1.52±0.24 after 24 hours and at 3.47±0.31 after 72 hours, suggesting a clear growth advantage of the Δ*bceAB* Δ*bcrC* double mutant over the Δ*bcrC* single mutant (Fig. 4.2). The CI values of the WT versus Δ*bceAB* mutant were 1.42±1.08 after 24 hours and 1.16±0.16 after 72 hours, which did not result in a significant growth difference upon Δ*bceAB* deletion (Fig. 4.2). The removal of *bceAB* appeared to be mainly advantageous when competing in a UPP-

accumulated environment, but seemed to have little to no impact in the wild-type background. This could be explained by BceAB having a low affinity to UPP alone, and upon accumulation of UPP it is more likely that this interaction happens. It became apparent that the CI became more veritable in the assays performed over 72 hours for both the WT versus Δ*bcrC* and the Δ*bcrC* versus Δ*bceAB* Δ*bcrC* pairs. It is possible that a growth difference between the WT and a Δ*bceAB* would take even longer to become detectable. Additionally, biological repeats and technical replicates of the CFUs will help to detect smaller differences. In the way the assay was conducted, it is not entirely clear whether the observed fitness advantage of the Δ*bceAB* Δ*bcrC* double mutant over the Δ*bcrC* single mutant is a result of faster growth, as the cells are only transferred into fresh medium after 24 h. This means that cells will enter various growth stages and accordingly experience alterations of growth rate as well as the underlying metabolism. It is thus possible that the competition benefit is a result of differential stationary phase survival or differences in outgrowth behaviour from lag-phase. To ensure the fitness advantage is due to faster growth, competing cells should be constrained to exponential growth as much as possible, rather than being allowed to transit into stationary phase. This could for example be achieved by dilution into fresh medium every two to three hours.

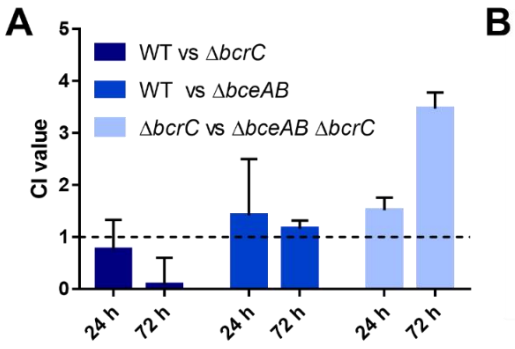

B

Strains	Competition index CI	
	24 hours	72 hours
WT vs Δ*bcrC*	0.76±0.06	0.08±0.52
WT vs Δ*bceAB*	1.42±1.08	1.16±0.16
Δ*bcrC* vs Δ*bceAB* Δ*bcrC*	1.52±0.24	3.47±0.31

Figure 4.2: The absence of BceAB seems only beneficial upon accumulation of UPP. For competition assays, *B. subtilis* strains were inoculated pairwise in a 50:50 ratio and grown in test tubes containing LB medium at 37 °C shaking incubation. Cultures were diluted 1:1000 into fresh LB medium every 24 h. Samples were taken, diluted and plated on LB agar with and without the appropriate selection after 0, 24 and 72 h. CFUs were counted after 24 h of incubation at 37 °C. **A:** Bar graphs show means ± standard deviation from at least 2 biological replicates. Comparison of CI values of the following pairs: WT versus a Δ*bcrC* mutant (TMB297, dark blue), WT versus Δ*bceAB* (SBG575, centre) and Δ*bcrC* versus Δ*bceAB* Δ*bcrC* (SGB01, lightest blue) after 24 and 72 h, values are listed in panel **B**. Displayed data were obtained in collaboration with Laura Richardson.

2.2 Changing amounts of the [target-AMP] complex has impact on BceAB activity.

In a second set of studies, we investigated whether the physiological substrate of BceAB was the complex of the AMP bound to its cellular target. For this, we first required a strategy to quantify transport activity in living cells. It has recently been shown that signalling within the Bce system is directly proportional to BceAB transport activity (Fritz *et al.*, 2015). As the signalling cascade ultimately leads to activation of the promoter controlling *bceAB* expression (P_{bceA}), the activity of a P_{bceA}-*luxABCDE* reporter fusion can be taken as a proxy for BceAB activity (SGB73, Fig. 4.3 A). Using this approach, we monitored BceAB activity in the WT strain under several sub-inhibitory bacitracin concentrations. In agreement with previously reported data (Fritz *et al.*, 2015), the threshold concentration to elicit detectable BceAB activity was 0.1 µg/ml bacitracin, and the activity gradually increased until maximum levels were reached at 30 µg/ml (Fig. 4.3 B). While this experiment showed that the transport activity increased with higher bacitracin concentrations, it did not directly allow us to distinguish whether the physiological substrate is free bacitracin or the complex between bacitracin and its cellular target UPP ([UPP-BAC]). This is because the concentration of [UPP-BAC] changes proportionally to the concentration of bacitracin added to the culture (Fig. 4.3 C).

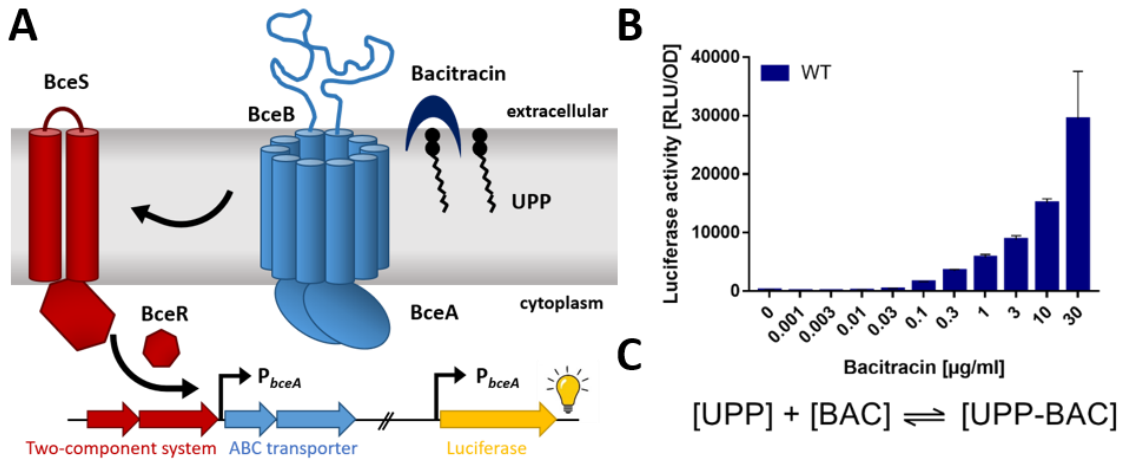

Figure 4.3: The flux-sensing mechanism as suitable strategy to monitor BceAB activity. A: Schematic of the BceAB-BceRS resistance system. In the presence of bacitracin, the transporter BceAB confers resistance against bacitracin. BceAB forms a sensory complex with the kinase BceS and the transport activity of BceAB induces a signalling cascade through the two component regulatory system BceRS, which ultimately activates transcription from the target promotor P_{bceA}. This results in increased production of BceAB, and therefore adjusted levels of resistance. As this signalling cascade is directly proportional to the transport activity, we can use the target promotor P_{bceA} upstream of a luciferase reporter to monitor the transport activity of BceAB. **B:** Using luciferase activity as a proxy, BceAB activity of wild-type *B. subtilis* W168 carrying the reporter fusion (SGB73) was determined as average of three measurements taken 25, 30 and 35 minutes after challenging the cells with sub-inhibitory concentrations of bacitracin. Measurements were performed during exponential growth phase in LB medium at 37 °C in a microplate reader. All data are depicted as mean ± standard deviation of at least three biological replicates. **C:** Binding reaction between free bacitracin and its cellular target UPP.

2.2.1 Accumulation of UPP increases BceAB activity at low concentrations of bacitracin.

To distinguish whether it was [UPP-BAC] or free bacitracin that triggered BceAB activity, we required a strategy to change the concentration of [UPP-BAC], while keeping the concentration of bacitracin constant. This should be possible by changing the UPP levels in the cell. If the [UPP-BAC] complex was the physiological substrate of BceAB, increased amounts of UPP should result in higher BceAB activity at the same bacitracin concentration.
To achieve such an increase in the level of UPP displayed on the extracellular face of the membrane, we deleted the UPP phosphatase encoding gene *bcrC*, which plays a prominent role in recycling of UPP to UP during exponential growth (Bernard *et al.*, 2005, Radeck *et al.*, 2017a, Zhao *et al.*, 2016). By this, we should reduce the rate of UPP dephosphorylation, and thus accumulate UPP. This assumption was supported by a computational model prediction by our collaborators (Piepenbreier & Fritz, data not shown). As expected from previous data (Radeck *et al.*, 2016b), deletion of *bcrC* resulted in an increased sensitivity to bacitracin, indicating an increased amount of UPP available for bacitracin to target. The MIC decreased from 160±20 µg/ml in the wild-type to 67±12 µg/ml in the Δ*bcrC* strain (SGB649).
Re-testing BceAB activity in the Δ*bcrC* strain showed that increasing the UPP concentration in the cell led to a more than 10-fold reduction in the minimal bacitracin concentration required to trigger transport activity (0.003 µg/ml, Fig. 4.4 A, turquoise). Likewise, maximum BceAB activity was observed at 0.3 µg/ml bacitracin (Fig. 4.4 A, turquoise), which is 100-fold less bacitracin than is required in the WT strain (SGB73) to reach similar activity (Fig. 4.4 A, dark blue). Between 0.3 and 30 µg/ml bacitracin the transport activity seemed to have reached a plateau. A seemingly decrease of activity with increasing bacitracin concentration was not statistically significant (one-way ANOVA with post-hoc test). A two-way ANOVA confirmed the variation observed between the two strains was significant ($p = 0.0075$). The huge disparity in BceAB activity between the Δ*bcrC* and the WT strain became particularly clear when comparing activity levels in the presence of 0.1 to 3 µg/ml bacitracin, as the *post-hoc* test performed showed *p*-values lower than 0.0001 at these concentrations. Further, a non-linear regression dose response curve was fitted on the normalised BceAB activity of each of the strains, allowing determination of the half maximal effective concentration of bacitracin (EC_{50}, Fig. 4.4 B). As the maximal activity of the WT strain has been previously determined to lie at a concentration around 30 µg/ml bacitracin (Rietkötter *et al.*, 2008, Fritz *et al.*, 2015), we assumed this concentration as a suitable end point.

The EC_{50} values, which describe the bacitracin concentration at which the BceAB activity is half its maximum, were 3.86 µg/ml in the WT and 0.059 µg/ml in the Δ*bcrC* mutant ($p < 0.0001$). This significant difference further confirmed the increased sensitivity upon UPP accumulation.

To explore if UPP alone could serve as the physiological substrate of BceAB, the activity was also compared in the absence of bacitracin. There was no detectable BceAB activity in either of the tested strains, which suggested that accumulation of UPP alone was not sufficient to trigger transport by BceAB.

To exclude that the observed sensitivity shift upon UPP accumulation was a result of an additional unknown regulatory effect on the P_{bceA} promoter, we uncoupled BceAB production from its native regulation. We re-tested the effect of UPP accumulation on BceAB activity in a strain lacking the native copy of *bceAB,* but carrying a xylose-inducible copy of *bceAB.* Ectopic expression of *bceAB* ensured equal BceAB production levels in all strains, independent of signalling activity and other regulatory influences. In agreement with previous observations (Kallenberg *et al.*, 2013), bacitracin resistance increased in a Δ*bceAB* single mutant (SGB218) as well as in the Δ*bceAB* Δ*bcrC* double mutant background (SGB677) upon xylose-induction of P_{xylA}-*bceAB* (MICs: Δ*bceAB* P_{xylA}-*bceAB* -xylose: 20 µg/ml, +xylose: 43.3±15.3 µg/ml; Δ*bceAB* Δ*bcrC* P_{xylA}-*bceAB* -xylose: < 1 µg/ml, +xylose: 13.3±5.8 µg/ml). This confirmed successful BceAB production. The minimal bacitracin concentration to induce detectable BceAB activity as well as the concentration at which maximal activity was observed were 30-fold lower in the Δ*bceAB* Δ*bcrC* double mutant than in the Δ*bceAB* background (Fig. 4.4 C). These findings suggest that the more sensitive response in BceAB activity upon UPP accumulation is independent of the level of BceAB produced, and the observed activity change therefore unlikely to be due to regulatory effects.

To further explore the effect of altered UPP levels on BceAB activity, we sought to decrease the pool of UPP displayed on the outer face of the membrane. To this end, we overproduced BcrC by placing an additional copy of *bcrC* under control of the xylose-inducible promoter P_{xylA} (SGB758). While the difference was not as pronounced as in the Δ*bcrC* strain, overproduction of BcrC still led to a small but consistent increase in MIC (WT: 160±20 µg/ml, P_{xylA}-*bcrC* + xylose: 173±12 µg/ml). Reduction of UPP levels in this way led to overall lower BceAB activities (Fig. 4.4 D, turquoise). The threshold concentration required to trigger detectable activity was increased three-fold, and even at the maximal concentration tested, the activity was less than half of that in the wild type.

The dose response curve fitted on the normalised data did not reveal a difference in sensitivity. However, the concentrations tested did not allow an adequate conclusion on whether 30 µg/ml bacitracin resulted in maximal BceAB activity for the BcrC overproduction strain, or if higher activities may have been achieved at even higher but still sub-lethal concentrations (Fig. 4.4 E). Therefore, the difference between the P_{xylA}-*bcrC* and the WT strain was shown by a two-way ANOVA (p = 0.0075). *Post-hoc* analysis revealed a significant difference between the WT and the BcrC overproduction strains at the concentrations of 10 µg/ml (p = 0.004) and 30 µg/ml bacitracin (p < 0.0001, Fig. 4.4 D). This suggests that BcrC overproduction and, therefore, reduced levels of the cellular target, are likely to lead to decreased BceAB activity. These findings were a first indication that the concentration of [UPP-BAC] complexes rather than bacitracin or UPP alone is the critical parameter determining BceAB activity.

Figure 4.4: Varying the cellular UPP concentration affects BceAB transport activity in the presence of bacitracin. Exponentially growing cells were challenged with varying concentrations of bacitracin, as indicated. Luminescence activity (RLU/OD) was determined as average of three measurements taken 25, 30 and 35 minutes after addition of AMPs. Experiments were performed in LB medium at 37 °C shaking incubation in a microplate reader. All data are shown as mean ± standard deviation of at least three biological replicates. **A:** Comparison of activities in the WT (SGB73, dark blue) and Δ*bcrC* strain (SGB649, turquoise) with varying bacitracin concentrations. **B:** Best-fit of dose response of BceAB activity for a Δ*bcrC* strain (turquoise) and the respective WT activity (dark blue). Non-linear regression curves were fitted on normalised activity data. The EC_{50} (half maximal effective concentration) was determined and statistical analyses performed on the $\log_{EC50}$ (****: p < 0.0001). **C:** Effect of Δ*bcrC* on BceAB activity in strains that carry a xylose-inducible copy of *bceAB* (P_{xylA}-*bceAB*), instead of the native copy *(*Δ*bceAB*). Experiments were performed in presence of 0.2 % xylose. **D:** BceAB activity of the BcrC overproduction strain (SGB758, P_{xylA}-*bcrC*) in the presence of 0.2 % xylose (turquoise) compared to WT activity (dark blue). For data displayed in panel A and D, a Bonferroni's multiple comparisons test was performed as *post-hoc* analysis after a two-way ANOVA (****: p < 0.0001, ***: p < 0.001, **: p < 0.01, *: 0.01 < p < 0.05). **E:** Best-fit of dose response of BceAB activity for a P_{xylA}-*bcrC* strains and the respective WT activity. Non-linear regression curves were fitted on normalised activity data.

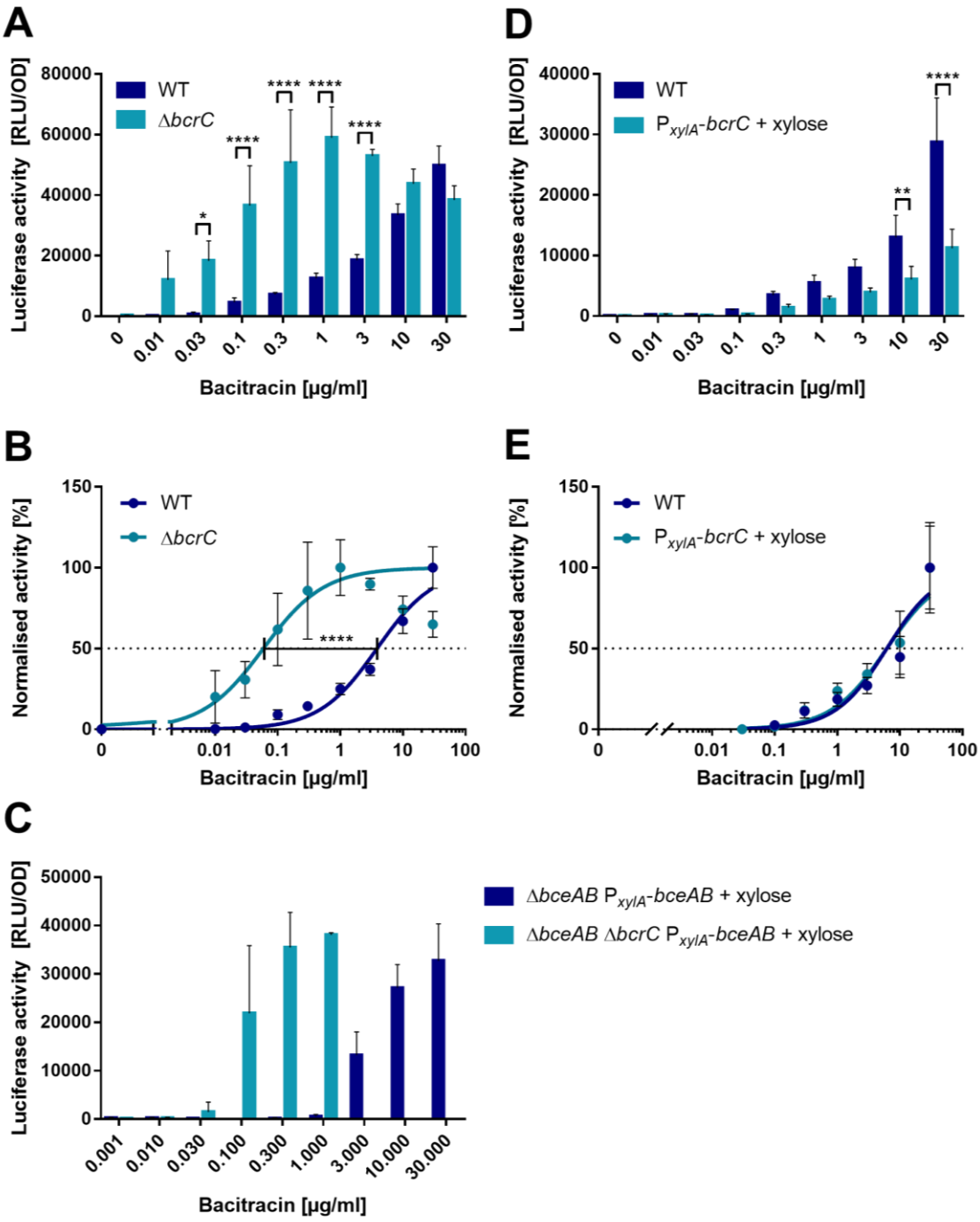
A
Luciferase activity [RLU/OD]
80000
60000
40000
20000
0
WT
ΔbcrC
*
****
****
****
****
0
0.01
0.03
0.1
0.3
1
3
10
30
Bacitracin [µg/ml]
D
Luciferase activity [RLU/OD]
40000
30000
20000
10000
0
WT
P$_{xylA}$-bcrC + xylose
**
****
0
0.01
0.03
0.1
0.3
1
3
10
30
Bacitracin [µg/ml]
B
Normalised activity [%]
150
100
50
0
WT
ΔbcrC
****
0
0.01
0.1
1
10
100
Bacitracin [µg/ml]
E
Normalised activity [%]
150
100
50
0
WT
P$_{xylA}$-bcrC + xylose
0
0.01
0.1
1
10
100
Bacitracin [µg/ml]
C
Luciferase activity [RLU/OD]
50000
40000
30000
20000
10000
0
0.001
0.010
0.030
0.100
0.300
1.000
3.000
10.000
30.000
Bacitracin [µg/ml]
ΔbceAB P$_{xylA}$-bceAB + xylose
ΔbceAB ΔbcrC P$_{xylA}$-bceAB + xylose

2.2.2 UPP accumulation does not affect transport activity upon addition of lipid II binding AMPs.

To exclude that the changed susceptibility of the cell caused by varying the levels of UPP phosphatase had general effects on BceAB activity, we had to ensure that the observed activity was indeed due to changes the amount of [UPP-BAC] in the cell. Therefore, we wanted to test if *bcrC* deletion or overexpression also altered BceAB activity in response to AMPs that do not interfere with UPP. To this end, we tested BceAB activity in response to two lipid II-binding AMPs, mersacidin and actagardine. If the changed BcrC levels had a specific effect on UPP concentrations, the BceAB activity should be the same as in the wild-type strain when mersacidin or actagardine were added. In contrast, more global effects on the cell envelope should result in a change of activity, regardless which AMP was used.

When re-testing the WT and the Δ*bcrC* strains (SGB73, SGB649), a gradual increase of BceAB activity could be observed with increasing amounts of mersacidin or actagardine (Fig. 4.5 A, C). Comparing the activities between the WT and Δ*bcrC* strains at each AMP concentration showed that changing the UPP levels in the cell had no effect on BceAB activity for these two AMPs. Statistical analysis using a two-way ANOVA confirmed the significant effect that the increased concentration of each AMP had on BceAB activity ($p < 0.0001$), but further showed that there was no significant variation between the two strains tested ($p = 0.7466$ and $p = 0.9987$ for mersacidin and actagardine, respectively).

As an additional control, the activity of the related *B. subtilis* transporter PsdAB upon UPP accumulation was tested. This transporter is a BceAB paralog and responds to and confers resistance against nisin, another lipid II-binding AMP. PsdAB activity was determined using the same luminescence-reporter assay as for BceAB, but with P_{psdA} activity as a proxy for transport. As before, transport activity increased significantly with concentration of nisin ($p < 0.0001$, Fig. 4.5 E). The minimal nisin concentration to induce PsdAB activity was 0.1 µg/ml, whereas the maximal activity was observed at 10 µg/ml. No difference between the WT (SGB74) and Δ*bcrC* (SGB681) strains at each AMP concentration could be determined ($p = 0.3530$). These findings indicate that *bcrC* deletion only affected the complex formation between UPP and bacitracin and did not have a general effect on BceAB or PsdAB function.

Re-testing transport activity upon addition of mersacidin and actagardine in a BcrC overproducing strain seemed to result in an overall decreased BceAB activity compared to WT levels (SGB758, SGB73, Fig. 4.5 B, D), similar to the effect seen upon bacitracin addition (Fig. 4.4 D). Statistically significant differences between WT and the P_{xylA}-*bcrC* strain at each

tested concentration were only found at 1 and 3 µg/ml mersacidin ($p < 0.0001$) using *post-hoc* analysis. These findings imply that overproduction of BcrC seemed to have a more global effect on BceAB activity. For example it could have affected not only UPP but also lipid II levels displayed on the extracellular face of the cell. Nevertheless, the largest difference in BceAB activity between the WT and the BcrC overproducing strain was seen in the presence of bacitracin (IV 2.2.1), hinting towards that the more prominent effect of BcrC overproduction is on the UPP pool.

The findings so far indicate that BceAB activity does not depend on the concentration of free antibiotic, but seemed to vary with the amount of the cellular target. This makes it more likely that [UPP-BAC], or more general the complex of cellular target and antimicrobial peptide is the physiological target rather than the AMP alone.

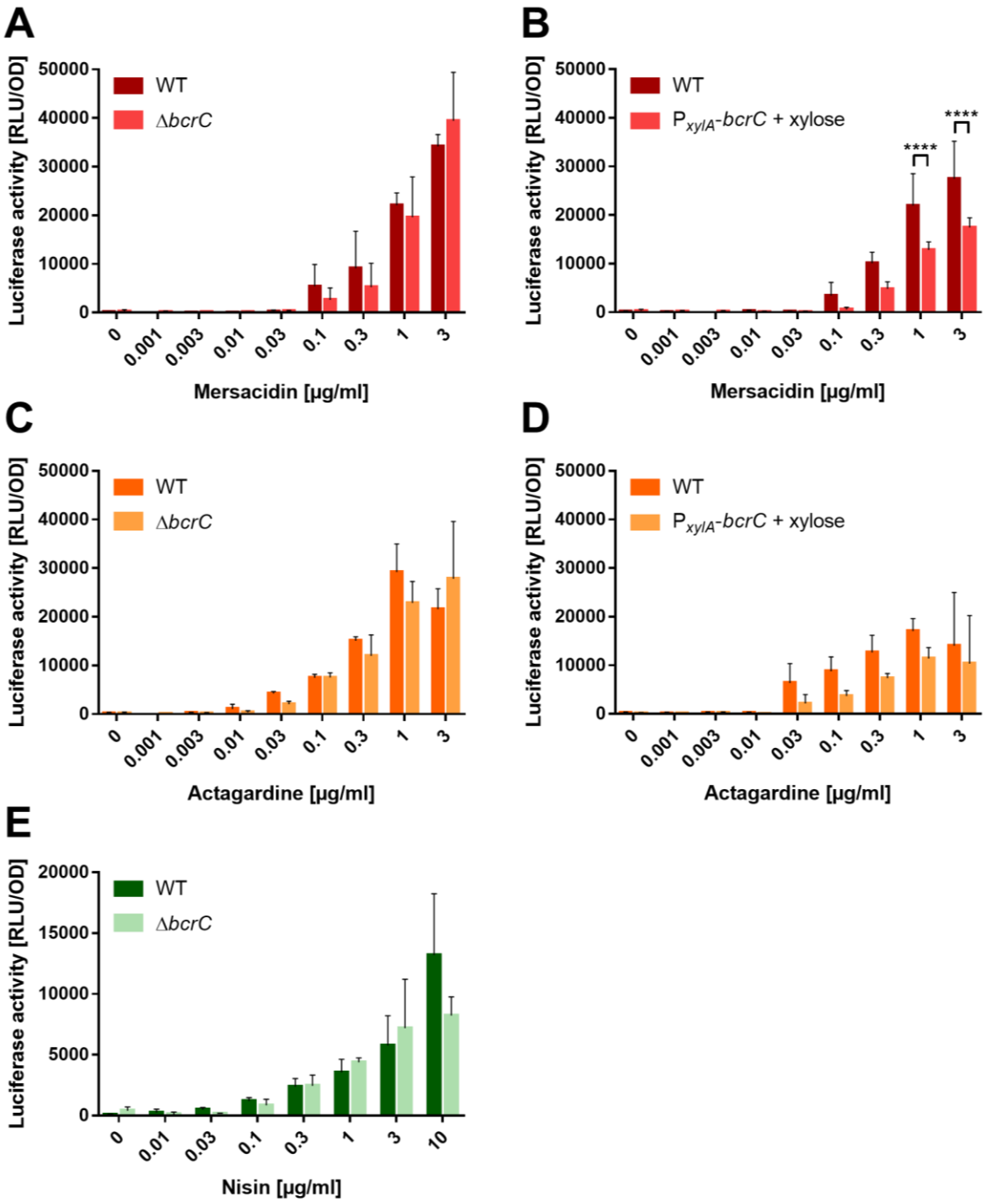
A
Luciferase activity [RLU/OD]
WT
ΔbcrC
Mersacidin [µg/ml]
B
WT
PxylA-bcrC + xylose
****
****
Mersacidin [µg/ml]
C
WT
ΔbcrC
Actagardine [µg/ml]
D
WT
PxylA-bcrC + xylose
Actagardine [µg/ml]
E
WT
ΔbcrC
Nisin [µg/ml]

Figure 4.5: Accumulation of UPP does not affect BceAB nor PsdAB transport activity in the presence of mersacidin, actagardine or nisin, respectively. Exponentially growing cells were challenged with varying concentrations of mersacidin, actagardine or nisin, as indicated. Luminescence activity (RLU/OD) was determined as average of three measurements taken 25, 30 and 35 minutes after addition of AMPs. All data are shown as mean ± standard deviation of at least three biological replicates. Bonferroni's multiple comparisons test was performed as *post-hoc* analysis after a two-way ANOVA (****: $p < 0.0001$, ***: $p < 0.001$, **: $p < 0.01$, *: $0.01 < p < 0.05$). **A+C:** Comparison of WT activities (SGB73, dark red/orange) and Δ*bcrC* strain (SGB649, light red/orange) with varying mersacidin or actagardine concentrations. **B+D:** BceAB activity of the BcrC overproduction strain (SGB758, P_{xylA}-*bcrC*) in the presence of 0.2 % xylose (light red/orange) compared to WT activity (dark red/orange). **E:** Comparison of PsdAB activities in the WT (dark green) and Δ*bcrC* strain (light green) with varying concentrations of nisin. PsdAB activity was obtained in the same manner as BceAB activity.

2.2.3 Accumulation of C_{35}-PP in the cell does not alter BceAB activity.

Manipulations of the isoprenoid biosynthesis pathway have previously been demonstrated to lead to accumulation of heptaprenyl diphosphate (C_{35}-PP). This effect occurs upon deletion of *ytpB*, a tetraprenyl-beta-curcumene synthase (Sato *et al.*, 2011), when the activity of MenA, a key enzyme in the menaquinone pathway, is simultaneously limited (Kingston *et al.*, 2014). C_{35}-PP was hypothesised to act as a competitive inhibitor and to block BceAB transport activity (Kingston *et al.*, 2014). In this case, BceAB activity should decrease upon C_{35}-PP accumulation.

As bacitracin has been shown to tightly bind the pyrophosphate of GPP (Economou *et al.*, 2013), the shorter precursor of UPP, it was expected that bacitracin would also bind C_{35}-PP. If [UPP-BAC] was the physiological substrate of BceAB, also [C_{35}-PP-BAC] is likely to be recognised by BceAB. Then, BceAB activity should not be affected.

To this end, we re-tested the BceAB activity of a Δ*ytpB* strain in the presence of bacitracin and compared it to wild type activity (SGB73, SGB798, Fig. 4.6). As the available a Δ*ytpB* MenA depletion strain was incompatible with our current luminescence reporter strain, BceAB activity experiments as well as MIC assays were performed in MH medium. In contrast to LB medium, MH contains lower amounts of tryptophan. In the tryptophan auxotroph *B. subtilis* W168 strain (*trpC2*), tryptophan depletion de-represses the biosynthesis thereof. Tryptophan biosynthesis in this strain is only disabled at the second-to-last step. This leads to a higher consumption of the central precursor chorismate, which in turn is thought to lead to reduced 1,4-dihydroxy-2-naphthoic acid (DHNA) biosynthesis. MenA uses DHNA as co-substrate of C_{35}-PP (Suvarna *et al.*, 1998). Depletion of DHNA reduces the activity of MenA, which thus mimics a genetic depletion strategy and should lead to C_{35}-PP accumulation (Kingston *et al.*, 2014).

As before, BceAB activity increased gradually with the bacitracin concentration added. The minimal concentration to trigger transport activity was 0.1 µg/ml bacitracin, maximal activity was observed at 30 µg/ml. There was no detectable difference in BceAB activity between the Δ*ytpB* strain and the WT at the same bacitracin concentration (Fig. 4.6).

This implies that under these conditions, C_{35}-PP or [C_{35}-PP-BAC] did not inhibit BceAB activity and suggests that BceAB cannot distinguish between [UPP-BAC] and [C_{35}-PP-BAC]. If BceAB is able to recognise both [UPP-BAC] and [C_{35}-PP-BAC] as substrate, the transporter is also likely to remove the bacitracin from the heptaprenyl diphosphate. In such case, the transport

activity was not expected to decrease. Taken together, these findings contradict that C_{35}-PP acts as a competitive inhibitor of BceAB.

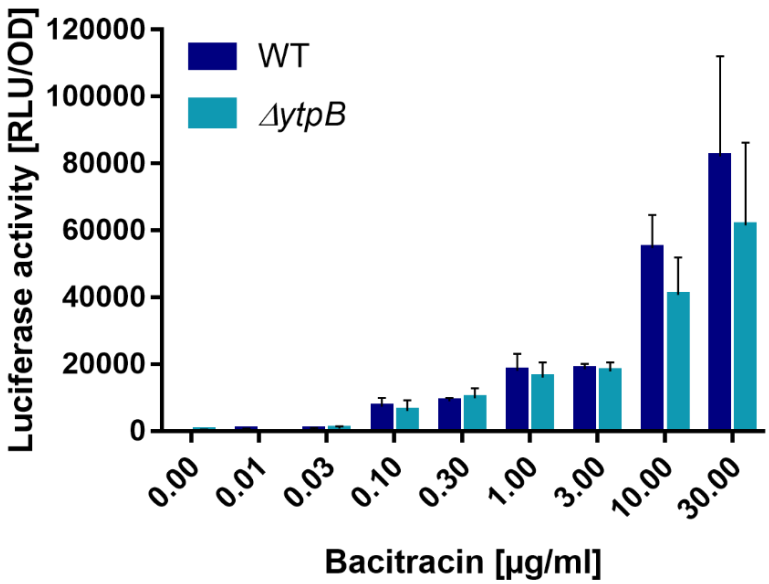

Figure 4.6: Accumulation of C_{35}-PP in the cell does not affect BceAB activity in presence to bacitracin, but leads to decrease in resistance. Comparison of activities in the WT (SGB73, dark blue) and Δ*ytpB* strain (SGB798, turquoise) in the presence of varying bacitracin concentrations. BceAB activities were determined as described in Fig. 4.4, but experiments were performed in MH media. Data are shown as mean ± standard deviation of at least three biological replicates. A two-way ANOVA did not show any significant contribution to variation by the strains.

3. Discussion

In this chapter, we aimed to identify the nature of the physiological substrate of the antimicrobial resistance transporter BceAB in the context of the living cell. Using *in vivo* assays combined with genetic manipulations that were expected to alter the levels of key players in the lipid II cycle, we intended to investigate changes in the interaction between the physiological target with BceAB and effects on its transport activity. The physiological substrate of BceAB had previously been proposed to be the [target-AMP] complex or either the AMP or the cellular target alone.

3.1 Our experimental data do not support a 'UPP import' model for BceAB.

A potential interaction between BceAB and the lipid carrier UPP was investigated using comparisons of the fastest doubling times and competition assays between strains that produced different levels of BceAB or lacked the transporter. In addition, this effect was tested in a UPP accumulation background. The absence of BceAB was expected to slow down growth in case the transporter acted as UPP importer, because slowed recycling of the lipid carrier reduces the rate of cell wall synthesis. In case UPP binding by the transporter could branch away some UPP from being recycled by UPP phosphatases, the removal of BceAB would facilitate faster growth. Deletion of *bceAB* imparted neither a benefit nor disadvantage on growth as determined by the fastest doubling times. It also did not cause any significant difference upon UPP accumulation. We were not able to reproduce the difference in growth observed by Radeck and colleagues (2016b) when comparing the fastest doubling time upon deletion of Δ*bceAB*. This can likely be explained by the fact that in the previous study the tested strains contained a P_{bceA} luminescence reporter. Luciferase catalyses the oxidation of reduced flavin mononucleotides ($FMNH_2$) and fatty aldehydes in the presence of molecular oxygen, which might come at a cost for the cell (Park *et al.*, 2013). A strain lacking BceAB might have therefore had a growth advantage. In support of this, we consistently observed growth differences between the WT (SGB73, *bceAB*$^+$) and Δ*bceAB* strains containing the P_{bceA}-*lux* reporter during routine growth for transport activity assays in this study (data not shown). This is would also be consistent with the hypothesis that cell wall synthesis itself is not rate-limiting during exponential growth. Cell wall synthesis, cell division, DNA replication and other mechanisms in the cell need to be tightly regulated and spatially and temporarily coordinated to ensure impeccable growth. Yet, fast-growing bacterial cells were found to

have elongated cell shapes (Chien *et al.*, 2012). In *B. subtilis*, fast-growing cells were only elongated and not increased in diameter, which results in a higher surface-to-volume ratio (Chien *et al.*, 2012). This indicates that the cell wall synthesis is not growth-limiting. Yet, it is unclear if the cell wall consists of as many layers of peptidoglycan as during slower growth, or whether fast-growing cells have a thinner cell wall.

The findings of the more sensitive competition assays suggested the deletion of *bceAB* to be advantageous over a *bceAB*$^{+}$ strain when competing in a UPP-accumulated environment, in which UPP recycling is diminished (Fig. 4.2). The absence of BceAB did not seem to make an obvious difference in the wild type background. This supports an interaction between BceAB and UPP, in which the transporter withholds some of the lipid carrier from being recycled. As this potential interaction seems to slow UPP turnover mainly when UPP recycling is impaired, we suspected a rather low affinity interaction.

Additionally, accumulation of UPP did not seem to trigger BceAB activity in the absence of AMPs, when BceAB transport activity was monitored using a luminescence reporter assay. This finding suggests that UPP alone is not enough to induce a signalling response of BceAB. This is consistent with the lipid carrier possibly being part of the physiological substrate as it is suggested for a 'hydrophobic vacuum cleaner' mechanism (Bernard *et al.*, 2007).

The recycling reaction of the lipid carrier, in which it is transported back across the membrane to the cytoplasmic face, is still far from understood. Cytosolic undecaprenyl phosphate (UP) stands as lipid carrier at the start of both, peptidoglycan and wall teichoic acid synthesis. Both pathways are known to release the lipid carrier in its pyrophosphate form (UPP) in the outer leaflet of the membrane after their respective cell wall building blocks have been incorporated into the cell wall (Scheffers & Pinho, 2005, Brown *et al.*, 2013). Because of its size and charge, UPP is thought to be imported actively rather than to flip spontaneously (Zhao *et al.*, 2017). Yet, the identity of the potential flippase remains unknown. It is further unclear if the lipid carrier is dephosphorylated before or after it is flipped across the membrane. In the search for answers to these fundamental questions, the membrane-based transporter BceAB seemed like a suitable candidate for UPP import. BceAB confers resistance against the UPP-targeting AMP bacitracin. Importing the lipid carrier back into the cell would effectively shelter it from the inhibitory grip of the AMP (Kingston *et al.*, 2014).

The growth advantage in the absence of BceAB stands against the hypothesis that the transporter acts as UPP or UP importer, which was proposed by Kingston *et al.* (2014). As importer, BceAB would increase UPP recycling and therefore lead to accelerated growth. The

lack of the transporter should have therefore resulted in a fitness cost, if this hypothesis was true.

Furthermore, BceAB also confers resistance against other AMPs, namely mersacidin, actagardine and the fungal defensin plectasin (Staron *et al.*, 2011, Mygind *et al.*, 2005). Instead of binding the lipid carrier, these AMPs were found to target lipid II (Breukink & de Kruijff, 2006, Schneider *et al.*, 2010). Import of UPP is not an appropriate strategy to provide resistance against them. Of course, import of lipid II before its peptidoglycan precursor is incorporated into the cell wall is a plausible way to shelter the molecule from AMPs. However, import of lipid II runs counter the process of cell wall biosynthesis, where PG precursors are required on the surface of the membrane. Lipid II import is therefore a not an effective way of protecting the cell from antimicrobial stress.

Taken together, our data suggest that UPP alone is unlikely to be the true physiological substrate of BceAB. Our experimental data and support from previous studies further argue against the hypothesis that BceAB acts according to a 'UPP import' model. Yet, the findings of this chapter are in support of a possible low-affinity interaction between BceAB and UPP in the absence of bacitracin. Even if not the signal-inducing agent or transported substrate, specific interactions between membrane-based transporters and their phospholipid environment are not unusual.

The tripartite drug efflux pump MacB was shown to specifically bind phosphatidylethanolamine molecules (Barrera *et al.*, 2009). The physiological role of this interaction is entirely unclear. It could be speculated whether also MacB recognised its substrates in a membrane-associated state, as macrolide antibiotics like erythromycin may weakly associate with phospholipids of biological membranes (Montenez *et al.*, 1999).

Further, the surrounding phospholipid environment was shown to affect substrate affinity and ATP hydrolysis of integral membrane proteins (Romsicki & Sharom, 1999, Miyamoto & Tokuda, 2007). Changes of the phospholipid environment as caused by bacitracin action or UPP phosphatase impairment could thus affect BceAB activity in some way. Because BceAB likely recognises the [UPP-BAC] complex, an affinity to the lipid carrier part alone is plausible, particularly under UPP accumulating conditions. It is also conceivable that the low affinity to the lipid carrier UPP could help BceAB with localisation near cell wall biogenesis sites. Further work needs to be carried out to understand the role of this potential interaction.

3.2 The [target-AMP] complex is likely the physiological substrate of BceAB.

After excluding UPP alone as physiological substrate of BceAB, we sought to determine whether the AMP alone was enough to trigger BceAB activity or whether the [target-AMP] complex was the physiological substrate of BceAB. To this end, we monitored the BceAB activity not only upon addition of the AMP, but also when levels of lipid carrier in the cells were altered by genetic manipulations. Both approaches are thought to alter the amount of [target-AMP] complex formed. We showed that addition of bacitracin as well as changing levels of UPP in the presence of bacitracin were able to alter BceAB activity (Fig. 4.4). We found this effect on BceAB activity to be specific for [UPP-BAC], as accumulation of UPP did not alter BceAB activity in the presence of the lipid II-binding AMPs (Fig. 4.5). These findings indicated that the physiological substrate is not bacitracin alone. As the activity changed according to two variables, the physiological substrate was suspected to be the complex of the AMP and its respective cellular target.

In an approach independent of alterations of the UPP phosphatase activity in the cell, we accumulated C_{35}-PP in the cell by deleting *ytpB* in an environment where MenA activity was reduced by substrate limitation (Sato *et al.*, 2011, Kingston *et al.*, 2014). Heptaprenyl diphosphate was expected to be a target of bacitracin, as it was shown that bacitracin only requires the pyrophosphate group and one adjacent isoprenoid moiety to bind its target with high affinity (Storm & Strominger, 1973, Economou *et al.*, 2013). Previously, C_{35}-PP or [C_{35}-PP-BAC] were proposed to interact with BceAB and to inhibit its activity (Kingston *et al.*, 2014). Our experimental data suggested that BceAB activity did not decrease significantly upon C_{35}-PP accumulation (Fig. 4.6). From this, we excluded C_{35}-PP or [C_{35}-PP-BAC] to have inhibitory function on BceAB. Our data rather indicated that BceAB cannot distinguish between [UPP-BAC] and [C_{35}-PP-BAC] and therefore might also recognise and process [C_{35}-PP-BAC] as a substrate. In contrast to BceAB being inhibited by C_{35}-PP, we thus propose that upon recognition of [C_{35}-PP-BAC], BceAB removes bacitracin from C_{35}-PP according to a 'hydrophobic vacuum cleaner' mechanism (Ohki *et al.*, 2003, Bernard *et al.*, 2007). Removal of bacitracin from the lipid II cycle intermediate UPP helps towards the turnover of the lipid II cycle and thus, towards cell wall biosynthesis. Releasing of C_{35}-PP from the grip of bacitracin, however, does not contribute to resistance against AMPs, as it is involved in sesquarterpene synthesis (Sato *et al.*, 2011). In agreement with this, deletion of *ytpB* led to an increased sensitivity to bacitracin (Kingston *et al.*, 2014). The effect was most prominent when the Δ*ytpB* strain was tested on solid medium, where bacitracin had a bacteriolytic

effect and led to early lysis. A moderate decrease of MIC was also observed in liquid culture (Kingston *et al.*, 2014). Our own MIC data from liquid cultures showed no noticeable difference between the Δ*ytpB* and the WT strain. The OD_{600} measurements from plate reader experiments, however, confirmed a slightly higher susceptibility of the Δ*ytpB* strain to bacitracin (data not shown).

The changes in sensitivity to bacitracin indicate that at the C_{35}-PP accumulated at the outer face of the membrane, where it is accessible to bacitracin. Membrane localisation of C_{35}-PP is expected due to its long isoprenoid chain. This is further supported, as C_{35}-PP is a precursor for some membrane-associated sesquarterpens and menaquinone-7 (Bramkamp & Lopez, 2015, Farrand & Taber, 1974). Yet, it remains puzzling whether C_{35}-PP is abundant at either face of the membrane or distributed asymmetrically.

Hence, it is possible that the Δ*ytpB* strain did not have enough C_{35}-PP accumulated at the outer face of the membrane at time the experiment was performed. It is therefore recommended to repeat the assay in a minimal medium containing even less tryptophan. Alternatively, BceAB activity should be re-tested in a Δ*ytpB menA* depletion strain, in which MenA activity is reduced by lower gene expression levels, rather than limited by substrate availability (Kingston *et al.*, 2014).

The findings of this chapter suggest the physiological substrate of BceAB to be the complex of cellular target and the AMP, rather than the free AMP or the target alone. Alternatively, it is also possible that the transporter only interacts with the bound version of the AMP alone, as these peptides are known to undergo conformational changes upon binding their target (Hsu *et al.*, 2003, Economou *et al.*, 2013). These structural changes might expose certain features required for substrate recognition by BceAB. The approaches used in this chapter were not laid out to distinguish between those two options.

3.3 The 'hydrophobic vacuum cleaner' model as proposed mechanism for BceAB.

The conclusions of this chapter are in support of a 'hydrophobic vacuum cleaner' model of BceAB action (Ohki *et al.*, 2003, Bernard *et al.*, 2007). Our proposed hypothesis is consistent with all previously published data on the mechanism of BceAB that we are aware of. Nevertheless, the identification of the physiological substrate does still not allow unwavering conclusions on the resistance mechanism, as, for example, the direction of transport is still unclear. Although the 'hydrophobic vacuum cleaner' hypothesis suggests export into the extracellular space, import of the substrate for degradation has not yet been ruled out experimentally. Upon recognition of the [target-AMP] complex, several alternative resistance mechanisms that have not been discussed in the literature, yet are plausible, might apply for BceAB. Rather than freeing the cellular target from the AMP, it is for example possible that the whole [target-AMP] complex is extracted from the membrane and released into the extracellular space. The resulting inactivation of the AMP would also prevent the re-attachment of the antimicrobial compound onto the membrane. In an alternative mechanism, BceAB could recognise the [target-AMP] complex, and in response export poly-isoprenoids from the membrane to the extracellular space, where the AMPs could be bound and inactivated. Although such a mechanism seems very costly for the cell, a recent study suggested a similar mechanism for daptomycin resistance in *S. aureus* (Pader *et al.*, 2016). Upon daptomycin stress, *S. aureus* releases the phospholipid phosphatidylglycerol, which is the target of daptomycin in the membrane (Tran *et al.*, 2015). In doing so, the antibiotic is inactivated in culture supernatants (Pader *et al.*, 2016).

To further investigate these possibilities, bacitracin transport assays from previous work by our laboratory were taken into account (Emenegger & Gebhard, unpublished data). These experiments were modified from the peptide release assays established by Otto and colleagues (1998) and were used in other studies to determine direction of AMP transport (Stein *et al.*, 2003, Stein *et al.*, 2005, Reiners *et al.*, 2017). The assay is based on the quantification of the AMP concentration that remains in the culture supernatant after incubating strains carrying or lacking the respective resistance determinant with the AMP.

No significant differences in the concentrations of residual biologically-active bacitracin could be determined between the culture supernatant of strains containing or lacking BceAB (*bceAB*$^{+}$ or Δ*bceAB*) and a control without cells (Fig. S4.1). An initial bacitracin concentration of 5 µg/ml was used and a slight reduction of bacitracin was observed even in the control without cells. This was likely due to oxidative deamination of bacitracin A to bacitracin F that

possesses lower antimicrobial activity (Storm & Strominger, 1973). As the remaining bacitracin in the supernatant did not decrease compared to this 'buffer-only' control, it was concluded that BceAB neither imported bacitracin into the cell nor led to inactivation or degradation of the AMP in the extracellular space. These findings make the alternative resistance mechanisms described above unlikely.

Further, a higher concentration of residual bacitracin was expected in the supernatant of the *bceAB*$^{+}$ strain compared to the Δ*bceAB* strain, if BceAB worked according to hydrophobic vacuum cleaner and expelled bacitracin from the membrane. However, no difference in concentration could be determined between them (Fig. S4.1). Notably, the bacitracin concentration of the cell suspensions did not seem to be decreased, compared to the buffer control. This implied that there was too little bacitracin attached to the cells to be detected. Therefore, we could not further confirm the expulsion of bacitracin from the membrane experimentally.

The idea of conferring resistance against lipid II-binding antibiotics via export of the AMP from the membrane to the extracellular space has previously been described for several LanFEG-type transporters. Otto and colleagues (1998) suggested the EpiFEG transporter of *S. epidermidis* to work by expelling epidermin and gallidermin derivatives from the membrane. Resistance against nisin in *Lactococcus lactis* is mediated by the transporter NisFEG, while *B. subtilis* ATCC6633 is protected against subtilin by SpaFEG. The self-protection mechanism provided by the transporters against both lantibiotics was shown to involve the transport of the lantibiotics from the membrane into the extracellular space (Stein *et al.*, 2003, 2005). Additionally, immunity against the lantibiotic nukacin ISK-1 in the producer *Straphylococcus warneri* ISK-1 was shown be conferred by NukFEG. Again, this transporter is thought to relocate the AMP away from the membrane, which was revealed by a transport assay using fluorescence-labelled nukacin ISK-1 (Okuda *et al.*, 2008). Recently, also the BceAB-like transporter NsrFG of *Streptococcus agalactiae* COH1 was shown to confer resistance by transporting nisin from the membrane to the extracellular space (Reiners *et al.*, 2017). In most studies, the remaining lantibiotic concentration was determined using HPLC, but none mentioned an increased amount of lipid II in the supernatant. These observations further supported that BceAB could provide resistance using a mechanism that recognises its substrate in the membrane and releases it into the extracellular space.

3.4 The challenges of manipulating the lipid II cycle intermediate levels of the cell wall biosynthesis

In Gram-positive bacteria, the cell wall is the outmost layer of protection against the environment, and thus cell wall biosynthesis is a main target for many antibiotics (Breukink & de Kruijff, 2006, Schneider & Sahl, 2010). In turn, bacteria have evolved to protect this mechanism by producing proteins with redundant function and by developing several stress response strategies that upregulate expression of alternative genes and pathways (Mascher *et al.*, 2003, Radeck *et al.*, 2016a, Helmann, 2016).

Most experiments described in this chapter focussed on the most prominent substrate of the BceAB transporter, bacitracin in complex with its cellular binding partner UPP. The extracellular UPP pool serves as an excellent target for antimicrobial action, yet we were seemingly able to alter the lipid carrier levels in the outer face of the membrane using genetic manipulations. This could potentially be explained by *B. subtilis* possessing alternative pathways to obtain the crucial lipid II cycle intermediate UP, when UPP recycling is impaired by the lack of the main UPP phosphatase BcrC or blocked by bacitracin. The bioneogenesis of UPP is catalysed by the undecaprenyl pyrophosphate synthetase UppS (Apfel *et al.*, 1999). Followed by dephosphorylation performed by functionally redundant UPP phosphatases (Zhao *et al.*, 2016, Radeck *et al.*, 2017a), this could still lead to lipid II formation and compensate for some of the deficiency. Further, Gram-positive bacteria are thought to store free undecaprenyl (C_{55}-OH) as a reserve pool of the lipid carrier (Bouhss *et al.*, 2008). In *B. subtilis*, UP shortage leads to increased phosphorylation of C_{55}-OH to UP by the undecaprenyl kinase DgkA (Jerga *et al.*, 2007, Radeck *et al.*, 2017a). Also recycling of UP from wall teichoic acid biosynthesis can potentially compensate for impaired UPP dephosphorylation (Brown *et al.*, 2013).

From the work presented in this chapter, we concluded that the [target-AMP] complex in general is the physiological target of BceAB. This means also the lipid II-binding AMPs, like mersacidin and actagardine, should be only recognised by BceAB when they are bound to their cellular target ([lipid II-AMP]). As a consequence, BceAB transport activity should also depend on the amount of [lipid II-AMP] complexes, which in turn should alter with varying lipid II levels in the cell. To test if the [target-AMP] complex principle also applies for lipid II-binding AMPs, it would be important to measure BceAB activity upon lipid II accumulation or reduction in the presence of mersacidin. Several alternative strategies to accumulate lipid II in the outer leaflet of the membrane have already been attempted for this study. These

included the deletion of *ponA,* which encodes penicillin binding protein 1. PBP1 is a class A PBP that possesses both, transglycosylation as well as transpeptidase activity during cell wall biosynthesis (Scheffers & Pinho, 2005). Deletion of *ponA* was shown to lead to slower growth, altered cell morphology (Popham & Setlow, 1995) and potentially to a decreased transglycosylation rate.

In an alternative strategy, we tried to accumulate lipid II without using genetic manipulations. A recent study showed that addition of moenomycin led to accumulation of lipid II in *S. aureus* and the same study successfully used vancomycin to accumulate lipid II in *B. subtilis* (Qiao *et al.*, 2017). Vancomycin binds to the terminal D-Ala-D-Ala residues of the peptidoglycan precursors stem peptide (Wang *et al.*, 2018). The glycopeptide should not affect the pyrophosphate and sugar moieties of lipid II that are recognised by mersacidin and actagardine and thus, not block their binding site. Therefore, we attempted to accumulate lipid II by combining the AMPs with vancomycin. A similar combinatory approach was performed using ampicillin.

BceAB activity was tested as described previously in this chapter, but now using these potentially lipid II-accumulating strains and conditions and upon the addition of mersacidin. None of the tested conditions resulted in significant changes of BceAB activity (Δ*ponA*: Fig. S4.2, vancomycin: Fig. S4.3, A, B, ampicillin: data not shown).

As we currently cannot measure the levels of lipid II cycle intermediates on the outer face of the membrane, no unwavering conclusions could be drawn from these experiments on whether the [lipid II-AMP] complex also serves as physiological substrate for BceAB. It is possible that BceAB can recognise bacitracin in complex with its cellular target UPP, but lipid II-binding AMPs might be recognised and dealt with in a different mechanism. In such a case, even successful alterations of the [lipid II-AMP] levels would have not led to changes in BceAB activity. However, lipid II, when located in the outer face of the membrane, is regarded as the Achilles' heel of cell wall synthesis and therefore should be particularly well-protected.

B. subtilis possesses three further PBPs with redundant transglycosylation activity (PBP2c, PBP2d, PBP4, Scheffers & Pinho, 2005). Even in absence of all of them, *B. subtilis* is able to grow (McPherson & Popham, 2003). A recent study revealed the transglycosylation activity of the RodA that can compensate for the loss of class A PBPs (Meeske *et al.*, 2016). This redundancy of function stresses the challenge to accumulate lipid II on the outer face by removal of just one PBPs. The cell seems to have several strategies to compensate for their loss and to secure the immediate incorporation of peptidoglycan precursors after 'just-in-time' delivery of lipid II.

When combining the AMPs with vancomycin, the growth of *B. subtilis* was analysed for potential synergistic interactions between the drug combinations that could point towards successful lipid II accumulation (Fig. S4.3, C, D). Although an antagonistic effect of the drug combinations can be excluded, the recorded data is not sufficient to conclude whether the antibiotics had additive or synergistic (super-additive) effects (Tallarida, 2001, Tallarida, 2006, Weinstein *et al.*, 2017). It is therefore still unclear if combining the two antibiotics led to alteration of the [lipid II-AMP] levels. Notably, the vancomycin concentration used for lipid II accumulation by Qiao *et al.* (2017) corresponded to eight-times the MIC, whereas our experiment required viable *B. subtilis* cells. Combining the AMPs with ampicillin could have potentially not led to successful accumulation of lipid II, as the beta-lactam irreversibly inhibits the transpeptidase activity of the PBPs, whereas their glycosyltransferase activity might remain functional. This implied that peptidoglycan precursors were taken off lipid II and incorporated into the glycan strands.

These experiments suggested accumulation of lipid II on the extracellular face of the membrane to be particularly challenging. The basal level of lipid II in *B. subtilis* was found to be comparatively low (Qiao *et al.*, 2017). In further support of this, our collaborators established a computational model for the lipid II cycle in *B. subtilis* (Piepenbreier & Fritz, unpublished). This model simulated the changes in cell wall synthesis upon addition of various AMPs and used the findings to deduce the AMP concentrations required to inhibit growth. For lipid II-binding AMPs a particularly large disparity between *in vitro* and *in vivo* activity was found (210-fold difference for nisin, *in vitro* K_d: 0.05 µM, Wiedemann *et al.* (2001), *in vivo* MIC: 11 µM). This was explained by the very small pool size of lipid II. With 1000 lipid II molecules per cell compared to 110 000 UPP molecules per cell, the model described the lipid II levels in the cell to be over 100-times lower than the UPP levels (Piepenbreier & Fritz, unpublished). This argues that *B. subtilis* is very good at protecting the lipid II pool on the extracellular face of the membrane and therefore the lipid II accumulation attempts so far might have not been successful.

Thus, we aimed to alter the levels of both, UPP and lipid II displayed on the outer face of the membrane. The cell wall synthesis is protected by several extracellular function (ECF) sigma factors (Helmann, 2016). The σ^M stress response is activated by conditions that disturb peptidoglycan synthesis, including antimicrobial stress caused by bacitracin. σ^M upregulates genes that are responsible for expression of the core machinery for cell wall biosynthesis, including PBPs (PBP1 and PbpX) and the UPP phosphatase BcrC (Eiamphungporn & Helmann, 2008, Helmann, 2016). Deletion of *sigM* was expected to cause changes in the lipid II cycle

intermediate levels and hence, alter the amounts of [target-AMP] complexes. Removal of σ^M did not lead to significant changes in BceAB activity upon addition of bacitracin or mersacidin (Fig. S4.4). Again, it was unclear whether the lipid II cycle intermediates levels on the outer face of the membrane were altered. The σ^M regulon comprises over 60 genes that potentially affect the lipid II cycle at different stages, which made accurate predictions difficult. Further, several genes are regulated by multiple σ factors, which could have compensated for the loss of σ^M. Particularly the σ^W and the σ^x stress response overlap to a significant degree with the σ^M regulon, which can be explained by highly similar consensus sequences in their respective promotor regions (Mascher *et al.*, 2007, Helmann, 2016). A well described example for this is the activation of expression of *bcrC* by both, σ^M and σ^x (Cao & Helmann, 2002). Double or even triple deletion strains might have clearer effects on the lipid II cycle intermediate levels. Although many of the described proteins and ECF σ factors seem functionally redundant and dispensable, other core genes of the cell wall synthesis are essential (Kobayashi *et al.*, 2003).
An alternative strategy to alter the total amount of lipid II cycle intermediates in the cell aimed at the manipulation of the undecaprenyl pyrophosphate synthetase, UppS. This enzyme catalyses the assembly of UPP from isoprenoid precursors (Apfel *et al.*, 1999). Overproduction of UppS was expected to lead to an increased amount of all lipid II cycle intermediates available to the cell, which should lead to increased amounts of [target-AMP]. However, overproduction of UppS did not lead to a significant change in BceAB activity upon addition of bacitracin (Fig. S4.5).
UPP assembly might not have been the rate limiting step of the lipid II cycle and thus, might have not led to accumulation on the extracellular face of the membrane. It is still open to debate whether *de novo* synthesised UPP is transported to the outer leaflet of the membrane before it is dephosphorylated to UP and imported back in, as the localisation of UPP phosphatases remains puzzling (Zhao *et al.*, 2016, Radeck *et al.*, 2017a). Overproduction of UppS therefore might have only resulted in small effects. In agreement with this, only a slight increase in resistance to bacitracin was found in a Δ*ytpB* strain upon overproduction of UppS (Kingston *et al.*, 2014).
To make availability of the lipid carrier the rate-limiting step of the lipid II cycle, we aimed to reduce UppS levels in the cell. By this, the lipid carrier levels should be decreased throughout all lipid II cycle pool levels, leading to lower amounts of [target-AMP] complexes. *uppS* is not only essential, but also transcribed as a polycistronic mRNA together with several other essential genes (Zhu & Stulke, 2018). Modifications of *uppS* were therefore challenging and

likely to impair transcription of the other genes in the operon. Deletion of the native *uppS* gene in a strain carrying an ectopic inducible copy of the gene failed, even in the presence of the inducer. Decreasing the translation levels of *uppS* as previously described by Lee and Helmann (2013) seemed promising at first, but problems with the control strain led us to disregard the data for now (not shown). The strain contained an antibiotic marker in the non-coding region before the *uppS* promoter region, which might have altered read-through of *uppS* and other essential downstream genes. To this end, other approaches, including conditional expression and CRISPRi (Hawkins *et al.*, 2015, Peters *et al.*, 2016) were attempted but failed due to technical reasons.

Aside from tackling technical issues, more work is required to understand changes of lipid II cycle intermediate levels more accurately and efficiently. Based on their to-date unpublished model of the lipid II cycle, predictions were attempted by our collaborators (Piepenbreier & Fritz, unpublished). While predictions of the lipid II cycle intermediate pool levels can forecast UPP accumulation on the outer face upon *bcrC* deletion, the model still has too many unknown parameters to allow accurate predictions of the less intuitive steps of cell wall synthesis. To accurately determine the rate limiting steps and alterations of pool sizes, the model would have to take resistance determinants and other stress responses into account. Analysing the global pattern of changes in promoter activities in response to genetic manipulations affecting the lipid II cycle would be a helpful step towards this goal.

All in all, this chapter described *in vivo* approaches to identify the physiological substrate of BceAB. Physiological assays, including growth and competition assays, identified a potential low-affinity interaction between BceAB and UPP when UPP dephosphorylation is impaired. Further, a P_{bceA}-*lux* reporter assay was used to investigate the BceAB transport activity in response to genetic manipulations of genes important to the lipid II cycle. Our data suggested the complex formed between the antimicrobial peptide and its corresponding cellular target as the physiological substrate of BceAB. Bacitracin transport assays argued against the import of bacitracin or its inactivation in the supernatant. This is in support of a 'hydrophobic vacuum cleaner' hypothesis as the resistance mechanism of BceAB, as it has been proposed before (Ohki *et al.*, 2003).

Chapter V

Conclusions and future perspectives

1. Summary and main conclusions

The overall aim of this thesis was to study the mechanisms of substrate recognition of the antimicrobial peptide resistance transporter BceAB of *B. subtilis*. The objectives of Chapter III were the purification and characterisation of the large extracellular domain of BceB (BceB-ECD), the putative binding domain. Further, the binding mechanism of this domain was investigated *in vitro*. The objectives of Chapter IV were aimed at the identification of the physiological substrate of BceAB using *in vivo* growth and luminescence reporter assays.

In Chapter III, we established an optimised strategy for the overproduction and purification of BceB-ECD, which led to greatly increased yield and solubility as well as high purity in only one purification step. As the *in silico* analysis suggested BceB-ECD to be highly flexible with intrinsically disordered regions, a substrate-induced coupled folding and binding process was proposed for BceB-ECD. Using steady-state ANS fluorescence and circular dichroism spectroscopy, the binding capacities of several refolded and soluble purified BceB-ECD samples were investigated. Yet, no binding activity between BceB-ECD and bacitracin alone could be detected. The cellular target of bacitracin, undecaprenyl pyrophosphate (UPP), had been proposed to be part of the physiological substrate of BceAB. Thus, investigations in the presence of geranyl pyrophosphate (GPP), which was used as surrogate for UPP, were performed. *In vitro* analyses did not reveal binding interactions between BceAB and GPP alone. The characterisation of a binding event between BceB-ECD and the [GPP-BAC] complex did not lead to unwavering conclusions, as the complex formation between GPP and bacitracin resulted in highly variable background signal.

Our investigations in Chapter IV therefore focussed on the identification of the physiological substrate *in vivo*. Accumulation of UPP alone did not induce BceAB activity. Additionally, a potential low-affinity binding event between BceAB and UPP was indicated by competition assays in the absence of bacitracin. By interacting with UPP, BceAB might withhold some UPP from dephosphorylation. These findings argued against a 'UPP importer' mechanism for BceAB.

A P_{bceA} luminescence reporter assay used as proxy for BceAB transport activity revealed that transport activity did not only vary with the amount of bacitracin but also when UPP levels were changed in the presence of bacitracin. Both variables specifically affected the amount of [UPP-BAC] complexes formed in the membrane. From this, we concluded that the most

likely physiological substrate is the complex between bacitracin and UPP or bacitracin alone, but in its target-bound conformation.

Combining our findings, we propose that BceAB recognised the [UPP-BAC] complex as its substrate, but seemed to only have little or no affinity to the components of the complex separately. Bacitracin undergoes an extensive conformational change when binding its target, adopting a truly amphipathic configuration (Economou *et al.*, 2013). Our data suggest that BceAB can differentiate between the 'free' and 'bound' form of bacitracin. The [UPP-BAC] complex is located at the membrane-interface; this is therefore likely where the substrate binding of BceAB takes place.

We thus propose that BceAB acts according to a hydrophobic vacuum cleaner, which takes up its substrate directly from the hydrophobic membrane environment and then expels it to the extracellular space. By this, the cellular target is released from the inhibitory grip of the AMP and can be processed by the next enzymatic step of the cell wall synthesis.

2. BceAB removes bacitracin from its membrane-bound target and releases the AMP into the extracellular space.

Taking the results and conclusions of this study into context with previous findings and the literature, we here propose a possible resistance mechanism of BceAB to bacitracin.

Generally, the resistance transporter BceAB is located in the membrane with its large domain facing the extracellular space (Rietkötter *et al.*, 2008). Upon antimicrobial stress, we propose that BceAB does not interact primarily with free bacitracin, nor with its cellular target UPP (Fig. 5.1 A). This is consistent with our *in vitro* data, in which no interaction between purified BceB-ECD and bacitracin or GPP alone was shown (Chapter III). Previously, a direct *in vitro* binding interaction between full-length BceB and bacitracin had been suggested (Dintner et al., 2014). However, the study could not exclude the possibility that BceAB recognised the complex formed between bacitracin and its target UPP that was possibly co-solubilised. Instead of free bacitracin, our *in vivo* studies (Chapter IV) suggest that BceAB recognises the [UPP-BAC] complex bacitracin as the physiological substrate and binds bacitracin in the membrane as suggested for a hydrophobic vacuum cleaner (Fig. 5.1 C, Mascher *et al.*, 2003, Ohki *et al.*, 2003).

When binding its membrane-anchored target, bacitracin undergoes a conformational change and adopts a truly amphipathic, dome-shaped configuration (Fig. 5.1 B, Economou *et al.*, 2013). Our ANS fluorescence and far-UV spectroscopy experiments in Chapter III confirmed the complex formation between bacitracin and its target and the associated conformational changes.

Substrate recognition and binding happen by a to-date unknown mechanism. We could not further confirm or exclude BceB-ECD as the substrate binding domain in this study. Large extracytoplasmic domains have been demonstrated to determine substrate specificity and mediate substrate binding of transporters that are homologous to BceAB (Mavrici *et al.*, 2014, Crow *et al.*, 2017, Greene *et al.*, 2018). Based on previous work (Rietkötter *et al.*, 2008, Coumes-Florens *et al.*, 2011, Hiron *et al.*, 2011) and the *in silico* predicted characteristics of BceB-ECD (III 2.1), we still assume that BceB-ECD acts as the binding domain (Fig. 5.1 C). We speculate that the large extracellular domain of BceAB undergoes a substrate-induced conformational change, as is characteristic for intrinsically disordered proteins (Wright & Dyson, 2009, Mittag *et al.*, 2010). It is possible that after a first weak interaction, BceB-ECD reels in its substrate according to a fly-casting mechanism (Shoemaker *et al.*, 2000, Huang & Liu, 2009).

BceAB removes bacitracin from its target, thereby releasing UPP (Fig. 5.1 D). This step is likely to be the ATP-dependent step of the resistance mechanism. Lacking the hydrophobic membrane environment and without its negatively charged target, bacitracin might lose its amphipathic configuration and changes its conformation back to its unbound form. BceB-ECD has much lower affinity to this conformation of bacitracin. In turn, bacitracin is released into the extracellular space (Fig. 5.1 E). By this, bacitracin is effectively 'transported' away from the membrane and UPP is unblocked. The proposed mechanism is consistent with findings on the BceAB-like transporter NsrFG of *S. agalactiae* COH1, in which the translocation of nisin by NsrFG from membrane-bound lipid II into the culture supernatant was shown (Reiners *et al.*, 2017).

As previous work showed no BceAB-mediated inactivation or degradation of bacitracin in the extracellular environment (Emenegger & Gebhard, unpublished), the AMP could now re-attach to its target in the membrane. However, UPP phosphatases are important resistance determinants themselves, and in the case of BcrC are also upregulated upon cell envelope stress (Cao & Helmann, 2002, Bernard *et al.*, 2005, Zhao *et al.*, 2016, Radeck *et al.*, 2017a). These enzymes dephosphorylate UPP to UP. Bacitracin has a much lower affinity to the single phosphate group (Storm & Strominger, 1973). Hence, UP no longer serves as target for

bacitracin (Fig. 5.1 F). The lipid carrier can therefore be recycled and cell wall synthesis can go forward.

Figure 5.1: BceAB is proposed to remove bacitracin from its target and to release the AMP into the extracellular space. A: BceAB is located in the membrane with its large domain facing the extracellular space. Flexibility of BceB-ECD is indicated by a dashed arrow. **B:** BceAB has very low affinity to unbound bacitracin. Upon binding its target, bacitracin undergoes a conformational change. **C:** BceAB recognises the bound form of bacitracin, potentially via its flexible extracellular domain. **D:** Bacitracin is removed from its target by an unknown mechanism. Substrate binding might and ATP hydrolysis induce conformational changes of BceAB. **E:** Without its target, bacitracin loses its amphipathic configuration. BceAB no longer has high enough affinity to bacitracin and releases the AMP into the extracellular space. **F:** Re-attachment of bacitracin to UPP is prevented by dephosphorylation of UPP to UP by UPP phosphatases. Grey: cell membrane, black: lipid carrier in its phosphorylated (UP) or pyrophosphorylated form (UPP), dark blue crescent: bacitracin, light blue: BceAB, red: molecular recognition feature within intrinsically disordered region, turquois: UPP phosphatase. Movements are indicated by dashed lines and arrows.

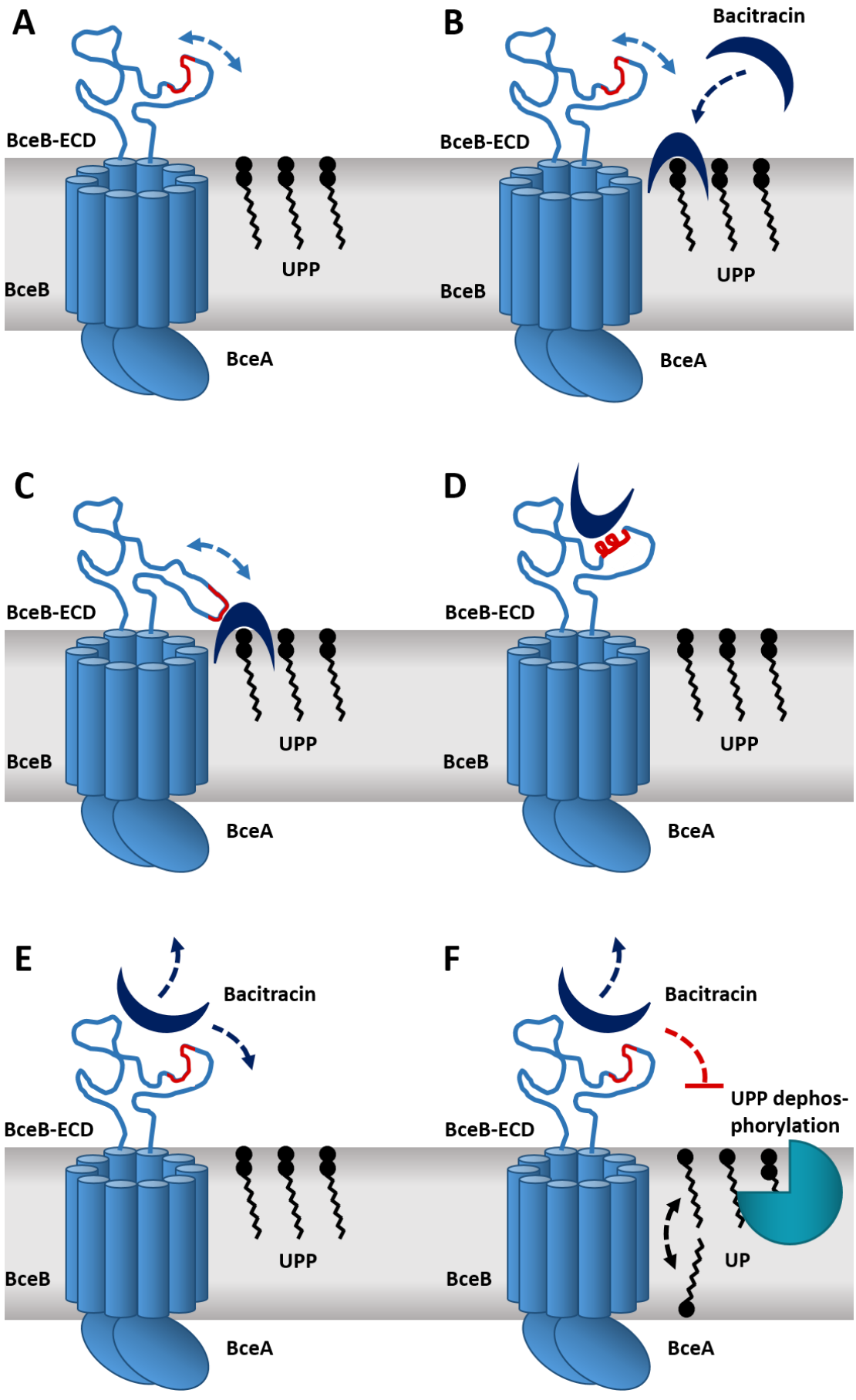
A
BceB-ECD
UPP
BceB
BceA
B
Bacitracin
BceB-ECD
UPP
BceB
BceA
C
BceB-ECD
UPP
BceB
BceA
D
BceB-ECD
UPP
BceB
BceA
E
Bacitracin
BceB-ECD
UPP
BceB
BceA
F
Bacitracin
UPP dephos-
phorylation
BceB-ECD
UP
BceB
BceA

3. BceAB is a mechanotransducer

3.1 Mechanotransmission rather than 'classic' transport

We here proposed that BceAB acts as a hydrophobic vacuum cleaner and takes up its substrate directly from the interface with the hydrophobic membrane environment (Gottesman & Pastan, 1993, Ohki *et al.*, 2003). BceAB then confers resistance by expelling bacitracin from the membrane into the extracellular space. Yet, this mechanism does not involve transportation of the AMP across any lipid bilayer, and thus should not be classified as transport in the 'classic' sense (Davidson & Chen, 2004).

This lack of transmembrane transport seems to be a characteristic feature of the type VII ABC superfamily (Greene *et al.*, 2018). This type of membrane protein from both Gram-positive and Gram-negative bacteria is known to be involved in lipoprotein trafficking (Ito *et al.*, 2006), regulation of cell division (Yang *et al.*, 2011, Mavrici *et al.*, 2014), toxin secretion (Yamanaka *et al.*, 2008), detoxification, or antibiotic resistance (Crow *et al.*, 2017, Greene *et al.*, 2018). While functionally highly variable, none of the so-far described transporters of this group were found to facilitate transport across the cytoplasmic membrane (Greene *et al.*, 2018). When transport across the outer membrane was reported at all, it was not mediated by the type VII ABC transporter located in the inner membrane alone. Some MacB-like transporters assemble to tripartite efflux pumps, for which adapter proteins and outer membrane channel proteins are required to span both, inner and outer membrane (Fitzpatrick *et al.*, 2017, Crow *et al.*, 2017, Yang *et al.*, 2018).

Instead of 'classic' import or export across the phospholipid bilayer (Davidson & Chen, 2004), the 'transporters' of the type VII ABC superfamily were proposed to act via mechanotransmission (Greene *et al.*, 2018). Mechanotransmission is defined as a mechanism in which ATP hydrolysis is coupled to conformational changes that lead to the performance of useful work in periplasm (Crow *et al.*, 2017, Greene *et al.*, 2018).

This definition of mechanotransmission instead of transport matches our proposed model for the resistance mechanism of BceAB. BceAB was shown to belong to the type VII superfamily (Chapter III, Greene *et al.*, 2018) and due to its homology to MacB, also mechanistic similarity seems evident. We thus conclude that BceAB is most likely a mechanotransducer rather than a classic transporter.

3.2 Could BceAB work according to an 'ATP-switch' model?

Our model proposed here does not yet include notions on the energy supply and ATP-usage required for the mechanotransmission mechanism of BceAB. Active transport or mechanotransmission of most ABC transporters is driven by ATP hydrolysis (Higgins & Linton, 2004, Locher, 2016), and also BceAB activity was abolished when conserved regions in the nucleotide binding domains were mutated (Rietkötter *et al.*, 2008). The homology of BceAB to MacB-like mechanotransducers might give first insights into the link between ATP binding and hydrolysis, and mechanotransmission.

MacB was proposed to use an 'ATP-switch' for its mechanotransmission mechanism (Higgins & Linton, 2004, Crow *et al.*, 2017, Greene *et al.*, 2018). ATP binding to the nucleotide binding domains (NBD) of MacB is thought to induce their dimerisation, with the nucleotides bound between the NBDs. In turn, the linked transmembrane domains undergo extensive conformational changes. This leads to the zip-like closing of the periplasmic domains, by which the substrate is thought to be extruded. In contrast, ATP hydrolysis drives disassociation of the NBD dimer (Higgins & Linton, 2004) and resets the closed conformation of the transmembrane and periplasmic domains back to their relaxed open state (Crow *et al.*, 2017). As this conformation revealed an interior cavity close to the substrate binding site, the substrate is thought to first associate with MacB in the relaxed state (Crow *et al.*, 2017).

Although not nearly as well understood as MacB, the energy supply of lipoprotein extractor LolCDE might function in a similar way. Upon ATP binding by its NBDs, LolCDE seemed to release its substrate, while in the absence of ATP or similar compounds the substrate was associated with the transporter (Ito *et al.*, 2006).

We thus wondered whether such an 'ATP switch' was a common feature of the type VII ABC superfamily and compatible with our current model for BceAB mechanotransmission. BceAB was shown to possess two conserved NBDs (BceA), and one large transmembrane segment (Dintner *et al.*, 2014). Based on recent experimental data from our laboratory, the BceA NBDs are thought to link to BceB at the cytoplasmic regions, between TMH2 and 3, and TMH8 and 9, respectively (M. Gibbon, unpublished). Further investigations have pointed out several residues located on one face of TMH8 (F538, S542, L546, Q550; M. Gibbon, unpublished). Mutations of these residues resulted in a hypersensitive signalling response through BceRS and are thought to have relaxed the coupling between substrate binding and ATP binding and hydrolysis. The correspondent region was identified to be the major coupling helix of MacB (Crow *et al.*, 2017).

Based on these similarities to MacB, the two BceA NBDs could also undergo dimerisation upon ATP binding in an ATP-switch-like manner (Higgins & Linton, 2004), thereby inducing conformational changes in the transmembrane segment and the ECD. This hypothesis is solely based on the homology to MacB-like transporters and requires further experimental evidence.

TMH8 (M526 to L548) is the direct link between the ECD and the ATPase. Thus, conformational changes induced by ATPase dimerisation are likely to be transferred by this transmembrane helix. A random mutagenesis approach had previously revealed the C-terminal half of BceB and TMH8 in particular as hotspot for amino acid replacements that affect either bacitracin signalling or resistance, or both (Kallenberg *et al.*, 2013). Topological analyses and experimental studies suggested that BceB does not undergo dimerisation, but rather forms a 'pseudo hetero-dimer' between its MacB-type repeat units (Khwaja *et al.*, 2005, Greene *et al.*, 2018). It is thus likely that TMH1 and TMH8 as well as TMH2 and TMH7 interact and potentially undergo a zip-like transition, similar to the one observed for MacB transmembrane and periplasmic segments (Crow *et al.*, 2017). To further investigate this, crosslinking experiments of the corresponding TMHs could be attempted.

While 'pseudo heterodimerisation' and an ATP switch-like mechanism seem to be a plausible scenario, it is unclear which effect the conformational changes would have on substrate binding. In a MacB-like scenario, the bellow movement of the transmembrane segments and periplasmic domains would actively expel bacitracin from the binding sites (Crow *et al.*, 2017). It is, however, presumable that initial substrate recognition by BceB-ECD is not enough to remove bacitracin from its target. The structural rearrangement of BceB-ECD induced by ATP binding could then facilitate dislodging bacitracin from UPP, while keeping bacitracin attached to the BceB-ECD binding site. As proposed in Fig. 5.1, in the absence of its membrane target bacitracin might lose its amphipathic configuration. In this case, BceB-ECD would rather passively release its substrate and BceAB would be reset into its initial conformation by ATP hydrolysis. In between such transport or mechanotransmission cycles, the 'ATP switch' model requires an initial step to facilitate ATP-binding and closed dimer formation in the first place. This signal is believed to be substrate binding (Higgins & Linton, 2004).

In Chapter III, we revealed that BceB-ECD has a highly similar predicted secondary structure pattern to MacB-like extracytoplasmic domains and that accordingly BceB-ECD can be subdivided in 'Porter' and 'Sabre' subdomains. For MacB, these periplasmic domains were proposed to harbour the substrate binding sites. Yet, one major difference between BceB

and MacB is that BceB only possesses one extracellular domain, without further dimerisation. MacB-like substrate binding at the interface between the heterodimeric periplasmic domains is thus rather unlikely.

Because of its predicted high flexibility and intrinsically-disordered regions (III), we proposed BceB-ECD to undergo conformational changes or potentially even a disorder-to-order transition upon substrate binding (Wright & Dyson, 2009). Such or similar substrate binding mechanisms are thought to transmit a conformational change to the NBDs, thereby enhancing ATP binding and lowering the activation energy for closed dimer formation of the NBD (Higgins & Linton, 2004). Several ABC transporters revealed substrate-induced conformational changes and concomitant increased affinity to ATP (Higgins & Linton, 2004). Amongst them is the hydrophobic vacuum cleaner P-glycoprotein for which both conformational changes and increased affinity to ATP were shown upon substrate binding (Liu & Sharom, 1996, Sonveaux *et al.*, 1999, Qu *et al.*, 2003, Higgins & Linton, 2004). As hardly any structures of transporters or mechanotransducers in complex with their substrates have been published, exact substrate binding sites and induced conformational changes remain puzzling, and more work is required to elucidate the underlying mechanisms.

3.3 Mechanotransmission directly couples transport activity with flux sensing.

The mechanotransmission mechanism proposed for BceAB further fits with our current understanding of bacitracin sensing and signalling through the two-component system BceRS. Unlike traditional histidine kinases, BceS lacks an obvious extracellular input domain (Mascher *et al.*, 2006). Even in the absence of bacitracin, BceB is known to form a complex with BceS (Dintner *et al.*, 2014). In agreement with this, the complex formation between the BceB-like mechanotransducer BraE and the BceS-like kinase NsaS of *S. aureus* was demonstrated recently (Randall *et al.*, 2018). While the interaction between BceB and BceS is thought to happen in the membrane (Mascher, 2014), the exact interaction sites are yet to be identified.

According to the flux-sensing mechanism described by Fritz and colleagues (2015), BceAB acts as sensor that directly signals its transport activity to BceS. The proposed mechanotransmission mechanism likely couples ATP hydrolysis with conformational changes that lead to the removal of bacitracin from its target. As the kinase is permanently attached to BceB (Dintner *et al.*, 2014), the conformational change of the BceB transmembrane segments is thought to affect the transmembrane helices of BceS. Recent work in our group

suggests that the transmembrane region of the kinase undergoes a piston-like displacement movement (A. Koh, unpublished). This is thought to lead to a rotation of the dimerisation histidine phosphotransfer (DHp) domain and to autophosphorylation of the kinase (A. Koh, unpublished, Mascher, 2014). In turn, the response regulator BceR that upregulates expression through P_{bceA} is activated and enables need-based production of BceAB (Fritz *et al.*, 2015).

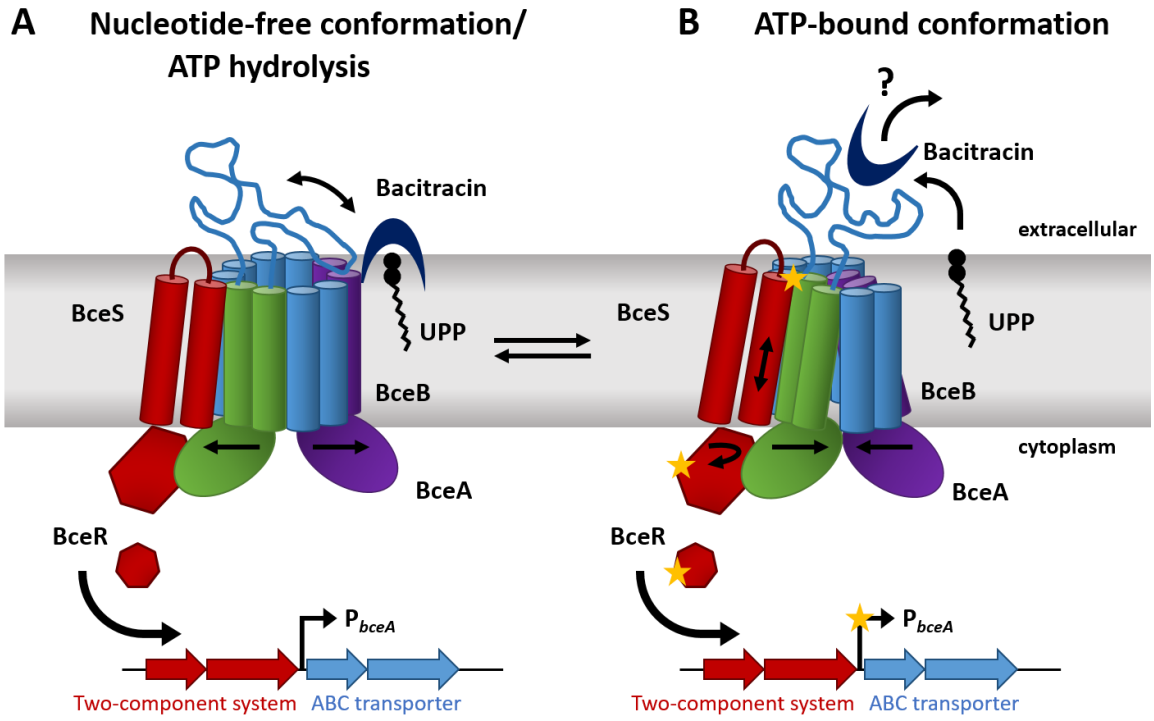

Figure 5.2: Mechanotransmission of BceAB can couple ATP-driven bacitracin resistance with flux-sensing response through BceRS. Schematics of BceAB-BceRS resistance system in its nucleotide-free (**A**) and ATP-bound (**B**) conformation. ATP-driven conformational changes of the BceB transmembrane segment are thought to lead to rotation and auto-phosphorylation of the attached histidine kinase BceS. Grey: cell membrane, black: lipid carrier in its pyrophosphorylated form (UPP), dark blue crescent: bacitracin, light blue: TMH3, 4, 5, 6, 9 and 10 of BceAB, purple: TMH1 and TMH2, with corresponding ATPase unit, green: TMH7 and TMH8, with corresponding ATPase unit, red: BceRS two component regulatory system. Stars indicate the signal transduction between BceB and BceS and the resulting flux-sensing cascade through BceRS, which eventually leads to expression of *bceAB*. Potential movements are indicated by arrows.

4. Target protection as resistance strategy

4.1 BceAB confers resistance by protecting its target

At a first glance, the proposed mechanotransmission mechanism of BceAB seems like a rather counter-intuitive strategy to confer bacitracin resistance. In contrast to canonical resistance mechanisms (Blair *et al.*, 2015, Andersson *et al.*, 2016, Du *et al.*, 2018), the antimicrobial peptide is not inactivated or degraded, nor is it imported or exported across a membrane, which could impede its reattachment. The resistance determinant itself does also not modify the target of the AMP. By removing bacitracin from its cellular target UPP, BceAB increases the disassociation rate of bacitracin and shifts the equilibrium towards unbound bacitracin in the environment. By this, BceAB facilitates the operability of the lipid II cycle, even if it is only for another round. The progression of the cell wall synthesis is under most conditions crucial for the viability of the bacterial cell. In *B. subtilis*, the upregulation of key enzymes of the lipid II cycle, like UPP phosphatase or PBPs, by ECF σ factors contributes to the effectiveness of this resistance mechanism (Helmann, 2016).

Based on current knowledge, this is the best model for the BceAB resistance mechanism. We thus believe that BceAB operates simply by protecting UPP and lipid II, respectively, from inhibition by AMPs. Such a resistance mechanism, called 'target protection', has been previously recognised but is widely underappreciated (Sharkey & O'Neill, 2018). Target protection seems particularly useful as measure of last resort to protect essential features of the cell or when traditional resistance mechanisms are limited in the first place. Modifications of the well-conserved intermediates of the lipid II cycle are uncommon, as the progress of the lipid II cycle should not be compromised. In agreement with this, the examples of target protection mechanisms described so far all focussed on safeguarding essential mechanisms of bacterial metabolism that involve well-conserved structures.

To the present day, the paradigm of target protection is the protection of the ribosome against the inhibitory actions of tetracyclines. The bacterial ribosome is responsible for the translation of genetic information from messenger RNAs into proteins and consists of structurally well-conserved subdomains. It thus serves as excellent target for antibiotics (Poehlsgaard & Douthwaite, 2005). Amongst others, tetracycline binds the A (aminoacyl) site and thereby sterically prevents tRNAs from access (Brodersen *et al.*, 2000).

Ribosomal protection proteins (RPRs) like Tet(O) and Tet(M) were shown to actively release tetracycline from ribosome in a GTP-driven mechanism (Trieber *et al.*, 1998, Burdett, 1996).

Both Tet(O) and Tet(M) binding sites of the ribosome overlap partly with the binding site of tetracycline and chase the antibiotic off by inducing conformational changes of the ribosome (Connell *et al.*, 2003b, Donhofer *et al.*, 2012). In doing so, the dissociation rate of tetracycline from the ribosome is effectively increased, which mediates resistance against tetracycline and secures protein biosynthesis (Connell *et al.*, 2003a).

In a similar drug displacement mechanism, also Antibiotic Resistance ATP-Binding Cassette-F (ARE ABC-F) proteins were recently shown to secure the functionality of the translational machinery (Sharkey *et al.*, 2016, Sharkey & O'Neill, 2018). ARE ABC-F proteins confer resistance against a vast range of antibiotic classes that target the 50 S subunit of the ribosome. Conversely for a protein previously classified as transporter (Dean *et al.*, 2001), this type of resistance proteins does not comprise any transmembrane segments. Its two ATPase domains are solely connected via an approximately 80 amino acid long linker. Akin to homologous regulatory proteins, ARE ABC-F proteins seem to recognise and bind the exit (E) site of the ribosome (Boel *et al.*, 2014, Chen *et al.*, 2014). Compared to regulatory proteins, the extended linker region of ARE ABC-F proteins enables them to reach into the peptidyl (P) site. The linker is thought to allosterically modulate the drug binding site by rRNA or P-site tRNA interactions (Sharkey *et al.*, 2016, Sharkey & O'Neill, 2018). By this, the binding affinity of the drug changes and the drug is dislodged from the ribosome, enabling protein biosynthesis.

In another ribosomal target protection mechanism, the ribosome is safeguarded from obstruction by fusidic acid (Cox *et al.*, 2012, Tomlinson *et al.*, 2016). Fusidic acid binds elongation factor G (EF-G) and inhibits the release thereof from the ribosome, after EF-G catalysed the translocation of peptidyl–tRNA from the A site to the P site (Tanaka *et al.*, 1968, Bodley *et al.*, 1969). Even in the absence of antibiotic stress, FusB-type proteins bind to EF-G and induce conformational changes which accelerate the disassociation of EF-G from the ribosome In the presence of fusidic acid, the FusB-induced release of EF-G from the ribosome directly counteracts the antibiotic's activity (Cox *et al.*, 2012, Tomlinson *et al.*, 2016). In doing so, FusB mediates resistance against fusidic acid and secures integer protein biosynthesis.

Other than ribosomal protection to ensure functionality of the translational machinery, also key players of the DNA replication seem to be protected by such a resistance mechanism in Gram-negative bacteria. Here, Qnr (quinolone resistance) proteins physically protect DNA gyrase and topoisomerase IV from quinolone inhibition (Ruiz, 2003, Tran *et al.*, 2005, Correia *et al.*, 2017).

Where mechanistic details are known, target protection mechanisms generally seem to lead to direct release of the target from the inhibitory action of the antibiotic. Yet, none of the protection determinants physically transfers the antibiotic across a membrane or inhibits its re-attachment in a similar way. By dislodging the antibiotics, the resistance determinants shift the equilibrium from target-bound towards the unbound antibiotic. Thereby, they facilitate proper accessibility and regular functionality of the target for at least one more time before the antibiotic could bind its target again, which is exactly what we expect BceAB to do. These examples stress that the proposed mechanotransmission mechanism for BceAB is both plausible and sufficient to effectively confer resistance against antimicrobial peptides.

4.2 Target protection of cell wall synthesis might be more common than anticipated.

The proposed mechanotransmission mechanism of BceAB is, to our knowledge, the first target protection mechanism that has been described for cell envelope stress. As the abundance of this resistance mechanism has been underappreciated so far, it is likely to be more widely distributed than previously anticipated.

Along the lines of BceAB-like mechanotransducers, we assume that also resistance against lantibiotics conferred by LanFEG transporters can be classified as a target protection mechanism. LanFEG transporters are known to extrude AMPs from its membrane-anchored target, however the mechanistic details remain puzzling (Otto *et al.*, 1998, Stein *et al.*, 2003, 2005, Okuda *et al.*, 2008, Colin *et al.*, 2008). Since lantibiotics generally bind targets in the outer face of the membrane, export across the cytoplasmic membrane is not a plausible strategy, and the Gram-positive lantibiotic producer strains do not possess an outer membrane that AMPs could be transported across. Considering that LanFEG transporters mostly confer self-protection to antimicrobial peptide producers (Colin *et al.*, 2008, Alkhatib *et al.*, 2012), many alternative resistance mechanisms seem rather counter-productive. Import into the cytoplasm for degradation, as well as degradation or inactivation by other means in the extracellular space are suitable strategies to confer protection against attacking AMPs. However, production of antimicrobial peptides is a cost-intensive approach to compete against other microbes (Hibbing *et al.*, 2010). By degrading or deactivating its newly produced agents, the bacterial cell would disarm its own weapon. Also alterations of the target are only contingently suitable. The targets of many lantibiotics are well-conserved intermediates of the lipid II cycle (Willey & van der Donk, 2007, Bierbaum & Sahl, 2009).

Modifications thereof might not only prevent antibiotics from binding but also disturb the interactions with their legitimate enzymes and binding partners, which might suspend the cell wall synthesis. A notable exception are the lipid II stem peptide alterations that cause vancomycin resistance. Yet, it seems like the most effective strategy for LanFEG transporters is to release the target from the inhibitory grip of the lantibiotic in a BceAB-like manner. Again, increasing the disassociation rate would allow the lipid II cycle intermediate to progress to the next stage of the lipid II cycle. Equally, the self-protection mechanism of bacitracin-producer *B. licheniformis* which is mediated by the putative 'hydrophobic vacuum cleaner' BcrAB would qualify as target protection (Podlesek *et al.*, 1995, Podlesek *et al.*, 2000). Interestingly, members of both transporter families were found to mediate resistance against exogenously produced AMPs in non-producer strains (Gebhard, 2012, Clemens *et al.*, 2017). Well-described examples are the bacitracin resistance conferred by BcrAB in *E. faecalis* (Manson *et al.*, 2004, Matos *et al.*, 2009) and the LanFEG homolog CprABC of *C. difficile* that confers resistance against nisin, gallidermin and polymyxin B (McBride & Sonenshein, 2011, Clemens *et al.*, 2017). This indicates that these resistance determinants are derived from the original self-resistance target protection mechanism and have been acquired by non-producer strains via horizontal gene transfer (Colin *et al.*, 2008).

Further, the resistance mechanism of most LanI-type proteins has not yet been elucidated in detail. As they do not seem to confer resistance cooperatively together with their respective LanFEG transporter, they too could mediate immunity via target protection. As described before (I 4.4.1), both SpaI and NisI immunity proteins are known to directly bind their substrate (Stein *et al.*, 2003, 2005, Takala *et al.*, 2004). Both proteins might remove their corresponding substrate from the membrane targets, rather than binding the unbound version of the lantibiotic in the extracellular periphery. In doing so, they would free the lipid II cycle intermediate and shift the binding equilibrium more towards the unbound lantibiotic. Immunity against the class I lantibiotic Pep5 is conferred by the PepI immunity protein (Reis *et al.*, 1994, Hoffmann *et al.*, 2004). PepI as well as Pep5 are highly positively charged peptides, which makes a direct binding interaction between them improbable. Instead, PepI was proposed to shield the membrane-located target from Pep5 action (Hoffmann *et al.*, 2004).

Interestingly, the transcription of all transporters and immunity proteins described here seems tightly coupled to the presence or absence of antimicrobial stress. Expression of protection determinants is generally regulated by kinase-response regulator two-component systems or transcription regulators that directly perceive the AMP stimulus (Gebhard *et al.*,

2009, Gebhard, 2012). In doing so, unnecessary costly protection of the host can be avoided, leading to an efficient resistance mechanism.

5. Future Perspectives

5.1 Investigations on the physiological substrate of BceAB for lipid II-binding AMPs.

In this study, we have pursued first steps to investigate whether the physiological substrate of BceAB, here established as [UPP-BAC], can be universally stated as the AMP in complex with its cellular target. According to this statement, BceAB would also only recognise lipid II-binding AMPs together with their target or when the AMPs have adopted their target-bound conformation (Hsu *et al.*, 2003). In Chapter IV, alterations of the lipid II pool as well as the total amount of lipid carrier in the cell were attempted, mainly using genetic manipulations. A computational model of the lipid II cycle (Fritz, unpublished) suggested the lipid II pool on the outer face of the membrane to be very small. Alterations to the amounts of lipid II in this pool, if possible at all without killing the cells, might therefore require more drastic measures than the ones tried so far.

In our study, neither removal of PBP1 to decrease the transglycosylation rate, nor attempts using antibiotic combinations resulted in obvious changes to BceAB activity. As already discussed, the redundancy in function of, in total, four class A PBPs that all possess transglycosylation activity might have prevented lipid II from accumulation (McPherson & Popham, 2003). The newly-discovered transglycosylation activity of RodA can just about compensate for the loss of all four PBPs (Meeske *et al.*, 2016). Testing the BceAB-activity in a quadruple deletion strain that lacks PBP1, PBP2c, PBP2d and PBP4, might decease the transglycoslyation activity enough to accumulate lipid II and change BceAB activity in the presence of mersacidin. Although *B. subtilis* is intrinsically resistant to moenomycin due to RodA activity, addition of moenomycin could effectively lead to the same decrease of transglycosylation (Ostash & Walker, 2010, Meeske *et al.*, 2016).

Although highly debated for a long time, recent studies suggest MurJ and Amj to be responsible for translocation of lipid II across the membrane (Sham *et al.*, 2014, Meeske *et al.*, 2015, Bolla *et al.*, 2018, Kumar *et al.*, 2018). Increasing this reaction by overproduction of the lipid II flippase could lead to the desired accumulation of lipid II on the outer face of the

membrane. Ultimately, combining increased flippase activity with reduced transglycosylation could be the key to allow changes in the level of this well-protected cell wall synthesis intermediate. On the other hand, also deletions or depletions of the lipid II flippases or enzymes crucial to lipid II assembly, like MraY or MurG, are potential strategies to affect the lipid II pool (Bouhss *et al.*, 2004, 2008).

To make the availability of the lipid carrier the rate-limiting step of the lipid II cycle, we aimed to reduce UppS levels in the cell, which is responsible for UPP assembly from precursors (Apfel *et al.*, 1999). While some attempts to alter UppS levels did not lead to clear results, other ideas could not be tested so far due to technical challenges (IV, 3.4).

To address this challenge in future attempts, two further strains that aim at the down-regulation of *uppS* expression should be tested (Sim & Fritz, unpublished). In the first strain (GFB0058), expression of *uppS* is uncoupled from its primary native regulation. The promoter region was replaced by the xylose-inducible P_{xylA} promotor, which makes the strains only conditionally viable. Any potential read-through from upstream genes to the *uppS* locus was inhibited by insertion of a chloramphenicol resistance cassette containing a terminator. The other strain (GFB0078) takes advantage of a CRISPRi knockdown of *uppS* (Hawkins *et al.*, 2015, Peters *et al.*, 2016). The strain carries a constitutively-expressed (P_{veg}) single guide (sg) RNA that is complementary to the *uppS* DNA sequence. It further contains a copy of *dCas9* which encodes a catalytically inactive variant of the endonuclease protein Cas9. The expression of *dCas9* is set under xylose-titratable regulation (P_{xylA}). Upon binding its DNA target, the sgRNA-dCas9 complex sterically hinders transcription (Hawkins *et al.*, 2015). In first trials, addition of 0.01 % xylose allowed wild-type growth of *B. subtilis*, while 0.1 % xylose was lethal (Sim & Fritz, personal communication).

Our current P_{bceA} luminescence reporter plasmid (Fritz *et al.*, 2015) was incompatible with these strains, as the same antibiotic marker for selection had been used. Testing BceAB activity in these promising strains, requires reconstruction of the current reporter construct. Attempts, including the replacement of the resistance cassette using homologous recombination and the transformation of *B. subtilis* with *de novo* assembled luminescence vectors carrying P_{bceA} were performed by a collaborator and have been unsuccessful so far (Fritz lab). A promising strategy to acquire P_{bceA} luminescence constructs with compatible antibiotic markers is the use of vectors that have been developed and evaluated for use in *B. subtilis* by Popp and colleagues (2017). Cloning P_{bceA} according to the BioBrick assembly standard RFC[10] (Knight, 2007) into the vectors pBS3E*lux* or pBS3K*lux* should lead to constructs very similar to our current plasmid and result in suitable P_{bceA} luminescence

reporter strains to test BceAB activity in *uppS* depletion strains. This approach was postponed due to time constraints, but successfully conducted after thesis submission.

When BceAB activity can successfully be tested in the strains described above, it is also advisable to re-test other mutants, for which no effect was observed in this study, but that potentially change the lipid II intermediate pool levels, in the now *uppS* depleted background. The potentially decreased UPP levels were found to alter the effects of other genetic manipulations related to the lipid II cycle on bacitracin sensitivity (*ΔsigM*, Lee & Helmann, 2013, *ΔytpB*, Kingston *et al.*, 2014).

As *uppS* is co-transcribed with other essential genes, some of which play a role in isoprenoid biosynthesis and membrane phospholipid production, also expression of these genes would be affected by alterations of the transcription levels. To avoid such down-stream effects, mutations that solely affect the integrity and function of UppS could be exploited. The mutation of residue 86 of *uppS* from threonine to isoleucine was shown to increase resistance to bacitracin and is thought to alter the available UPP pool size (Inaoka & Ochi, 2012).

Without the ability to directly monitor the lipid II cycle intermediate levels on the cell surface and lacking improved predictions on effects of genetic manipulations on the lipid II cycle, the described approaches are mostly trial and error experiments and we cannot yet distinguish whether lipid II accumulation or reduction was successful or if BceAB activity is independent from the [lipid II-AMP] complex.

In an approach independent from genetic manipulations, cells could be incubated with synthesised or previously extracted lipid II as described by Breukink *et al.* (2003), Welzel (2005), or Qiao *et al.* (2017). The hydrophobic tail of lipid II is likely to escape the hydrophilic culture medium and might insert into the hydrophobic bacterial membrane, thereby increasing the lipid II pool size on the outer face of the membrane. This could lead to the desired accumulation of [lipid II-AMP] complex and in turn result in alterations of the BceAB activity. Lipid II or maybe a more soluble variant thereof, with a shorter prenyl chain, could bind lipid II-targeting AMPs like mersacidin already in the supernatant and thereby inhibit its antimicrobial activity. Nevertheless, if the extracellular domain is involved in substrate binding and under conditions in which the mersacidin binding of lipid II is saturated, the transporter might still recognise the formed [lipid II-MERS] complex and adjust transport activity. A similar approach is plausible with the [UPP-BAC] or [GPP-BAC] complex, as a positive control. Addition of UPP/GPP to cultures for membrane insertion or formation of [UPP/GPP-BAC] in the extracellular space should increase the overall amounts of [UPP-BAC]

that BceAB can recognise and thus, increase its activity. As mersacidin is not commercially available and therefore potentially the bottleneck of this approach, this hypothesis could be tested with the nisin-inducible PsdAB transporter (Staron *et al.*, 2011). In this case, nisin and extracted lipid II would be added to exponentially growing *B. subtilis* cells.

5.2 *In vivo* investigation of potential BceB-ECD binding site for target-bound bacitracin.

An important, yet still puzzling question about BceAB-like mechanotransducers is the molecular basis of their substrate specificity. BceAB-like transporters often have a broad substrate range, but within this range only bind a specific, diverse subset of AMPs. Although indications suggest the ECD to be involved in substrate binding (Rietkötter *et al.*, 2008, Hiron *et al.*, 2011), this could not be confirmed in this study using *in vitro* binding assays. Future work targeting the molecular recognition of the substrates could therefore make use of an *in vivo* approach to identify binding sites.

The *in silico* analysis of this study (Chapter III, 2.1) suggested the extracellular domain of BceB to be highly flexible and indicated molecular recognition features (MoRF) that are often involved in binding interactions (Mohan *et al.*, 2006). One of these predicted regions comprises the amino acids residues 370 to 384, encoding Glu^--Met-Gln-Gly-Asp^--Pro-Gly-Asn-Met-Gln (Chapter III, Fig. 3.1, green). This stretch contains several negatively charged (X^-) and polar residues (grey). Polar residues are known to form hydrogen bonds with other polar residues, while negatively charged residues can form electrostatic ionic bonds with positively charged amino acid side chains. When binding its target, bacitracin was shown to adopt a highly amphipathic configuration with polar and non-polar residues distinctly separated (Economou *et al.*, 2013). Non-polar residues were found at the hydrophobic membrane lipid interface, while most polar residues interacted with the metals or pyrophosphate group of UPP. Amongst the polar residues are several positively charged residues (Lys, Orn, His). As these residues should be easiest to access for the large extracellularly located domain of BceAB, we suggest this MoRF as the potential bacitracin binding site within BceB-ECD.

Previous random mutagenesis approaches of BceAB did not result in any mutations in the ECD (Kallenberg *et al.*, 2013). In future work, a site-directed mutagenesis approach could focus on this MoRF to identify potential binding interactions and to confirm BceB-ECD as binding domain. Amino acids with polar and charged side chains in particular should be replaced by neutral amino acids (e.g. alanine) to investigate their possible contribution to

recognition of bacitracin. The resulting effect on signalling can be examined using the same *in vivo* luminescence assay that was used in this study (Chapter IV). Likewise, changes in bacitracin resistance should be monitored by MIC assays. To further investigate the findings of the alanine scanning mutagenesis, residues of interest could be replaced with amino acids with similar or opposite properties. Complete or partial loss or possibly even gain of function could indicate a binding interaction between BceB-ECD and bacitracin in its amphipathic, bound form.

BceAB also confers resistance against the lantibiotics mersacidin and actagardine. Yet, both have quite different charge distribution and chemical properties to bacitracin (Staron *et al.*, 2011). Neither of them contain any amino acids with positively charged side chains and hardly any polar residues. A glutamate residue in the lipid II-binding motif seems to be the only conserved charged residue in the peptides that are otherwise enriched in non-polar, hydrophobic residues (Böttiger *et al.*, 2009). The binding domain of BceAB for mersacidin and actagardine might therefore differ from the one that was here suggested for bacitracin.

Another MoRF of BceB-ECD was predicted to lie around amino acid residue 432 (Lys^{+}-Val-Lys^{+}-Ser-Lys^{+}-His^{+}-Glu^{-}-Thr-Gln-Pro, Chapter III, Fig. 3.1, yellow). This region contains some polar residues (grey), but strikingly many positively charged amino acids, like histidine and lysine (X^{+}). Although intuitively not necessarily suitable for bacitracin binding, this domain might be important for other interactions, for example, with the negatively-charged mersacidin and actagardine.

It would be very interesting to investigate differences in the signalling response of BceAB containing mutated MoRF residues when mersacidin is administered instead of bacitracin. If the signalling response was, for example, partly impaired upon addition of bacitracin but did not alter in the presence mersacidin, this could imply that the MoRF is a binding site specific for bacitracin.

If this hypothesis held true, this would be a suitable strategy to confirm BceB-ECD as bacitracin binding-domain, while avoiding challenges that might be encountered with *in vitro* assays. The sequence alignment between bacitracin-related permeases in this study did not find the amino acid sequence of the MoRF to be conserved at all. Yet, if the MoRF was revealed as the bacitracin binding site by site-directed mutagenesis, further insights gained from the experimental data might point out a prevailing bacitracin binding motif that could be searched for in other ECDs.

5.3 Analysis of the natural membrane environment and localisation of BceAB.

The growth assays performed in Chapter IV indicated a low-affinity interaction between BceAB and UPP upon deletion of *bcrC.* Impaired dephosphorylation of UPP leads to a very similar effect as the addition of bacitracin, namely the accumulation of UPP. One possible explanation is that UPP is recognised by BceAB as part of the substrate, and a low binding affinity is present even in the absence of bacitracin. It is also conceivable that BceAB monitors the UPP levels in the cell or that BceAB uses the abundance of UPP for localisation in the membrane. In the absence of bacitracin, basal BceAB levels in the cell are low, yet the signalling response of BceAB to addition of bacitracin happens rapidly (Fritz *et al.*, 2015). To further investigate this interaction, the natural lipid environment of BceAB should be examined *in vitro*.

The membrane phospholipid composition is under normal conditions tightly regulated. AMPs can perturb this regulation change the membrane composition and lead to the formation of lipid domains (Muchova *et al.*, 2011, Strahl *et al.*, 2014). Lipid domains were shown have increased lipid fluidity *in vivo*. This can disturb the overall lipid homeostasis and affect membrane protein localisation. Daptomycin, for example, was shown to cause an extensive rearrangement of fluid lipid domains, affecting the membrane viscosity. This leads to the detachment of the lipid II synthase MurG and thus results in the discontinuation of the cell wall synthesis (Muller *et al.*, 2016). Further, the synthetic cyclic hexapeptide cWFW leads to the formation of distinct membrane domains and rapidly reduces the membrane fluidity of *B. subtilis* (Scheinpflug *et al.*, 2017). This causes membrane protein disorganisation, which is followed by the inhibition of cell wall synthesis. These examples stress that changes of the membrane composition caused can affect the membrane viscosity or the lateral pressure onto membrane proteins (Muchova *et al.*, 2011, Lee, 2004, van den Brink-van der Laan *et al.*, 2004). This can have effects on the helix-helix interactions of integral membrane proteins and change their activity.

For example, the well-described multidrug efflux pump P-glycoprotein is thought to access its substrates from the membrane, according to a hydrophobic vacuum cleaner mechanism (Higgins & Gottesman, 1992, Gottesman & Pastan, 1993). However, the membrane phospholipid environment was shown to modulate the substrate interactions with P-glycoprotein (Romsicki & Sharom, 1999). The tested drugs had, for example, a substantially higher affinity when surrounded by phosphatidylcholine compared to phosphatidyl-

ethanolamine. In addition, the ATPase activity that drives P-glycoprotein efflux varied accordingly with the encompassing environment (Romsicki & Sharom, 1999).

Similarly, the activity lipoprotein extractor LolCDE seems to depend on phospholipid composition (Miyamoto & Tokuda, 2007). The common phospholipids phosphatidylglycerol, phosphatidylethanolamine and cardiolipin affected the lipoprotein sorting and release ability as well as ATPase activity of LolCDE, each in their own way. Similar effects may also affect BceAB activity.

As briefly mentioned in Chapter III, styrene maleic acid (SMA) copolymers and similar compounds have revolutionised work on bacterial membranes, and integral membrane proteins in particular, over the last decade (Knowles *et al.*, 2009, Dorr *et al.*, 2016). The SMA copolymers form so-called SMA lipid particles (SMALP) or SMA nanodiscs, which encompass the protein of interest and patches of the original lipid bilayer. With this method, membrane proteins can be characterised using standard biochemical and biophysical approaches (Knowles *et al.*, 2009). Aside from often maintained functionality and increased stability of protein complexes, SMALPs also preserve the natural lipid environment of the membrane protein (Swainsbury *et al.*, 2014). SMA copolymers have the ability to insert into membrane bilayers and extract membrane proteins directly from intact membranes, without the use of detergent (Scheidelaar *et al.*, 2015, Stroud *et al.*, 2018). Due to this quality, SMA co-polymers found use as tool to investigate protein-lipid interaction and lipid preferences (Dorr *et al.*, 2014, 2016). Generally, SMA itself does not seem to have any significant preference to solubilise a certain phospholipid species (Dominguez Pardo *et al.*, 2017). Thus, comparison between the lipid content of the SMA nanodiscs containing the protein of interest with the average abundance of phospholipids in other nanodiscs might point out specific affinities of the protein under investigation to certain types of phospholipids. The phospholipid content of nanodiscs can be analysed by several techniques including thin layer chromatography, gas chromatography, high-performance liquid chromatography or variations thereof, e.g. reverse-phase chromatography (Peterson & Cummings, 2006, Scheidelaar *et al.*, 2015, Dominguez Pardo *et al.*, 2017). Using this method could further test the interaction between full-length BceAB and UPP *in vitro* under different conditions. If the substrate recognition mechanism of BceAB is the same for lipid II binding AMPs, BceAB could also have also an affinity to lipid II alone. Successful solubilisation of the BceAB complex in SMA nanodiscs would also open the doors for structural analysis using electron microscopy (Postis *et al.*, 2015, Parmar *et al.*, 2018).

As key player in the cell wall synthesis, the localisation of lipid II in the cell is well-studied. In elongated cells like *B. subtilis*, *de novo* synthesised peptidoglycan is not only inserted around the division septum but also in domains along the lateral walls of the cell in a helical pattern (Daniel & Errington, 2003). Microscopy studies could give insights into where BceAB localises in the cell *in vivo* and whether this distribution correlates with the abundance of labelled lipid II or UPP. Localisation of fluorescent-tagged BceAB could also be studied in the presence or absence of antimicrobial stress or other conditions that disrupt cell wall synthesis. The depletion of precursors, amongst others, leads to the disorganisation of peptidoglycan synthesis and to alterations in the distributions of lipids in the membrane (Muchova *et al.*, 2011). Particularly, depletion of UPP phosphatases might be important for localisation of BceAB in the cell.

In this thesis, we shed light on the nature of the physiological substrate of the antimicrobial resistance transporter BceAB of *B. subtilis*. By identifying the most likely physiological substrate to be bacitracin in complex with its cellular target UPP, rather than unbound bacitracin, we now understand that substrate recognition and binding are likely to happen in the hydrophobic membrane environment. Thereby, we gained further insights into the resistance mechanism that has been elusive for decades. Together with experimental evidence from previous studies, these insights support the hypothesis that bacitracin is removed from its cellular target and released into the extracellular space. BceAB likely confers resistance against AMPs by shifting the equilibrium of membrane-bound AMPs towards unbound AMPs in the surrounding environment, according to a target protection mechanism. As this resistance mechanism does not involve transport of the AMP across a membrane, BceAB was classified as a mechanotransducer rather than a transporter.

Identifying the physiological substrate of the paradigm transporter BceAB and understanding the underlying resistance mechanism are of great importance to counteracting emerging antimicrobial resistance, as this and similar mechanisms are presumably wide spread in immunity and resistance against AMPs in numerous bacterial genera. The ability to differentiate between the membrane-bound and free version might constitute a key concept of AMP recognition in resistance determinants beyond this and similar types of transporters. The findings of this study thus open up exciting future perspectives to further investigate BceAB-like transporters and other resistance determinants. Better understanding of resistance mechanisms will facilitate the development of AMPs for medical treatment that can circumvent these resistance determinants and reveal new targets and strategies to combat the global threat that antimicrobial resistance poses to mankind.

References

Aires, J.R. & H. Nikaido, (2005) Aminoglycosides are captured from both periplasm and cytoplasm by the AcrD multidrug efflux transporter of *Escherichia coli*. *J Bacteriol* **187**: 1923-1929.

Alanis, A.J., (2005) Resistance to antibiotics: are we in the post-antibiotic era? *Arch Med Res* **36**: 697-705.

Alkhatib, Z., A. Abts, A. Mavaro, L. Schmitt & S.H. Smits, (2012) Lantibiotics: how do producers become self-protected? *J Biotechnol* **159**: 145-154.

Anderson, R.J., Groundwater, P.W., Todd, A., Worsley, A.J. , (2012) Antibacterial agents : chemistry, mode of action, mechanisms of resistance and clinical applications.

Andersson, D.I., D. Hughes & J.Z. Kubicek-Sutherland, (2016) Mechanisms and consequences of bacterial resistance to antimicrobial peptides. *Drug Resist Updat* **26**: 43-57.

Andersson, H. & G. von Heijne, (1993) Sec dependent and sec independent assembly of *E. coli* inner membrane proteins: the topological rules depend on chain length. *EMBO J* **12**: 683-691.

Andersson, H. & G. von Heijne, (1994a) Membrane protein topology: effects of delta mu H+ on the translocation of charged residues explain the 'positive inside' rule. *EMBO J* **13**: 2267-2272.

Andersson, H. & G. von Heijne, (1994b) Positively charged residues influence the degree of SecA dependence in protein translocation across the *E. coli* inner membrane. *FEBS Lett* **347**: 169-172.

Aoki, W. & M. Ueda, (2013) Characterization of Antimicrobial Peptides toward the Development of Novel Antibiotics. *Pharmaceuticals (Basel)* **6**: 1055-1081.

Apfel, C.M., B. Takacs, M. Fountoulakis, M. Stieger & W. Keck, (1999) Use of genomics to identify bacterial undecaprenyl pyrophosphate synthetase: cloning, expression, and characterization of the essential *uppS* gene. *J Bacteriol* **181**: 483-492.

Aso, Y., K. Okuda, J. Nagao, Y. Kanemasa, N. Thi Bich Phuong, H. Koga, K. Shioya, T. Sashihara, J. Nakayama & K. Sonomoto, (2005) A novel type of immunity protein, NukH, for the lantibiotic nukacin ISK-1 produced by *Staphylococcus warneri* ISK-1. *Biosci Biotechnol Biochem* **69**: 1403-1410.

Auerbuch, V., L.L. Lenz & D.A. Portnoy, (2001) Development of a Competitive Index Assay To Evaluate the Virulence of *Listeria monocytogenes actA* Mutants during Primary and Secondary Infection of Mice. *Infection and Immunity* **69**: 5953-5957.

Bader, M.W., S. Sanowar, M.E. Daley, A.R. Schneider, U. Cho, W. Xu, R.E. Klevit, H. Le Moual & S.I. Miller, (2005) Recognition of antimicrobial peptides by a bacterial sensor kinase. *Cell* **122**: 461-472.

Barbe, V., S. Cruveiller, F. Kunst, P. Lenoble, G. Meurice, A. Sekowska, D. Vallenet, T. Wang, I. Moszer, C. Medigue & A. Danchin, (2009) From a consortium sequence to a unified sequence: the *Bacillus subtilis* 168 reference genome a decade later. *Microbiology* **155**: 1758-1775.

Barrera, N.P., S.C. Isaacson, M. Zhou, V.N. Bavro, A. Welch, T.A. Schaedler, M.A. Seeger, R.N. Miguel, V.M. Korkhov, H.W. van Veen, H. Venter, A.R. Walmsley, C.G. Tate & C.V. Robinson, (2009) Mass spectrometry of membrane transporters reveals subunit stoichiometry and interactions. *Nat Methods* **6**: 585-587.

Barreteau, H., S. Magnet, M. El Ghachi, T. Touze, M. Arthur, D. Mengin-Lecreulx & D. Blanot, (2009) Quantitative high-performance liquid chromatography analysis of the pool

levels of undecaprenyl phosphate and its derivatives in bacterial membranes. *J Chromatogr B Analyt Technol Biomed Life Sci* **877**: 213-220.

Becker, P., R. Hakenbeck & B. Henrich, (2009) An ABC transporter of *Streptococcus pneumoniae* involved in susceptibility to vancoresmycin and bacitracin. *Antimicrob Agents Chemother* **53**: 2034-2041.

Bernard, R., M. El Ghachi, D. Mengin-Lecreulx, M. Chippaux & F. Denizot, (2005) BcrC from *Bacillus subtilis* acts as an undecaprenyl pyrophosphate phosphatase in bacitracin resistance. *J Biol Chem* **280**: 28852-28857.

Bernard, R., A. Guiseppi, M. Chippaux, M. Foglino & F. Denizot, (2007) Resistance to bacitracin in *Bacillus subtilis*: unexpected requirement of the BceAB ABC transporter in the control of expression of its own structural genes. *J Bacteriol* **189**: 8636-8642.

Bertani, G., (1951) Studies on lysogenesis. I. The mode of phage liberation by lysogenic *Escherichia coli*. *J Bacteriol* **62**: 293-300.

Bierbaum, G., H. Brotz, K.P. Koller & H.G. Sahl, (1995) Cloning, sequencing and production of the lantibiotic mersacidin. *FEMS Microbiol Lett* **127**: 121-126.

Bierbaum, G. & H.G. Sahl, (2009) Lantibiotics: mode of action, biosynthesis and bioengineering. *Curr Pharm Biotechnol* **10**: 2-18.

Blair, J.M., M.A. Webber, A.J. Baylay, D.O. Ogbolu & L.J. Piddock, (2015) Molecular mechanisms of antibiotic resistance. *Nat Rev Microbiol* **13**: 42-51.

Bodley, J.W., F.J. Zieve, L. Lin & S.T. Zieve, (1969) Formation of the ribosome-G factor-GDP complex in the presence of fusidic acid. *Biochemical and Biophysical Research Communications* **37**: 437-443.

Boel, G., P.C. Smith, W. Ning, M.T. Englander, B. Chen, Y. Hashem, A.J. Testa, J.J. Fischer, H.J. Wieden, J. Frank, R.L. Gonzalez, Jr. & J.F. Hunt, (2014) The ABC-F protein EttA gates ribosome entry into the translation elongation cycle. *Nat Struct Mol Biol* **21**: 143-151.

Bolanos-Garcia, V.M. & O.R. Davies, (2006) Structural analysis and classification of native proteins from *E. coli* commonly co-purified by immobilised metal affinity chromatography. *Biochim Biophys Acta* **1760**: 1304-1313.

Bolla, J.R., J.B. Sauer, D. Wu, S. Mehmood, T.M. Allison & C.V. Robinson, (2018) Direct observation of the influence of cardiolipin and antibiotics on lipid II binding to MurJ. *Nat Chem* **10**: 363-371.

Böttiger, T., T. Schneider, B. Martinez, H.G. Sahl & I. Wiedemann, (2009) Influence of Ca^{2+} ions on the activity of lantibiotics containing a mersacidin-like lipid II binding motif. *Appl Environ Microbiol* **75**: 4427-4434.

Bouhss, A., M. Crouvoisier, D. Blanot & D. Mengin-Lecreulx, (2004) Purification and characterization of the bacterial MraY translocase catalyzing the first membrane step of peptidoglycan biosynthesis. *J Biol Chem* **279**: 29974-29980.

Bouhss, A., A.E. Trunkfield, T.D. Bugg & D. Mengin-Lecreulx, (2008) The biosynthesis of peptidoglycan lipid-linked intermediates. *FEMS Microbiol Rev* **32**: 208-233.

Boutet, E., D. Lieberherr, M. Tognolli, M. Schneider & A. Bairoch, (2007) Uniprotkb/swiss-prot. In: Plant bioinformatics. Springer, pp. 89-112.

Bramkamp, M. & D. Lopez, (2015) Exploring the existence of lipid rafts in bacteria. *Microbiol Mol Biol Rev* **79**: 81-100.

Breukink, E. & B. de Kruijff, (2006) Lipid II as a target for antibiotics. *Nat Rev Drug Discov* **5**: 321-332.

Breukink, E., P. Ganz, B. de Kruijff & J. Seelig, (2000) Binding of Nisin Z to Bilayer Vesicles As Determined with Isothermal Titration Calorimetry. *Biochemistry* **39**: 10247-10254.

Breukink, E., H.E. van Heusden, P.J. Vollmerhaus, E. Swiezewska, L. Brunner, S. Walker, A.J. Heck & B. de Kruijff, (2003) Lipid II is an intrinsic component of the pore induced by nisin in bacterial membranes. *J Biol Chem* **278**: 19898-19903.

Breukink, E., I. Wiedemann, C.v. Kraaij, O.P. Kuipers, H.-G. Sahl & B. de Kruijff, (1999) Use of the Cell Wall Precursor Lipid II by a Pore-Forming Peptide Antibiotic. *Science* **286**: 2361-2364.

Brodersen, D.E., W.M. Clemons, A.P. Carter, R.J. Morgan-Warren, B.T. Wimberly & V. Ramakrishnan, (2000) The Structural Basis for the Action of the Antibiotics Tetracycline, Pactamycin, and Hygromycin B on the 30S Ribosomal Subunit. *Cell* **103**: 1143-1154.

Brötz, H., G. Bierbaum, K. Leopold, P.E. Reynolds & H.G. Sahl, (1998a) The lantibiotic mersacidin inhibits peptidoglycan synthesis by targeting lipid II. *Antimicrob Agents Chemother* **42**: 154-160.

Brötz, H., G. Bierbaum, P.E. Reynolds & H.G. Sahl, (1997) The lantibiotic mersacidin inhibits peptidoglycan biosynthesis at the level of transglycosylation. *Eur J Biochem* **246**: 193-199.

Brötz, H., M. Josten, I. Wiedemann, U. Schneider, F. Götz, G. Bierbaum & H.-G. Sahl, (1998b) Role of lipid-bound peptidoglycan precursors in the formation of pores by nisin, epidermin and other lantibiotics. *Molecular Microbiology* **30**: 317-327.

Brown, S., J.P. Santa Maria, Jr. & S. Walker, (2013) Wall teichoic acids of gram-positive bacteria. *Annu Rev Microbiol* **67**: 313-336.

Bugg, T.D., D. Braddick, C.G. Dowson & D.I. Roper, (2011) Bacterial cell wall assembly: still an attractive antibacterial target. *Trends Biotechnol* **29**: 167-173.

Burdett, V., (1996) Tet(M)-promoted release of tetracycline from ribosomes is GTP dependent. *J Bacteriol* **178**: 3246-3251.

Cao, M. & J.D. Helmann, (2002) Regulation of the *Bacillus subtilis bcrC* Bacitracin Resistance Gene by Two Extracytoplasmic Function σ Factors. *Journal of Bacteriology* **184**: 6123-6129.

Chen, B., G. Boel, Y. Hashem, W. Ning, J. Fei, C. Wang, R.L. Gonzalez, Jr., J.F. Hunt & J. Frank, (2014) EttA regulates translation by binding the ribosomal E site and restricting ribosome-tRNA dynamics. *Nat Struct Mol Biol* **21**: 152-159.

Chen, Y. & M.D. Barkley, (1998) Toward understanding tryptophan fluorescence in proteins. *Biochemistry* **37**: 9976-9982.

Chien, A.C., N.S. Hill & P.A. Levin, (2012) Cell size control in bacteria. *Curr Biol* **22**: R340-349.

Christ, N.A., S. Bochmann, D. Gottstein, E. Duchardt-Ferner, U.A. Hellmich, S. Dusterhus, P. Kotter, P. Guntert, K.D. Entian & J. Wohnert, (2012a) The First structure of a lantibiotic immunity protein, SpaI from *Bacillus subtilis*, reveals a novel fold. *J Biol Chem* **287**: 35286-35298.

Christ, N.A., E. Duchardt-Ferner, S. Dusterhus, P. Kotter, K.D. Entian & J. Wohnert, (2012b) NMR resonance assignment of the autoimmunity protein SpaI from *Bacillus subtilis* ATCC 6633. *Biomol NMR Assign* **6**: 9-13.

Clemens, R., J. Zaschke-Kriesche, S. Khosa & S.H.J. Smits, (2017) Insight into Two ABC Transporter Families Involved in Lantibiotic Resistance. *Front Mol Biosci* **4**: 91.

Colin, H., A.D. Lorraine, R.P. Ross & D.C. Paul, (2008) Lantibiotic Immunity. *Current Protein & Peptide Science* **9**: 39-49.

Collins, B., N. Curtis, P.D. Cotter, C. Hill & R.P. Ross, (2010) The ABC transporter AnrAB contributes to the innate resistance of *Listeria monocytogenes* to nisin, bacitracin, and various beta-lactam antibiotics. *Antimicrob Agents Chemother* **54**: 4416-4423.

Commission, E., (2017) European One Health Action Plan against Antimicrobial Resistance.

Connell, S.R., D.M. Tracz, K.H. Nierhaus & D.E. Taylor, (2003a) Ribosomal protection proteins and their mechanism of tetracycline resistance. *Antimicrob Agents Chemother* **47**: 3675-3681.

Connell, S.R., C.A. Trieber, G.P. Dinos, E. Einfeldt, D.E. Taylor & K.H. Nierhaus, (2003b) Mechanism of Tet(O)-mediated tetracycline resistance. *The EMBO journal* **22**: 945-953.

Correia, S., P. Poeta, M. Hebraud, J.L. Capelo & G. Igrejas, (2017) Mechanisms of quinolone action and resistance: where do we stand? *J Med Microbiol* **66**: 551-559.

Cotter, P.D., C. Hill & R.P. Ross, (2005) Bacteriocins: developing innate immunity for food. *Nat Rev Microbiol* **3**: 777-788.

Cotter, P.D., R.P. Ross & C. Hill, (2013) Bacteriocins - a viable alternative to antibiotics? *Nat Rev Microbiol* **11**: 95-105.

Coumes-Florens, S., C. Brochier-Armanet, A. Guiseppi, F. Denizot & M. Foglino, (2011) A new highly conserved antibiotic sensing/resistance pathway in firmicutes involves an ABC transporter interplaying with a signal transduction system. *PLoS One* **6**: e15951.

Courvalin, P., (2006) Vancomycin Resistance in Gram-Positive Cocci. *Clinical Infectious Diseases* **42**: S25-S34.

Cox, G., G.S. Thompson, H.T. Jenkins, F. Peske, A. Savelsbergh, M.V. Rodnina, W. Wintermeyer, S.W. Homans, T.A. Edwards & A.J. O'Neill, (2012) Ribosome clearance by FusB-type proteins mediates resistance to the antibiotic fusidic acid. *Proc Natl Acad Sci U S A* **109**: 2102-2107.

Cromwell, M.E.M., E. Hilario & F. Jacobson, (2006) Protein aggregation and bioprocessing. *The AAPS journal* **8**: E572-E579.

Crow, A., N.P. Greene, E. Kaplan & V. Koronakis, (2017) Structure and mechanotransmission mechanism of the MacB ABC transporter superfamily. *Proc Natl Acad Sci U S A* **114**: 12572-12577.

Daniel, R.A. & J. Errington, (2003) Control of cell morphogenesis in bacteria: two distinct ways to make a rod-shaped cell. *Cell* **113**: 767-776.

Darnell, R.L., Y. Nakatani, M.K. Knottenbelt, S. Gebhard & G.M. Cook, (2019) Functional characterization of BcrR: a one-component transmembrane signal transduction system for bacitracin resistance. *Microbiology* **165**: 475-487.

Davidson, A.L. & J. Chen, (2004) ATP-binding cassette transporters in bacteria. *Annu Rev Biochem* **73**: 241-268.

Davies, J., (2006) Where have All the Antibiotics Gone? *The Canadian journal of infectious diseases & medical microbiology* **17**: 287-290.

Dawson, R.J., K. Hollenstein & K.P. Locher, (2007) Uptake or extrusion: crystal structures of full ABC transporters suggest a common mechanism. *Mol Microbiol* **65**: 250-257.

de Kruijff, B., V. van Dam & E. Breukink, (2008) Lipid II: a central component in bacterial cell wall synthesis and a target for antibiotics. *Prostaglandins Leukot Essent Fatty Acids* **79**: 117-121.

Dean, M., A. Rzhetsky & R. Allikmets, (2001) The human ATP-binding cassette (ABC) transporter superfamily. *Genome Res* **11**: 1156-1166.

Desai, J., Y.D. Wang, K.D. Wang, S.R.D. Malwal & E. Oldfield, (2016) Isoprenoid Biosynthesis Inhibitors Targeting Bacterial Cell Growth. *ChemMedChem* **11**: 2205-2215.

Dintner, S., R. Heermann, C. Fang, K. Jung & S. Gebhard, (2014) A sensory complex consisting of an ATP-binding cassette transporter and a two-component regulatory system controls bacitracin resistance in *Bacillus subtilis*. *J Biol Chem* **289**: 27899-27910.

Dintner, S., A. Staron, E. Berchtold, T. Petri, T. Mascher & S. Gebhard, (2011) Coevolution of ABC transporters and two-component regulatory systems as resistance modules against antimicrobial peptides in Firmicutes Bacteria. *J Bacteriol* **193**: 3851-3862.

Dischinger, J., S. Basi Chipalu & G. Bierbaum, (2014) Lantibiotics: promising candidates for future applications in health care. *Int J Med Microbiol* **304**: 51-62.

Disfani, F.M., W.L. Hsu, M.J. Mizianty, C.J. Oldfield, B. Xue, A.K. Dunker, V.N. Uversky & L. Kurgan, (2012) MoRFpred, a computational tool for sequence-based prediction and characterization of short disorder-to-order transitioning binding regions in proteins. *Bioinformatics* **28**: i75-83.

Dominguez Pardo, J.J., J.M. Dorr, A. Iyer, R.C. Cox, S. Scheidelaar, M.C. Koorengevel, V. Subramaniam & J.A. Killian, (2017) Solubilization of lipids and lipid phases by the styrene-maleic acid copolymer. *Eur Biophys J* **46**: 91-101.

Donhofer, A., S. Franckenberg, S. Wickles, O. Berninghausen, R. Beckmann & D.N. Wilson, (2012) Structural basis for TetM-mediated tetracycline resistance. *Proc Natl Acad Sci U S A* **109**: 16900-16905.

Dorr, J.M., M.C. Koorengevel, M. Schafer, A.V. Prokofyev, S. Scheidelaar, E.A. van der Cruijsen, T.R. Dafforn, M. Baldus & J.A. Killian, (2014) Detergent-free isolation, characterization, and functional reconstitution of a tetrameric K^+ channel: the power of native nanodiscs. *Proc Natl Acad Sci U S A* **111**: 18607-18612.

Dorr, J.M., S. Scheidelaar, M.C. Koorengevel, J.J. Dominguez, M. Schafer, C.A. van Walree & J.A. Killian, (2016) The styrene-maleic acid copolymer: a versatile tool in membrane research. *Eur Biophys J* **45**: 3-21.

Dosztanyi, Z., V. Csizmok, P. Tompa & I. Simon, (2005a) IUPred: web server for the prediction of intrinsically unstructured regions of proteins based on estimated energy content. *Bioinformatics* **21**: 3433-3434.

Dosztanyi, Z., V. Csizmok, P. Tompa & I. Simon, (2005b) The pairwise energy content estimated from amino acid composition discriminates between folded and intrinsically unstructured proteins. *J Mol Biol* **347**: 827-839.

Draper, L.A., P.D. Cotter, C. Hill & R.P. Ross, (2015) Lantibiotic resistance. *Microbiol Mol Biol Rev* **79**: 171-191.

Drozdetskiy, A., C. Cole, J. Procter & G.J. Barton, (2015) JPred4: a protein secondary structure prediction server. *Nucleic Acids Res* **43**: W389-394.

Du, D., X. Wang-Kan, A. Neuberger, H.W. van Veen, K.M. Pos, L.J.V. Piddock & B.F. Luisi, (2018) Multidrug efflux pumps: structure, function and regulation. *Nat Rev Microbiol*.

Dunker, A.K., J.D. Lawson, C.J. Brown, R.M. Williams, P. Romero, J.S. Oh, C.J. Oldfield, A.M. Campen, C.M. Ratliff, K.W. Hipps, J. Ausio, M.S. Nissen, R. Reeves, C. Kang, C.R. Kissinger, R.W. Bailey, M.D. Griswold, W. Chiu, E.C. Garner & Z. Obradovic, (2001) Intrinsically disordered protein. *J Mol Graph Model* **19**: 26-59.

Dunker, A.K. & Z. Obradovic, (2001) The protein trinity—linking function and disorder. *Nature Biotechnology* **19**: 805.

Dunker, A.K., C.J. Oldfield, J. Meng, P. Romero, J.Y. Yang, J.W. Chen, V. Vacic, Z. Obradovic & V.N. Uversky, (2008a) The unfoldomics decade: an update on intrinsically disordered proteins. *BMC Genomics* **9 Suppl 2**: S1.

Dunker, A.K., I. Silman, V.N. Uversky & J.L. Sussman, (2008b) Function and structure of inherently disordered proteins. *Curr Opin Struct Biol* **18**: 756-764.

Economou, N.J., S. Cocklin & P.J. Loll, (2013) High-resolution crystal structure reveals molecular details of target recognition by bacitracin. *Proc Natl Acad Sci U S A* **110**: 14207-14212.

Eiamphungporn, W. & J.D. Helmann, (2008) The *Bacillus subtilis* sigmaM regulon and its contribution to cell envelope stress responses. *Mol Microbiol* **67**: 830-848.

El Ghachi, M., A. Derbise, A. Bouhss & D. Mengin-Lecreulx, (2005) Identification of multiple genes encoding membrane proteins with undecaprenyl pyrophosphate phosphatase (UppP) activity in *Escherichia coli*. *J Biol Chem* **280**: 18689-18695.

El Zoeiby, A., F. Sanschagrin & R.C. Levesque, (2003) Structure and function of the Mur enzymes: development of novel inhibitors. *Mol Microbiol* **47**: 1-12.

Elkins, C.A. & H. Nikaido, (2002) Substrate Specificity of the RND-Type Multidrug Efflux Pumps AcrB and AcrD of *Escherichia coli* Is Determined Predominately by Two Large Periplasmic Loops. *Journal of Bacteriology* **184**: 6490-6498.

Ellermeier, C.D., E.C. Hobbs, J.E. Gonzalez-Pastor & R. Losick, (2006) A three-protein signaling pathway governing immunity to a bacterial cannibalism toxin. *Cell* **124**: 549-559.

Emami, K., A. Guyet, Y. Kawai, J. Devi, L.J. Wu, N. Allenby, R.A. Daniel & J. Errington, (2017) RodA as the missing glycosyltransferase in *Bacillus subtilis* and antibiotic discovery for the peptidoglycan polymerase pathway. *Nat Microbiol* **2**: 16253.

Epand, R.M. & R.F. Epand, (2009) Lipid domains in bacterial membranes and the action of antimicrobial agents. *Biochim Biophys Acta* **1788**: 289-294.

Epand, R.M., C. Walker, R.F. Epand & N.A. Magarvey, (2016) Molecular mechanisms of membrane targeting antibiotics. *Biochim Biophys Acta* **1858**: 980-987.

Erickson, H.P., (2009) Size and shape of protein molecules at the nanometer level determined by sedimentation, gel filtration, and electron microscopy. *Biol Proced Online* **11**: 32-51.

Farrand, S.K. & H.W. Taber, (1974) Changes in menaquinone concentration during growth and early sporulation in *Bacillus subtilis*. *Journal of Bacteriology* **117**: 324-326.

Field, D., T. Blake, H. Mathur, P.M. O'Connor, P.D. Cotter, R.P. Ross & C. Hill, (2018) Bioengineering Nisin to overcome the Nisin Resistance Protein. *Mol Microbiol*.

Fischer, E., (1894) Einfluss der Configuration auf die Wirkung der Enzyme. *Berichte der deutschen chemischen Gesellschaft* **27**: 2985-2993.

Fitzpatrick, A.W.P., S. Llabres, A. Neuberger, J.N. Blaza, X.C. Bai, U. Okada, S. Murakami, H.W. van Veen, U. Zachariae, S.H.W. Scheres, B.F. Luisi & D. Du, (2017) Structure of the MacAB-TolC ABC-type tripartite multidrug efflux pump. *Nat Microbiol* **2**: 17070.

Franke, C.A. & D.E. Hruby, (1993) Expression and single-step purification of enzymatically active vaccinia virus thymidine kinase containing an engineered oligohistidine domain by immobilized metal affinity chromatography. *Protein Expr Purif* **4**: 101-109.

Frelet, A. & M. Klein, (2006) Insight in eukaryotic ABC transporter function by mutation analysis. *FEBS Lett* **580**: 1064-1084.

Frick, I.M., P. Akesson, M. Rasmussen, A. Schmidtchen & L. Bjorck, (2003) SIC, a secreted protein of *Streptococcus pyogenes* that inactivates antibacterial peptides. *J Biol Chem* **278**: 16561-16566.

Fritz, G., S. Dintner, N.S. Treichel, J. Radeck, U. Gerland, T. Mascher & S. Gebhard, (2015) A New Way of Sensing: Need-Based Activation of Antibiotic Resistance by a Flux-Sensing Mechanism. *MBio* **6**: e00975.

Fujinami, D., A.A. Mahin, K.M. Elsayed, M.R. Islam, J.I. Nagao, U. Roy, S. Momin, T. Zendo, D. Kohda & K. Sonomoto, (2018) The lantibiotic nukacin ISK-1 exists in an equilibrium between active and inactive lipid-II binding states. *Commun Biol* **1**: 150.

Garti-Levi, S., R. Hazan, J. Kain, M. Fujita & S. Ben-Yehuda, (2008) The FtsEX ABC transporter directs cellular differentiation in *Bacillus subtilis*. *Mol Microbiol* **69**: 1018-1028.

Gasteiger E., H.C., Gattiker A., Duvaud S., Wilkins M.R., Appel R.D., Bairoch A., (2005) *Protein Identification and Analysis Tools on the ExPASy Server,* p. 571-607.

Gasymov, O.K. & B.J. Glasgow, (2007) ANS fluorescence: potential to augment the identification of the external binding sites of proteins. *Biochim Biophys Acta* **1774**: 403-411.

Gauntlett, J.C., S. Gebhard, S. Keis, J.M. Manson, K.M. Pos & G.M. Cook, (2008) Molecular analysis of BcrR, a membrane-bound bacitracin sensor and DNA-binding protein from *Enterococcus faecalis*. *J Biol Chem* **283**: 8591-8600.

Gebhard, S., (2012) ABC transporters of antimicrobial peptides in Firmicutes bacteria - phylogeny, function and regulation. *Mol Microbiol* **86**: 1295-1317.

Gebhard, S., C. Fang, A. Shaaly, D.J. Leslie, M.R. Weimar, F. Kalamorz, A. Carne & G.M. Cook, (2014) Identification and characterization of a bacitracin resistance network in *Enterococcus faecalis*. *Antimicrob Agents Chemother* **58**: 1425-1433.

Gebhard, S., A. Gaballa, J.D. Helmann & G.M. Cook, (2009) Direct stimulus perception and transcription activation by a membrane-bound DNA binding protein. *Mol Microbiol* **73**: 482-491.

Gebhard, S. & T. Mascher, (2011) Antimicrobial peptide sensing and detoxification modules: unravelling the regulatory circuitry of *Staphylococcus aureus*. *Mol Microbiol* **81**: 581-587.

González-Pastor, J.E., E.C. Hobbs & R. Losick, (2003) Cannibalism by Sporulating Bacteria. *Science* **301**: 510-513.

Gottesman, M.M. & I. Pastan, (1993) Biochemistry of multidrug resistance mediated by the multidrug transporter. *Annu Rev Biochem* **62**: 385-427.

Graumann, P., (2007) *Bacillus: Cellular and Molecular Biology*. Caister Academic Press.

Greene, N.P., E. Kaplan, A. Crow & V. Koronakis, (2018) Antibiotic Resistance Mediated by the MacB ABC Transporter Family: A Structural and Functional Perspective. *Front Microbiol* **9**: 950.

Greenfield, N.J., (2006) Using circular dichroism spectra to estimate protein secondary structure. *Nat Protoc* **1**: 2876-2890.

Guzman, L.M., D. Belin, M.J. Carson & J. Beckwith, (1995) Tight regulation, modulation, and high-level expression by vectors containing the arabinose PBAD promoter. *Journal of Bacteriology* **177**: 4121-4130.

Hacker, C., N.A. Christ, E. Duchardt-Ferner, S. Korn, L. Berninger, P. Kotter, K.D. Entian & J. Wohnert, (2015a) NMR resonance assignments of the lantibiotic immunity protein NisI from *Lactococcus lactis*. *Biomol NMR Assign* **9**: 293-297.

Hacker, C., N.A. Christ, E. Duchardt-Ferner, S. Korn, C. Gobl, L. Berninger, S. Dusterhus, U.A. Hellmich, T. Madl, P. Kotter, K.D. Entian & J. Wohnert, (2015b) The Solution Structure of the Lantibiotic Immunity Protein NisI and Its Interactions with Nisin. *J Biol Chem* **290**: 28869-28886.

Hall, T., I. Biosciences & C. Carlsbad, (2011) BioEdit: an important software for molecular biology. *GERF Bull Biosci* **2**: 60-61.

Hall, T.A., (1999) BioEdit: a user-friendly biological sequence alignment editor and analysis program for Windows 95/98/NT. In: Nucleic acids symposium series. London, Information Retrieval Ltd., c1979-c2000., pp. 95-98.

Hancock, R. & P.C. Fitz-James, (1964) Some differences in the action of penicillin, bacitracin and vancomycin on *Bacillus megaterium*. *Journal of Bacteriology* **87**: 1044-1050.

Hancock, R.E. & H.G. Sahl, (2006) Antimicrobial and host-defense peptides as new anti-infective therapeutic strategies. *Nat Biotechnol* **24**: 1551-1557.

Hancock, R.E.W. & D.S. Chapple, (1999) Peptide Antibiotics. *Antimicrobial Agents and Chemotherapy* **43**: 1317-1323.

Hasper, H.E., B. de Kruijff & E. Breukink, (2004) Assembly and stability of nisin-lipid II pores. *Biochemistry* **43**: 11567-11575.

Hasper, H.E., N.E. Kramer, J.L. Smith, J.D. Hillman, C. Zachariah, O.P. Kuipers, B. de Kruijff & E. Breukink, (2006) An Alternative Bactericidal Mechanism of Action for Lantibiotic Peptides That Target Lipid II. *Science* **313**: 1636-1637.

Hawkins, J.S., S. Wong, J.M. Peters, R. Almeida & L.S. Qi, (2015) Targeted Transcriptional Repression in Bacteria Using CRISPR Interference (CRISPRi). *Methods Mol Biol* **1311**: 349-362.

Heijne, G., (1986) The distribution of positively charged residues in bacterial inner membrane proteins correlates with the trans-membrane topology. *EMBO J* **5**: 3021-3027.

Helmann, J.D., (2016) *Bacillus subtilis* extracytoplasmic function (ECF) sigma factors and defense of the cell envelope. *Curr Opin Microbiol* **30**: 122-132.

Hibbing, M.E., C. Fuqua, M.R. Parsek & S.B. Peterson, (2010) Bacterial competition: surviving and thriving in the microbial jungle. *Nat Rev Microbiol* **8**: 15-25.

Higgins, C.F. & M.M. Gottesman, (1992) Is the Multidrug Transporter a Flippase. *Trends in Biochemical Sciences* **17**: 18-21.

Higgins, C.F. & K.J. Linton, (2004) The ATP switch model for ABC transporters. *Nat Struct Mol Biol* **11**: 918-926.

Hiron, A., M. Falord, J. Valle, M. Debarbouille & T. Msadek, (2011) Bacitracin and nisin resistance in *Staphylococcus aureus*: a novel pathway involving the BraS/BraR two-component system (SA2417/SA2418) and both the BraD/BraE and VraD/VraE ABC transporters. *Mol Microbiol* **81**: 602-622.

Hirst, J.D. & C.L. Brooks, 3rd, (1994) Helicity, circular dichroism and molecular dynamics of proteins. *J Mol Biol* **243**: 173-178.

Hoffmann, A., T. Schneider, U. Pag & H.G. Sahl, (2004) Localization and functional analysis of PepI, the immunity peptide of Pep5-producing *Staphylococcus epidermidis* strain 5. *Appl Environ Microbiol* **70**: 3263-3271.

Hofler, C., J. Heckmann, A. Fritsch, P. Popp, S. Gebhard, G. Fritz & T. Mascher, (2016) Cannibalism stress response in *Bacillus subtilis*. *Microbiology* **162**: 164-176.

Hofmann, K., (1993) TMbase-A database of membrane spanning proteins segments. *Biol. Chem. Hoppe-Seyler* **374**: 166.

Hottenrott, S., T. Schumann, A. Pluckthun, G. Fischer & J.U. Rahfeld, (1997) The *Escherichia coli* SlyD is a metal ion-regulated peptidyl-prolyl cis/trans-isomerase. *J Biol Chem* **272**: 15697-15701.

Hsu, S.T., E. Breukink, G. Bierbaum, H.G. Sahl, B. de Kruijff, R. Kaptein, N.A. van Nuland & A.M. Bonvin, (2003) NMR study of mersacidin and lipid II interaction in dodecylphosphocholine micelles. Conformational changes are a key to antimicrobial activity. *J Biol Chem* **278**: 13110-13117.

Hsu, S.T., E. Breukink, E. Tischenko, M.A. Lutters, B. de Kruijff, R. Kaptein, A.M. Bonvin & N.A. van Nuland, (2004) The nisin-lipid II complex reveals a pyrophosphate cage that provides a blueprint for novel antibiotics. *Nat Struct Mol Biol* **11**: 963-967.

Huang, Y. & Z. Liu, (2009) Kinetic advantage of intrinsically disordered proteins in coupled folding-binding process: a critical assessment of the "fly-casting" mechanism. *J Mol Biol* **393**: 1143-1159.

Inaoka, T. & K. Ochi, (2012) Undecaprenyl pyrophosphate involvement in susceptibility of *Bacillus subtilis* to rare earth elements. *J Bacteriol* **194**: 5632-5637.

Ishida, T. & K. Kinoshita, (2007) PrDOS: prediction of disordered protein regions from amino acid sequence. *Nucleic Acids Res* **35**: W460-464.

Ito, Y., K. Kanamaru, N. Taniguchi, S. Miyamoto & H. Tokuda, (2006) A novel ligand bound ABC transporter, LolCDE, provides insights into the molecular mechanisms underlying membrane detachment of bacterial lipoproteins. *Mol Microbiol* **62**: 1064-1075.

Jeong, J.H. & S.C. Ha, (2018) Crystal Structure of NisI in a Lipid-Free Form, the Nisin Immunity Protein, from *Lactococcus lactis*. *Antimicrob Agents Chemother* **62**.

Jerga, A., Y.J. Lu, G.E. Schujman, D. de Mendoza & C.O. Rock, (2007) Identification of a soluble diacylglycerol kinase required for lipoteichoic acid production in *Bacillus subtilis*. *J Biol Chem* **282**: 21738-21745.

Johnson, B.A., H. Anker & F.L. Meleney, (1945) Bacitracin: a new antibiotic produced by a member of the *B. subtilis* group. *Science* **102**: 376-377.

Joo, H.S., C.I. Fu & M. Otto, (2016) Bacterial strategies of resistance to antimicrobial peptides. *Philos Trans R Soc Lond B Biol Sci* **371**.

Kaletta, C., K.-D. Entian, R. Kellner, G. Jung, M. Reis & H.-G. Sahl, (1989) Pep5, a new lantibiotic: structural gene isolation and prepeptide sequence. *Archives of Microbiology* **152**: 16-19.

Kallenberg, F., S. Dintner, R. Schmitz & S. Gebhard, (2013) Identification of regions important for resistance and signalling within the antimicrobial peptide transporter BceAB of *Bacillus subtilis*. *J Bacteriol* **195**: 3287-3297.

Kaluarachchi, H., J.F. Siebel, S. Kaluarachchi-Duffy, S. Krecisz, D.E. Sutherland, M.J. Stillman & D.B. Zamble, (2011) Metal selectivity of the *Escherichia coli* nickel metallochaperone, SlyD. *Biochemistry* **50**: 10666-10677.

Kaluarachchi, H., D.E.K. Sutherland, A. Young, I.J. Pickering, M.J. Stillman & D.B. Zamble, (2009) The Ni(II)-Binding Properties of the Metallochaperone SlyD. *Journal of the American Chemical Society* **131**: 18489-18500.

Kelly, S.M., T.J. Jess & N.C. Price, (2005) How to study proteins by circular dichroism. *Biochim Biophys Acta* **1751**: 119-139.

Khosa, S., Z. AlKhatib & S.H. Smits, (2013) NSR from *Streptococcus agalactiae* confers resistance against nisin and is encoded by a conserved nsr operon. *Biol Chem* **394**: 1543-1549.

Khosa, S., B. Frieg, D. Mulnaes, D. Kleinschrodt, A. Hoeppner, H. Gohlke & S.H. Smits, (2016a) Structural basis of lantibiotic recognition by the nisin resistance protein from *Streptococcus agalactiae*. *Sci Rep* **6**: 18679.

Khosa, S., M. Lagedroste & S.H. Smits, (2016b) Protein Defense Systems against the Lantibiotic Nisin: Function of the Immunity Protein NisI and the Resistance Protein NSR. *Front Microbiol* **7**: 504.

Khwaja, M., Q. Ma & M.H. Saier, Jr., (2005) Topological analysis of integral membrane constituents of prokaryotic ABC efflux systems. *Res Microbiol* **156**: 270-277.

Kingston, A.W., H. Zhao, G.M. Cook & J.D. Helmann, (2014) Accumulation of heptaprenyl diphosphate sensitizes *Bacillus subtilis* to bacitracin: implications for the mechanism of resistance mediated by the BceAB transporter. *Mol Microbiol* **93**: 37-49.

Kleerebezem, M., (2004) Quorum sensing control of lantibiotic production; nisin and subtilin autoregulate their own biosynthesis. *Peptides* **25**: 1405-1414.

Knerr, P.J. & W.A. van der Donk, (2012) Discovery, biosynthesis, and engineering of lantipeptides. *Annu Rev Biochem* **81**: 479-505.

Knight, T., (2007) Draft Standard for Biobrick Biological Parts, http://parts.igem.org/Help:Assembly_standard_10.

Knowles, T.J., R. Finka, C. Smith, Y.P. Lin, T. Dafforn & M. Overduin, (2009) Membrane proteins solubilized intact in lipid containing nanoparticles bounded by styrene maleic acid copolymer. *J Am Chem Soc* **131**: 7484-7485.

Kobayashi, K., S.D. Ehrlich, A. Albertini, G. Amati, K.K. Andersen, M. Arnaud, K. Asai, S. Ashikaga, S. Aymerich, P. Bessieres, F. Boland, S.C. Brignell, S. Bron, K. Bunai, J. Chapuis, L.C. Christiansen, A. Danchin, M. Debarbouille, E. Dervyn, E. Deuerling, K. Devine, S.K. Devine, O. Dreesen, J. Errington, S. Fillinger, S.J. Foster, Y. Fujita, A. Galizzi, R. Gardan, C. Eschevins, T. Fukushima, K. Haga, C.R. Harwood, M. Hecker, D. Hosoya, M.F. Hullo, H. Kakeshita, D. Karamata, Y. Kasahara, F. Kawamura, K. Koga, P. Koski, R. Kuwana, D. Imamura, M. Ishimaru, S. Ishikawa, I. Ishio, D. Le Coq, A. Masson, C. Mauel, R. Meima, R.P. Mellado, A. Moir, S. Moriya, E. Nagakawa, H. Nanamiya, S. Nakai, P. Nygaard, M. Ogura, T. Ohanan, M. O'Reilly, M. O'Rourke, Z. Pragai, H.M. Pooley, G. Rapoport, J.P. Rawlins, L.A. Rivas, C. Rivolta, A. Sadaie, Y. Sadaie, M. Sarvas, T. Sato, H.H. Saxild, E. Scanlan, W. Schumann, J.F. Seegers, J. Sekiguchi, A. Sekowska,

S.J. Seror, M. Simon, P. Stragier, R. Studer, H. Takamatsu, T. Tanaka, M. Takeuchi, H.B. Thomaides, V. Vagner, J.M. van Dijl, K. Watabe, A. Wipat, H. Yamamoto, M. Yamamoto, Y. Yamamoto, K. Yamane, K. Yata, K. Yoshida, H. Yoshikawa, U. Zuber & N. Ogasawara, (2003) Essential Bacillus subtilis genes. *Proc Natl Acad Sci U S A* **100**: 4678-4683.

Kobayashi, N., K. Nishino & A. Yamaguchi, (2001) Novel Macrolide-Specific ABC-Type Efflux Transporter in *Escherichia coli*. *Journal of Bacteriology* **183**: 5639-5644.

Koo, B.M., G. Kritikos, J.D. Farelli, H. Todor, K. Tong, H. Kimsey, I. Wapinski, M. Galardini, A. Cabal, J.M. Peters, A.B. Hachmann, D.Z. Rudner, K.N. Allen, A. Typas & C.A. Gross, (2017) Construction and Analysis of Two Genome-Scale Deletion Libraries for *Bacillus subtilis*. *Cell Syst* **4**: 291-305 e297.

Kordel, M., F. Schüller & H.-G. Sahl, (1989) Interaction of the pore forming-peptide antibiotics Pep 5, nisin and subtilin with non-energized liposomes. *FEBS Letters* **244**: 99-102.

Koshland Jr., D.E., (1995) The Key–Lock Theory and the Induced Fit Theory. *Angewandte Chemie International Edition in English* **33**: 2375-2378.

Kramer, N.E., E.J. Smid, J. Kok, B. de Kruijff, O.P. Kuipers & E. Breukink, (2004) Resistance of Gram-positive bacteria to nisin is not determined by lipid II levels. *FEMS Microbiol Lett* **239**: 157-161.

Kriwacki, R.W., L. Hengst, L. Tennant, S.I. Reed & P.E. Wright, (1996) Structural studies of p21Waf1/Cip1/Sdi1 in the free and Cdk2-bound state: conformational disorder mediates binding diversity. *Proceedings of the National Academy of Sciences* **93**: 11504-11509.

Kuipers, O., M.M. Beerthuyzen, P.G. de Ruyter, E.J. Luesink & W. De Vos, (1995) *Autoregulation of Nisin Biosynthesis in Lactococcus lactis by Signal Transduction,* p. 27299-27304.

Kumar, S., F.A. Rubino, A.G. Mendoza & N. Ruiz, (2018) The bacterial lipid II flippase MurJ functions by an alternating-access mechanism. *J Biol Chem*.

Kunst, F., N. Ogasawara, I. Moszer, A.M. Albertini, G. Alloni, V. Azevedo, M.G. Bertero, P. Bessières, A. Bolotin, S. Borchert, R. Borriss, L. Boursier, A. Brans, M. Braun, S.C. Brignell, S. Bron, S. Brouillet, C.V. Bruschi, B. Caldwell, V. Capuano, N.M. Carter, S.K. Choi, J.J. Codani, I.F. Connerton, N.J. Cummings, R.A. Daniel, F. Denizot, K.M. Devine, A. Düsterhöft, S.D. Ehrlich, P.T. Emmerson, K.D. Entian, J. Errington, C. Fabret, E. Ferrari, D. Foulger, C. Fritz, M. Fujita, Y. Fujita, S. Fuma, A. Galizzi, N. Galleron, S.Y. Ghim, P. Glaser, A. Goffeau, E.J. Golightly, G. Grandi, G. Guiseppi, B.J. Guy, K. Haga, J. Haiech, C.R. Harwood, A. Hénaut, H. Hilbert, S. Holsappel, S. Hosono, M.F. Hullo, M. Itaya, L. Jones, B. Joris, D. Karamata, Y. Kasahara, M. Klaerr-Blanchard, C. Klein, Y. Kobayashi, P. Koetter, G. Koningstein, S. Krogh, M. Kumano, K. Kurita, A. Lapidus, S. Lardinois, J. Lauber, V. Lazarevic, S.M. Lee, A. Levine, H. Liu, S. Masuda, C. Mauël, C. Médigue, N. Medina, R.P. Mellado, M. Mizuno, D. Moestl, S. Nakai, M. Noback, D. Noone, M. O'Reilly, K. Ogawa, A. Ogiwara, B. Oudega, S.H. Park, V. Parro, T.M. Pohl, D. Portetelle, S. Porwollik, A.M. Prescott, E. Presecan, P. Pujic, B. Purnelle*, et al.*, (1997) The complete genome sequence of the Gram-positive bacterium Bacillus subtilis. *Nature* **390**: 249.

Kunst, F. & G. Rapoport, (1995) Salt stress is an environmental signal affecting degradative enzyme synthesis in *Bacillus subtilis*. *J Bacteriol* **177**: 2403-2407.

Lai, Y. & R.L. Gallo, (2009) AMPed up immunity: how antimicrobial peptides have multiple roles in immune defense. *Trends Immunol* **30**: 131-141.

Leavitt, S. & E. Freire, (2001) Direct measurement of protein binding energetics by isothermal titration calorimetry. *Curr Opin Struct Biol* **11**: 560-566.

Lee, A.G., (2004) How lipids affect the activities of integral membrane proteins. *Biochim Biophys Acta* **1666**: 62-87.

Lee, P.A., G. Buchanan, N.R. Stanley, B.C. Berks & T. Palmer, (2002) Truncation Analysis of TatA and TatB Defines the Minimal Functional Units Required for Protein Translocation. *Journal of Bacteriology* **184**: 5871-5879.

Lee, W., K. Schaefer, Y. Qiao, V. Srisuknimit, H. Steinmetz, R. Muller, D. Kahne & S. Walker, (2016) The Mechanism of Action of Lysobactin. *J Am Chem Soc* **138**: 100-103.

Lee, Y.H. & J.D. Helmann, (2013) Reducing the Level of Undecaprenyl Pyrophosphate Synthase Has Complex Effects on Susceptibility to Cell Wall Antibiotics. *Antimicrob Agents Chemother* **57**: 4267-4275.

Letunic, I. & P. Bork, (2018) 20 years of the SMART protein domain annotation resource. *Nucleic Acids Res* **46**: D493-D496.

Letunic, I., T. Doerks & P. Bork, (2015) SMART: recent updates, new developments and status in 2015. *Nucleic Acids Res* **43**: D257-260.

Li, Q., M. Montalban-Lopez & O.P. Kuipers, (2018) Increasing Antimicrobial Activity of Nisin-based Lantibiotics Against Gram-negative Pathogens. *Appl Environ Microbiol*.

Li, Y., V. Lubchenko & P.G. Vekilov, (2011) The use of dynamic light scattering and brownian microscopy to characterize protein aggregation. *Rev Sci Instrum* **82**: 053106.

Lin, T.Y. & D.B. Weibel, (2016) Organization and function of anionic phospholipids in bacteria. *Appl Microbiol Biotechnol* **100**: 4255-4267.

Linding, R., L.J. Jensen, F. Diella, P. Bork, T.J. Gibson & R.B. Russell, (2003) Protein disorder prediction: implications for structural proteomics. *Structure* **11**: 1453-1459.

Ling, L.L., T. Schneider, A.J. Peoples, A.L. Spoering, I. Engels, B.P. Conlon, A. Mueller, T.F. Schäberle, D.E. Hughes, S. Epstein, M. Jones, L. Lazarides, V.A. Steadman, D.R. Cohen, C.R. Felix, K.A. Fetterman, W.P. Millett, A.G. Nitti, A.M. Zullo, C. Chen & K. Lewis, (2015) A new antibiotic kills pathogens without detectable resistance. *Nature* **517**: 455.

Liu, R. & F.J. Sharom, (1996) Site-Directed Fluorescence Labeling of P-Glycoprotein on Cysteine Residues in the Nucleotide Binding Domains. *Biochemistry* **35**: 11865-11873.

Liu, Y. & E. Breukink, (2016) The Membrane Steps of Bacterial Cell Wall Synthesis as Antibiotic Targets. *Antibiotics* **5**.

Liu, Y., L. Liu, J. Li, G. Du & J. Chen, (2018) Synthetic Biology Toolbox and Chassis Development in Bacillus subtilis. *Trends Biotechnol*.

Locher, K.P., (2016) Mechanistic diversity in ATP-binding cassette (ABC) transporters. *Nat Struct Mol Biol* **23**: 487-493.

Lopez, D. & R. Kolter, (2010) Extracellular signals that define distinct and coexisting cell fates in *Bacillus subtilis*. *FEMS Microbiol Rev* **34**: 134-149.

Lovering, A.L., L.H. de Castro, D. Lim & N.C.J. Strynadka, (2007) Structural Insight into the Transglycosylation Step of Bacterial Cell-Wall Biosynthesis. *Science* **315**: 1402-1405.

Löw, C., (2012) Metallochaperone SlyD. In: Encyclopedia of Inorganic and Bioinorganic Chemistry. pp.

Lullien, V. & C. Balny, (2002) High-pressure as a tool to study some proteins' properties: Conformational modification, activity and oligometric dissociation. *Innovative Food Science & Emerging Technologies* **3**: 209-221.

Mader, J.S. & D.W. Hoskin, (2006) Cationic antimicrobial peptides as novel cytotoxic agents for cancer treatment. *Expert Opin Investig Drugs* **15**: 933-946.

Maeno, A. & K. Akasaka, (2015) High-Pressure Fluorescence Spectroscopy. *Subcell Biochem* **72**: 687-705.

Maher, S. & S. McClean, (2006) Investigation of the cytotoxicity of eukaryotic and prokaryotic antimicrobial peptides in intestinal epithelial cells *in vitro*. *Biochem Pharmacol* **71**: 1289-1298.

Mahlapuu, M., J. Hakansson, L. Ringstad & C. Bjorn, (2016) Antimicrobial Peptides: An Emerging Category of Therapeutic Agents. *Front Cell Infect Microbiol* **6**: 194.

Manat, G., S. Roure, R. Auger, A. Bouhss, H. Barreteau, D. Mengin-Lecreulx & T. Touze, (2014) Deciphering the metabolism of undecaprenyl-phosphate: the bacterial cell-wall unit carrier at the membrane frontier. *Microb Drug Resist* **20**: 199-214.

Manson, J.M., S. Keis, J.M. Smith & G.M. Cook, (2004) Acquired bacitracin resistance in *Enterococcus faecalis* is mediated by an ABC transporter and a novel regulatory protein, BcrR. *Antimicrob Agents Chemother* **48**: 3743-3748.

Marr, A.K., W.J. Gooderham & R.E. Hancock, (2006) Antibacterial peptides for therapeutic use: obstacles and realistic outlook. *Curr Opin Pharmacol* **6**: 468-472.

Martino, L., Y. He, K.L. Hands-Taylor, E.R. Valentine, G. Kelly, C. Giancola & M.R. Conte, (2009) The interaction of the *Escherichia coli* protein SlyD with nickel ions illuminates the mechanism of regulation of its peptidyl-prolyl isomerase activity. *FEBS J* **276**: 4529-4544.

Mascher, T., (2014) Bacterial (intramembrane-sensing) histidine kinases: signal transfer rather than stimulus perception. *Trends Microbiol* **22**: 559-565.

Mascher, T., A.B. Hachmann & J.D. Helmann, (2007) Regulatory overlap and functional redundancy among *Bacillus subtilis* extracytoplasmic function sigma factors. *J Bacteriol* **189**: 6919-6927.

Mascher, T., J.D. Helmann & G. Unden, (2006) Stimulus perception in bacterial signal-transducing histidine kinases. *Microbiol Mol Biol Rev* **70**: 910-938.

Mascher, T., N.G. Margulis, T. Wang, R.W. Ye & J.D. Helmann, (2003) Cell wall stress responses in *Bacillus subtilis*: the regulatory network of the bacitracin stimulon. *Molecular Microbiology* **50**: 1591-1604.

Matos, R., V.V. Pinto, M. Ruivo & F. Lopes Mde, (2009) Study on the dissemination of the bcrABDR cluster in *Enterococcus* spp. reveals that the BcrAB transporter is sufficient to confer high-level bacitracin resistance. *Int J Antimicrob Agents* **34**: 142-147.

Mavrici, D., M.J. Marakalala, J.M. Holton, D.M. Prigozhin, C.L. Gee, Y.J. Zhang, E.J. Rubin & T. Alber, (2014) *Mycobacterium tuberculosis* FtsX extracellular domain activates the peptidoglycan hydrolase, RipC. *Proc Natl Acad Sci U S A* **111**: 8037-8042.

May, K.L. & T.J. Silhavy, (2017) Making a membrane on the other side of the wall. *Biochim Biophys Acta Mol Cell Biol Lipids* **1862**: 1386-1393.

McBride, S.M. & A.L. Sonenshein, (2011) Identification of a genetic locus responsible for antimicrobial peptide resistance in *Clostridium difficile*. *Infect Immun* **79**: 167-176.

McPherson, D.C. & D.L. Popham, (2003) Peptidoglycan Synthesis in the Absence of Class A Penicillin-Binding Proteins in *Bacillus subtilis*. *Journal of Bacteriology* **185**: 1423-1431.

Medeiros-Silva, J., S. Jekhmane, A.L. Paioni, K. Gawarecka, M. Baldus, E. Swiezewska, E. Breukink & M. Weingarth, (2018) High-resolution NMR studies of antibiotics in cellular membranes. *Nat Commun* **9**: 3963.

Meeske, A.J., E.P. Riley, W.P. Robins, T. Uehara, J.J. Mekalanos, D. Kahne, S. Walker, A.C. Kruse, T.G. Bernhardt & D.Z. Rudner, (2016) SEDS proteins are a widespread family of bacterial cell wall polymerases. *Nature* **537**: 634-638.

Meeske, A.J., L.T. Sham, H. Kimsey, B.M. Koo, C.A. Gross, T.G. Bernhardt & D.Z. Rudner, (2015) MurJ and a novel lipid II flippase are required for cell wall biogenesis in *Bacillus subtilis*. *Proc Natl Acad Sci U S A* **112**: 6437-6442.

Meisner, J., P. Montero Llopis, L.T. Sham, E. Garner, T.G. Bernhardt & D.Z. Rudner, (2013) FtsEX is required for CwlO peptidoglycan hydrolase activity during cell wall elongation in *Bacillus subtilis*. *Mol Microbiol* **89**: 1069-1083.

Menges, F., (2016) Spekwin32-optical spectroscopy software, http://www.effemm2.de/spekwin/.

Michna, R.H., F.M. Commichau, D. Todter, C.P. Zschiedrich & J. Stulke, (2014) SubtiWiki-a database for the model organism *Bacillus subtilis* that links pathway, interaction and expression information. *Nucleic Acids Res* **42**: D692-698.

Mileykovskaya, E. & W. Dowhan, (2005) Role of membrane lipids in bacterial division-site selection. *Curr Opin Microbiol* **8**: 135-142.

Miller, M.B. & B.L. Bassler, (2001) Quorum Sensing in Bacteria. *Annual Review of Microbiology* **55**: 165-199.

Ming, L.-J. & J.D. Epperson, (2002) Metal binding and structure–activity relationship of the metalloantibiotic peptide bacitracin. *Journal of Inorganic Biochemistry* **91**: 46-58.

Mittag, T., L.E. Kay & J.D. Forman-Kay, (2010) Protein dynamics and conformational disorder in molecular recognition. *J Mol Recognit* **23**: 105-116.

Miyamoto, S. & H. Tokuda, (2007) Diverse effects of phospholipids on lipoprotein sorting and ATP hydrolysis by the ABC transporter LolCDE complex. *Biochim Biophys Acta* **1768**: 1848-1854.

Mizutani, M., K. Mukaiyama, J. Xiao, M. Mori, R. Satou, S. Narita, S. Okuda & H. Tokuda, (2013) Functional differentiation of structurally similar membrane subunits of the ABC transporter LolCDE complex. *FEBS Lett* **587**: 23-29.

Mohammadi, T., V. van Dam, R. Sijbrandi, T. Vernet, A. Zapun, A. Bouhss, M. Diepeveen-de Bruin, M. Nguyen-Disteche, B. de Kruijff & E. Breukink, (2011) Identification of FtsW as a transporter of lipid-linked cell wall precursors across the membrane. *EMBO J* **30**: 1425-1432.

Mohan, A., C.J. Oldfield, P. Radivojac, V. Vacic, M.S. Cortese, A.K. Dunker & V.N. Uversky, (2006) Analysis of molecular recognition features (MoRFs). *J Mol Biol* **362**: 1043-1059.

Montenez, J.P., F. Van Bambeke, J. Piret, R. Brasseur, P.M. Tulkens & M.P. Mingeot-Leclercq, (1999) Interactions of Macrolide Antibiotics (Erythromycin A, Roxithromycin, Erythromycylamine [Dirithromycin], and Azithromycin) with Phospholipids: Computer-Aided Conformational Analysis and Studies on Acellular and Cell Culture Models. *Toxicology and Applied Pharmacology* **156**: 129-140.

Moszer, I., L.M. Jones, S. Moreira, C. Fabry & A. Danchin, (2002) SubtiList: the reference database for the *Bacillus subtilis* genome. *Nucleic Acids Research* **30**: 62-65.

Motulsky, H. & A. Christopoulos, (2004) *Fitting models to biological data using linear and nonlinear regression: a practical guide to curve fitting*. Oxford University Press.

Muchova, K., A.J. Wilkinson & I. Barak, (2011) Changes of lipid domains in *Bacillus subtilis* cells with disrupted cell wall peptidoglycan. *FEMS Microbiol Lett* **325**: 92-98.

Muller, A., M. Wenzel, H. Strahl, F. Grein, T.N.V. Saaki, B. Kohl, T. Siersma, J.E. Bandow, H.G. Sahl, T. Schneider & L.W. Hamoen, (2016) Daptomycin inhibits cell envelope synthesis by interfering with fluid membrane microdomains. *Proc Natl Acad Sci U S A* **113**: E7077-E7086.

Murakami, S., R. Nakashima, E. Yamashita & A. Yamaguchi, (2002) Crystal structure of bacterial multidrug efflux transporter AcrB. *Nature* **419**: 587.

Mygind, P.H., R.L. Fischer, K.M. Schnorr, M.T. Hansen, C.P. Sonksen, S. Ludvigsen, D. Raventos, S. Buskov, B. Christensen, L. De Maria, O. Taboureau, D. Yaver, S.G. Elvig-Jorgensen, M.V. Sorensen, B.E. Christensen, S. Kjaerulff, N. Frimodt-Moller, R.I.

Lehrer, M. Zasloff & H.H. Kristensen, (2005) Plectasin is a peptide antibiotic with therapeutic potential from a saprophytic fungus. *Nature* **437**: 975-980.

Nakashima, R., K. Sakurai, S. Yamasaki, K. Nishino & A. Yamaguchi, (2011) Structures of the multidrug exporter AcrB reveal a proximal multisite drug-binding pocket. *Nature* **480**: 565-569.

Narita, S. & H. Tokuda, (2006) An ABC transporter mediating the membrane detachment of bacterial lipoproteins depending on their sorting signals. *FEBS Lett* **580**: 1164-1170.

Narita, S.I. & H. Tokuda, (2017) Bacterial lipoproteins; biogenesis, sorting and quality control. *Biochim Biophys Acta Mol Cell Biol Lipids* **1862**: 1414-1423.

Nawrocki, K.L., E.K. Crispell & S.M. McBride, (2014) Antimicrobial Peptide Resistance Mechanisms of Gram-Positive Bacteria. *Antibiotics (Basel)* **3**: 461-492.

Neuhaus, F.C. & J. Baddiley, (2003) A Continuum of Anionic Charge: Structures and Functions of D-Alanyl-Teichoic Acids in Gram-Positive Bacteria. *Microbiology and Molecular Biology Reviews* **67**: 686-723.

Neumüller, A.M., D. Konz & M.A. Marahiel, (2001) The two-component regulatory system BacRS is associated with bacitracin 'self-resistance' of *Bacillus licheniformis* ATCC 10716. *European Journal of Biochemistry* **268**: 3180-3189.

Ng, V. & W.C. Chan, (2016) New Found Hope for Antibiotic Discovery: Lipid II Inhibitors. *Chemistry* **22**: 12606-12616.

O'Neill, J., (2014) The Review on Antimicrobial Resistance: Tackling a crisis for the health and wealth of nations.

O'Neill, J., (2016) Tackling drug-resistant infections globally: final report and recommendations.

Ogura, K., T. Koyama & H. Sagami, (1997) Polyprenyl Diphosphate Synthases. In: Cholesterol: Its Functions and Metabolism in Biology and Medicine. R. Bittman (ed). Boston, MA: Springer US, pp. 57-87.

Ohki, R., Giyanto, K. Tateno, W. Masuyama, S. Moriya, K. Kobayashi & N. Ogasawara, (2003) The BceRS two-component regulatory system induces expression of the bacitracin transporter, BceAB, in *Bacillus subtilis*. *Molecular Microbiology* **49**: 1135-1144.

Okada, U., E. Yamashita, A. Neuberger, M. Morimoto, H.W. van Veen & S. Murakami, (2017) Crystal structure of tripartite-type ABC transporter MacB from Acinetobacter baumannii. *Nat Commun* **8**: 1336.

Okuda, K., Y. Aso, J. Nagao, K. Shioya, Y. Kanemasa, J. Nakayama & K. Sonomoto, (2005) Characterization of functional domains of lantibiotic-binding immunity protein, NukH, from *Staphylococcus warneri* ISK-1. *FEMS Microbiol Lett* **250**: 19-25.

Okuda, K., Y. Aso, J. Nakayama & K. Sonomoto, (2008) Cooperative transport between NukFEG and NukH in immunity against the lantibiotic nukacin ISK-1 produced by *Staphylococcus warneri* ISK-1. *J Bacteriol* **190**: 356-362.

Okuda, S. & H. Tokuda, (2009) Model of mouth-to-mouth transfer of bacterial lipoproteins through inner membrane LolC, periplasmic LolA, and outer membrane LolB. *Proceedings of the National Academy of Sciences* **106**: 5877-5882.

Oppedijk, S., (2017) Identification, purification and elucidation of the mode of action of (novel) antimicrobial substances. *ProefschriftMaken*

Oppedijk, S.F., N.I. Martin & E. Breukink, (2016) Hit 'em where it hurts: The growing and structurally diverse family of peptides that target lipid-II. *Biochim Biophys Acta* **1858**: 947-957.

Organization, World Health, (2015) Global action plan on antimicrobial resistance.

Organization, World Health, (2019) Key facts on antimicrobial resistance, https://www.who.int/antimicrobial-resistance/en/.

Ostash, B. & S. Walker, (2010) Moenomycin family antibiotics: chemical synthesis, biosynthesis, and biological activity. *Nat Prod Rep* **27**: 1594-1617.

Otto, M., A. Peschel & F. Gotz, (1998) Producer self-protection against the lantibiotic epidermin by the ABC transporter EpiFEG of *Staphylococcus epidermidis* Tu3298. *FEMS Microbiol Lett* **166**: 203-211.

Ouyang, J., X.L. Tian, J. Versey, A. Wishart & Y.H. Li, (2010) The BceABRS four-component system regulates the bacitracin-induced cell envelope stress response in *Streptococcus mutans*. *Antimicrob Agents Chemother* **54**: 3895-3906.

Pader, V., S. Hakim, K.L. Painter, S. Wigneshweraraj, T.B. Clarke & A.M. Edwards, (2016) *Staphylococcus aureus* inactivates daptomycin by releasing membrane phospholipids. *Nat Microbiol* **2**: 16194.

Parisot, J., S. Carey, E. Breukink, W.C. Chan, A. Narbad & B. Bonev, (2008) Molecular mechanism of target recognition by subtilin, a class I lanthionine antibiotic. *Antimicrob Agents Chemother* **52**: 612-618.

Park, M., S.L. Tsai & W. Chen, (2013) Microbial biosensors: engineered microorganisms as the sensing machinery. *Sensors (Basel)* **13**: 5777-5795.

Parmar, M., S. Rawson, C.A. Scarff, A. Goldman, T.R. Dafforn, S.P. Muench & V.L.G. Postis, (2018) Using a SMALP platform to determine a sub-nm single particle cryo-EM membrane protein structure. *Biochim Biophys Acta Biomembr* **1860**: 378-383.

Pedersen, L.B., E.R. Angert & P. Setlow, (1999) Septal localization of penicillin-binding protein 1 in *Bacillus subtilis*. *J Bacteriol* **181**: 3201-3211.

Percy, M.G. & A. Grundling, (2014) Lipoteichoic acid synthesis and function in gram-positive bacteria. *Annu Rev Microbiol* **68**: 81-100.

Perego, M., P. Glaser, A. Minutello, M.A. Strauch, K. Leopold & W. Fischer, (1995) Incorporation of D-alanine into lipoteichoic acid and wall teichoic acid in *Bacillus subtilis*. Identification of genes and regulation. *J Biol Chem* **270**: 15598-15606.

Peschel, A., R.W. Jack, M. Otto, L.V. Collins, P. Staubitz, G. Nicholson, H. Kalbacher, W.F. Nieuwenhuizen, G. Jung, A. Tarkowski, K.P.M. van Kessel & J.A.G. van Strijp, (2001) *Staphylococcus aureus* Resistance to Human Defensins and Evasion of Neutrophil Killing via the Novel Virulence Factor Mprf Is Based on Modification of Membrane Lipids with L-Lysine. *The Journal of Experimental Medicine* **193**: 1067-1076.

Peters, J.M., A. Colavin, H. Shi, T.L. Czarny, M.H. Larson, S. Wong, J.S. Hawkins, C.H.S. Lu, B.M. Koo, E. Marta, A.L. Shiver, E.H. Whitehead, J.S. Weissman, E.D. Brown, L.S. Qi, K.C. Huang & C.A. Gross, (2016) A Comprehensive, CRISPR-based Functional Analysis of Essential Genes in Bacteria. *Cell* **165**: 1493-1506.

Peterson, B.L. & B.S. Cummings, (2006) A review of chromatographic methods for the assessment of phospholipids in biological samples. *Biomed Chromatogr* **20**: 227-243.

Pettersen, E.F., T.D. Goddard, C.C. Huang, G.S. Couch, D.M. Greenblatt, E.C. Meng & T.E. Ferrin, (2004) UCSF Chimera--a visualization system for exploratory research and analysis. *J Comput Chem* **25**: 1605-1612.

Pierce, M.M., C.S. Raman & B.T. Nall, (1999) Isothermal titration calorimetry of protein-protein interactions. *Methods* **19**: 213-221.

Podlesek, Z., A. Comino, B. Herzog-Velikonja & M. Grabnar, (2000) The role of the bacitracin ABC transporter in bacitracin resistance and collateral detergent sensitivity. *FEMS Microbiol Lett* **188**: 103-106.

Podlesek, Z., A. Comino, B. Herzog-Velikonja, D. Zgur-Bertok, R. Komel & M. Grabnar, (1995) *Bacillus licheniformis* bacitracin-resistance ABC transporter: relationship to mammalian multidrug resistance. *Mol Microbiol* **16**: 969-976.

Poehlsgaard, J. & S. Douthwaite, (2005) The bacterial ribosome as a target for antibiotics. *Nat Rev Microbiol* **3**: 870-881.

Pollock, N.L., S.C. Lee, J.H. Patel, A.A. Gulamhussein & A.J. Rothnie, (2018) Structure and function of membrane proteins encapsulated in a polymer-bound lipid bilayer. *Biochim Biophys Acta Biomembr* **1860**: 809-817.

Popham, D.L. & P. Setlow, (1995) Cloning, nucleotide sequence, and mutagenesis of the *Bacillus subtilis ponA* operon, which codes for penicillin-binding protein (PBP) 1 and a PBP-related factor. *J Bacteriol* **177**: 326-335.

Popp, P.F., M. Dotzler, J. Radeck, J. Bartels & T. Mascher, (2017) The *Bacillus* BioBrick Box 2.0: expanding the genetic toolbox for the standardized work with *Bacillus subtilis*. *Sci Rep* **7**: 15058.

Pos, K.M., (2009) Drug transport mechanism of the AcrB efflux pump. *Biochim Biophys Acta* **1794**: 782-793.

Postis, V., S. Rawson, J.K. Mitchell, S.C. Lee, R.A. Parslow, T.R. Dafforn, S.A. Baldwin & S.P. Muench, (2015) The use of SMALPs as a novel membrane protein scaffold for structure study by negative stain electron microscopy. *Biochim Biophys Acta* **1848**: 496-501.

Powell, E.O., (1956) Growth rate and generation time of bacteria, with special reference to continuous culture. *J Gen Microbiol* **15**: 492-511.

Prince, A., P. Sandhu, P. Ror, E. Dash, S. Sharma, M. Arakha, S. Jha, Y. Akhter & M. Saleem, (2016) Lipid-II Independent Antimicrobial Mechanism of Nisin Depends On Its Crowding And Degree Of Oligomerization. *Sci Rep* **6**: 37908.

Provencher, S.W. & J. Glockner, (1981) Estimation of globular protein secondary structure from circular dichroism. *Biochemistry* **20**: 33-37.

Provencher, S.W. & J. Gloeckner, (1981) Estimation of globular protein secondary structure from circular dichroism. *Biochemistry* **20**: 33-37.

Qiao, Y., V. Srisuknimit, F. Rubino, K. Schaefer, N. Ruiz, S. Walker & D. Kahne, (2017) Lipid II overproduction allows direct assay of transpeptidase inhibition by beta-lactams. *Nat Chem Biol* **13**: 793-798.

Qu, Q., P.L. Russell & F.J. Sharom, (2003) Stoichiometry and Affinity of Nucleotide Binding to P-Glycoprotein during the Catalytic Cycle. *Biochemistry* **42**: 1170-1177.

Quinn, P.J., (2002) Plasma membrane phospholipid asymmetry. *Subcell Biochem* **36**: 39-60.

Radeck, J., G. Fritz & T. Mascher, (2016a) The cell envelope stress response of *Bacillus subtilis*: from static signaling devices to dynamic regulatory network. *Curr Genet*.

Radeck, J., S. Gebhard, P.S. Orchard, M. Kirchner, S. Bauer, T. Mascher & G. Fritz, (2016b) Anatomy of the bacitracin resistance network in *Bacillus subtilis*. *Mol Microbiol* **100**: 607-620.

Radeck, J., K. Kraft, J. Bartels, T. Cikovic, F. Dürr, J. Emenegger, S. Kelterborn, C. Sauer, G. Fritz, S. Gebhard & T. Mascher, (2013) The *Bacillus* BioBrick Box: generation and evaluation of essential genetic building blocks for standardized work with *Bacillus subtilis*. *J Biol Eng* **7**: 29.

Radeck, J., N. Lautenschlager & T. Mascher, (2017a) The Essential UPP Phosphatase Pair BcrC and UppP Connects Cell Wall Homeostasis during Growth and Sporulation with Cell Envelope Stress Response in *Bacillus subtilis*. *Front Microbiol* **8**: 2403.

Radeck, J., D. Meyer, N. Lautenschlager & T. Mascher, (2017b) *Bacillus* SEVA siblings: A Golden Gate-based toolbox to create personalized integrative vectors for *Bacillus subtilis*. *Sci Rep* **7**: 14134.

Raetz, C. & W. Dowhan, (1990) Biosynthesis and function of phospholipids in *Escherichia coli*. *Journal of Biological Chemistry* **265**: 1235-1238.

Randall, C.P., A. Gupta, B. Utley-Drew, S.Y. Lee, G. Morrison-Williams & A.J. O'Neill, (2018) Acquired Nisin Resistance in *Staphylococcus aureus* Involves Constitutive Activation of an Intrinsic Peptide Antibiotic Detoxification Module. *mSphere* **3**.

Reiners, J., M. Lagedroste, K. Ehlen, S. Leusch, J. Zaschke-Kriesche & S.H.J. Smits, (2017) The N-terminal Region of Nisin Is Important for the BceAB-Type ABC Transporter NsrFP from *Streptococcus agalactiae* COH1. *Front Microbiol* **8**: 1643.

Reis, M., M. Eschbach-Bludau, M.I. Iglesias-Wind, T. Kupke & H.G. Sahl, (1994) Producer immunity towards the lantibiotic Pep5: identification of the immunity gene pepI and localization and functional analysis of its gene product. *Applied and Environmental Microbiology* **60**: 2876-2883.

Revilla-Guarinos, A., S. Gebhard, T. Mascher & M. Zuniga, (2014) Defence against antimicrobial peptides: different strategies in Firmicutes. *Environ Microbiol* **16**: 1225-1237.

Rietkötter, E., D. Hoyer & T. Mascher, (2008) Bacitracin sensing in *Bacillus subtilis*. *Mol Microbiol* **68**: 768-785.

Rogers, L.A., (1928) The Inhibiting Effect of *Streptococcus Lactis* on *Lactobacillus Bulgaricus*. *J Bacteriol* **16**: 321-325.

Romsicki, Y. & F.J. Sharom, (1999) The membrane lipid environment modulates drug interactions with the P-glycoprotein multidrug transporter. *Biochemistry* **38**: 6887-6896.

Rouquette-Loughlin, C.E., J.T. Balthazar & W.M. Shafer, (2005) Characterization of the MacA-MacB efflux system in *Neisseria gonorrhoeae*. *J Antimicrob Chemother* **56**: 856-860.

Roy, A., A. Kucukural & Y. Zhang, (2010) I-TASSER: a unified platform for automated protein structure and function prediction. *Nat Protoc* **5**: 725-738.

Rudolph, R. & H. Lilie, (1996) In vitro folding of inclusion body proteins. *FASEB J* **10**: 49-56.

Ruiz, J., (2003) Mechanisms of resistance to quinolones: target alterations, decreased accumulation and DNA gyrase protection. *J Antimicrob Chemother* **51**: 1109-1117.

Ruiz, N., (2008) Bioinformatics identification of MurJ (MviN) as the peptidoglycan lipid II flippase in *Escherichia coli*. *Proc Natl Acad Sci U S A* **105**: 15553-15557.

Ruiz, N., (2015) Lipid Flippases for Bacterial Peptidoglycan Biosynthesis. *Lipid Insights* **8**: 21-31.

Ruzin, A., G. Singh, A. Severin, Y. Yang, R.G. Dushin, A.G. Sutherland, A. Minnick, M. Greenstein, M.K. May, D.M. Shlaes & P.A. Bradford, (2004) Mechanism of Action of the Mannopeptimycins, a Novel Class of Glycopeptide Antibiotics Active against Vancomycin-Resistant Gram-Positive Bacteria. *Antimicrobial Agents and Chemotherapy* **48**: 728-738.

Saaf, A., H. Andersson, G. Gafvelin & G. von Heijne, (1995) SecA-dependence of the translocation of a large periplasmic loop in the *Escherichia coli* MalF inner membrane protein is a function of sequence context. *Mol Membr Biol* **12**: 209-215.

Sato, T., S. Yoshida, H. Hoshino, M. Tanno, M. Nakajima & T. Hoshino, (2011) Sesquarterpenes (C35 terpenes) biosynthesized via the cyclization of a linear C_{35} isoprenoid by a tetraprenyl-beta-curcumene synthase and a tetraprenyl-beta-curcumene cyclase: identification of a new terpene cyclase. *J Am Chem Soc* **133**: 9734-9737.

Sauvage, E., F. Kerff, M. Terrak, J.A. Ayala & P. Charlier, (2008) The penicillin-binding proteins: structure and role in peptidoglycan biosynthesis. *FEMS Microbiol Rev* **32**: 234-258.

Sauvage, E. & M. Terrak, (2016) Glycosyltransferases and Transpeptidases/Penicillin-Binding Proteins: Valuable Targets for New Antibacterials. *Antibiotics (Basel)* **5**.

Scheffers, D.J. & M.G. Pinho, (2005) Bacterial cell wall synthesis: new insights from localization studies. *Microbiol Mol Biol Rev* **69**: 585-607.

Scheffers, D.J. & M.B. Tol, (2015) LipidII: Just Another Brick in the Wall? *PLoS Pathog* **11**: e1005213.

Scheidelaar, S., M.C. Koorengevel, J.D. Pardo, J.D. Meeldijk, E. Breukink & J.A. Killian, (2015) Molecular model for the solubilization of membranes into nanodisks by styrene maleic Acid copolymers. *Biophys J* **108**: 279-290.

Scheinpflug, K., M. Wenzel, O. Krylova, J.E. Bandow, M. Dathe & H. Strahl, (2017) Antimicrobial peptide cWFW kills by combining lipid phase separation with autolysis. *Sci Rep* **7**: 44332.

Schmidt, K.L., N.D. Peterson, R.J. Kustusch, M.C. Wissel, B. Graham, G.J. Phillips & D.S. Weiss, (2004) A Predicted ABC Transporter, FtsEX, Is Needed for Cell Division in *Escherichia coli*. *Journal of Bacteriology* **186**: 785-793.

Schneider, T., T. Kruse, R. Wimmer, I. Wiedemann, V. Sass, U. Pag, A. Jansen, A.K. Nielsen, P.H. Mygind, D.S. Raventos, S. Neve, B. Ravn, A.M. Bonvin, L. De Maria, A.S. Andersen, L.K. Gammelgaard, H.G. Sahl & H.H. Kristensen, (2010) Plectasin, a fungal defensin, targets the bacterial cell wall precursor Lipid II. *Science* **328**: 1168-1172.

Schneider, T. & H.G. Sahl, (2010) An oldie but a goodie - cell wall biosynthesis as antibiotic target pathway. *Int J Med Microbiol* **300**: 161-169.

Schnell, N., K.-D. Entian, U. Schneider, F. Götz, H. Zähner, R. Kellner & G. Jung, (1988) Prepeptide sequence of epidermin, a ribosomally synthesized antibiotic with four sulphide-rings. *Nature* **333**: 276.

Scholz, C., B. Eckert, F. Hagn, P. Schaarschmidt, J. Balbach & F.X. Schmid, (2006) SlyD proteins from different species exhibit high prolyl isomerase and chaperone activities. *Biochemistry* **45**: 20-33.

Schonbrunn, E., D.I. Svergun, N. Amrhein & M.H. Koch, (1998) Studies on the conformational changes in the bacterial cell wall biosynthetic enzyme UDP-N-acetylglucosamine enolpyruvyltransferase (MurA). *Eur J Biochem* **253**: 406-412.

Sham, L.T., E.K. Butler, M.D. Lebar, D. Kahne, T.G. Bernhardt & N. Ruiz, (2014) MurJ is the flippase of lipid-linked precursors for peptidoglycan biogenesis. *Science* **345**: 220-222.

Sham, L.T., K.R. Jensen, K.E. Bruce & M.E. Winkler, (2013) Involvement of FtsE ATPase and FtsX extracellular loops 1 and 2 in FtsEX-PcsB complex function in cell division of *Streptococcus pneumoniae* D39. *MBio* **4**.

Sharkey, L.K., T.A. Edwards & A.J. O'Neill, (2016) ABC-F Proteins Mediate Antibiotic Resistance through Ribosomal Protection. *MBio* **7**: e01975.

Sharkey, L.K.R. & A.J. O'Neill, (2018) Antibiotic Resistance ABC-F Proteins: Bringing Target Protection into the Limelight. *ACS Infect Dis* **4**: 239-246.

Shen, H.H., T. Lithgow & L. Martin, (2013) Reconstitution of membrane proteins into model membranes: seeking better ways to retain protein activities. *Int J Mol Sci* **14**: 1589-1607.

Shin, J.M., J.W. Gwak, P. Kamarajan, J.C. Fenno, A.H. Rickard & Y.L. Kapila, (2016) Biomedical applications of nisin. *J Appl Microbiol* **120**: 1449-1465.

Shoemaker, B.A., J.J. Portman & P.G. Wolynes, (2000) Speeding molecular recognition by using the folding funnel: the fly-casting mechanism. *Proc Natl Acad Sci U S A* **97**: 8868-8873.

Silhavy, T.J., D. Kahne & S. Walker, (2010) The bacterial cell envelope. *Cold Spring Harb Perspect Biol* **2**: a000414.

Singer, S.J. & G.L. Nicolson, (1972) The Fluid Mosaic Model of the Structure of Cell Membranes. *Science* **175**: 720-731.

Singh, A., V. Upadhyay & A.K. Panda, (2015) Solubilization and refolding of inclusion body proteins. *Methods Mol Biol* **1258**: 283-291.

Singh, S.M. & A.K. Panda, (2005) Solubilization and refolding of bacterial inclusion body proteins. *J Biosci Bioeng* **99**: 303-310.

Sohlenkamp, C. & O. Geiger, (2016) Bacterial membrane lipids: diversity in structures and pathways. *FEMS Microbiol Rev* **40**: 133-159.

Sonveaux, N., C. Vigano, A.B. Shapiro, V. Ling & J.-M. Ruysschaert, (1999) Ligand-mediated Tertiary Structure Changes of Reconstituted P-glycoprotein: a tryptophan fluorescence quenching analysis. *Journal of Biological Chemistry* **274**: 17649-17654.

Sreerama, N. & R.W. Woody, (2000) Estimation of protein secondary structure from circular dichroism spectra: comparison of CONTIN, SELCON, and CDSSTR methods with an expanded reference set. *Anal Biochem* **287**: 252-260.

Staron, A., D.E. Finkeisen & T. Mascher, (2011) Peptide antibiotic sensing and detoxification modules of *Bacillus subtilis*. *Antimicrob Agents Chemother* **55**: 515-525.

Stein, T., S. Heinzmann, S. Dusterhus, S. Borchert & K.D. Entian, (2005) Expression and functional analysis of the subtilin immunity genes *spaIFEG* in the subtilin-sensitive host *Bacillus subtilis* MO1099. *J Bacteriol* **187**: 822-828.

Stein, T., S. Heinzmann, I. Solovieva & K.D. Entian, (2003) Function of *Lactococcus lactis* nisin immunity genes *nisI* and *nisFEG* after coordinated expression in the surrogate host *Bacillus subtilis*. *J Biol Chem* **278**: 89-94.

Stetefeld, J., S.A. McKenna & T.R. Patel, (2016) Dynamic light scattering: a practical guide and applications in biomedical sciences. *Biophys Rev* **8**: 409-427.

Stone, K.J. & J.L. Strominger, (1971) Mechanism of action of bacitracin: complexation with metal ion and C 55 -isoprenyl pyrophosphate. *Proc Natl Acad Sci U S A* **68**: 3223-3227.

Storm, D.R., (1974) Mechanism of bacitracin action: a specific lipid-peptide interaction. *Ann N Y Acad Sci* **235**: 387-398.

Storm, D.R. & J.L. Strominger, (1973) Complex formation between bacitracin peptides and isoprenyl pyrophosphates. The specificity of lipid-peptide interactions. *J Biol Chem* **248**: 3940-3945.

Storm, D.R. & J.L. Strominger, (1974) Binding of bacitracin to cells and protoplasts of *Micrococcus lysodeikticus*. *J Biol Chem* **249**: 1823-1827.

Strahl, H., F. Burmann & L.W. Hamoen, (2014) The actin homologue MreB organizes the bacterial cell membrane. *Nat Commun* **5**: 3442.

Strahl, H. & J. Errington, (2017) Bacterial Membranes: Structure, Domains, and Function. *Annu Rev Microbiol* **71**: 519-538.

Stroud, Z., S.C.L. Hall & T.R. Dafforn, (2018) Purification of membrane proteins free from conventional detergents: SMA, new polymers, new opportunities and new insights. *Methods* **147**: 106-117.

Sun, Z., J. Zhong, X. Liang, J. Liu, X. Chen & L. Huan, (2009) Novel mechanism for nisin resistance via proteolytic degradation of nisin by the nisin resistance protein NSR. *Antimicrob Agents Chemother* **53**: 1964-1973.

Suvarna, K., D. Stevenson, R. Meganathan & M.E.S. Hudspeth, (1998) Menaquinone (vitamin K-2) biosynthesis: Localization and characterization of the *menA* gene from Escherichia coli. *Journal of Bacteriology* **180**: 2782-2787.

Swainsbury, D.J., S. Scheidelaar, R. van Grondelle, J.A. Killian & M.R. Jones, (2014) Bacterial reaction centers purified with styrene maleic acid copolymer retain native membrane functional properties and display enhanced stability. *Angew Chem Int Ed Engl* **53**: 11803-11807.

Takahashi, I. & K. Ogura, (1982) Prenyltransferases of *Bacillus subtilis*: Undecaprenyl Pyrophosphate Synthetase and Geranylgeranyl Pyrophosphate Synthetase1. *The Journal of Biochemistry* **92**: 1527-1537.

Takala, T., O. Koponen, M. Qiao & P. Saris, (2004) Lipid-free NisI: interaction with nisin and contribution to nisin immunity via secretion. *FEMS Microbiology Letters* **237**: 171-177.

Tallarida, R.J., (2001) Drug synergism: its detection and applications. *J Pharmacol Exp Ther* **298**: 865-872.

Tallarida, R.J., (2006) An overview of drug combination analysis with isobolograms. *J Pharmacol Exp Ther* **319**: 1-7.

Tanaka, N., T. Kinoshita & H. Masukawa, (1968) Mechanism of protein synthesis inhibition by fusidic acid and related antibiotics. *Biochemical and Biophysical Research Communications* **30**: 278-283.

Taniguchi, N. & H. Tokuda, (2008) Molecular events involved in a single cycle of ligand transfer from an ATP binding cassette transporter, LolCDE, to a molecular chaperone, LolA. *J Biol Chem* **283**: 8538-8544.

Thompson, J.D., T.J. Gibson & D.G. Higgins, (2003) Multiple sequence alignment using ClustalW and ClustalX. *Current protocols in bioinformatics*: 2.3. 1-2.3. 22.

Thorne, K. & E. Kodicek, (1966) The structure of bactoprenol, a lipid formed by lactobacilli from mevalonic acid. *Biochemical Journal* **99**: 123-127.

Tikhonova, E.B., V.K. Devroy, S.Y. Lau & H.I. Zgurskaya, (2007) Reconstitution of the *Escherichia coli* macrolide transporter: the periplasmic membrane fusion protein MacA stimulates the ATPase activity of MacB. *Mol Microbiol* **63**: 895-910.

Tipper, D.J. & J.L. Strominger, (1965) Mechanism of action of penicillins: a proposal based on their structural similarity to acyl-D-alanyl-D-alanine. *Proceedings of the National Academy of Sciences* **54**: 1133-1141.

Tomlinson, J.H., G.S. Thompson, A.P. Kalverda, A. Zhuravleva & A.J. O'Neill, (2016) A target-protection mechanism of antibiotic resistance at atomic resolution: insights into FusB-type fusidic acid resistance. *Sci Rep* **6**: 19524.

Tran, J.H., G.A. Jacoby & D.C. Hooper, (2005) Interaction of the plasmid-encoded quinolone resistance protein QnrA with *Escherichia coli* topoisomerase IV. *Antimicrob Agents Chemother* **49**: 3050-3052.

Tran, T.T., J.M. Munita & C.A. Arias, (2015) Mechanisms of drug resistance: daptomycin resistance. *Ann N Y Acad Sci* **1354**: 32-53.

Trieber, C.A., N. Burkhardt, K.H. Nierhaus & D.E. Taylor, (1998) Ribosomal protection from tetracycline mediated by Tet(O): Tet(O) interaction with ribosomes is GTP-dependent. *Biol Chem* **379**: 847-855.

Tsirigos, K.D., C. Peters, N. Shu, L. Kall & A. Elofsson, (2015) The TOPCONS web server for consensus prediction of membrane protein topology and signal peptides. *Nucleic Acids Res* **43**: W401-407.

Tsuda, H., Y. Yamashita, Y. Shibata, Y. Nakano & T. Koga, (2002) Genes involved in bacitracin resistance in *Streptococcus mutans*. *Antimicrob Agents Chemother* **46**: 3756-3764.

Tsumoto, K., D. Ejima, I. Kumagai & T. Arakawa, (2003) Practical considerations in refolding proteins from inclusion bodies. *Protein Expr Purif* **28**: 1-8.

van den Brink-van der Laan, E., J.A. Killian & B. de Kruijff, (2004) Nonbilayer lipids affect peripheral and integral membrane proteins via changes in the lateral pressure profile. *Biochim Biophys Acta* **1666**: 275-288.

van der Heide, T. & B. Poolman, (2002) ABC transporters: one, two or four extracytoplasmic substrate-binding sites? *EMBO Rep* **3**: 938-943.

van Heijenoort, J., (1998) Assembly of the monomer unit of bacterial peptidoglycan. *Cellular and Molecular Life Sciences CMLS* **54**: 300-304.

van Heijenoort, J., (2007) Lipid intermediates in the biosynthesis of bacterial peptidoglycan. *Microbiol Mol Biol Rev* **71**: 620-635.

van Heijenoort, Y., M. Gómez, M. Derrien, J. Ayala & J. van Heijenoort, (1992) Membrane intermediates in the peptidoglycan metabolism of *Escherichia coli*: possible roles of PBP 1b and PBP 3. *Journal of Bacteriology* **174**: 3549-3557.

Villaverde, A. & M.M. Carrio, (2003) Protein aggregation in recombinant bacteria: biological role of inclusion bodies. *Biotechnol Lett* **25**: 1385-1395.

Vollmer, W., D. Blanot & M.A. de Pedro, (2008) Peptidoglycan structure and architecture. *FEMS Microbiol Rev* **32**: 149-167.

von Heijne, G., (1992) Membrane protein structure prediction. Hydrophobicity analysis and the positive-inside rule. *J Mol Biol* **225**: 487-494.

Walker, S., L. Chen, Y. Hu, Y. Rew, D. Shin & D.L. Boger, (2005) Chemistry and Biology of Ramoplanin: A Lipoglycodepsipeptide with Potent Antibiotic Activity. *Chemical Reviews* **105**: 449-476.

Wang, D., K. Chen, J.L. Kulp Iii & P.S. Arora, (2006) Evaluation of biologically relevant short alpha-helices stabilized by a main-chain hydrogen-bond surrogate. *J Am Chem Soc* **128**: 9248-9256.

Wang, F., H. Zhou, O.P. Olademehin, S.J. Kim & P. Tao, (2018) Insights into Key Interactions between Vancomycin and Bacterial Cell Wall Structures. *ACS Omega* **3**: 37-45.

Wang, W., S. Nema & D. Teagarden, (2010) Protein aggregation--pathways and influencing factors. *Int J Pharm* **390**: 89-99.

Weidenmaier, C. & A. Peschel, (2008) Teichoic acids and related cell-wall glycopolymers in Gram-positive physiology and host interactions. *Nat Rev Microbiol* **6**: 276-287.

Weininger, U., C. Haupt, K. Schweimer, W. Graubner, M. Kovermann, T. Bruser, C. Scholz, P. Schaarschmidt, G. Zoldak, F.X. Schmid & J. Balbach, (2009) NMR solution structure of SlyD from *Escherichia coli*: spatial separation of prolyl isomerase and chaperone function. *J Mol Biol* **387**: 295-305.

Weinstein, Z.B., A. Bender & M. Cokol, (2017) Prediction of synergistic drug combinations. *Current Opinion in Systems Biology* **4**: 24-28.

Welzel, P., (2005) Syntheses around the transglycosylation step in peptidoglycan biosynthesis. *Chem Rev* **105**: 4610-4660.

Whitmore, L. & B.A. Wallace, (2004) DICHROWEB, an online server for protein secondary structure analyses from circular dichroism spectroscopic data. *Nucleic Acids Res* **32**: W668-673.

Whitmore, L. & B.A. Wallace, (2008) Protein secondary structure analyses from circular dichroism spectroscopy: methods and reference databases. *Biopolymers* **89**: 392-400.

Wiedemann, I., E. Breukink, C. van Kraaij, O.P. Kuipers, G. Bierbaum, B. de Kruijff & H.G. Sahl, (2001) Specific binding of nisin to the peptidoglycan precursor lipid II combines pore formation and inhibition of cell wall biosynthesis for potent antibiotic activity. *J Biol Chem* **276**: 1772-1779.

Willey, J.M. & W.A. van der Donk, (2007) Lantibiotics: peptides of diverse structure and function. *Annu Rev Microbiol* **61**: 477-501.

Wiser, M.J. & R.E. Lenski, (2015) A Comparison of Methods to Measure Fitness in *Escherichia coli*. *PLoS One* **10**: e0126210.

Wood, W.B., (1966) Host specificity of DNA produced by *Escherichia coli*: bacterial mutations affecting the restriction and modification of DNA. *J Mol Biol* **16**: 118-133.

Wright, P.E. & H.J. Dyson, (1999) Intrinsically unstructured proteins: re-assessing the protein structure-function paradigm. *J Mol Biol* **293**: 321-331.

Wright, P.E. & H.J. Dyson, (2009) Linking folding and binding. *Curr Opin Struct Biol* **19**: 31-38.

Yakushi, T., K. Masuda, S.-i. Narita, S.-i. Matsuyama & H. Tokuda, (2000) A new ABC transporter mediating the detachment of lipid-modified proteins from membranes. *Nature Cell Biology* **2**: 212.

Yamanaka, H., H. Kobayashi, E. Takahashi & K. Okamoto, (2008) MacAB is involved in the secretion of *Escherichia coli* heat-stable enterotoxin II. *J Bacteriol* **190**: 7693-7698.

Yang, D.C., N.T. Peters, K.R. Parzych, T. Uehara, M. Markovski & T.G. Bernhardt, (2011) An ATP-binding cassette transporter-like complex governs cell-wall hydrolysis at the bacterial cytokinetic ring. *Proc Natl Acad Sci U S A* **108**: E1052-1060.

Yang, H.B., W.T. Hou, M.T. Cheng, Y.L. Jiang, Y. Chen & C.Z. Zhou, (2018) Structure of a MacAB-like efflux pump from *Streptococcus pneumoniae*. *Nat Commun* **9**: 196.

Yang, J. & Y. Zhang, (2015) I-TASSER server: new development for protein structure and function predictions. *Nucleic Acids Res* **43**: W174-181.

Yoshida, Y., M. Matsuo, Y. Oogai, F. Kato, N. Nakamura, M. Sugai & H. Komatsuzawa, (2011) Bacitracin sensing and resistance in *Staphylococcus aureus*. *FEMS Microbiol Lett* **320**: 33-39.

Young, K.D., (2014) Microbiology. A flipping cell wall ferry. *Science* **345**: 139-140.

Yu, E.W., J.R. Aires & H. Nikaido, (2003) AcrB Multidrug Efflux Pump of *Escherichia coli*: Composite Substrate-Binding Cavity of Exceptional Flexibility Generates Its Extremely Wide Substrate Specificity. *Journal of Bacteriology* **185**: 5657-5664.

Zaffiri, L., J. Gardner & L.H. Toledo-Pereyra, (2012) History of antibiotics. From salvarsan to cephalosporins. *J Invest Surg* **25**: 67-77.

Zhang, C., P.L. Freddolino & Y. Zhang, (2017) COFACTOR: improved protein function prediction by combining structure, sequence and protein-protein interaction information. *Nucleic Acids Res* **45**: W291-W299.

Zhang, Y.M. & C.O. Rock, (2008) Membrane lipid homeostasis in bacteria. *Nat Rev Microbiol* **6**: 222-233.

Zhao, H., V. Patel, J.D. Helmann & T. Dorr, (2017) Don't let sleeping dogmas lie: new views of peptidoglycan synthesis and its regulation. *Mol Microbiol* **106**: 847-860.

Zhao, H., D.M. Roistacher & J.D. Helmann, (2018) Aspartate deficiency limits peptidoglycan synthesis and sensitizes cells to antibiotics targeting cell wall synthesis in *Bacillus subtilis*. *Mol Microbiol* **109**: 826-844.

Zhao, H., Y. Sun, J.M. Peters, C.A. Gross, E.C. Garner & J.D. Helmann, (2016) Depletion of Undecaprenyl Pyrophosphate Phosphatases Disrupts Cell Envelope Biogenesis in *Bacillus subtilis*. *J Bacteriol* **198**: 2925-2935.

Zheng, S., L.-T. Sham, F.A. Rubino, K.P. Brock, W.P. Robins, J.J. Mekalanos, D.S. Marks, T.G. Bernhardt & A.C. Kruse, (2018) Structure and mutagenic analysis of the lipid II flippase MurJ from *Escherichia coli*. *Proceedings of the National Academy of Sciences* **115**: 6709-6714.

Zhou, L., A.J. van Heel, M. Montalban-Lopez & O.P. Kuipers, (2016) Potentiating the Activity of Nisin against *Escherichia coli*. *Front Cell Dev Biol* **4**: 7.

Zhu, B. & J. Stulke, (2018) SubtiWiki in 2018: from genes and proteins to functional network annotation of the model organism *Bacillus subtilis*. *Nucleic Acids Res* **46**: D743-D748.

Zwama, M., S. Yamasaki, R. Nakashima, K. Sakurai, K. Nishino & A. Yamaguchi, (2018) Multiple entry pathways within the efflux transporter AcrB contribute to multidrug recognition. *Nat Commun* **9**: 124.

Supplement

Chapter II

Table S1: *E. coli* strains used in this study.

Strain	Description[a]	Source/Reference
DH5α	*fhuA2*Δ(*argF-lacZ*)U169 *phoA glnV44* ϕ80 Δ(*lac-Z*) M15 *gyrA96 recA1 relA1 end A1 thi-1 hsdR17*	Laboratory stock
BL21(DE3)	*fhuA2 [lon] ompT gal (λ DE3) [dcm]* Δ*hsdS λ DE3 = λ sBamHIo* Δ*EcoRI-B int::(lacI::PlacUV5::T7gene1) i21* Δ*nin5*	New England BioLabs Inc.
SGE09	DH5α pSG1601, amp^r	Susanne Gebhard
SGE156	XL1-blue pNTSB104, amp^r	Nicole Treichel
SGE162	XL1-blue pNT2E01, amp^r	Nicole Treichel
SGE420	DH5α pCKET1601, amp^r	This study
SGE421	DH5α pCKET1602, amp^r	This study
SGE422	DH5α pCKET1603, amp^r	This study
SGE423	DH5α pCKET1604, amp^r	This study
SGE426	Top10 pCKpUC571, kan^r	This study
SGE427	Top10 pCKpUC572, kan^r	This study
SGE435	DH5α pCKBAD2404, amp^r	This study
SGE436	DH5α pCKBAD2405, amp^r	This study
SGE469	DH5α pCKDR1, amp^r	This study
SGE507	DH5α pCKC301, cm^r	This study
SGE508	DH5α pCK4S01, amp^r	This study
GFC473	DH5α pANM-1_145, spec^r	Annis Newmann
GFC474	DH5α pANM-1_146, spec^r	Annis Newmann
GFC475	DH5α pANM-1_147, spec^r	Annis Newmann

[a]amp^r: resistance to ampicillin, cm^r: chloramphenicol, kan^r: kanamycin, spec^r: spectinomycin.

Table S2: *B. subtilis* strains used in this study.

Strain	Description[a]	Source/Reference
W168	laboratory wild type strain, *trpC*2	Laboratory stock
SGB01	*bceAB*::kan *bcrC*::*tet*, kan^r, tet^r	Susanne Gebhard
SGB73	*sacA*::P$_{bceA}$-*luxABCDE*, cm^r	(Fritz *et al.*, 2015)
SGB74	*sacA*::P$_{psdA}$-*luxABCDE,* cm^r	Sebastian Dintner
SGB79	*bceAB*::kan *sacA*::P$_{bceA}$-*lux*, cm^r	(Kallenberg *et al.*, 2013)
SGB170	*bceAB*::kan pXT-*bceAB*, kan^r, spec^r	(Kallenberg *et al.*, 2013)
SGB218	*bceAB*::kan *sacA*::P$_{bceA}$-*lux lacA*::P$_{xyl}$-*bceAB*, kan^r, cm^r, mls^r	Nicole Treichel
SGB575	*bceAB*::kan, kan^r	This study
SGB576	*lacA*::P$_{xyl}$-*bceAB* (pNT2E01), mls^r	This study
SGB577	*bceAB*::kan *lacA*::P$_{xyl}$-*bceAB* (pNT2E01), kan^r, mls^r	This study
SGB648	*bceAB*::kan *bcrC*::tet *sacA*::P$_{bceA}$-*lux*, kan^r, cm^r, tet^r	This study
SGB649	*bcrC*::tet *sacA*::P$_{bceA}$-*lux*, cm^r, tet^r	This study
SGB650	*amyE*::P$_{hy_spank}$-*uppS* (pCKDR1), spec^r	This study
SGB651	*sacA*::P$_{bceA}$-*lux amyE*::P$_{hy_spank}$-*uppS*, cm^r, spec^r	This study
SGB677	*bcrC*::tet *bceAB*::kan *sacA*::P$_{bceA}$-*lux lacA*::P$_{xyl}$-*bceAB,* tet^r, kan^r, cm^r, mls^r	This study
SGB678	*bcrC*::tet *bceAB*::kan *sacA*::P$_{bceA}$-*lux lacA*::P$_{xyl}$-*bceAB*WalkerB,* tet^r, kan^r, cm^r, mls^r	This study
SGB681	*bcrC*::tet *sacA*::P$_{psdA}$-*lux,* tet^r, cm^r	This study
SGB713	*thrC*::P$_{xylA}$-*uppS*, spec^r	This study
SGB714	*thrC*::P$_{xylA}$-*uppS sacA*::P$_{bceA}$-*lux,* spec^r, cm^r	This study
SGB745	P$_{uppS}$::kan-*uppS1*, kan^r	This study
SGB746	*sacA*::P$_{bceA}$-*lux* P$_{uppS}$::kan-*uppS1,* cm^r, kan^r	This study
SGB758	*sacA*::P$_{bceA}$-*lux lacA*:: P$_{xylA}$-*bcrC*, cm^r, mls^r	This study
SGB798	*ytpB*::mls *sacA*::P$_{bceA}$-*lux*, cm^r, mls^r	This study
SGB810	*ponA*::kan *sacA*::P$_{bceA}$-*lux,* cm^r, kan^r	This study
SGB812	*sigM*::kan *sacA*::P$_{bceA}$-*lux,* cm^r, kan^r	This study
SGB870	P$_{uppS}$::kan-*uppS$^+$ sacA*::P$_{bceA}$-*lux,* kan^r, cm^r	This study
SGB871	P$_{uppS}$::kan-*uppS1 sacA*::P$_{bceA}$-*lux,* kan^r, cm^r	This study

TMB035	*bceAB*::kan, kan^r	(Rietkötter *et al.*, 2008)
TMB297	*bcrC*::tet, tet^r	(Rietkötter *et al.*, 2008)
HB13321	*ytpB*::mls, mls^r	(Kingston *et al.*, 2014)
HB13647	P_{uppS}::kan-*uppS*$^+$, kan^r	(Lee & Helmann, 2013)
HB13648	P_{uppS}::kan-*uppS1*, kan^r	(Lee & Helmann, 2013)
GFB058	P_{uppS}::*cat*-P_{xylA}, cm^r	Andre Sim
GFB078	*lacA*:: P_{xylA}-*dcas9 amyE*::P_{veg}-*uppS*-sgRNA, mls^r, cm^r	Andre Sim
BKK09520	*sigM*::kan, kan^r	(Koo *et al.*, 2017)
BKK22320	*ponA*::kan, kan^r	(Koo *et al.*, 2017)
TMB035	*bceAB*::kan, kan^r	(Rietkötter *et al.*, 2008)

[a]All *B. subtilis* strains used in this study are derived from strain W168. amp^r: resistance to ampicillin, cm^r: chloramphenicol, kan^r: kanamycin, mls^r: macrolide-lincosamide-streptogramin B, spec^r: spectinomycin, tet^r: tetracycline.

Table S3: Vectors used in this study.

	Vectors	Description[a]	Source/Reference
03	**pET-16b**	PT7, His•tag®, tT7, *lacI*, *ori*(pBR322), amp^r	pET system manual, 11th ed., Novagen®
20	**pBAD24**	arabinose-inducible promoter pBAD; ribosome binding site on vector, amp^r	(Guzman *et al.*, 1995)
78	**pBS4S**	pDG1731 derived, *rfp*-cassette, *thrC* integration, amp^r	(Radeck *et al.*, 2013)
81	**pSB1C3**	*ori* pMB1 , *rfp*-cassette in BioBrick multiple cloning site, cm^r	(Radeck *et al.*, 2013)
101	**pDR111**	P_{hy_spank}-multiple cloning site, IPTG-inducible, *amyE* integration	David Rudner

[a] amp^r: resistance to ampicillin, cm^r: chloramphenicol.

Table S4: Plasmids used in this study.

Plasmids		Description[a]	Source/Reference
11	**pSG1601**	*bceB*-ECD (A310-G525) in pET-16b, N-terminal His•tag® (NdeI/XhoI)	Susanne Gebhard
153	**pNTSB104**	P_{xylA} in pSB1A3 (EcoRI/SpeI, TM2341/2342)	Nicole Treichel
159	**pNT2E01**	P_{xylA}-*bceAB* in pBS2E (EcoRI/PstI)	Nicole Treichel
418	**pCKET1601**	*bceB*-ECD (Y315-Q520) in pET-16b, N-terminal His•tag® (NdeI/BamHI, SG0183/185)	This study
419	**pCKET1602**	*bceB*-ECD (T320-D515) in pET-16b, N-terminal His•tag® (NdeI, BamHI, SG0184/186)	This study
420	**pCKET1603**	*bceB*-ECD (Y315-D515) in pET-16b, N-terminal His•tag® (NdeI/BamHI, SG0183/186)	This study
421	**pCKET1604**	*bceB*-ECD (T320-Q520) in pET-16b, N-terminal His•tag® (NdeI/BamHI, SG0184/185)	This study
429	**pCKpUC571**	H1-*bceb*-ECD (A310-G525)-Strep•tag® II in pUC57-kan, synthesized (EcoRI/PstI)	This study
430	**pCKpUC572**	H1-*bceb*-ECD (A310-G525)-H2-Strep•tag® II in pUC57-kan, synthesized (EcoRI/PstI)	This study
433	**pCKBAD2404**	H1-*bceb*-ECD (A310-G525)-Strep•tag® II in pBAD24, synthesized (EcoRI/PstI)	This study
434	**pCKBAD2405**	H1-*bceb*-ECD (A310-G525)-H2-Strep•tag® II in pUC57-kan, synthesized (EcoRI/PstI)	This study
465	**pCKDR1**	P_{hy_spank}-*uppS*, in pDR111 (SalI/NheI, SG495/496)	This study
510	**pCKC301**	*uppS* in pSB1C3, (EcoRI/PstI, SG587/588)	This study
511	**pCK4S01**	P_{xylA}-*uppS* in pBS4S (BioBrick assembly)	This study
pANM-1_145		*sacA*::*cat*-P_{bceA}-*luxABCDE* (MoClo method)	Annis Newmann
pANM-1_146		*sacA*::spec-P_{bceA}-*luxABCDE* (MoClo method)	Annis Newmann
pANM-1_147		*sacA*::mls-P_{bceA}-*luxABCDE* (MoClo method)	Annis Newmann

[a]Restriction enzymes used for cloning are given in brackets (enzyme for 5'/enzyme for 3'). Primers used for PCRs are stated in bracktes, where applicable (primer for 5'/primer for 3').

Table S5: Oligonucleotides used in this study.

Primers	Target	Sequence (5' → 3')
SG0183	BceB_Y315_NdeI_F	AATTCATATGTACTCGTCGGAAAAGACCGC
SG0184	BceB_T320_NdeI_F	AATTCATATGACCGCTGAACAAAATGTAGCG
SG0185	BceB_Q520_BamHI_R	AATTGGATCCTCATTGCGCAGCGCTTGTATC
SG0186	BceB_D515_BamHI_R	AATTGGATCCTCAATCTAGTCTTGATAAATGCTCG
SG0416	pETcheck_up	ATGCGTCCGGCGTAGA
SG0417	pET_check_down	GTTAAATTGCTAACGCAGTCA
SG0418	pBAD_check_up	ATGCCATAGCATTTTTATCC
SG0419	pBAD_check_down	GATTTAATCTGTATCAGG
SG0427	pUC check_f (M13)	CCCAGTCACGACGTTGTAAAACG
SG0428	pUC check_r (M13)	AGCGGATAACAATTTCACACAGG
SG0495	UppS_SalI_F	AATTGTCGACATGCTCAACATACTCAAAAATTGGAAG
SG0496	UppS_NheI_R	AATTGCTAGCCTAAATTCCGCCAAACCTCCGGCC
SG0506	AmyE check(F)	GTAAGCGTTAACAAAATTCTC
SG0507	AmyE check(R)	TTATATTGTGCAACACTTCACA
SG0587	UppS_ENX_F	ATTGAATTCGCGGCCGCTTCTAGAGATGCTCAACATACTCAAAAATTGGAAG
SG0588	UppS_SNP_R	AGCCTGCAGCGGCCGCTACTAGTACTAAATTCCGCCAAACCTCCGGCC
SG0599	pSB1C3_seq_F	TGCCACCTGACGTCTAAG
SG0600	pSB1C3_seq_R	ATTACCGCCTTTGAGTGA
SG0601	pBS4S_seq_F	CAGTCAACCCTTACCGCATTG
SG0602	pBS4S_seq_R	CCTCCTCACTATTTTGATTAGTACC
SG0626	UppS_up_F	TGAATCAGCTGTTAAGTATGAATCAC
SG0627	UppS_up_R	CCTATCACCTCAAATGGTTCGCTGTGTACATAGTTTTTCATTAAACTTCCA CGAGCGCCTACGAGGAATTTGTATCGACTGTTGATTACATTGATTATCAGCA
SG0628	UppS_do_F	GGGAATGTAACCTTTTTGGGTGACGGAGGCATCTCATGCTCAACATAC
SG0629	UppS_do_R	TACTCAGCCTTATCTCGCCG
SG0637	menA_up_F	CCGTACACAAGGATAGGAGA
SG0638	menA_up_R	CCTATCACCTCAAATGGTTCGCTGGCCAAAGGATCTGCCCCAT
SG0639	menA_do_F	CGAGCGCCTACGAGGAATTTGTATCGCTGGGTTGTCGGCTTGGTT
SG0640	menA_do_R	GAAGGCGAAAGCATCTGACA
SG0701	sigM_up	CGGGCCAATGCACCTGATAAAG
SG0702	sigM_do	CAACCCGTTCATTCCCTACGG
SG0703	ponA_up	GCCGTTATACACAAAAAGCCGAC
SG0704	ponA_do	GCGCAGTCTTGGCCAGAAGAG

Chapter III

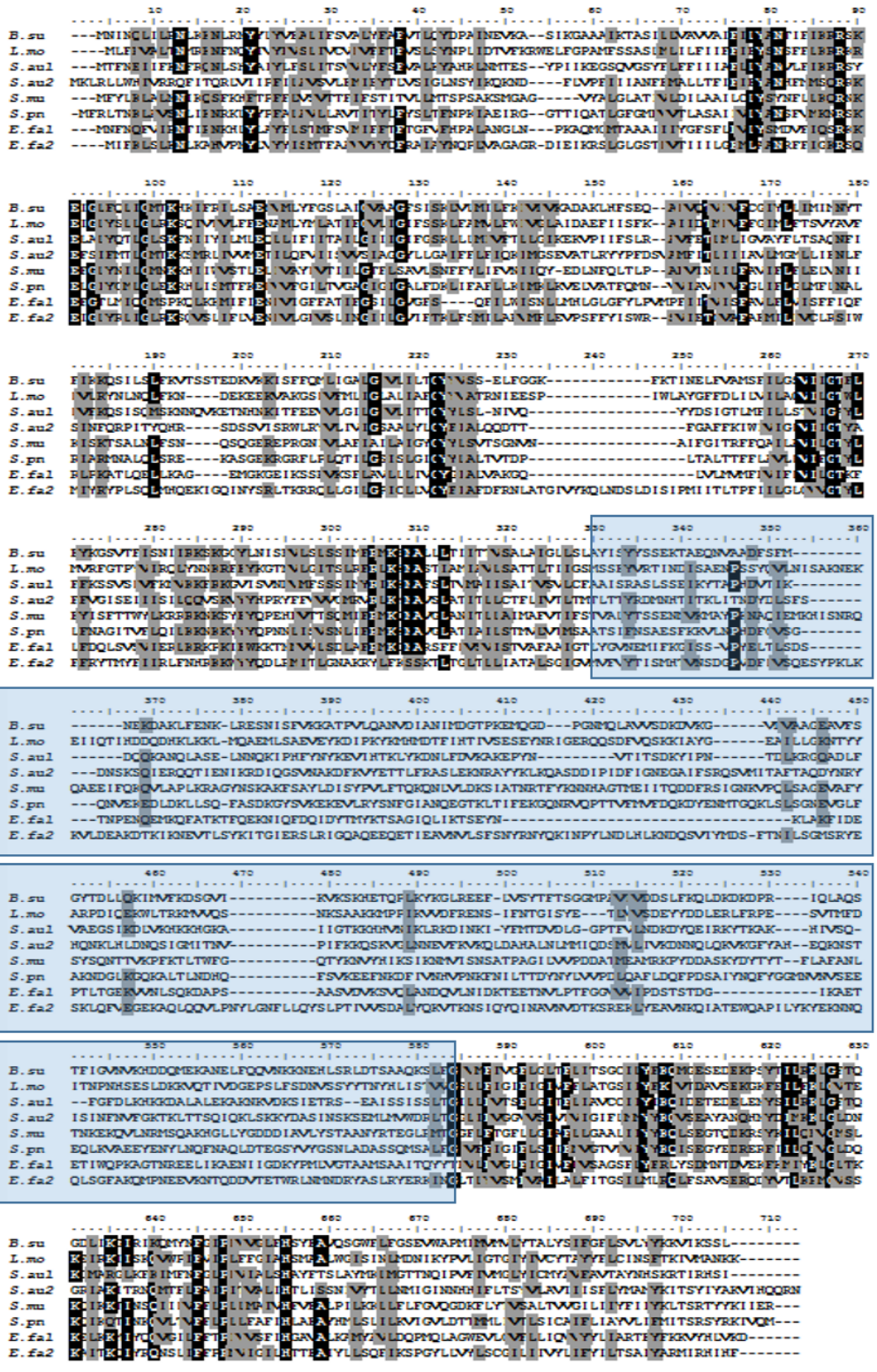

Figure S3.1: The extracellular domains of bacitracin resistance-related BceB-like permeases have only poor amino acid conservation. Sequence alignment of eight BceB-like permeases that sense bacitracin or confer resistance against the AMP. Amino acid sequences were aligned using the application ClustalW built into the sequence analysing tool BioEdit. Identical amino acid residues are shaded in back, amino acids with similar properties are shaded grey (75%). The extracellular domains are highlighted by a blue box. 1: BceB, *B. subtilis* (O34741, Ohki *et al.*, 2003), 2: AnrB, *Listeria monocytogenes* (Q8Y5E9, Collins *et al.*, 2010), 3: BraE, *Staphylococcus aureus*, (A0A0H3JWA4, Hiron *et al.*, 2011), 4: VraG, *Staphylococcus aureus* (A0A0H3K6M3, Hiron *et al.*, 2011), 5: MbrB, *Streptococcus mutans* (Q8VUH1, Tsuda *et al.*, 2002, Ouyang *et al.*, 2010), 6: Spr0813, *Streptococcus pneumoniae* (Q8DQ76, Becker *et al.*, 2009), 7: EF_2049, *Enterococcus faecalis* (Q833B5, Gebhard *et al.*, 2014), 8: EF_2751, *Enterococcus faecalis* (Q830M8, Gebhard *et al.*, 2014). Uniprot accession numbers are given in brackets (Boutet *et al.*, 2007).

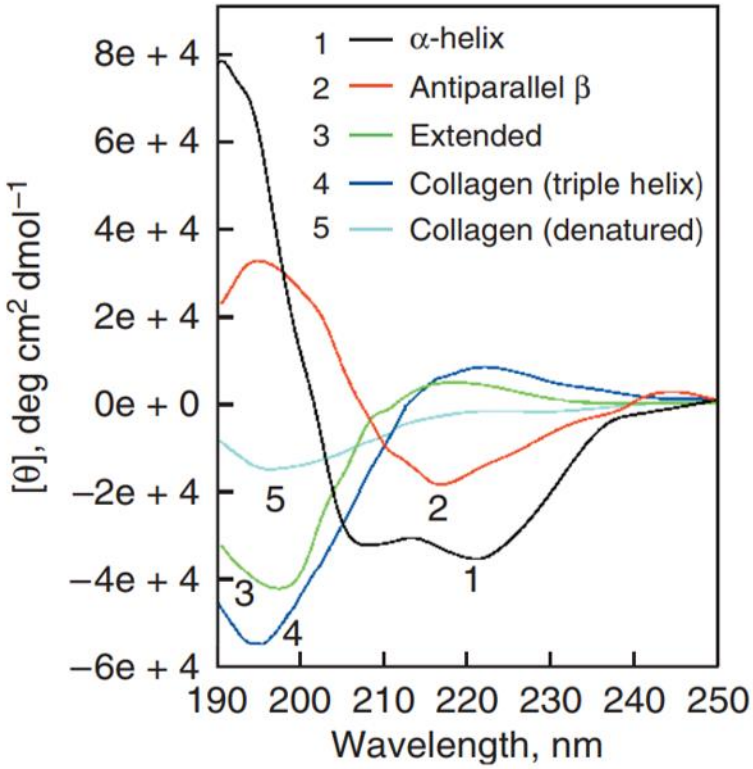

Figure S3.2: Circular dichroism spectra of polypeptides and proteins with representative secondary structures. 1: α-helical conformation (black), 2: antiparallel β-sheet conformation (red), 3: random coil or disorder (green), 4+5: collagen in native (blue) and denatured (cyan) forms. Modified from Greenfield (2006).

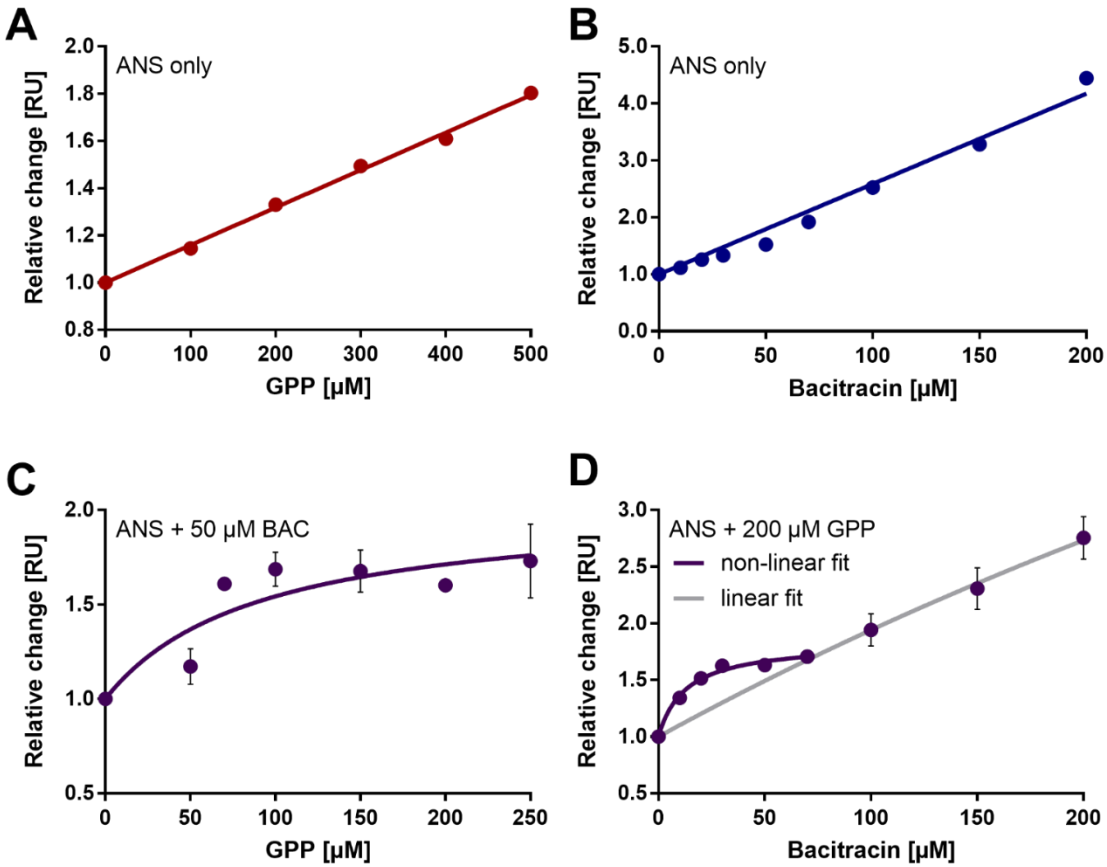

Figure S3.3: Complex formation between bacitracin and GPP results in saturation at 50 µM BAC and 200 µM GPP. Steady-state ANS fluorescence experiments of bacitracin and GPP were performed as described in Fig. 3.4. No buffer spectra were subtracted. **A+B:** Dose response of ANS fluorescence upon addition of various concentrations of A: GPP and B: bacitracin. Data points were fit with a linear regression line. **C:** Dose response of ANS fluorescence signal upon gradual addition of GPP to bacitracin. Data points were fit with a non-linear single site binding curve. **D:** Dose response of ANS fluorescence emission upon titration of bacitracin to GPP. Data points were approximated with a non-linear single site binding curve (purple) for lower and according to a linear regression fit (grey) at higher bacitracin concentrations. Data in C+D are depicted as mean ± standard deviation of two independent measurements.

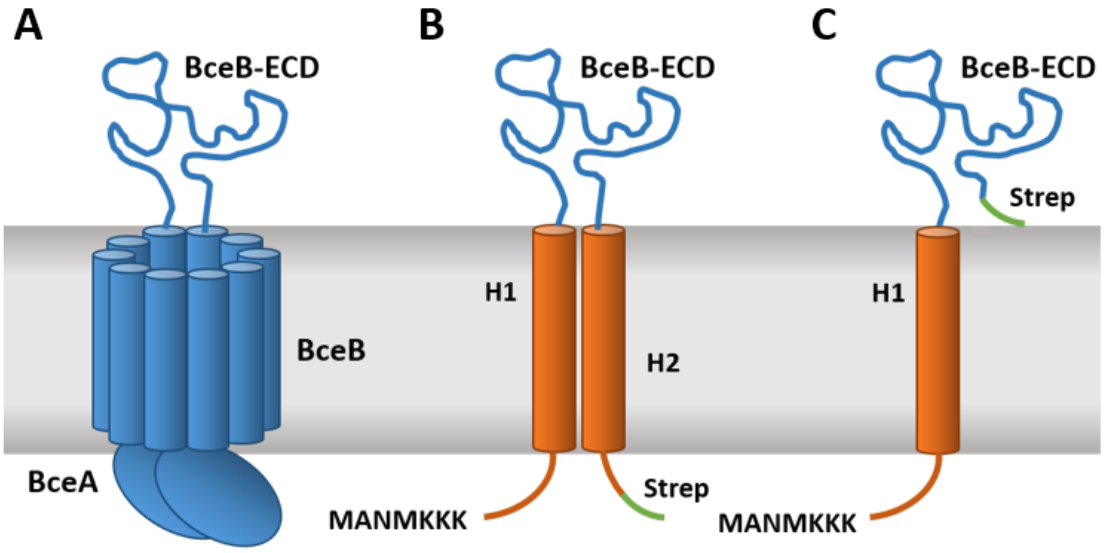

Figure S3.4. Schematic of BceB-ECD hybrid membrane proteins. Two different BceB-ECD hybrid membrane constructs were designed for gene synthesis (B and C). **B:** The first protein was designed to comprise two TMH (H1 + H2, orange) with the *bceB*-ECD encoding sequence in between (blue). **C:** The second hybrid protein contained a single TMH (H1, orange), followed by the *bceB*-ECD coding sequence. Both constructs were C-terminally-tagged with a Strep-Tag® II (green, IBA GmbH) and cloned into the same arabinose-inducible vector that were used for overproduction of full-length BceAB (**A**, pBAD24). The sequence of the membrane helices originated from the *E. coli* protein LepB. To ensure the correct topology in the membrane with the ECD located on the extracellular side of the membrane, additional positive amino acids (KKK) were added into the N-terminal region of the fusion protein, and positive residues in the native loop region of LepB were exchanged as suggested by Andersson and von Heijne (1993). The orientation of membrane proteins is based on the so-called 'positive-inside rule' which has been extensively studied and is used for topology predictions of membrane proteins (von Heijne, 1992, Andersson & von Heijne, 1994a, 1994b). According to this rule, bacterial inner membrane proteins contain a much higher amount of positively charged amino acid residues in their cytoplasmic regions rather than in the periplasm or extracellularly (Heijne, 1986). The correct topology of the BceB-ECD hybrid constructs was confirmed using the TOPCONS web server for consensus prediction of membrane protein topology (data not shown, Tsirigos *et al.*, 2015).

Chapter IV

A

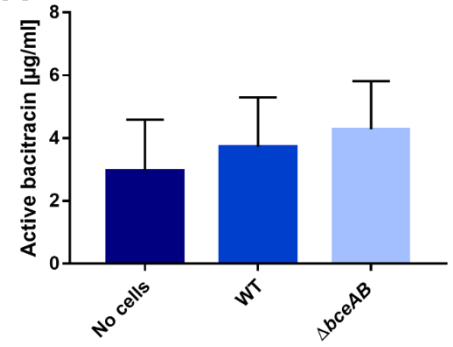

B

Strains	Active bacitracin [µg/ml]
No cells	2.96±1.62
WT	3.72±1.57
Δ*bceAB*	4.29±1.52

Figure S4.1: AMP transport assay suggests bacitracin is neither imported nor inactivated by BceAB. *B. subtilis* W168 (WT) and a Δ*bceAB* mutant (TMB035) were grown, harvested and resuspended to an OD_{600} of 10. Bacitracin was added to cultures and a control without cells to a final concentration of 5 µg/ml and incubated for 30 minutes. Supernatants were collected and the remaining bacitracin activity was determined using a bio-assay. Supernatants were filled into wells in an agar plate with a bacitracin-sensitive strain (Δ*bceAB* Δ*bcrC* double mutant, SGB01) as indicator strain. Residual bacitracin concentrations were quantified from the diameter of inhibition zones and calibrated against a series of standards. Data are shown as mean ± standard deviation of at least three biological replicates. **A:** Comparison of remaining biologically active bacitracin in the supernatant of WT and Δ*bceAB* cultures and samples without cells. Values are stated in panel **B**. No significant difference could be determined using a one-way ANOVA.

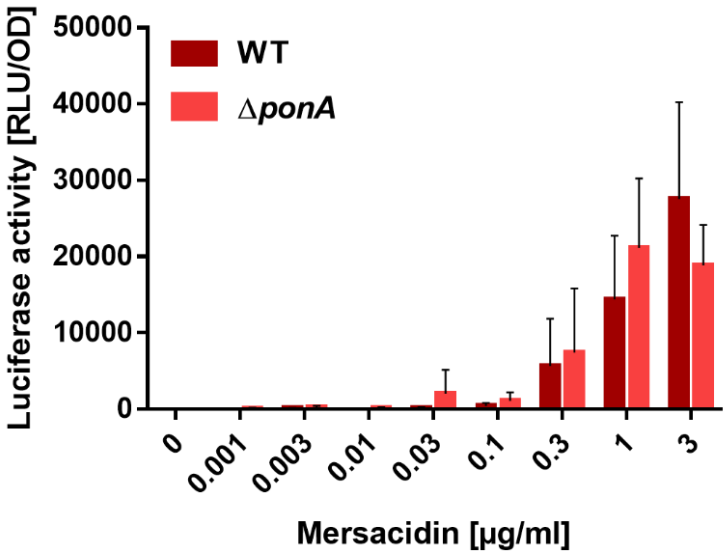

Figure S4.2: Deletion of *ponA* does not lead to changes in BceAB activity. Comparison of BceAB activities in the WT (SGB73, dark red) and a Δ*ponA* strain (SGB810, light red) in the presence of varying mersacidin concentrations. BceAB activities were determined as described in Fig. 4.4. Data are shown as mean ± standard deviation of at least three biological replicates. A two-way ANOVA did not reveal any significant contribution to variation by the strains.

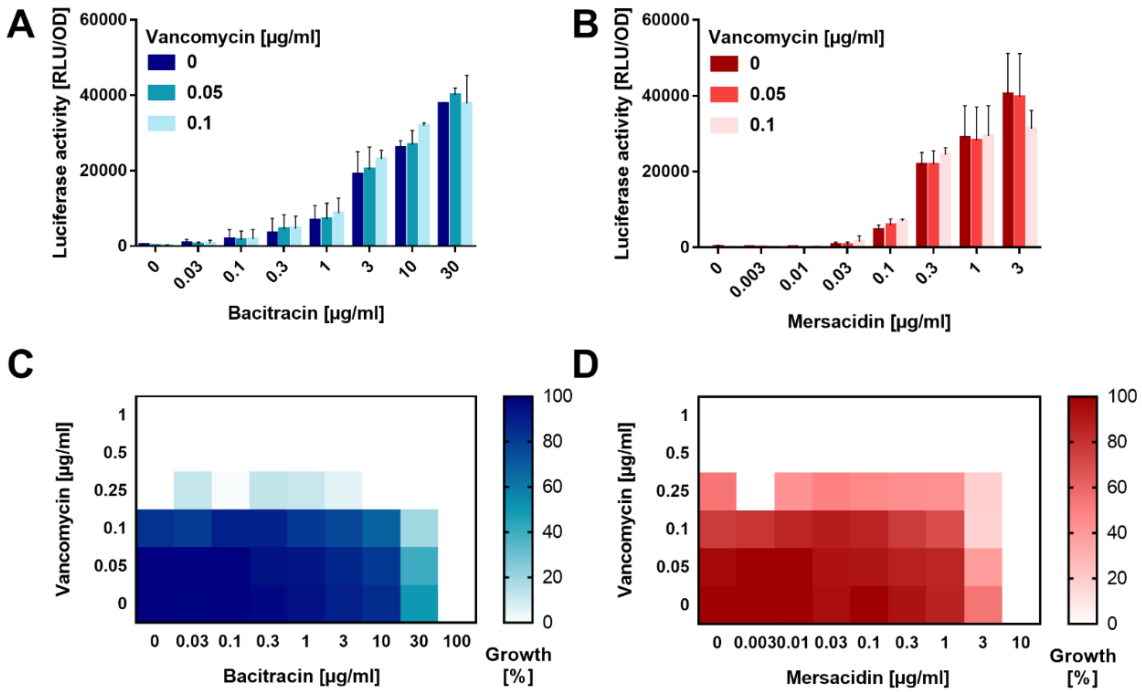

Figure S4.3: Combination of bacitracin or mersacidin with vancomycin does not alter BceAB activity. A+B: BceAB activity in presence of bacitracin or mersacidin in combination with 0, 0.05, 0.1 µg/ml vancomycin (dark to lighter colour). Exponentially growing cells were challenged with varying concentrations of vancomycin and bacitracin or mersacidin, as indicated BceAB activities were determined as described in Fig. 4.4. **C+D:** Growth of the WT strain (SGB73) in presence of bacitracin or mersacidin combined with vancomycin. OD_{600} measurements taken 55, 60 and 65 minutes after addition were averaged and normalised (100 % corresponding to maximum growth, darkest blue/red). All data are shown as mean of two biological replicates. Standard deviation of BceAB activity is indicated in bar graphs of panel A and B. A two-way ANOVA did not show any significant contribution to variation by the strains.

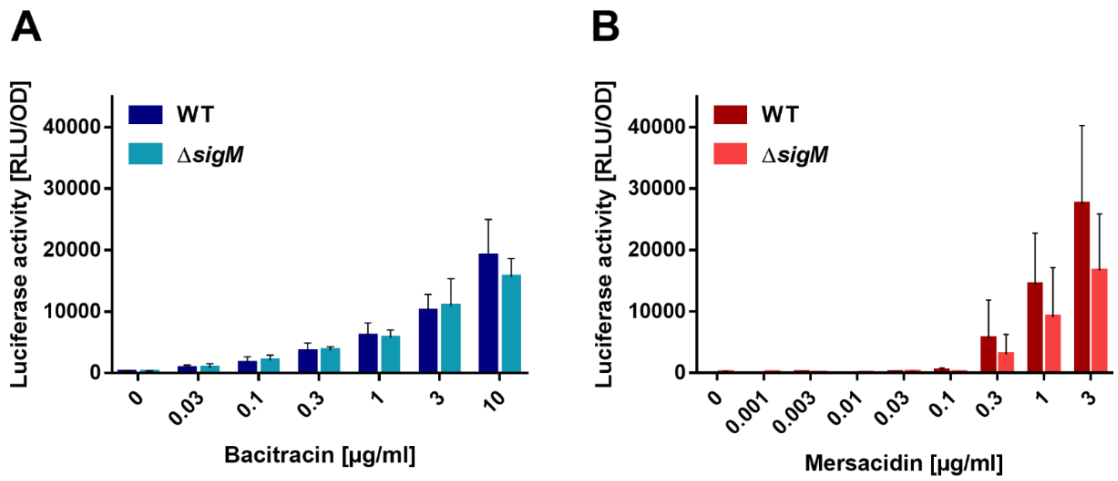

Figure S4.4: Deletion of *sigM* does not result in significant changes in the BceAB activity. BceAB activity of a Δ*sigM* strain (SGB, 812turquois/light red) compared to WT activity (SGB73 darker blue/red) in the presence of sub-inhibitory concentrations of **A:** bacitracin and **B:** mersacidin. BceAB activities were determined as described in Fig. 4.4. All data are shown as mean ± standard deviation of at least three biological replicates. A two-way ANOVA did not show any significant contribution to variation by the strains.

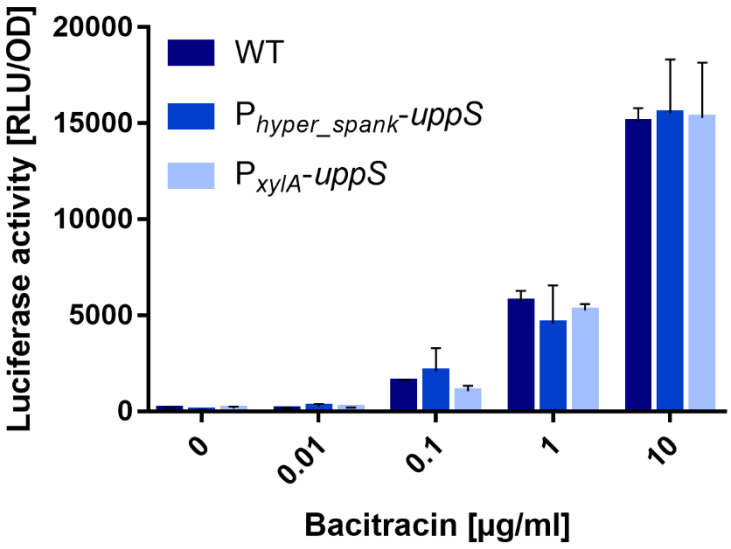

Figure S4.5: Overproduction of UppS does not alter BceAB activity. Comparison of BceAB activities in the WT (SGB73, dark blue) and IPTG-/ xylose-inducible UppS overproduction strains (SGB651, blue and light blue) in the presence of varying bacitracin concentrations. BceAB activities were determined as described in Fig. 4.4, in the presence of 1 mM IPTG or 0.2 % xylose. Data are shown as mean ± standard deviation of at least three biological replicates. A two-way ANOVA did not show any significant contribution to variation by the strains.